Adriana Isabel do Vale Marcelo

Stress granules in Polyglutamine diseases: new targets for therapeutic intervention?

UNIVERSIDADE DO ALGARVE

Faculdade de Medicina e Ciências Biomédicas

2021

Adriana Isabel do Vale Marcelo

Stress granules in Polyglutamine diseases: new targets for therapeutic intervention?

PhD Program in Biomedical Sciences

This work was done under the supervision of:

Clévio Nóbrega, PhD

Luís Pereira de Almeida, PhD

UNIVERSIDADE DO ALGARVE

Faculdade de Medicina e Ciências Biomédicas

2021

Stress granules in Polyglutamine diseases: new targets for therapeutic intervention?

Declaração de autoria de trabalho

Declaro ser a autora deste trabalho, que é original e inédito. Autores e trabalhos consultados estão devidamente citados no texto e constam da listagem de referências incluída.

_____

(Adriana Isabel do Vale Marcelo)

Copyright © 2021 Adriana Isabel do Vale Marcelo

A Universidade do Algarve reserva para si o direito, em conformidade com o disposto no Código do Direito de Autor e dos Direitos Conexos, de arquivar, reproduzir e publicar a obra, independentemente do meio utilizado, bem como de a divulgar através de repositórios científicos e de admitir a sua cópia e distribuição para fins meramente educacionais ou de investigação e não comerciais, conquanto seja dado o devido crédito ao autor e editor respetivos

Aos meus pais Manuela e Marcelo e à minha irmã Mariana pelo eterno amor, apoio e incentivo.

Agradecimentos

Após quatro anos de trabalho árduo, a primeira reflexão que faço é que terminar esta etapa profissional muito desejada não seria possível sem a ajuda e o apoio constante de diversas pessoas. Chega assim a hora de agradecer a todos vós:

Ao Professor Doutor Clévio Nóbrega, quero começar por agradecer por todas as oportunidades que me foram criadas e por ter acreditado e confiado em mim desde início para realizar este projecto, pela disponibilidade para me orientar e ajudar neste trabalho, pela paciência, por todos os ensinamentos e conhecimentos transmitidos, pelos conselhos e amizade.

Ao Professor Doutor Luís Pereira de Almeida, agradeço a oportunidade de realizar este projeto sob a sua co-orientação e pela disponibilidade para me ajudar sempre que precisei.

Aos meus colegas e amigos de laboratório, Sofia, Inês, Rebekah, Rafa, Ricardo, Carlos, Sara, Joana, André, Leonardo, agradeço toda ajuda que me deram, os bons momentos e toda a amizade.

Finalmente quero agradecer ao meu namorado Marcelo pelo apoio constante e pelo incentivo nas horas mais difíceis, às princesas Carolina, Mousinho, Helena, Sofia e Sara, a todos os meus amigos de infância que apesar de estarem longe foram sempre os melhores amigos do mundo, e aos meus familiares.

O meu maior agradecimento vai para os meus pais, Manuela e Marcelo, e para a minha irmã Mariana, os três grandes pilares da minha vida. Obrigada por todas oportunidades que me proporcionaram ao longo da minha vida. Sem eles não seria a pessoa que sou hoje e a eles devo tudo.

A todos vós,
Um sincero Obrigado!

Table of contents

Abbreviations

ALS	amyotrophic lateral sclerosis
AMPK	adenosine monophosphate-activated protein kinase
ASOs	antisense oligonucleotides
Atx	Ataxin
BAC	bacterial artificial chromosome
C. elegans	Caernorhabditis elegans
CACNA1A	calcium voltage-gated channel subunit alpha 1A
CAG	Cytosine-Adenine-Guanine
CARHSP1	calcium-regulated heat stable protein 1
CBP	cAMP-response element binding-binding protein
CDK5	cyclin-dependent kinase-5
Cr-Carhsp1	CRISPR-Cas 9 system guided for Carhsp1
Cr-CT	control construct
CREB	cAMP-response element binding
CRISPR	Clustered Regularly Interspaced Short Palindromic Repeats
DAPI	4′,6′-Diamidino-2′-phenylindole
DDX6	DEAD/H-box RNA helicase
DMEM	Dulbecco’s modified Eagle’s medium
DRPLA	dentatorubral-pallidoluysian atrophy
DTI	diffusion tensor imaging
DUB	deubiquitinating enzyme
EGFP	enhanced green fluorescent protein
EGFR	epidermal growth factor receptor
EIF2AK1	eIF2α kinase 1
EIF2AK3	eIF2α kinase 3
EIF2AK4	eIF2α kinase 4
eIF2α	Eukaryotic translation initiation factor 2A
eIF4F	Eukaryotic initiation factor 4F

ER	endoplasmic reticulum
ERAD	endoplasmic reticulum-associated degradation
ERES	endoplasmic reticulum exit sites
FBS	fetal bovine serum
FMRP	fragile X mental retardation protein
FOXO	forkhead box
G3BP1	ras GTPase-activating protein-binding protein 1
GCN2	general control non-derepressible-2
HA	N-terminal haemagglutinin
HD	Huntington’s disease
HDAC	histone deacetylase
HDAC3	histone deacetylase
HEK	human embryonic kidney
HHR23A/B	yeast DNA repair protein Rad23 A and B
hMSCs	human mesenchymal stromal cells
HRI	haem-regulated inhibitor
HSG	heat-stress granules
HSP	heat shock proteins
HSP90	heat shock protein 90
IDDs	intrinsically disordered domains
InsP3R1	1 inositol 1,4,5-trisphosphate
IP	intraperitoneal injection
iPSC	induced pluripotent stem cell
JD	Josephin domain
KI	knock-in
KPNA3	karyopherin alpha 3
Lsm	Like-sm
LsmAD	Lsm-associated
LTD	long-term depression
LV	lentiviral vectors

MAP2	microtubule-associated protein 2
miRNA	microRNA
MJD	Machado-Joseph disease
MRI	magnetic resonance imaging
mRNPs	messenger ribonucleoprotein
MRS	magnetic resonance spectroscopy
MSC	mesenchymal stromal cells
MTK1	MAP 3 kinase
N2A	neuroblastoma line-derived cells
NAA	N-acetylaspartate
NCOR1	nuclear receptor co-repressor 1
P-bodies	processing bodies
PABP	poly(A)-binding protein
PAM	protospacer adjacent motif
PANTHER	Protein ANalysis THrough Evolutionary Relationships
PBS	1M phosphate buffer solution
PCAF	p300/CREBBP associated factor
Pcp2	Purkinje cell protein 2
PEI	polyethylenimine
PEK	pancreatic eIF2α kinase
PERK	PKR-like ER kinase
PFA	paraformaldehyde
PGK	phosphoglycerate kinase 1
PKR	protein kinase R
PLDs	prion-like domains
PLIC1	protein linking IAP to the cytoskeleton
PNAs	peptide nuclei acid
PolyQ	Polyglutamine
PUM1	Pumilio homolog
Q	glutamines

Qn	polyQ tract
RACK1	receptor of activated protein C kinase 1
RBP	RNA-binding protein
RT	room temperature
SBMA	spinal and bulbar muscular atrophy
SCA2	Spinocerebellar ataxia type 2
SCAs	spinocerebellar ataxias
sgRNA	single guide RNA
SGs	stress granules
shRNA	short hairpin RNA
siRNA	small interfering RNA
SK	potassium channels
SNALPs	stable nuclei acid lipid particles
SOD2	manganese superoxide dismutase 2
ss-siRNAs	single-stranded silencing RNAs
TBP	TATA-binding protein
TIA-1	T-cell intracellular antigen-1
TIAR	TIA-1 related
TNF-α	tumor necrosis factor alpha
TRDs	trinucleotide repeat diseases
TTP	tristetraprolin
UIMs	ubiquitin interactor domains
UPS	ubiquitin-proteasome system
UTR	untranslated region
VCP/p97	valosin-containing protein or ATPase p97
WT	wild-type
YAC	yeast artificial chromosome

Abstract

Polyglutamine (PolyQ) diseases are a group of hereditary and incurable neurodegenerative pathologies, caused by abnormal expansion of CAG trinucleotide repeats in the disease-causing genes. In these disorders, the formation of toxic aggregated species from the expanded protein leads to dysfunction of several biological systems, ultimately resulting in neuronal degeneration and death widespread across different brain regions. Dysfunction of cellular pathways also correlates with stress responses, such as the formation of stress granules (SGs). Recently, multiple evidence suggested that SGs and its components play a role in the pathogenesis of PolyQ diseases. Therefore, the general goal of this project was to clarify the SGs role in the context of PolyQ diseases pathogenesis, trying to identify new pathways and targets for a therapeutic intervention, using spinocerebellar ataxia type 3 (SCA3) and type 2 (SCA2) as PolyQ disease models. We found that several SGs components have their gene expression levels altered in these two diseases, including regulated heat stable protein 1 (CARHSP1) and Pumilio homolog 1 (PUM1), which have their levels upregulated in SCA3 and SCA2 diseases. We found that the downregulation of CARHSP1 resulted in reduced mutant protein aggregation in SCA3 cellular and mouse models, as well as amelioration of motor and neuropathological abnormalities. On the other hand, knockdown of PUM1 levels led to increased aggregation of polyQ-expanded protein, as well as worsening of motor deficits in mouse models of SCA3 disease. We further assessed the downregulation of CARHP1 in a novel striatal lentiviral mouse of SCA2, although no alterations in neuropathological features were observed. Overall, our study contributes to the putative involvement of SGs in PolyQ disease and showed that the modulation of CARHSP1 SGs component could be potential therapeutic approach for SCA3 disease. Future studies are needed to fully understand SGs and its components importance in the context of PolyQ and other neurodegenerative diseases.

Key words: Polyglutamine diseases, spinocerebellar ataxia type 3, spinocerebellar ataxia type 2, stress granules, stress granules components, disease mouse models

Resumo

As doenças de poliglutaminas são um grupo de nove doenças neurodegenerativas causadas pelo mesmo tipo de mutação genética. Estas patologias resultam de uma repetição aberrante do códão CAG na região codificante dos genes responsáveis por cada uma destas doenças. Esta mutação genética traduz-se numa expansão tóxica de glutaminas nas respetivas proteínas traduzidas, que sofrem alterações conformacionais levando à formação de agregados proteicos em diversas populações de neurónios. Apesar de serem causadas por genes e proteínas diferentes, as doenças de poliglutaminas partilham vários mecanismos de patogénese, que incluem a desregulação de diversos sistemas celulares essenciais à sobrevivência celular. Para além disto, a expressão de proteínas com expansões de poliglutaminas conduz a aumento dos níveis de stress celular, induzindo a formação de grânulos de stress. Diversos estudos sugeriram que os grânulos de stress podem desempenhar um papel relevante na patogénese das doenças de poliglutaminas e de outras doenças neurodegenerativas. Assim, o objetivo global deste trabalho foi estudar o papel dos grânulos de stress e dos seus componentes nestas doenças, de forma a tentar identificar novas vias celulares envolvidas nestas patologias e novos alvos com um potencial terapêutico, utilizando a ataxia espinocerebelosa do tipo 3 (SCA3, do inglês *spinocerebellar ataxia type 3*) e do tipo 2 (SCA2, do inglês *spinocerebellar ataxia type 2*), como modelos das doenças de poliglutaminas. Estas duas doenças resultam da expansão anormal de poliglutaminas nas proteínas ataxina-3 e ataxina-2, respetivamente.

Neste trabalho, começámos por analisar quais os componentes dos grânulos de stress que estavam diferencialmente expressos, utilizando a análise de dados de transcriptómica, de modelos de murganho de cada uma das doenças modelo. Estes resultados demonstraram que as proteínas, CARHSP1 (do inglês *calcium regulated heat stable protein 1*) e PUM1 (do inglês Pumilio homolog 1) tinham os seus níveis aumentados, comparados com animais saudáveis. De seguida, decidimos avaliar se a diminuição dos níveis destas proteínas através da ferramenta de edição génica CRISPR-Cas (do inglês *clustered regularly short palindromic repeats-CRISPR associated nucleases*) poderia ter um impacto em diversas caraterísticas da SCA3. Os resultados obtidos demonstraram que a

diminuição de CARHSP1 levou a uma redução da agregação da proteína ataxina-3 expandida em modelos celulares e animais desta doença. Para além disto, observou-se a melhoria do fenótipo motor e das características neuropatológicas em murganhos de SCA3. Por outro lado, a diminuição dos níveis de PUM1 resultou no aumento dos níveis de agregação da proteína mutante e no agravamento da função motora na doença de SCA3. Assim, estes resultados demonstraram que a diminuição dos níveis de CARHSP1 teve um efeito benéfico nos modelos de doença de SCA3.

De forma a podermos testar o efeito do componente dos SGs, CARHSP1, na doença SCA2, procedemos ao desenvolvimento de um novo modelo de murganho desta doença com patologia no estriado. Para isto, recorremos ao uso de vetores lentivirais para expressar a construção com o gene mutante de SCA2. A caraterização deste modelo revelou a expressão da proteína mutante resulta na formação de agregados dentro dos neurónios do estriado, levando à depleção de marcadores neuronais, à morte neuronal e à indução de inflamação no estriado. O modelo lentiviral de murganho de SCA2 criado revelou-se como uma ferramenta útil para estudar novos mecanismos de doenças e testar novos potencias alvos terapêuticos.

De seguida, fomos então avaliar se a diminuição dos níveis de CARHSP1 poderia ter o mesmo papel benéfico na doença SCA2. Após a modulação dos níveis de CARHSP1, não observámos alterações significativas na neuropatologia dos animais com SCA2.

Em conclusão, este trabalho identificou a proteína CARHSP1, componente dos SGs, como um potencial alvo terapêutico para o tratamento da doença de PolyQ SCA3. Por outro lado, este alvo não resultou em melhorias no modelo de doença de SCA2. Assim, estudos futuros em outras doenças de PolyQ devem ser feitos para validar o CARHSP1 como alvo terapêutico para estas doenças.

Palavras-chave: doenças de Poliglutaminas, ataxia espinocerebelosa do tipo 3, ataxia espinocerebelosa do tipo 2, grânulos de stress, componentes dos grânulos de stress, modelos de ratinho de doenças

Chapter 1. Introduction

1.1 Trinucleotide Repeat Disorders

The trinucleotide repeat diseases (TRDs) are a group of genetic pathologies caused by abnormal expansion of triplet repeats in coding or non-coding DNA regions (Fig. 1.1) (Spada et al., 1994). Repetitive nucleotide sequences occur commonly in the human genome and normally are referred as microsatellite regions (Srivastava et al., 2019). Usually, these sites of tandem repeats are linked to gene regulation and play an important role in evolutionary plasticity (Sreenu et al., 2006). Nonetheless, when the number of repeats extend beyond a certain threshold, it could give rise to an abnormal protein, triggering downstream pathogenic mechanisms (Orr and Zoghbi, 2007). The mutagenic events that lead to this expansion of repetitive sequences have been characterized for several TRDs. In a specific group of these diseases, Mittelman and colleagues reported that upon inhibition of the heat shock protein 90 (HSP90), Cytosine-Adenine-Guanine (CAG) trinucleotide repeats mutate more frequently in human cells, suggesting a role of HSP90 in modulating trinucleotide repeat tracts (Mittelman et al., 2010). The relation between impairment of HSP90 normal function and a stressed environment hinted that stress factors could induce expansion of trinucleotide repeat regions (Fonville et al., 2011). The association of environmental stress and mutagenesis of trinucleotide repeats in human cells was proposed by Chatterjee et al. who showed that cold, heat, hypoxia and oxidative stress stimulus increased CAG triplet mutagenesis (Chatterjee et al., 2015). Moreover, they reported that stress-induced trinucleotide repeats mutations could be decreased by modulation of the stress-response players levels. Regardless the mutagenic trigger or the pathogenic mechanism behind the TRDs, all disorders are unstably transmitted to the offspring resulting in a high range of clinical phenotypes and disease severity (McMurray, 2010). The number of repeats tends to increase in the successive generations leading to earlier disease onset and symptoms worsening, in a phenomenon called genetic anticipation (Friedman, 2011).

So far, 16 neurological disorders manifesting either during early human development or in latter adult life, were reported to be caused by unstable trinucleotide repeats (Orr and Zoghbi, 2007). These disorders can be classified according to the mechanism underlying disease pathogenesis. Fragile X

Syndrome (Richards et al., 1981), Fragile XE Syndrome (Mulley et al., 1995) and Friedreich ataxia (Cossée et al., 1997) are caused by loss-of-function mechanisms of the mutated proteins. Other TRDs result from RNA-mediated-gain-of-function which include Myotonic dystrophy type 1 (Fu et al., 1992), Myotonic dystrophy type 2 (Liquori et al., 2001) and Fragile X-Associated Tremor Ataxia Syndrome (Hagerman et al., 2001). The monogenic group of Polyglutamine (PolyQ) diseases are characterized by a toxic-gain-of-action (Bunting et al., 2021), constituting the largest group of monogenic neurogenerative diseases and will be discussed in more detail in the following section.

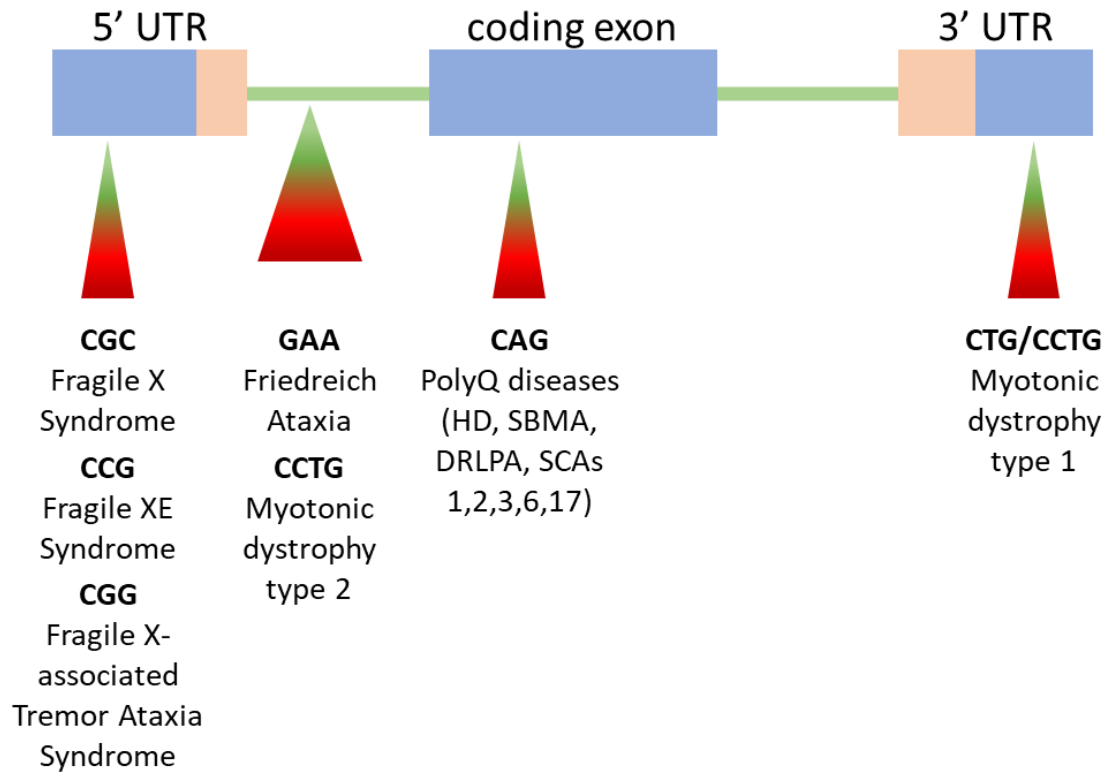

Fig. 1.1: **Neurological trinucleotide repeat disorders (TRDs) gene expansions**. Trinucleotide repeat disorders are caused by triplet unstable expansions in different gene regions. The expanded sequence varies among the different disorders as well as the site of its location inside the genomic sequence, which could occur in non-coding (5' untranslated region (UTR), intronic zones and 3' UTR region) or inside the exonic coding regions. (Adapted from Budworth & McMurray, 2013).

1.2 Polyglutamine diseases

Polyglutamine (PolyQ) diseases comprises a group of 9 hereditary rare neurodegenerative pathologies caused by the same type of genetic mutation (Table 1.2). They are caused by an abnormal expansion of the trinucleotide CAG in the disease-causing genes coding region, resulting in a toxic glutamine (polyQ) stretch in the translated proteins (Fig. 1.2) (Nóbrega and Pereira de Almeida, 2018). Huntington's disease (HD), dentatorubral-pallidoluysian atrophy (DRPLA) and the spinocerebellar ataxias (SCAs) type 1, 2, 3, 6, 7 and 17 are inherited in an autosomal dominant manner, while spinal and bulbar muscular atrophy (SBMA) has a X-linked recessive inheritance (Bunting et al., 2021). Besides carrying the CAG/polyQ repeat expansion, genes and proteins associated with these group of diseases do not share significant homology, having distinct biological functions (Paulson, 2018). Nevertheless, all polyglutamine expanded proteins tend to aggregate in large insoluble multiprotein inclusions inside neuronal cells of specific brain regions (Gatchel and Zoghbi, 2005).

While different, PolyQ diseases share several features, including common pathogenic mechanisms. In all PolyQ diseases, there is a positive correlation between the number of CAG repeats and the onset age and severity of the symptoms, meaning that longer polyQ stretches result in earlier and aggravated symptomatic manifestations (Zoghbi and Orr, 2000). The CAG repeat expansions are very dynamic and unstable often increasing when transmitted to the progeny, resulting in anticipation and worsening of the symptoms in successive generations, a phenomenon common in other TRDs (McMurray, 2010; Paulson, 2018). Another characteristic recurrently observed in PolyQ diseases is the presence of intracellular pathogenic aggregates in patients' neuronal tissues, as observed in other neurogenerative diseases (Ross et al., 1999). Although the molecular mechanism underlying PolyQ diseases pathogenesis are fully understood, several toxic events have already been proposed: formation of toxic RNA polyQ transcriptions; mutated protein toxic gain of function; resulting in aberrant molecular interactions, transcriptional changes, mitochondrial alterations, protein clearance systems, among others (Gatchel and Zoghbi, 2005; Bauer and Nukina, 2009; La Spada and Taylor, 2010). The comparable features observed in the different PolyQ diseases fostered researchers to investigate new

targets that could be potential therapeutic targets for all these pathologies, taking also into consideration the differences existing in each disorder.

Table 1.2: **Polyglutamine diseases: names, genetics, neuropathology and symptoms.**

Disease	Gene mutated	Protein	Normal CAG repeats	Disease CAG repeats	Major affected regions	Major clinical features
HD	*HTT* (autosomal)	Huntingtin	10-35	40-250	Caudate nucleus, putamen, globus pallidus and substantia nigra	Chorea, dystonia, rigidity, depression, anxiety
DRLPA	*ATN1* (autosomal)	Atrophin 1	6-35	48-93	Cerebellum, red nucleus, globus pallidus, subthalamic nucleus	Ataxia, epilepsy, choreoathetosis, dementia
SBMA	*AR* (X-linked)	Androgen receptor	5-34	37-70	Motor neurons in anterior horn of the spinal cord and in brainstem	Weakness and atrophy of bulbar, facial and limb muscles
SCA1	*ATXN1* (autosomal)	Ataxin-1	19-36	43-81	Cerebellum, red nucleus, inferior olive, pons, pyramidal tracts	Ataxia, slurred speech, spasticity, cognitive impairment
SCA2	*ATXN2* (autosomal)	Ataxin-2	13-31	33-200	Cerebellum, ocular brainstem, spinal cord	Ataxia, slow saccades, dysarthria, nystagmus
SCA3	*ATXN3* (autosomal)	Ataxin-3	10-44	61-87	Cerebellum, fourth ventricle enlargement, dentate nucleus	Ataxia, dysarthria, spasticity, oculomotor dysfunction, dystonia
SCA6	*CACNA1A* (autosomal)	Calcium voltage-gated channel subunit α1 A	4-18	19-33	Cerebellum, thalamus, putamen, pallidum	Ataxia, dysarthria, nystagmus
SCA7	*ATXN7* (autosomal)	Ataxin-7	4-35	36-460	Cerebellum, brainstem, macula, inferior olive	Ataxia, slow eye movement, ophthalmoplegia, dysphagia, pyramidal signs
SCA17	*TBP* (autosomal)	TATA box-binding protein	25-40	41-66	Cerebellum, cortex, caudate and putamen	Ataxia, dementia, chorea, dystonia

Abbreviations: HD, Huntington's disease; DRPLA, dentatorubral-pallidoluysian atrophy; SBMA, spinal and bulbar muscular atrophy; SCA, spinocerebellar ataxia. (Adapted from Afonso-Reis et al., 2021; Bunting et al., 2022; Nóbrega & Pereira de Almeida, 2018).

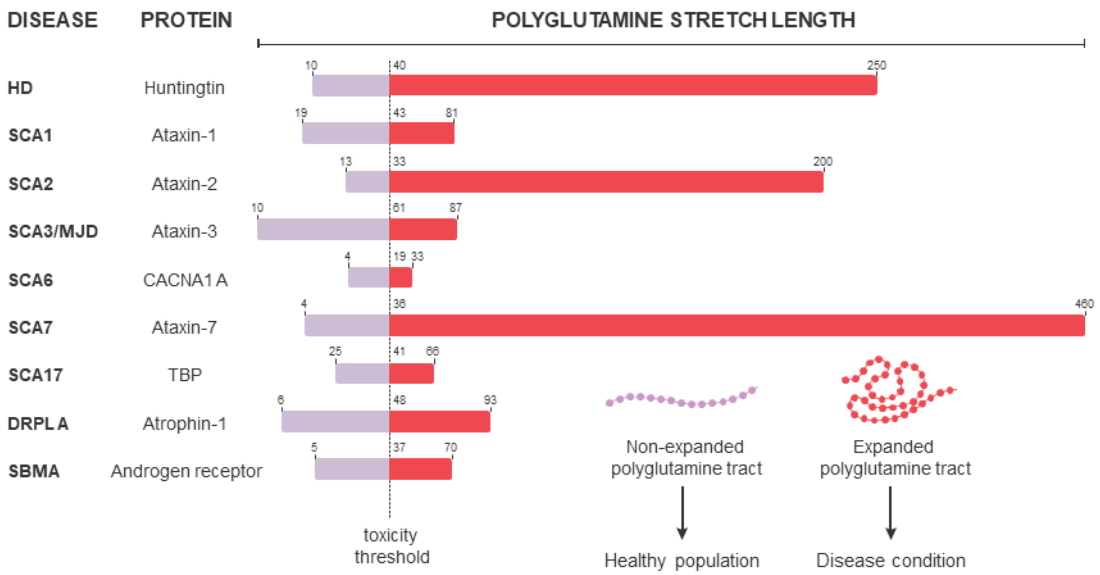

Fig. 1.2: **Representation of polyQ-stretch length for each protein involved in PolyQ diseases**. Abbreviations: HD, Huntington's disease; SCA, spinocerebellar ataxia; DRPLA, dentatorubral-pallidoluysian atrophy; SBMA, spinal and bulbar muscular atrophy. (Adapted from Nóbrega et al., 2020).

1.3 Spinocerebellar ataxia type 3 / Machado-Joseph disease

1.3.1 History and epidemiology

Spinocerebellar ataxia type 3 (SCA3), also known as Machado-Joseph disease (MJD), was first described between 1972 and 1977 in four families living in the United States of America, who were Portuguese descendants from the Azores archipelago. The high variability of clinical manifestations, presented by affected individuals, led to the definition of four different dominantly inherited genetic diseases: “Machado disease” (Nakano et al., 1972), “nigro-spino-dentatal degeneration” (Woods and Schaumburg, 1972), “Joseph disease” (Rosenberg et al., 1976) and “Azorean disease of the nervous system” (Romanul et al., 1977). In 1978, Coutinho and Andrade reported a study on 15 families from Flores and São Miguel Azorean Islands that displayed common symptoms, such as cerebellar ataxia, progressive external ophthalmoplegia, pyramidal and extrapyramidal signs and distal muscular atrophy (Coutinho and Andrade, 1978). They suggested that the previous studies of neurological disorders observed in Azorean lineages were clinical variations of the same pathology and proposed the name “Machado-Joseph disease” which was adopted in 1980.

Currently, SCA3 is the most common SCA worldwide, affecting around 1,5 in 100.000 individuals (Orphanet, 2021). Comparing to other SCAs, SCA3 is particularly frequent in China (62.1%), Brazil (59.6%), Thailand (46.5%), Germany (42%), Singapore (41%), Taiwan (32%), France (32%), Japan (28%), The Netherlands (28%), Venezuela (25%), the USA (21%) and Spain (15%) (Nóbrega and Pereira de Almeida, 2018). In the case of Portugal, SCA3 has a frequency of 56% in overall SCA patients, with a prevalence of 3,1 in 100.000 individuals in the mainland (Coutinho et al., 2013). In the Azorean Islands, the prevalence reaches a higher prevalence of 39 in 100.000 individuals, with particular focus in the Islands of Flores (1 in 158 individuals) and Corvo (1 in 143 individuals) (de Araújo et al., 2016).

1.3.2 Clinical features

SCA3 patients usually display their first symptoms during adulthood, around 40 years of age, however, it was described disease onset ages at 4 years (Carvalho et al., 2008) and 70 years of age (Bettencourt and Lima, 2011). The disease progresses rapidly and irreversibly during an average period of 21 years (ranging from 7 to 29 years), leading to premature death (Kieling et al., 2007). SCA3 patients present clinically heterogenous manifestations which mainly results from the involvement of cerebellar, pyramidal, extrapyramidal, motor neuron and oculomotor systems (Rosenberg, 1992). Nevertheless, the clinical hallmark is cerebellar ataxia, defined as uncoordinated involuntary movements, reported as first symptom in 92% of diagnosed cases (Bettencourt and Lima, 2011). Patients can also experience progressive external ophthalmoplegia, pyramidal signs (rigidity, spasticity), extrapyramidal signs (bradykinesia and dystonia), dysarthria, dysphagia, tremors, motor neuropathy, muscle atrophy, Parkinsonism, among others (Rosenberg, 1992). The complex clinical presentation resulted in the definition of four distinct disease subtypes (Coutinho and Andrade, 1978; Suite et al., 1986). In type I, the age of onset occurs between 5 to 30 years old, and symptoms have a faster progression, which include limb and gait ataxia, dystonia, pyramidal deficits, progressive external ophthalmoplegia. The most common SCA3 type is II, starting around 36 years old and manifesting through ataxia, pyramidal traits and progressive external ophthalmoplegia. SCA3 disease type III is the second most frequent, presenting a later age of onset between 40-75 years. Besides ataxia and progressive external ophthalmoplegia, patients present peripheral signs as motor neuropathy and muscle atrophy. The rarest clinical presentation is SCA3 type IV characterized by parkinsonism symptoms, fasciculations and peripheral neuropathy, typical in patients with short CAG repeat expansions (onset age 38-47 years). Posteriorly, an SCA3 type V was proposed, as rare cases of pure spastic paraplegia were diagnosed (Landau et al., 2000). Cognitive impairments and non-motor symptoms have also been described in SCA3 cases. These include: (1) sleep disorders (restless legs syndrome, rapid eye movement, sleep behavior disorder, periodic limb movement during sleep, sleep apnea, insomnia, and excessive daytime sleepiness); (2) cognitive deficits (executive dysfunction, visual information and

visual attention processing problems, verbal and visual memory deficits); (3) psychiatric symptoms (depression, anxiety); (4) olfactory dysfunction; (5) peripheral neuropathy (muscle atrophy, distal weakness with foot drop and fasciculations); (6) fatigue; (7) cramps (affect lower limbs, arms, trunk, face and abdominal muscles); (8) autonomic dysfunction (urinary incontinence, cold intolerance, sweating disorders); and (9) weight loss (Kinoshita et al., 1995; Kanai et al., 2003; Yeh et al., 2005; Cecchin et al., 2007; Friedman and Amick, 2008; Rüb et al., 2008; D'Abreu et al., 2009b; Braga-Neto et al., 2012b, 2012a; Pedroso et al., 2013).

1.3.3 Neuropathology

The severe and heterogeneous clinical manifestations observed and described in SCA3 patients are a result of an extensive degeneration in several regions of the central nervous system (Table 1.3). Histological analysis demonstrated neuronal loss in the cerebellum (spinocerebellar pathways, medial cerebellar peduncle and dentate nucleus); in the brainstem (pons, medulla oblongata); in the basal ganglia (substantia nigra, striatum, globus pallidus); in the thalamus; in cranial nerves (particularly the oculomotor-III and the hypoglossoal-XII); and in the spinal cord (anterior horn cells, the Clarke's column and the dorsal columns) (Rosenberg, 1992; Sudarsky and Coutinho, 1995; Riess et al., 2008; Rüb et al., 2008; Bettencourt and Lima, 2011).

More recently, neuroimaging techniques allowed the analysis in more detail the brain of SCA3 patients. Magnetic resonance imaging (MRI) studies demonstrated atrophy of several structures, suggested by volumetric measures. Regarding the infratentorial structures (cerebellum), it was observed reduced volume of cerebellar vermis and hemisphere, and brainstem. The level of volumetric reduction is positively correlated with the polyQ expansion length. In supratentorial structures, MRI allowed the detection of reduced volume in basal ganglia (caudate nuclei, putamen, and thalami). In this case, the extent of atrophy did not correlate with disease severity (Schulz et al., 2010; D'Abreu et al., 2012; Rezende et al., 2015). Diffusion tensor imaging (DTI) studies revealed white matter damage in the cerebellum (dentate and other nuclei), cerebellar peduncles and brainstem (midbrain and pons) (Guimarães et al., 2013). Furthermore,

magnetic resonance spectroscopy (MRS) analyses identified a reduction of the neuronal-axonal integrity marker N-acetylaspartate (NAA) at the deep white matter (D'Abreu et al., 2009a), and at cerebellar hemispheres vermis in SCA3 affected individuals (Lirng et al., 2012).

Table 1.3: **Central nervous pathways and systems affected during the neurodegenerative process of SCA3 and their main clinical consequences.**

Affected central nervous pathway	Major lesions	Associated clinical manifestations
Cerebellothalamocortical motor loop	Cerebellar cortex, dentate and fastigial nuclei; pontine nuclei; thalamic ventral lateral nucleus; giant Betz pyramidal cells of the primary motor cortex; anterior horn motoneurons of the spinal cord	Ataxia; dysarthria; intentional tremor; amyotrophy; fasciculations; weakness of muscles; spasticity; hyperreflexia
Basal ganglia–thalamocortical motor loop	Pallidum; subthalamic nucleus; thalamic ventral lateral and reticular nuclei	Ataxia; bradykinesia; dystonia; myoclonia
Visual system	Lateral and inferior nuclei of the pulvinar; lateral geniculate body of the thalamus	Visual attentional deficits; abnormal visual evoked potentials
Auditory system	Colliculus inferior; nuclei of the lateral lemniscus; superior olive; cochlear nuclei	Abnormal brainstem auditory evoked potentials
Somatosensory system	All somatosensory nuclei of the thalamus, pons, and medulla oblongata; Clarke's column of the spinal cord	Ataxia; falls; decreased sense of vibration; decreased temperature discrimination; abnormal somatosensory evoked potentials
Vestibular system	Superior, lateral, medial, spinal, and interstitial vestibular nuclei	Postural instability; falls; horizontal gaze-evoked nystagmus; impaired vestibulo-ocular reaction and optokinetic nystagmus
Oculomotor system	Oculomotor, trochlear, and abducens nuclei; rostral interstitial nucleus of the medial longitudinal fascicle; reticulotegmental nucleus of the pons; area of the excitatory burst neurons for horizontal saccades; raphe interpositus nucleus; prepositus hypoglossal nucleus	Diplopia; saccadic smooth pursuits; dysmetrical saccades; slowed saccades; vertical and horizontal gaze palsy
Ingestion-related brainstem system	All somatosensory, somatomotor, viscerosensory and visceromotor ingestion-related brainstem nuclei; ingestion-related regions of the brainstem reticular formation	Dysphagia; malfunctions of the preparatory phase of ingestion; dysfunctions detrimental to the lingual, pharyngeal, and oesophageal phases of swallowing
Precerebellar brainstem system	Arcuate nucleus; red nucleus; pontine nuclei; reticulotegmental nucleus of the pons; vestibular nuclei; lateral reticular nucleus; external cuneate nucleus; prepositus hypoglossal nucleus; dorsal paramedian reticular nucleus; nucleus Roller; inferior olive	Ataxia; dysarthria; horizontal gaze-evoked nystagmus
Midbrain dopaminergic system	Mesostriatal dopaminergic system (substantia nigra); mesolimbic dopaminergic system (nuclei of the ventral tegmental area)	Parkinsonian features (akinesia, rigidity)
Midbrain cholinergic system	Pedunculopontine nucleus	Rapid eye movement sleep disorder
Pontine noradrenergic system	Locus coeruleus	Rapid eye movement sleep disorder

(Adapted from Rüb et al., 2008)

1.3.4 Genetics and protein physiology

The causative gene of SCA3, the *ATXN3* gene (also known as *MJD1* or *MJD* gene), was mapped in the long arm of chromosome 14 (14q24.3-q32) by Takiyama et al., 1993. In 1994, a study identified an expansion of CAG repeats in the *ATXN3* gene mapped to chromosome 14q32.1, in all members of a family with pathologically confirmed SCA3 (Kawaguchi et al., 1994). This work stablished the genetic cause underlying SCA3 and associated it as an inherited trinucleotide repeat disease. The complete genomic structure of *ATXN3* gene was later described by Ichikawa et al., 2001 (Fig. 1.3). The gene has 48kb and is composed of 11 exons and was found to be ubiquitously expressed throughout the organism. The CAG expansion localizes to exon 10 inside the gene (Ichikawa et al., 2001). In wild-type (WT) alleles, the number of trinucleotide repeats varies between 10 to 44, while expanded alleles range from 61 to 87 CAG consecutive repeats (Maciel et al., 2001). Intermediate size alleles from 45 to 60 repeats have also been reported to be associated with SCA3 disease, although these appear rarely and display incomplete penetrance as development of a pathologic condition might not occur (Bettencourt and Lima, 2011).

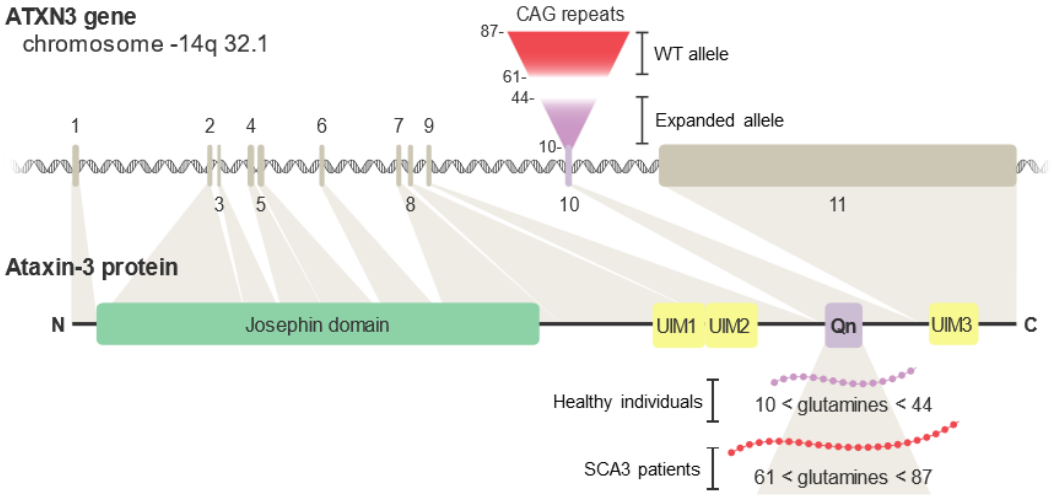

Fig. 1.3: **Schematic representation of *ATXN3* gene and ataxin-3 protein**. *ATXN3* gene is mapped in 14q32.1 chromosome, containing 11 exons. The gene product is Atx3 deubiquitinating protein, constituted by the Josephin domain in the N-terminal region and two or three ubiquitin interactor domains (UIMs) in the C-terminal tail. SCA3-associated CAG repeats expansion is localized in exon 10, which is translated into a polyQ tract (Qn) in the Atx3 protein. Healthy individuals have gene alleles/proteins containing between 10-44 CAG/glutamine repeats, whereas SCA3 patients express longer expansions ranging from 61 to 87 CAG/glutamine repeats. (Adapted from Nóbrega et al., 2020).

The *ATXN3* gene encodes for the protein ataxin-3 (ATXN3), a deubiquitinating enzyme with a normal molecular weight of 40-43 kilodalton (kDa), that comprises in its structure 339 amino acids along with a variable number of glutamine residues (Kawaguchi et al., 1994). Atx3 is composed by the structured globular Josephin domain (JD) in the N-terminal tail. On the other end, the C-terminal end has a more variable arrangement depending on alternative splicing events. The C-terminal end contains two or three ubiquitin interaction motifs (UIMs) and the polymorphic polyQ tract (Qn) (Burnett et al., 2003; Masino et al., 2003) (Fig. 1.3). So far, 12 isoforms of Atx3 protein have been identified and published (Gene ID: 4287, Uniprot ID: P54252). The most studied and characterized are ataxin-3a (or MJD1a) (Kawaguchi et al., 1994) and ataxin-3c (or MJD1-1) (Goto et al., 1997) gene products that differ in the number of UIMs: isoform-a contains only two UIMs in C-terminal tail, while isoform-c has a third UIM.

As described for the *ATXN3* mRNA, Atx3 protein is ubiquitously expressed in neuronal and non-neuronal tissues, localized both to the nucleus and the cytoplasm of several cell populations (Paulson et al., 1997a). Regarding the human brain, Atx3 was found to have a widespread expression, including cerebellum, cerebral cortex, spinal cord, caudate nucleus, hippocampus, substantia nigra and thalamus (Paulson et al., 1997a). In neuronal cells, Atx3 has mostly a cytoplasmic localization, distributed around the soma, dendrites, and axons. However, the nuclear presence of Atx3 has also been reported (Paulson et al., 1997b, 1997a; Schmidt et al., 1998; Trottier et al., 1998).

Although several studies have attempted to disclose the role of Atx3 in biological mechanisms, the exact physiological functions of the protein are not fully understood. Modelling Atx3 levels in *Caernorhabditis elegans* (*C. elegans*) and mouse showed that Atx3 knockout did not develop significant impairments, suggesting it as a nonessential protein (Rodrigues et al., 2007; Schmitt et al., 2007). However, it is plausible that JD-like containing proteins (Ataxin-3 Like, JosD1 and JosD2) counteract Atx3 absence by performing similar functions (Todi and Paulson, 2011). Moreover, the significance of Atx3 functions could be reflected by the fact that more than 40 proteins were identified as Atx3 interactors, as well as over 90 putative interactors, which could imply that Atx3 might be involved in several signaling pathways (Costa and Paulson, 2012). The first hints about Atx3 functions arose from the analysis of its structure, as protein

motifs UIMs were shown to interact with proteins bound to ubiquitin monomers or chains, thus suggesting a role in the protein degradation ubiquitin-proteasome pathway (Polo et al., 2002; Shih et al., 2002). In agreement with this hypothesis, Burnett and colleagues reported that Atx3 binds ubiquitylated proteins, specifically chains containing four or more ubiquitin moieties (Burnett et al., 2003). Moreover, their work also suggested that Atx3 is a ubiquitin protease, which is evidenced by its role in removing polyubiquitin chains and cleaving ubiquitin proteasome substrates. Additionally, it was shown that the edition of polyubiquitin chains by Atx3 occurs through binding to K48 and K63-linked chains and contributes to proteasomal degradation of ubiquitinated proteins (Chai et al., 2004; Winborn et al., 2008; Wang et al., 2012). *In vivo* findings corroborated the role of Atx3 as a deubiquitinating enzyme (DUB). The characterization of a knockout mouse model for *ATXN3* showed that the lack of this protein led to a notable increase in levels of ubiquitinated proteins in animals brain (Schmitt et al., 2007). Besides its function as a DUB, Atx3 was shown to target substrates for proteasomal degradation through complexation with the valosin-containing protein or ATPase p97 (VCP/p97) and with the human homologs of the yeast DNA repair protein Rad23 A and B (HHR23A/B). The VCP/Atx3 and HHR23A/B/Atx3 conjugations function in shuttling polyubiquitinated proteins for degradation in the ubiquitin proteasome system (Doss-Pepe et al., 2003). Additionally, the VCP/Atx3 complex has been shown to regulate endoplasmic reticulum-associated degradation (ERAD), through interaction with endoplasmic reticulum (ER) components, controlling the exportation to the cytosol and degradation by the proteasome of misfolded proteins and unassembled complex constituents (Wang et al., 2006; Zhong and Pittman, 2006). Likewise, Atx3 has been linked to other functional roles in protein quality systems, such as the formation of aggresomes. These perinuclear inclusions contribute to the maintenance of cellular proteostasis, as they assemble when the UPS is compromised or saturated (Kopito, 2000; Markossian and Kurganov, 2004). Wild-type Atx3 was reported to regulate aggresome formation, co-localizing also with aggresome and preaggresome like particles (Burnett and Pittman, 2005). Moreover, Atx3 was shown to interact with other players in the aggresome organization, including dynein, histone deacetylase 6 (HDAC6), protein linking

IAP to the cytoskeleton (PLIC1) and microtubules (Burnett and Pittman, 2005; Heir et al., 2006; Mazzucchelli et al., 2009).

The interaction of Atx3 with cytoskeleton constituents, dynein, and microtubule-associated protein 2 (MAP2), clued on a possible role of Atx3 in the organization of the cytoskeleton. In fact, it was observed in human and cell lines that the absence of Atx3 led to morphological and structural alterations such as: rounder shape; disorganization of microtubule, microfilament and intermediate filament networks; cell-extracellular matrix connection loss accompanied by reduced levels of talin and α1 integrin subunit expression (Rodrigues et al., 2010). In the specific case of myogenesis of mouse embryos, silencing of Atx3 resulted in immature cytoskeleton, compromising the differentiation of myoblasts into muscle fibers. These alterations occurred due to Atx3 stabilization of α5 integrin subunits levels in a DUB activity-dependent manner, repressing the degradation of this protein via proteasome (do Carmo Costa et al., 2010).

Other studies inferred the involvement of Atx3 in the transcription process, most likely as a transcriptional co-repressor (Li et al., 2002). Atx3 was predicted to have two independent co-repressor activities. First, Atx3 inhibits transcription through C-terminal domain interaction with the major histone acetyltransferases: cAMP-response element binding (CREB)-binding protein (CBP); p300; and p300/CREBBP associated factor (PCAF) (Li et al., 2002). Second, Atx3 inhibits p300-mediated histone acetylation and promotes histone deacetylation, which could result in transcriptional repression, through N-terminal domain interaction with histone deacetylase (HDAC3) and nuclear receptor co-repressor 1 (NCOR1) (Evert et al., 2006). Posteriorly, Araujo and collaborators reported a role of Atx3 in modulating transcriptional activation of manganese superoxide dismutase 2 gene (*SOD 2*). In response to oxidative stress, Atx3 and the forkhead box (FOXO) transcription factor FOXO4 are recruited to the nucleus, concomitantly bind to *SOD2* gene promoter and increase the expression levels of the antioxidant enzyme SOD2 (Araujo et al., 2011).

In summary, studies exploring Atx3 biochemical characteristics and interactions suggested that this protein has been mainly linked to three biological processes: (i) protein quality control systems, including the ubiquitin-proteasome pathway, ERAD and aggresome assembly; (ii) cytoskeleton organization and myogenesis; and (iii) transcriptional regulation (Fig. 1.4).

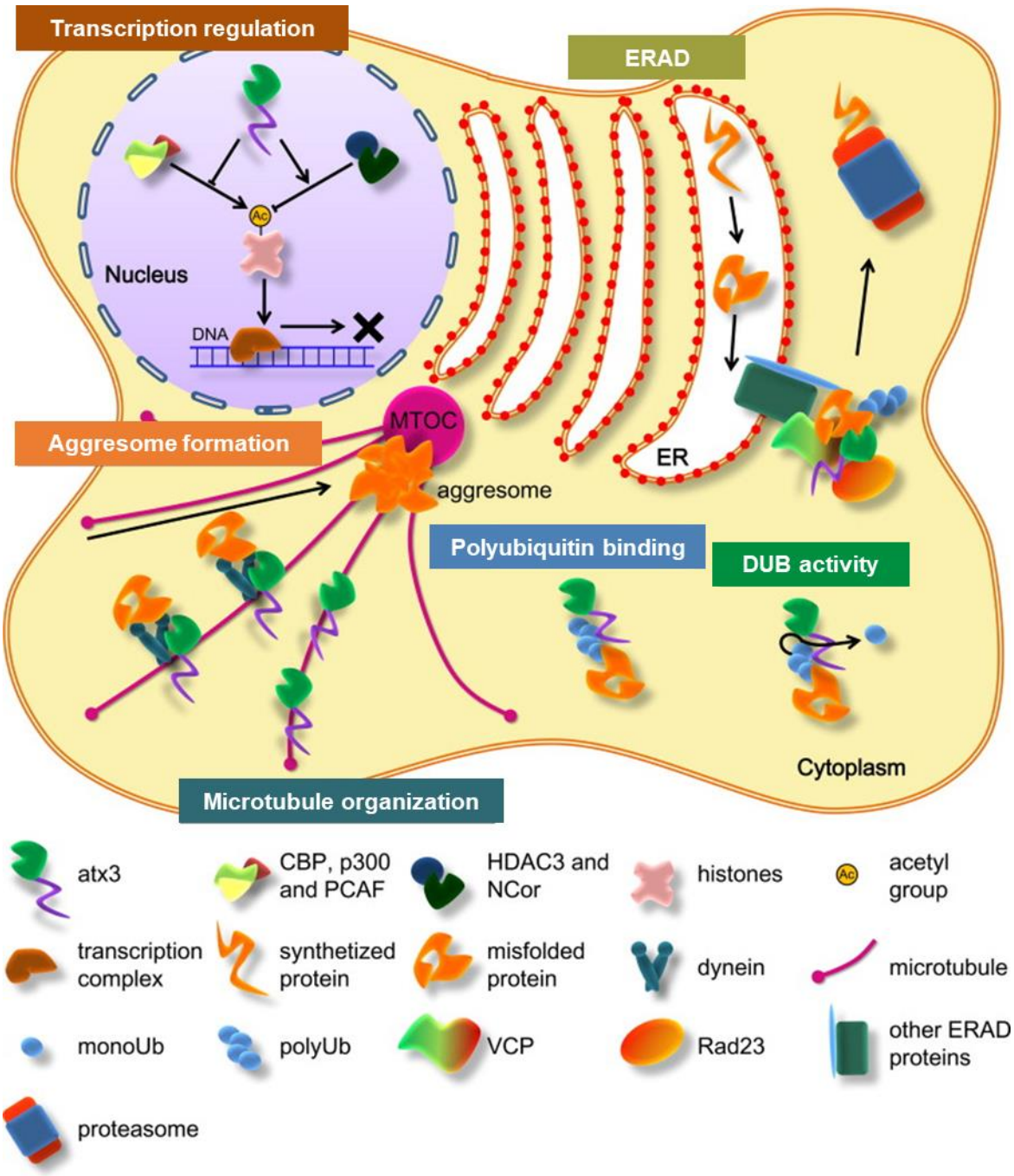

Fig. 1.4. **Representation of Atx3 proposed physiological roles and reported interactions**. Atx3 exhibits deubiquitinase (DUB) activity and binds to and edits polyubiquitinated chains from misfolded proteins for ubiquitin-proteasome clearance. Atx3 conjugates with VCP and Rad23, shuttling ubiquitinated substrates for proteasome and regulating misfolded proteins degradation by ERAD. Atx3 interacts with cytoskeleton components (dyneins and microtubules), interfering with aggresome formation and cytoskeleton organization processes. Atx3 interacts with transcription coactivators (CBP, p300 and PCAF) and corepressors (histones and HDAC3 and NCOR) being implicated in regulation of the transcriptional pathway. (Adapted from Matos et al., 2011).

1.3.5 SCA3 animal models

Although neuroimaging techniques and histological analyses of post-mortem brain samples provided diverse insights into the degeneration process of SCA3 disease, several aspects of pathogenic mechanisms cannot be studied in human patients. Thus, the development and characterization of disease models is an essential tool to investigate the pathophysiology behind SCA3 disorder and new potential therapeutic targets that could be effective in treating affected patients. Though most commonly used model organism contain an endogenous orthologue of the human *ATNX3* gene, polyQ repeats beyond a pathogenic threshold occurring in non-human organism have not been described so far (Matos et al., 2011). So, the generation of SCA3 disease models could be mediated by transfection with a viral construct, transgenic development approaches or by integration of an expanded polyQ stretch in the endogenous *ATXN3* orthologue (knock-in models). While simple organisms like *C. elegans* and *Drosophila* have been useful for screening studies and for the identification of pathogenic events, mammalian models like *Mus musculus* resemble major SCA3 human disease traits and allow the validation of mechanisms and new therapeutic approaches. The diverse models created to study SCA3 disease and the strategies used are extensively reviewed elsewhere (Schmidt and Schmidt, 2018; Cendelin et al., 2021).

In 2002, Cemal and co-workers generated a mouse model using a yeast artificial chromosome (YAC) spanning human full-length *ATNX3* gene including all the regulatory elements (Cemal et al., 2002). Several transgenic lines were described, including a control line with 15 CAG (SCA3-Q15) repeats and a mutant line carrying an expansion of 84 CAGs (SCA3-Q84). Motor function analysis revealed that mutant transgenic mice presented ataxic gait, tremors, hypoactivity, clasping and loss of weight. Moreover, neuropathological alterations included cell loss in diverse brain regions also affected in human disease, such as pons, deep cerebellar nuclei, and cerebellum, as well as the presence of mutant Atx3 intranuclear inclusions.

A different transgenic mouse model expressing a truncated form of human *ATXN3* gene with 69 CAG repeats and under the expression of Purkinje cell specific promoter L7 (SCA3-Q69) was developed by Torashima and colleagues

in 2008. This transgenic model manifests severe motor impairments as early as 3 weeks of age, including decreased performance in motor coordination tests. Neuropathological characterization showed severe cerebellar atrophy, accompanied with the presence of mutant Atx3 aggregates and loss of Purkinje cells.

On the other hand, the development of SCA3 disease mouse models using lentiviral vectors (LVs), as a fast alternative to the transgenic and knock-in approaches, have been described. Alves and co-authors used LVs to express mutant Atx3 in different brain regions of rat (Alves et al., 2008b). Only after 4 weeks of LVs expression, it was observed the presence of the typical mutant protein inclusions. Moreover, several signs of degeneration, including the loss of neuronal markers and cell death, were also detected. Posteriorly, the same research group used a similar strategy to develop a lentiviral mouse model with cerebellar pathology, which manifested motor incoordination and an ataxic gait (Nóbrega et al., 2013a). Thus, animal models based on lentiviral approaches represent several advantages including the use of adult mice, reduced costs comparing to the generation and maintenance of a transgenic model and the possibility to study pathology in specific tissues.

Overall, the development of mouse models has provided large insights into SCA3 pathogenesis, while also allowing assessment of novel potential targets and its limitations in experimental therapy.

1.3.6 Pathogenic mechanisms and involved pathways

The genetic cause behind SCA3 is well established, nonetheless the complete events underlying the molecular pathogenesis are still unclear. In fact, several cellular mechanisms and pathways were reported to be involved in SCA3 pathogenesis and are discussed in this section (Fig. 1.5).

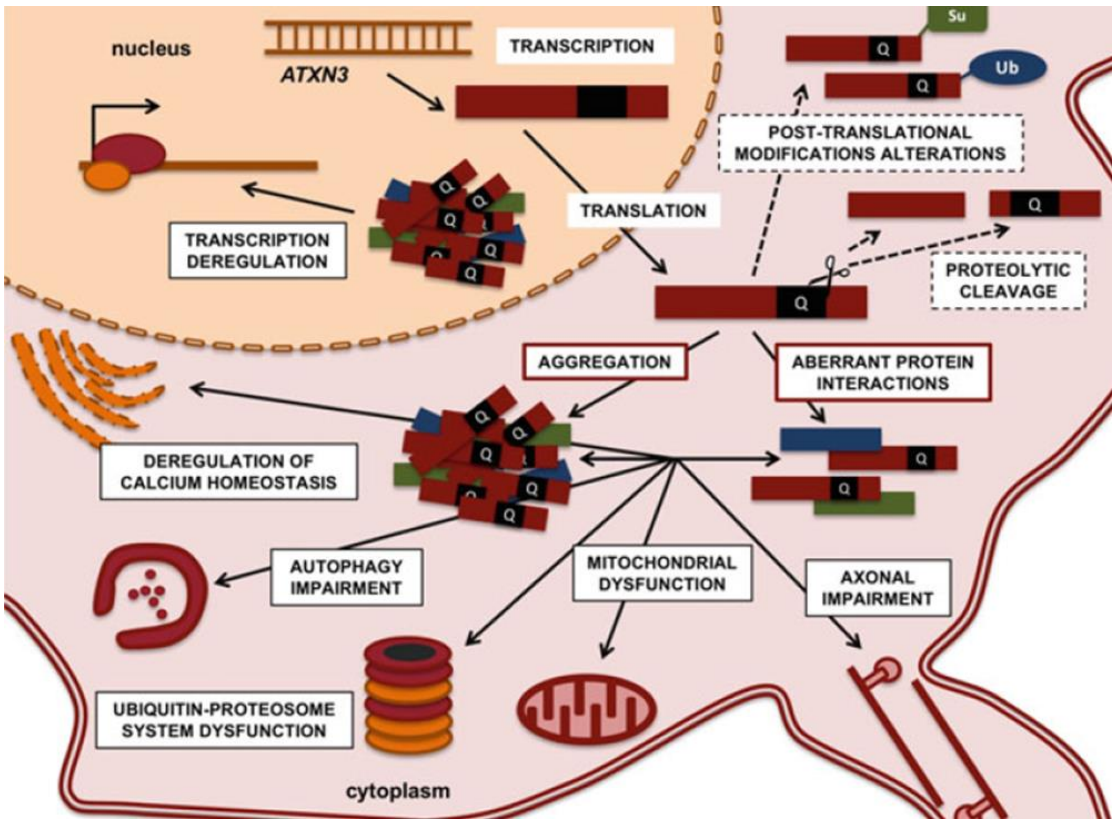

Fig. 1.5. **Cellular mechanisms and pathways involved in SCA3 pathogenesis**. Several molecular events have been put forth as potential toxic mechanisms underlying SCA3 pathogenesis, including induced-toxicity by mutant Atx3 aggregation, proteolytic cleavage of polyQ-expanded Atx3, aberrant protein interactions, protein clearance systems failure, mitochondrial dysfunction, oxidative stress, axonal transport impairments, calcium dysregulation, transcriptional deregulation, and post-translational modifications defects. (Adapted from Nóbrega & Pereira de Almeida, 2018).

1.3.6.1 PolyQ expansion-induced toxicity

The presence of mutant polyQ-expanded aggregates inside neuronal cells of affected brain areas is a neuropathological hallmark of SCA3, and of the other PolyQ diseases (Paulson et al., 1997b; Schmidt et al., 1998). *In vitro* studies showed that wild-type Atx3 form has already an intrinsic predisposition to aggregate. This aggregation is a one-step process, which is induced by self-

association of the protein domain JD into dimers, independently of the polyQ tract. Posteriorly, the dimers assemble into spheroidal oligomers followed by formation of SDS-soluble elongated fibrils, resembling amyloid-like fibrils (Ellisdon et al., 2006; Masino et al., 2011). On the other hand, expanded-Atx3 aggregation goes through a two-stage process. Although displaying fastest aggregation kinetics, the first step is like normal Atx3 and involves the formation of SDS-soluble fibrils. The second phase consists in generation of SDS-insoluble aggregates and depends on the polyQ segment (Ellisdon et al., 2006). Herein, it occurs glutamine side-chain hydrogen bonding of the polyQ expansion, leading to SDS-insolubility (Natalello et al., 2011). Therefore, Atx3 conformational alterations are not only induced by the polyQ tract but also by intrinsic propensity of the protein to misfold, resulting in irreversible and insoluble aggregates (Ellisdon et al., 2007). Although Atx3 is preferentially a cytoplasmic protein, the pathological inclusions are mainly found in the nucleus of specific neuronal populations (Paulson et al., 1997b). However, the mechanisms through which mutant Atx3 aggregates cause cellular toxicity and neuronal death remains uncertain. In fact, there is a controversial debate among the scientific community about whether aggregation is sufficient to cause cell degeneration (Sisodia, 1998; Michalik and Van Broeckhoven, 2003). A study on a transgenic mouse model resembling late onset SCA3 disease, demonstrated that appearance of intranuclear aggregates occurred at an advanced age (around 18 months old), while behavioral and motor alterations were observed between the first months and 12 months of age (Boy et al., 2010). This study supports the claim that neuronal dysfunction precedes the formation of nuclear inclusions. Contrastingly, Bichelmeier et. al. reported that nuclear localization of mutant Atx3 is necessary for disease pathogenesis and symptoms manifestation. This hypothesis is based in a different SCA3 transgenic mouse model, revealing that mice expressing mutant Atx3 directed to the nucleus showed pronounced neuropathological inclusions and earlier death, while mice expressing mutant Atx3 attached to a nuclear export signal developed a milder phenotype, with fewer protein aggregates (Bichelmeier et al., 2007). Additionally, it was noted that mutant Atx3 aggregates recruit several other key proteins, such as chaperones, ubiquitin, proteasomal players and transcription co-activators (Chai et al., 1999a, 2001; McCampbell et al., 2000). These observations suggest that polyQ-expanded Atx3

acquires a toxic gain-of-function, interfering with numerous cellular pathways and processes, which might be depleted of crucial participants. Nevertheless, further studies are required to elucidate the exact cascade of pathologic events triggered by mutant Atx3.

1.3.6.2 Proteolytic cleavage

Multiple lines of evidence imply that proteolytic cleavage of polyQ-expanded proteins contributes to disease pathogenesis, commonly referred as the toxic fragment hypothesis (Ferrigno and Silver, 2000; Matos et al., 2017). In the case of SCA3, a study reported that the expression of polyQ expanded Atx3 fragments increases aggregation and cellular toxicity, whereas no pathologic alterations were found upon expression of full-length protein form (Ikeda et al., 1996). In this line, a mutant Atx3 putative-cleavage fragment was detected in a transgenic mouse model and post-mortem brain samples of SCA3 affected individuals. Moreover, the overexpression of this Atx3 fragment above a critical concentration, resulted in cellular cytotoxicity (Goti et al., 2004). Altogether, these studies seem to support a role of mutant Atx3 proteolysis in SCA3 disease progression.

The proteolytic cleavage of mutant Atx3 has been shown to occur either via caspases or via calpains proteases. Wellington and collaborators demonstrated that both caspase-1 and caspase-3 originated Atx3 proteolytic products, although polyQ-expanded Atx3 was preferentially cleaved by caspase-1 (Wellington et al., 1998). Through site-directed mutagenesis assays, a cluster of aspartate residues inside the UIM2 motif were mapped as a major cleavage site in Atx3 protein (Berke et al., 2004). Diversely, calpains were also suggested to cleave Atx3 in mouse neuroblastoma cells (Haacke et al., 2007) and in SCA3 patient induced pluripotent stem cell (iPSC)-derived neurons (Koch et al., 2011). Both studies showed that calpain proteolytic activity generated detergent-insoluble aggregates, while this process could be prevented by calpain inhibition. Hübener and colleagues further clarified that Atx3 is a substrate of calpain-1 and calpain-2 (Hübener et al., 2013). Nevertheless, elucidating which exact proteases trigger the proteolytic cleavage of mutant Atx3 could shed light on disease pathogenic events and identify potential therapeutic targets.

1.3.6.3 Aberrant Protein Interactions

Several studies have pointed out the importance of abnormal interactions of polyQ-expanded Atx3, with its native protein partners or novel interactors, in SCA3 disease pathogenesis. As already mentioned, more than 40 proteins have been so far identified as Atx3 interactors (Costa and Paulson, 2012). As Atx3 is implicated in several signaling pathways, altered and abnormal protein interactions could help explaining the selective neuronal degeneration found in the disease (Takahashi et al., 2010). For example, wild-type Atx3 is found in nuclear inclusions of SCA2 patients brain, while normal Atx2 is observed in mutant aggregates present in SCA3 individuals (Uchihara et al., 2001b). Moreover, polyQ-expansion induces altered interactions between Atx3 and CHIP and parkin proteins, causing depletion of these neuroprotective proteins ins SCA3 disease (Costa and Paulson, 2012). Future studies tackling wild-type and mutant Atx3 functions in specific protein interactions might help understanding cellular dysfunction and death upon polyQ expansion.

1.3.6.4 Ubiquitin-Proteasome System and Autophagy Impairment

Protein quality control and clearance systems, such as ubiquitin-proteasome system (UPS) and autophagy pathways, are highly important to maintain cellular homeostasis, as they degrade misfolded and insoluble aggregate-prone proteins (Williams et al., 2006; Kleiger and Mayor, 2014). Strikingly, either UPS, autophagy and molecular chaperones have been involved in refolding and in the clearance of mutant Atx3 (Chai et al., 1999a; Ravikumar et al., 2002; Berger et al., 2006). However, several studies reported failure of these systems in SCA3 disease. In earlier disease stages, polyQ-expanded Atx3 activates cellular stress mechanisms, leading to higher levels of molecular chaperones. These chaperones perform a neuroprotective role by reducing mutant Atx3 misfolding and aggregation (Chai et al., 1999a; Warrick et al., 1999; Bilen and Bonini, 2007; Chou et al., 2008). As the disease progresses, it is observed a downregulation of heat-shock chaperones HSP70, HSP40 and HSP27 in SCA3 cellular and transgenic mouse models, suggesting dysfunction of neurons stress-response induced by mutant Atx3 (Huen and Chan, 2005; Chou et al., 2008; Chang et al.,

2009). Likewise, other studies support a role of autophagic impairment in SCA3 pathogenesis. This pathway has been implicated in clearing preferentially mutant Atx3 form rather than wild-type protein (Menzies et al., 2010). However, analysis of post mortem brain samples revealed an abnormal accumulation of autophagic markers, including p62, Atg16L and LC3B in SCA3 patients tissue (Nascimento-Ferreira et al., 2011). Studies using *in vivo* models of SCA3 disease also reported a higher number of p62-positive aggregates that co-localized with ubiquitinated mutant Atx3 inclusions. In latter disease stages, deposition of autophagosomes was observed in neurons cytoplasm (Nascimento-Ferreira et al., 2011). Moreover, the autophagic marker beclin-1, required for the autophagic function, was shown to be decreased in SCA3 patients fibroblasts and transgenic mice striatum, as well as shown to co-localize with nuclear polyQ-expanded Atx3 aggregates (Nascimento-Ferreira et al., 2011). Other authors also support that the accumulation of misfolded proteins can overload or prevent UPS activity, worsening dysfunction of cellular mechanisms (Bence et al., 2001). Therefore, the failure of protein clearance and degradation systems is consistent with accumulation of mutant Atx3 in SCA3 disease, supporting a role in pathogenic events.

1.3.6.5 Mitochondrial Dysfunction and Oxidative Stress

Mitochondrial function defects have been described for several polyQ diseases, including HD (Orr et al., 2008), SBMA (Beauchemin et al., 2001), DRLPA (Lodi et al., 2000) and SCA1 (Kish et al., 1999). Mitochondrial-related alterations have also been observed in SCA3, when Matsuishi et. al. reported a metabolic disruption in the cerebrospinal fluid of SCA3 affected individuals (Matsuishi et al., 1996). After, *in vitro* studies on SCA3 models showed that the expression of polyQ-expanded Atx3 results in increased mitochondrial-mediated cell death, via apoptosis and reduced mitochondrial DNA copy number (Tsai et al., 2004; Chou et al., 2006; Yu et al., 2009). Later, the analysis of SCA3 transgenic mouse blood and brain samples showed mitochondrial DNA damage (Ramos et al., 2015). Additionally, some authors suggested that cells expressing mutant Atx3 are more susceptible to oxidative stress. Araujo and collaborators found that longer polyQ tracts in the Atx3 structure reduces its ability to activate *SOD2* transcription,

mediated through interaction with FOXO4, an important player in mitochondrial reactive oxygen species clearance (Araujo et al., 2011). As well, the levels of the antioxidant HSP27 were found downregulated in mutant Atx3-expressing cells (Chang et al., 2009). Hence, all these findings suggest that mitochondrial function and oxidative stress defense mechanisms might be compromised in SCA3 disease.

1.3.6.6 Axonal Transport Impairments

In SCA3 disease, the presence of insoluble mutant Atx3 aggregates is mainly found inside the nucleus of neuronal cells. However, Seidel and colleagues detected widespread distribution of ubiquitin- and p62-positive mutant aggregates in axons of nerve tracts undergoing neurodegeneration (Seidel et al., 2010). This data implies that mutant Atx3 might interfere with axonal transport activity, and this might contribute to neuronal degeneration. This hypothesis is supported by observations in *C. elegans* and *Drosophila* models for SCA3, in which were found that mutant Atx3 deposits promote swelling and abnormal branching of neuronal processes, deteriorating synaptic transmission (Gunawardena and Goldstein, 2005; Khan et al., 2006). The findings connecting axonal transport impairment to SCA3 pathogenesis are in line with motor neuropathy or neuronopathy observed in affected patients (Klockgether et al., 1999).

1.3.6.7 Intracellular Ca^{2+} Homeostasis Disruption

Calcium ions (Ca^{2+}) are signaling molecules responsible for regulating a wide range of biological functions in eukaryotic cells. Particularly in neurons, Ca^{2+} homeostasis is crucial for several functions, including neurotransmitters release, synaptic plasticity, gene expression and neurite outgrowth (Zhivotovsky and Orrenius, 2011). In line with these important functions in neurons, multiple evidence suggest that Ca^{2+} dysregulation plays an important role in neurodegenerative diseases, including polyQ pathologies (Pchitskaya et al., 2018). Ionic homeostasis alterations have also been reported in SCA3 disease. Specifically, the polyQ-expanded protein, but not normal Atx3, was described to bind type 1 inositol 1,4,5-trisphosphate (InsP3R1) intracellular calcium channel

present in the ER, enhancing its susceptibility to be active by InsP3 and potentiating Ca^{2+} release from ER components (Chen et al., 2008). Pellistri and colleagues also reported that Atx3 oligomers interact with the lipid raft ganglioside GM1, glutamatergic receptors and voltage dependent calcium channels, resulting in increased influx of Ca^{2+} ions inside cells of the cerebellar granular layer (Pellistri et al., 2013). Consequently, the excess of intracellular calcium ions could contribute to mitochondrial dysfunction, oxidative stress, cytoskeletal disorganization and activation of calpains, thus promoting cell toxicity and death (Zhivotovsky and Orrenius, 2011).

1.3.6.8 Transcriptional Dysregulation

Several reports demonstrated that transcriptional factors are sequestered into intranuclear inclusions of expanded polyQ proteins, suggesting a role of transcriptional dysregulation in disease pathogenesis (McCampbell et al., 2000; Yamada et al., 2000). In SCA3 disease, the presence of transcription regulators, as TATA-binding protein (TBP) and CBP, in mutant Atx3 nuclear aggregates was also reported (Chai et al., 2001). A pathogenic altered transcription role in SCA3 is further reinforced by atypical interactions of mutant Atx3, which have been shown to compromise its function as transcriptional regulator. It was shown that, the Atx3 C-terminus bearing the pathological polyQ stretch binds more efficiently to the transcriptional coactivators CBP, p300 and PCAF, compared to wild-type Atx3, indicating a pathological inhibition of the transcription process (Li et al., 2002). On the other hand, mutant expanded Atx3 exhibits aberrant DNA and chromatin binding, decreasing its ability to deacetylase histones and repress transcription (Evert et al., 2006). Moreover, mutant Atx3 displays reduced capability to activate *SOD2* gene transcription, via interaction with FOXO4 factor, resulting in increased cellular vulnerability to oxidative stress (Araujo et al., 2011). Therefore, taking into consideration the aberrant interactions of mutant Atx3 with transcriptional components, alterations in gene expression levels are expected. In this line, transcriptomic analysis of a SCA3 cell and mouse models revealed a downregulation of genes involved in glutamatergic neurotransmission, intracellular calcium signaling/mobilization, $GABA_{A/B}$ receptor subunits, HSPs, and transcription factors involved in neuronal survival and differentiation

pathways. On the contrary, genes associated with neuroinflammation and cell death were found to be upregulated (Evert et al., 2001, 2003; Chou et al., 2008). Furthermore, microRNA (miRNA) biogenesis and machinery were described to be downregulated in different SCA3 disease models (Carmona et al., 2017). This study also reported that miR-9, miR-181a, and miR-494 miRNAs had their expression profile altered in SCA3 postmortem brain samples. The fact that miRNAs negatively regulate post-transcription of ATXN3 mediated by interaction with 3'UTR region, strengthens the hypothesis of transcriptional dysfunction in SCA3.

1.3.6.9 Post-translational Modifications Defects

Few works reported a toxic role of irreversible post-translational modifications of mutant Atx3 in the pathogenesis of SCA3 disease. A study showed that conversion of serine 256 to alanine residue prevented Atx3 phosphorylation by glycogen synthase kinase 3β, leading to increased aggregation of polyQ-expanded Atx3 (Fei et al., 2007). Moreover, Matos and colleagues reported that serine 12 plays a role in pathogenesis of expanded Atx3 and that phosphorylation of this residue reverted the loss of dendrites and synapses observed (Matos et al., 2016). The ubiquitination of Atx3 has also been described to induce post-translational alterations in both wild-type and mutant forms. *In vitro* studies revealed that enzymatic activity of both Atx3 forms were equally activated by ubiquitination. However, an increased ubiquitination of polyQ-expanded Atx3 was observed in brain lysates of SCA3 transgenic mice (Todi et al., 2009). Additionally, Atx3 protein can be modified by SUMO-1 at specific lysine sites, a process called SUMOylation. A study demonstrated that covalent bonding of SUMO at lysine 356 of Atx3 promotes decreased aggregation of ataxin-3. Besides, this post-translational alteration led to decreased formation of mutant Atx3 inclusions in cortical neurons (Almeida et al., 2015). While these studies show that post-translational modifications might impact the SCA3 pathogenesis, further studies are required to fully understand the possible implications of these modifications in the disease.

1.3.7 Therapeutic perspectives for SCA3

SCA3 is a highly debilitating and fatal neurodegenerative disease that progresses rapidly resulting in severe consequences for affected patients and their families. Although huge efforts have been made searching for a disease-modifying target/approach, currently there are no therapies able to stop or delay disease progression, which leads to premature death of SCA3 patients (Matos et al., 2019). Several approaches have been researched in the last years and are outlined in the next pages (Fig. 1.6).

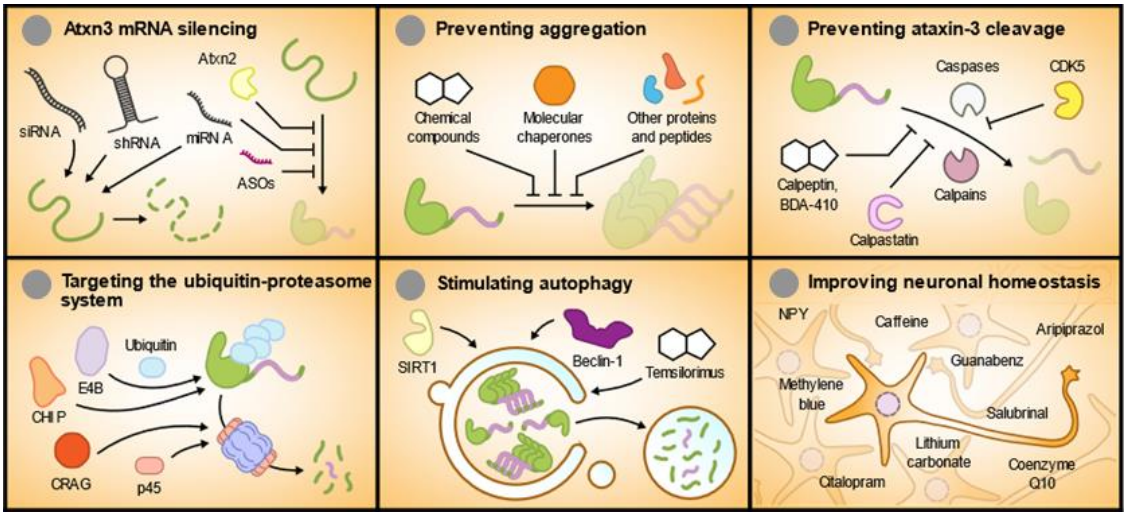

Fig. 1.6. **Potential therapeutic strategies developed for SCA3 targeting different pathogenic pathways**. Several approaches targeting the different pathways proposed to be involved in SCA3 pathogenesis have been tested, such as silencing the mutant *ATXN3* mRNA; preventing mutant Atx3 protein aggregation, preventing Atx3 proteolytic cleavage; enhancing UPS and autophagy clearance systems; and improving neuronal homeostasis and survival. Abbreviations: ASOs, antisense oligonucleotides; Atxn2, ataxin-2; Atxn3, ataxin-3; CDK5, cyclin-dependent kinase5; CHIP, C-terminus of 70 kDa heat-shock protein-interacting protein; CRAG, collapsin response mediator protein-associated molecule-associated GTPase; miRNA, microRNA; mRNA, messenger RNA; NPY, neuropeptide Y; RNA, RNA interference; shRNA, short hairpin RNA; siRNA, small interfering RNA; SIRT1, sirtuin-1. (Adapted from Matos et al., 2019).

1.3.7.1 Targeting mutant ATXN3 RNA

As CAG-expanded RNA is a precursor of mutant Atx3 translation, several strategies targeting the mutant RNA or molecular players involved in RNA processing have been investigated. In 2008, Alves and collaborators took advantage of a single nucleotide polymorphism that is present in 70% of SCA3

affected individuals and designed a short hairpin RNA (shRNA) that specifically targeted this region, resorting to LVs as delivery system (Alves et al., 2008a). The allele-specific silencing of mutant Atx3 resulted in a significant reduction of the neuropathological abnormalities observed in a striatal lentiviral mouse model of SCA3. Posteriorly, the same group assessed the shRNA therapeutic potential in SCA3 transgenic mice and in a cerebellar lentiviral mouse model, which mimics motor deficits and cerebellar neuropathological alterations observed in SCA3 patients (Nóbrega et al., 2013b, 2014). The cerebellar injection of LVs encoding for the shRNA sequence ameliorated the motor performance and the neuropathological deficits in SCA3 mice, demonstrating the potential of RNA silencing as a therapeutic approach for this disease. Later, a small interfering RNA (siRNA) targeting mutant Atx3, was administered in a SCA3 striatal lentiviral model and in a SCA3 transgenic mouse model, using a non-viral nanoparticle delivery approach. The injection of the stable nuclei acid lipid particles (SNALPs), encapsulating the siRNA, led to efficient reduction of mutant Atx3 levels, decreasing the neuropathology and motor function deficits associated with the SCA3 disease.

Several other authors developed strategies aiming to silence mutant expanded RNA. In 2011, Hu et. al. designed peptide nuclei acid (PNAs), a duplex RNA species in which nucleotide bases are linked by an amide backbone, complementary to CAG repeats. The administration of this PNA was evaluated in fibroblast cell lines derived from SCA3 patients, leading to the inhibition of mutant *ATXN3* gene expression, without causing toxicity or affecting the levels of other genes with CAG repeats (Hu et al., 2009). Later, Liu and collaborators showed that single-stranded silencing RNAs (ss-siRNAs) are allele-selective inhibitors of Atx3 expression by blocking translation or affecting alternative splicing, depending on ss-siRNA design used (Liu et al., 2013). Although these approaches were successful in reducing mutant Atx3 levels, they were only assessed in *in vitro* models. The silencing of mutant Atx3 RNA was also achieved by development of antisense oligonucleotides (ASOs), a short single strand of chemically modified oligonucleotides that bind mRNA, mediating its cleavage by RNase H. The ASOs administration resulted in reduced mutant Atx3 levels in two different transgenic mouse models of SCA3, rescuing molecular, pathological, electrophysiological and behavioral disease hallmarks (Moore et al., 2017;

McLoughlin et al., 2018). Another study in a mouse model found that the administration of an antisense oligonucleotide (ASO) mediating exon skipping, did not altered Atx3 functions, and did not report toxic effects due to the generation of a new truncated protein (Evers et al., 2013). In a subsequent study, the same strategy proved to be successful in reducing insoluble Atx3 levels and its nuclear accumulation in a transgenic mouse model of SCA3 (Toonen et al., 2016). Approaches aiming to target the microRNA pathway were as well evaluated in cellular and *in vivo* models of SCA3 disease (Bilen and Bonini, 2007; Do Carmo Costa et al., 2013; Rodríguez-Lebrón et al., 2013; Huang et al., 2014; Carmona et al., 2017). These approaches were successful in reducing Atx3 protein levels leading to the mitigation of neurodegeneration observed in the disease models, while rescue of motor deficits were not reported.

1.3.7.2 Targeting mutant Atx3 aggregation

Several therapeutic strategies attempting to decrease or stop aberrant protein aggregation have also been studied, as formation of insoluble multiprotein neuronal inclusions are a hallmark of SCA3. Numerous compounds have been shown to prevent fibrillogenesis and aggregation of expanded Atx3, decreasing toxicity and cell death in SCA3 cellular, *C. elegans*, and *Drosophila* models. These include chemical compounds (epigallocatechin-3-gallate (Bonanomi et al., 2014); 17-(allylamino)-17-demethoxygeldanamycin (Fujikake et al., 2008); ectoine (Furusho et al., 2005)) and natural aqueous extracts of *Glycyrrhiza inflata* (Chen et al., 2014a) and *Paeonia lactiflora* (Chang et al., 2013). Moreover, a range of molecular targets were demonstrated to be effective in suppressing mutant Atx3 aggregation, including: the polyQ binding peptide QBP1 (Nagai et al., 2003) and the human cytomegalovirus UL97 kinase (Tower et al., 2011). The class of heat shock proteins (HSP), as polyQ protein refolding chaperones have also been widely explored in the context of expanded Atx3 aggregation. A genome-wide screening study for Atx3 modifiers in *Drosophila* reported that chaperones HSP70, HSP40 and HSJ2 decreased Atx3 protein inclusions (Bilen and Bonini, 2007). Cushman-Nick and collaborators also demonstrated that the upregulation of HSP104 reduced toxicity associated with a fragment of the Atx3 C-terminal with expanded polyQ tract, however it had the oppositive effect on the

full-length mutant Atx3 protein (Cushman-Nick et al., 2013). Likewise, the use of drugs that stabilize proteins, termed chemical chaperones, reduced the aggregation process and toxicity in *in vitro* models of SCA3 (Yoshida et al., 2002). Though, the few *in vivo* studies using these molecules showed limited efficacy in ameliorating SCA3 phenotype, as for example the administration of valproic acid (Esteves et al., 2015). More recently, DNAJC8 (Ito et al., 2016), HSPB7 (Wu et al., 2019) and SRCP1, the novel *Dictyostelium* chaperone (Santarriaga et al., 2018), were shown to suppress early polyQ aggregation steps, thus being suggested as potential therapeutic targets for SCA3 disease. In SCA3 mouse models, the presence of expanded Atx3 inside the nuclear compartment was described to be required for symptoms manifestations and to induce more toxicity, as compared to a cytoplasmic localization (Bichelmeier et al., 2007). In line with this, karyopherin alpha 3 (KPNA3) importin proved to be essential in transporting mutant Atx3 to the nucleus. In this line, the downregulation of *KPNA3* in *Drosophila* and mouse models of SCA3, alleviated the neurological phenotype induced by polyQ-expanded Atx3, stressing the importance of nuclear localization to disease pathogenesis (Sowa et al., 2018).

1.3.7.3 Targeting the proteolytic cleavage of Atx3

The presence of toxic polyQ-expanded fragments resulting from the irreversible proteolytic cleavage of mutant Atx3 polypeptide chain, by either caspases or calpains enzymes, has been associated with SCA3 disease (Matos et al., 2017). Therefore, several studies targeting mutant Atx3 proteolysis attempted to reduce generation of polyQ-expanded oligomers and thus prevent neuronal toxicity. The use of an ASOs-mediated exon skipping strategy resulted in the removal of diverse expected cleavage sites in mutant Atx3 protein, preventing the formation of toxic fragment species, although phenotypic alterations were not assessed (Toonen et al., 2017). Additionally, approaches aiming to regulate caspases and calpains levels have also been tested. The cyclin-dependent kinase-5 (CDK5) showed a protective effect against ataxin-3-induced degeneration and toxicity in cellular and *Drosophila* models, by regulating caspase cleavage (Liman et al., 2014). Later, it was also demonstrated that suppression of calpains, mediated by calpeptin, blocked the formation of mutant Atx3 fragments, as well as the

assembly of aggregates (Haacke et al., 2007). Likewise, the administration of calpeptin compound in a SCA3 zebrafish model also proved successful in preventing ataxin-3 fragmentation and in mitigating motor deficits (Watchon et al., 2017). The inhibition of calpain activity as a potential therapeutic approach for SCA3 disease was further strengthen by two pre-clinical studies using SCA3 striatal and cerebellar lentiviral mouse models. Firstly, the authors showed that molecular overexpression of calpastatin, an endogenous calpain repressor, decreased the generation of polyQ-expanded Atx3 oligomers, resulting in lower nuclear aggregation and toxicity (Simões et al., 2012). After, the same group described that oral treatment using the calpain inhibitor BDA-410 compound led to reduced fragmentation of mutant Atx3, suppressing mutant aggregation and preventing cell injury in the lentiviral mouse models (Simões et al., 2014). Overall, preventing generation of toxic mutant Atx3 fragments by impairing proteolytic cleavage could be a promising approach to treat SCA3 disease, however the inhibition of proteases is not a specific strategy and could negatively impact the normal function of other cellular targets.

1.3.7.4 Targeting the ubiquitin-proteasome system and the autophagic pathway

The correct UPS functioning is highly important to maintain cellular proteostasis by clearing and degrading misfolded proteins. An UPS impairment in SCA3 disease was early suggested, as players of the proteasome pathway are found in mutant Atx3 neuronal inclusions (Chai et al., 1999b). Therefore, strategies aiming to enhance UPS activity have been assessed in the context of SCA3 pathology. It was reported that the expression of a ubiquitin chain assembly factor (E4B) in cell lines, induced clearance of polyQ-expanded mutant Atx3, and mitigated the neurodegeneration phenotype in a SCA3 *Drosophila* model (Matsumoto et al., 2004). Moreover, a study demonstrated that augmentation of CHIP levels led to enhanced ubiquitination and posterior degradation of mutant Atx3 protein, decreasing aggregation levels and promoting cell survival in a mouse-derived cell line, while its downregulation speeded disease progression in a SCA3 transgenic mice (Jana et al., 2005; Williams et al., 2009). Likewise, the overexpression of the 19S proteasomal subunit, the ATPase p45, resulted in increased Atx3 degradation rates (Wang et al., 2007). More recently, a pre-

clinical work in a SCA3 *Drosophila* model revealed that downregulation of the shuttling factor Rad23 promoted reduced Atx3-induced cytotoxicity, indicating its potential as therapeutic target for SCA3.

Another key mechanism responsible for the degradation of aggregate-prone proteins, including mutant Atx3, is the autophagic pathway (Menzies et al., 2010). As discussed above, impairments in the autophagic process contributes to the pathogenesis of SCA3 disease, as well as to other polyQ disorders (Cortes and La Spada, 2015). Therefore, several studies extensively explored the potential of autophagic enhancement for the treatment of SCA3. Menzies et. al. revealed that upon administration of temsirolimus, an antagonist of the mammalian target of rapamycin, autophagic levels were increased leading to decreased soluble levels and number of mutant Atx3 aggregates in a transgenic mouse model of SCA3 (Menzies et al., 2010). A previous study from our group demonstrated that the administration of cordycepin activates autophagy, via adenosine monophosphate-activated protein kinase (AMPK) pathway, ameliorating neuropathological and behavior deficits in mouse models of SCA3 and SCA2 diseases (Marcelo et al., 2018, 2021a). Furthermore, other studies also reported beneficial effects of autophagy stimulation using compounds in SCA3 disease models (Silva-Fernandes et al., 2014; Cunha-Santos et al., 2016; Watchon et al., 2017). Furthermore, Nascimento-Ferreira and collaborators investigated the potential of gene therapy to activate autophagy, by overexpressing the autophagic protein beclin-1. The authors observed that beclin-1 overexpression decreased the levels of mutant Atx3, mitigating neuropathological abnormalities in a striatal lentiviral rat model of SCA3 (Nascimento-Ferreira et al., 2011). Posteriorly, the same strategy was evaluated in two SCA3 mouse models, where overexpression of beclin-1 rescued the motor phenotypic alterations characteristics of these models, reinforcing the this autophagic marker as a promising target to treat SCA3 disease (Nascimento-Ferreira et al., 2013). Overall, approaches targeting the protein quality control systems, UPS, and autophagy, showed encouraging results, and emerged as potential therapeutic strategies for SCA3 that should be further explored.

1.3.7.5 Promoting neuronal homoeostasis and protection

Several cell and gene therapy-based studies targeting neuroprotective strategies have also been explored as potential benefic therapeutic approaches for SCA3 disease. In 2015, Duarte-Neves and collaborators demonstrated that the overexpression of neuropeptide Y, using LV-mediated delivery, ameliorated the neuropathological and motor abnormalities in SCA3 lentiviral and transgenic mouse models (Duarte-Neves et al., 2015). Moreover, Nóbrega et. al. revealed that ataxin-2 (Atx2) mRNA and protein levels were decreased in SCA3 patients and animal models. Strikingly, the restoration of Atx2 levels, through LV injection, resulted in reduced levels of mutant Atx3, leading to mitigation of neuropathological deficits and improvement in motor function in different SCA3 mouse models (Nóbrega et al., 2015a). In 2016, Cunha-Santos and colleagues reported a beneficial effect of caloric restriction in a transgenic mouse model of SCA3, resulting in rescued motor behavioral phenotype and neuropathological alterations. This effect was possibly mediated by SIRT1 promoting autophagic activation (Cunha-Santos et al., 2016). Additionally, the use of cellular therapies, such as administration cerebellar neural stem cells or mesenchymal stromal stem cells, alleviated motor deficits and neuropathological alterations in SCA3 cellular and animal models (Mendonça et al., 2015; Oliveira Miranda et al., 2018). Therefore, different neuroprotective approaches based on gene or cell therapies could be promising therapeutic strategies for SCA3 disease, however further pre-clinical and clinical studies addressing toxicity and efficacy are needed.

1.4 Spinocerebellar ataxia type 2

1.4.1 History and epidemiology

Spinocerebellar ataxia type 2 (SCA2) was primarily discovered and described in 9 families native from India by Wadia and Swami in 1971 (Wadia and Swami, 1971). These patients presented pronounced cerebellar ataxia accompanied by other motor symptoms, such as chorea and facial weakness, like those observed in other familial spinocerebellar degenerations, previously described in Europe. Contrary to previous reports, these group of affected individuals showed unusual slow eye movements, leading to the characterization of the disease as “a new form of heredo-familial spinocerebellar degeneration”. Later in 1989, a group of neurologists described a form of dominantly inherited olivopontocerebellar atrophy affecting individuals living in Cuba, with Spanish ancestry (Orozco et al., 1989). These patients also suffered from gait ataxia accompanied by slow saccadic eye movements, clinical hallmarks that are characteristic of SCA2 disease. The classification of both these pathologies as spinocerebellar ataxia type 2 only occurred in 1996, upon discovery of the genetic mutation underlying the disease.

Currently, SCA2 is the world second most common subtype of autosomal dominant cerebellar ataxia (15%), after SCA3 disease (21%), with a worldwide prevalence of 1.5 affected individuals in 100.000 (Bird, 1998; Orphanet, 2021). Global epidemiological analysis revealed that SCA2 has a large geographical distribution across the world, representing the most frequent SCA in specific regions such as Cuba, India, Mexico and southern Italy (Bird, 1998). Particularly, Cuba has the largest prevalence rates with 6.57 cases per 100.000 inhabitants and 28.51 mutation carriers per 100.000 individuals (including patients and preclinical carries), due to a prominent founder effect (Auburger et al., 1990; Velázquez Pérez et al., 2009). Moreover, the highest frequency of normal unstable large alleles, considered reservoirs for mutated alleles, is found in Cuba, giving continuously rise of novel SCA2 cases (Laffita-Mesa et al., 2011, 2014). Within Cuba island, the Holguin province holds the greatest frequency with 40.18 cases and 182.75 carries per 100.000 residents (Velázquez Pérez et al., 2009).

1.4.2 Clinical features

SCA2 has an average disease onset around 35 years old, initiating during adult life as happens for SCA3 and other SCAs disorders (Diallo et al., 2018). However, disease onset is highly variable among SCA2 families, ranging from 2 to 68 years of age, while 25% of the patients have a juvenile onset, presenting clinical manifestations before 22 years (Mederos et al., 2008). As observed for other polyQ diseases, the age of onset of SCA2 is closely dependent on the length of CAG repeats, as longer number of repeats results in earlier and more severe symptomatic manifestations (Klockgether et al., 1998). However, a recent study on the Cuban SCA2 founder population established that genetic modifiers, including DNA repair, mitochondrial fission and oxidoreductase activity, could also affect disease onset age (Figueroa et al., 2017). Several studies in SCA2 Cuban, Spanish and Italian populations revealed that survival rates from birth to death and after disease onset depends on the geographical location and ethnical groups. Hence, longer survival rates are observed in Italy (mean survival of 67 years; mean survival of 25 years from onset) (Antenora et al., 2018), compared to relatively lower survival rates reported in Spain (mean survival of 54 years; mean survival of 17 years from onset) (Infante et al., 2005) and in Cuba (mean survival of 52 years; mean survival of 22 years from onset) (Almaguer-Mederos et al., 2013).

SCA2 patients present a complex picture of motor and non-motor clinical manifestations implying that SCA2 is a multisystem disorder. As observed in SCA3, the clinical hallmark and first presenting symptom in SCA2 is cerebellar gait ataxia, reported in 97% of affected individuals (Cancel et al., 1997). However, SCA2 is characterized by a wide range of progressive motor cerebellar manifestations, including postural tremor, cerebellar dysarthria, dysmetria, and dysdiadochokinesia (Cancel et al., 1997; Geschwind et al., 1997; Filla et al., 1999; Velázquez-Pérez et al., 2011a). Moreover, SCA2 patients might also experience a broad spectrum of non-cerebellar symptoms. The most prominent oculomotor perturbation is the occurrence of slow horizontal saccadic eye movements, detected in 98% of affected patients and defined as a distinct sign of SCA2 disease (Bürk et al., 1999a). The slowing of saccadic movements positively correlates with CAG repeat expansion length (Velázquez-Pérez et al.,

2004), and gradually deteriorates over disease progression along with saccadic latency and dysmetria (Rodríguez-Labrada et al., 2011, 2016). SCA2 patients also present reduced saccadic pursuits, reduced vestibulo-ocular reflex and ophthalmoplegia (Bürk et al., 1999a; Stephen and Schmahmann, 2019). Other non-motor signs present in SCA2 clinical condition include: (1) corticospinal tract dysfunction symptoms (extensor plantar response, hyperreflexia and spasticity); (2) motor neuron degeneration signs (fasciculations and distal amyotrophy); (3) extrapyramidal features (resting tremor, dystonia, myoclonus, rigidity, chorea/dyskinesia, parkinsonism); (4) peripheral neuropathy (hypo/areflexia, paresthesia, hypoesthesia, hypopallesthesia, muscle atrophy and distal weakness); (5) muscle cramps (lower limbs, abdominal and trunk muscles); (6) sleep disorders (restless legs syndrome, periodic legs movements syndrome, rapid eye movement, insomnia, and nocturnal leg cramps); (7) cognitive deficits (early frontal-executive dysfunctions, verbal memory impairments and attentional deficits; (8) psychiatric symptoms (depression, anxiety, psychosis); (9) autonomic dysfunction (urogenital, cardiovascular, gastrointestinal and thermoregulatory impairment, nocturia, pollakiuria, dysphagia and constipation); and (10) olfactory dysfunction (Orozco et al., 1989; Bürk et al., 1999b; Sánchez-Cruz et al., 2001; Reynaldo-Armiñán et al., 2002; Velázquez-Pérez et al., 2011a, 2011b, 2017; Tuin et al., 2006; Velázquez-Pérez et al., 2006; Schmitz-Hübsch et al., 2008; Takao et al., 2011; Linnemann et al., 2015; Lo et al., 2016).

1.4.3 Neuropathology

The severe features observed in SCA2 patients are usually the result of a widespread neurodegenerative process (Table 1.3). Macroscopic analysis of *post-mortem* brain samples showed an overall brain size shrinkage accompanied by substantial atrophy of the cerebellum, brainstem, frontal, temporal and occipital lobes, medial and inferior cerebellar peduncles and cranial nerves, midbrain *substantia nigra* whiteness and diminished cerebral and cerebellar white matter (Scherzed et al., 2012; Seidel et al., 2012). Histological findings in the cerebellum revealed premature and substantial loss of neurons in the cerebellar Purkinje cell layer, as well as diminished dendritic arborizations and axonal abnormal shape remodeling. Moreover, a significant degeneration is observed in the brainstem, including neuronal loss in inferior olive, pontine and other pre-cerebellar brainstem nuclei, along with a marked decrease of neuronal cells in the substantia nigra. Also, a widespread degeneration is noticed in the cerebral cortex, basal forebrain, thalamus and spinal cord (Estrada et al., 1999; Gierga et al., 2005; Rüb et al., 2007; Seidel et al., 2012). Neuroimaging techniques provided additional insight of the neurodegenerative process in SCA2 patients' brain. Voxel-based morphometry demonstrated a widespread pattern of brain atrophy, with substantial volume loss observed in: (1) infratentorial structures, such as cerebellar hemisphere, vermis, pons, mesencephalon and thalamus; and (2) supratentorial regions, including right orbitofrontal cortex, right temporomesial cortex and primary sensory motor cortex (Brenneis et al., 2003). Furthermore, proton magnetic resonance spectrometry revealed decreased NAA levels in the pons and cerebellar hemispheres (Chen et al., 2014b).

Table 1.3: **Review of central nervous systems affected during the neurodegenerative process of SCA2 and principal clinical consequences.**

Affected central nervous pathway	Major lesions	Associated clinical manifestations
Cerebellothalamocortical motor loop	Cerebellar cortex and nuclei; pontine nuclei; thalamic ventral lateral nucleus; Betz pyramidal cells of the primary motor cortex	Ataxia; dysdiadochokinesia; dysarthria; dysmetria; postural tremor
Basal ganglia-thalamocortical motor loop	Pallidum; subthalamic nucleus; thalamic ventral anterior and reticular nuclei	Ataxia; dystonia; myoclonia; resting tremor; rigidity; chorea/dyskinesia; extensor plantar response
Visual system	Lateral and inferior nuclei of the pulvinar; lateral geniculate body of the thalamus	Visual attentional deficits; abnormal visual evoked potentials
Auditory system	Colliculus inferior; nuclei of the lateral lemniscus; superior olive; cochlear nuclei	Abnormal brainstem auditory evoked potentials
Somatosensory system	All somatosensory nuclei of the thalamus, pons, and medulla oblongata	Ataxia; falls; decreased proprioception; decreased sense of vibration; decreased temperature discrimination
Vestibular system	Superior, lateral, medial, spinal and interstitial vestibular nuclei	Postural instability; falls; horizontal gaze-evoked nystagmus; impaired vestibulo-ocular reaction and optokinetic nystagmus
Oculomotor system	Oculomotor, trochlear, and abducens nuclei; rostral interstitial nucleus of the medial longitudinal fascicle; reticulotegmental nucleus of the pons; raphe interpositus nucleus; prepositus hypoglossal nucleus	Slowed horizontal saccades; reduced saccadic pursuits; dysmetrical saccades; reduced vestibulo-ocular reflex; ophthalmoplegia
Ingestion-related brainstem system	All ingestion-related brainstem nuclei and associated regions of the brainstem reticular formation	Dysphagia; malfunctions of the preparatory phase of ingestion; dysfunctions detrimental to the lingual, pharyngeal and oesophageal phases of swallowing
Precerebellar brainstem system	Red nucleus; pontine nuclei; vestibular nuclei; arcuate nucleus; lateral reticular nucleus; external cuneate nucleus; dorsal paramedian reticular nucleus; inferior olive	Ataxia; dysarthria
Midbrain dopaminergic system	Mesostriatal dopaminergic system (substantia nigra); mesolimbic dopaminergic system (nuclei of the ventral tegmental area)	Parkinsonian features (rigidity)
Midbrain cholinergic system	Pedunculopontine nucleus	Rapid eye movement sleep disorder
Pontine noradrenergic system	Locus coeruleus	Rapid eye movement sleep disorder

(Adapted from Rüb et al., 2013)

1.4.4 Genetics and protein physiology

The locus of the causative gene of SCA2 was initially mapped to chromosome 12 (Pulst et al., 1993), more precisely to the long arm 24 (Gispert et al., 1993). The *ATXN2* gene (12q24.12) was only identified later in 1996 by three different research groups (Imbert et al., 1996; Pulst et al., 1996; Sanpei et al., 1996). These studies demonstrated that the mutation underlying SCA2 consisted in an unstable expansion of CAG repeats in the coding region of the *ATXN2* gene, associating the disease to the heterogeneous group of polyQ disorders. Characterization of the gene genomic structure showed that *ATXN2* spans a total of 147kb and consists of 25 exons (Sahba et al., 1998), and has ubiquitous expression in all tissues (Nechiporuk et al., 1998) (Fig. 1.7). Regarding SCA2 genetic mutation, the CAG repeat tract is localized to exon 1. The triplet repeats vary from 13 to 31 CAG in healthy individuals, while the most common wild-type alleles found contain 22-23 CAG repeats interrupted by CAA sequences [$(CAG)_8$-CAA-$(CAG)_4$-CAA-$(CAG)_8$]. The CAA interruptions were reported to carry out an important role in maintaining CAG repeat stability, while its absence prompts alleles to undergo pathological repeat expansion (Choudhry et al., 2001). On the other hand, tandemly-repeated pure CAG sequences over 32 (≥ 33) cause SCA2 disease (Fernandez et al., 2000). Intermediate alleles harboring 27-33 trinucleotide repeats were associated with predisposition to develop amyotrophic lateral sclerosis (ALS) (present in ~4.7% of ALS cases) (Elden et al., 2010), while trinucleotide repeats of 35-36 were associated with SCA2 presenting as parkinsonism (Gwinn–Hardy et al., 2000).

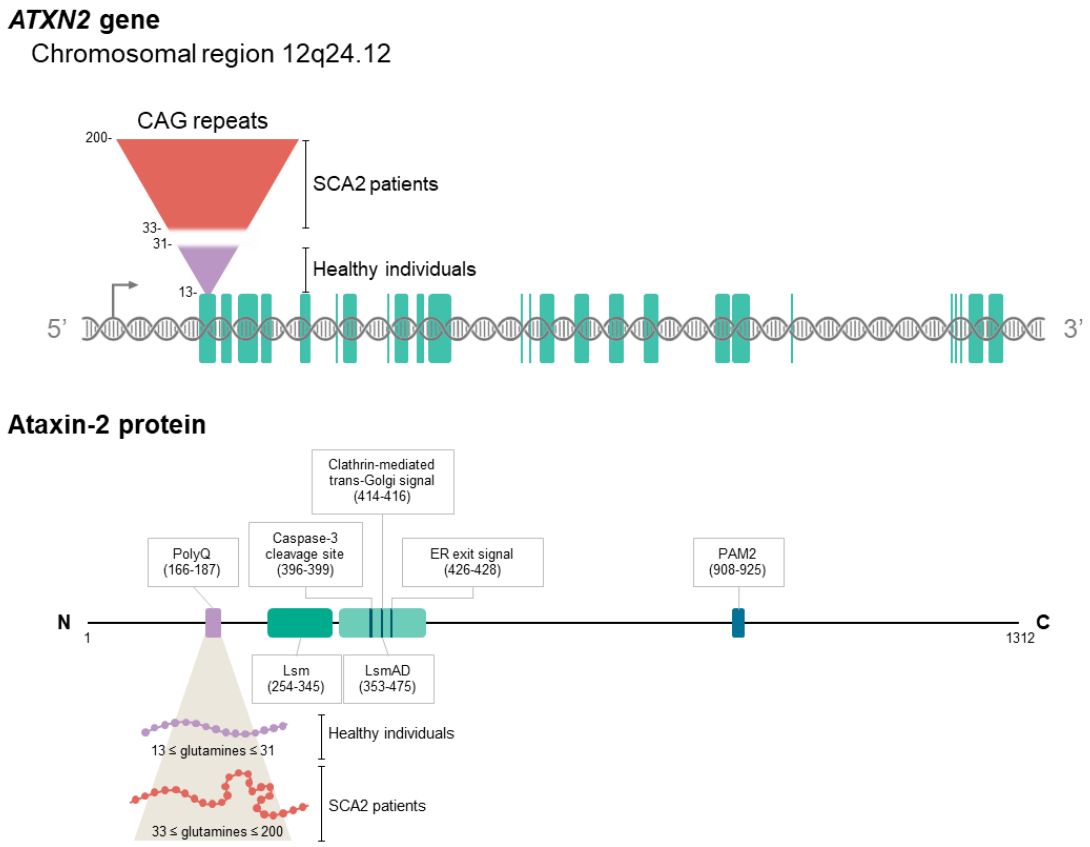

Fig. 1.7: **Schematic representation of *ATXN2* gene and ataxin-2 protein**. The *ATXN2* gene is mapped to 12q24.12 chromosome, containing 25 exons. The gene product is the Atx2 RNA-binding protein, constituted by an acidic region with the Lsm and LsmAD domains, and a PABP interacting domain in the C-terminal tail. SCA2-associated CAG repeats expansion is localized in exon 1, which is translated into a polyQ tract in the Atx2 protein. Healthy individuals have gene alleles/proteins containing between 13-31 CAG/glutamine repeats, whereas SCA2 patients express longer expansions ranging from 33 up to more than 200 CAG/glutamine repeats. (Adapted from Costa, 2021).

The *ATXN2* gene encodes for the protein Atx2, with a normal molecular weight of ~140 kDa, which comprises in its structure 1312 amino acids (Pulst et al., 1996; Ostrowski et al., 2017). However, translation from a second start codon present upstream of the CAG repeat within *ATXN2* gene produces a ~124 kDa peptide (Sahba et al., 1998; Scoles et al., 2012). Atx2 is a highly basic protein, apart from one acidic region with 46 acidic amino acids located downstream of the polyQ site (Fig. 1.7). This region consists in two globular domains designated Lsm (Like-sm) and LsmAD (Lsm-associated). The LsmAD domain bears a clathrin-mediated trans-Golgi signal and an endoplasmic reticulum exist signal. Outside of the Lsm and LsmAD motifs, Atx2 is intrinsically unstructured containing nonglobular and flexible N- and C-terminal tails. The polyQ region is localized in exon 1 in the N-terminal tail, while the C-terminal region contains a PABP

(poly(A)-binding protein) interacting motif, designated PAM2 (Albrecht et al., 2004).

Atx2 has a ubiquitous expression in human tissues, including the brain, heart, liver, skeletal muscle, pancreas, and placenta. In the brain, Atx2 is found in the amygdala, caudate nucleus, corpus callosum, hippocampus, hypothalamus, substantia nigra, subthalamic nucleus and thalamus. Particularly, increased levels of Atx2 with age are observed in cerebellar Purkinje cells (Pulst et al., 1996; Sanpei et al., 1996; Huynh et al., 1999). At a cellular level, Atx2 is mainly found in the cytoplasm, while subcellularly this protein is located ate the Golgi apparatus and rough ER membranes (Huynh et al., 1999, 2003; van de Loo et al., 2009).

Although the exact biological functions of Atx2 are not fully disclosed, numerous studies on cellular and animal models shed light on the role of this protein (Carmo-Silva et al., 2017). Knockout of Atx2 generated viable mice that displayed no major histological abnormalities, suggesting that Atx2 might not be essential for embryonic development or adult survival (Kiehl et al., 2006). Nevertheless, absence of Atx2 resulted in obesity, dyslipidemia and insulin resistance in mice, as well as changes in the circadian system in mice and *Drosophila* (Kiehl et al., 2006; Lastres-Becker et al., 2008a; Lim and Allada, 2013; Pfeffer et al., 2017).

Further studies on Atx2 putative domains and its interactors provided some hints into the protein molecular role (Table IV). The Lsm and LsmAD domains were shown to interact directly with RNA, implying that Atx2 could be an RNA-binding protein (RBP) (Wilusz and Wilusz, 2005; Satterfield and Pallanck, 2006). In fact, Yokoshi and collaborators performed high-throughput screening of Atx2-bound RNAs prepared by photoactivatable-ribonucleoside-enhanced crosslinking followed by immunoprecipitation (PAR-CLIP), revealing that Atx2 binds directly to over 4000 mRNA molecules (Yokoshi et al., 2014). They found that Atx2 interacts with these molecules through binding of LSm domain to uridine-rich elements within 3' UTRs of targeted mRNAs. Moreover, gene expression analysis upon Atx2 downregulation or overexpression showed that Atx2 stabilizes targeted mRNAs molecules, increasing the levels of the respective translated proteins. The proteins predominantly upregulated by Atx2 are involved in RNA splicing, polyadenylation, and end processing, thus suggesting an important role in RNA metabolism. Besides its role in mRNA stability, a study on a Atx2-knockout mouse model suggested that absence of Atx2 leads to global decrease

in protein synthesis, suggesting a function in promoting the translation process (Fittschen et al., 2015). Accordingly, Nóbrega and co-workers reported that Atx2 regulates the translation of mutant Atx3 protein, through interaction with PABP (Nóbrega et al., 2015b).

A study aiming to understand the interaction of PABP with Atx2 via PAM2 domain hinted about a role in stress granules (SGs) and processing bodies (P-bodies) assembly, which are dynamic cytoplasmic structures formed in response to cellular stress (Ralser et al., 2005). In this report, Atx2 and PABP were found to colocalize in stress granules upon application of heat-shock *stimulus* in a fibroblast-like cell line derived from monkey kidney tissue (COS1). Later, the same research group characterized the interaction of Atx2 with DEAD/H-box RNA helicase (DDX6), a SGs and P-bodies component, through Lsm and LsmAD motifs (Nonhoff et al., 2007). Moreover, the authors also established that reduced levels of Atx2 lead to impaired SGs formation, while increased levels of Atx2, decreased the number of P-bodies inside the cells, suggesting Atx2 functions in regulating the dynamics of these structures and possibly mediating the cellular responses to stress.

Importantly, the fact that Atx2 and its molecular functions are evolutionary conserved in numerous species, ranging from *Saccharomyces cerevisiae* (yeast) to *Pan troglodytes* (chimpanzee) and human, suggests that this protein might impact several physiological processes. Indeed, Atx2 has been reported to be involved in embryonic development, actin development, apoptosis, cellular proliferation among other biological pathways (Ostrowski et al., 2017).

Table 1.4: **The role of Atx2 in physiological mechanisms in different species, according to its interaction and possible implications upon dysregulation**

Atx2 Target	Species	Physiological function of Atx2	Implications of Atx2 dysregulation
TORC1	*S. cerevisiae* *C. elegans* *M. musculus* *H. sapiens*	Regulates TORC1-mediated nutrient responses via sequestration to stress granules	Possible defects in various TORC1-mediated metabolic pathways
PER1	*Drosophila*	Regulates circadian rhythms via activating translation of PER1	Impaired circadian clock, specifically a longer period of constant darkness
polyQ-expanded Atx3	*M. musculus*	Regulates mutante Atx3 translation via interaction with PABP	Increased mutant Atx3 aggregation and Aggravates SCA3 disease
Caspase activation	*H. sapiens*	Targets neuroblastoma cells for apoptosis	Reduction in apoptotic activity
Endophilin-A1 and -A2	*S. cerevisiae* *M. musculus* *H. sapiens*	Potential role(s) in plastin-associated pathways and receptor endocytosis	Possible implications in actin development and structure / alteration of the epidermal growth factor receptor (EGFR) internalization at the plasma membrane
Insulin receptor	*M. musculus*	Potential role in translation of Insr mRNA translation and / or regulation of Insr proteins	Obesity and infertility
pAktERES	*Drosophila*	Development of peripheral tissue by regulating the formation of endoplasmic reticulum exit sites (ERES) formation in larval fat body	Defects in ERES development and cellular growth
Grb2	*H. sapiens*	Role in cell proliferation by regulating Grb2 levels	Gain of function: increase in proliferation Loss of function: impaired developmental processes
Ccr4 and Kdh1	*S. cerevisiae*	Directly interacts with Rpl12a and Rpl12b proteins to regulate Ccr4 and Khd1 mediated cell growth	Possible growth defects
CZY-20	*C. elegans*	Regulates centrosome assembly and levels of centrosome-associated microtubules	Defects in cytokinesis
PAR-5 and ZEN-4	*C. elegans*	Promotes cell division via regulation of PAR-5 which in turn modulates a cytokinesis pathway that targets ZEN-4 to the spindle midzone	Defects in spindle alignment and midzone assembly

Abbreviations: *S. cerevisiae*, *Saccharomyces cerevisiae*; *C. elegans*, *Caenorhabditis elegans*; *M. musculus*, *Mus musculus*; *H. sapiens*, *Homo sapiens*. (Adapted from Nóbrega et al., 2015b; Ostrowski et al., 2017).

1.4.5 SCA2 animal models

The understanding of SCA2 disease was highly improved by the development of disease model systems. Firstly, the establishment of basic SCA2 models like yeast, *C. elegans* and *Drosophila* has been crucial to explore the functional roles of ataxin-2 protein (Kiehl et al., 2000; Satterfield and Pallanck, 2006). On the other hand, the development and characterization of more complex models like *Mus musculus* have provided valuable insights into SCA2 pathogenesis. Importantly, these models have offered an important opportunity to test and assess potential therapeutic strategies that could be further translated into a clinical context (Alves-Cruzeiro et al., 2016). So far, four transgenic and two knock-in (KI) murine animals modelling SCA2 disease have been developed and will be briefly reviewed below, focusing on the main motor and neuropathological abnormalities observed (Table 1.5).

1.4.5.1 SCA2-Q58 transgenic mouse model

In 2000, Huynh and colleagues developed the first SCA2 transgenic mouse model that express human full length ataxin-2 protein containing 58 consecutive glutamine repeats (Q58), under the regulation of the heterologous Purkinje cell protein 2 (Pcp2) promoter (L7) (Huynh et al., 2000). The authors also developed a control transgenic line expressing human full length ataxin-2 protein with 22 glutamine repeats (Q22). Both transgenes were expressed in mice cerebellar Purkinje cells, a neuronal population severely affected in SCA2 patients' brain. Regarding the motor features, Q58 animals exhibited limb clasping (abnormal limb flexion upon mice lifting) at 32 weeks of age. Also, mutant Q58 mice showed decreased stride length (19%) and reduced latency to fall of the rotarod apparatus (50%), indicating ataxic gait and balance incoordination when compared to Q22 and WT groups at 16 weeks of age. These motor deficits worsened over disease progression leading to severe impairments at 26 weeks of age. Later, a study also reported significant lack of balance and coordination in Q58 mice at 32 weeks of age, suggested by foot slips and longer times to cross the beam walking bar (Liu et al., 2009). The first neuropathological alteration observed in this model was reduced immunostaining for the neuronal marker calbindin-28K at 4 weeks

of age, that declined progressively from 7 to 14 weeks. Later, at 24-27 weeks of age, Q58 mice cerebellum presented a substantial loss in the number of Purkinje cells (around 50%) contrary to healthy animals. Moreover, mutant cytoplasmic microaggregates are observed in these cells. A different study on Purkinje cells electrophysiological profile using Q58 transgenic model reported a reduction in the number and frequency of firing cells in mutant mice (Kasumu et al., 2012b). Overall, the SCA2-Q58 transgenic mice is as a model with robust motor and neuropathological deficits, as well as a suitable tool to study Purkinje cells dysfunction. However, the expression of the transgene limited to one neuronal population could represent a disadvantage of this model.

1.4.5.2 SCA2-Q75 transgenic mouse model

Later in 2006, a different transgenic mouse model was created, also using pronuclear microinjection of human full-length *ATXN2* gene isolated from a Cuban patient with 75 CAG repeats (Aguiar et al., 2006). The transgene expression was under the regulation of the self-human SCA2 promoter, thus resulting in ubiquitous expression of mutant ataxin-2 mRNA and protein across different tissues, including lungs, kidney, skeletal muscle, liver, and brain. Motor behavioral analysis revealed a significant decline in rotarod test performance in heterozygous mice at 12 weeks of age, whereas homozygous mice showed earlier motor deficits at 6 weeks of age, in comparison to WT littermates. The motor dysfunction correlated with neuropathological alterations, as cerebellar Purkinje cells presented reduced immunoreactivity for calbindin-28k marker, along with reduced dendritic arbor and shrinkage of cell bodies, at 52 weeks of age. Intriguingly, only Purkinje cells were found to be degenerated, despite the ubiquitous expression of the mutant *ATXN2* transgene. Therefore, the SCA2-Q75 transgenic mouse model expressed mutant Atx2 ubiquitously, resembling physiological levels found in patients, and exhibited an early onset of motor abnormalities, making it a suitable model to study new targets for therapy. On the other hand, this model displayed few behavioral symptoms showing only motor incoordination, while a control transgenic line with normal CAG repeats was not developed for more accurate comparisons.

1.4.5.3 SCA2-Q42 knock-in mouse model

The KI mouse model of SCA2 disease was published by Damrath and colleagues in 2012 (Damrath et al., 2012). The authors of this study took advantage of the homologous recombination in embryonic stem cells to insert a CAG expansion with 42 repeats into the murine *ATXN2* gene. The mutant gene product, under the regulation of the endogenous murine *ATXN2* promoter, was found in the cortex and cerebellum tissues, both at the transcript and protein levels. Phenotypic assessment of SCA2-Q42 KI model revealed a significant weight loss (19%) already at 1 week of age, compared to WT littermates, a trait also noted in moderate and severe cases of SCA2 patients (Rodriguez-Graña et al., 2021). Surprisingly, only a very mild ataxic phenotype was observed in this model, as no differences in open field (assesses exploratory behavior and general activity), grip (assesses muscular strength) or footprint (assesses gait pattern) tests were observed in 42 KI mice. At 72 weeks of age, homozygous mice presented significant reduced latency to fall off the rotarod apparatus, while heterozygous animals did not show significant motor impairments at any age, when compared to WT group. Consistent with motor coordination observations, only subtle and late-onset neuropathological alterations were detected in this KI mouse model. The most noticeable trait was the presence of cytoplasmic Atx2-positive insoluble inclusions inside Purkinje cells, at 56 weeks of age, while no signs of neurodegeneration were observed. Therefore, the SCA2-Q42 KI model has the advantage of a targeted transgene genome insertion, compared to the method of pronuclear injection used in the previous transgenic models, thus preventing random integration in the DNA. However, this model also exhibited very mild and late-onset phenotypic and neuropathological alterations, representing an unsuitable model to evaluate potential disease-modifying targets.

1.4.5.4 SCA2-Q127 transgenic mouse model

Another transgenic mouse model expressing a larger CAG expansion (127 repeats), compared to the other reported models, was developed and characterized by Hansen and colleagues in 2013 (Hansen et al., 2013). The transgene inserted, under the control of Pcp2 promoter, encoded for a mutant form of human full-length Atx2 with 127 glutamines. Behavioral testing of SCA2-

Q127 mice showed more robust motor features, compared to previous SCA2 murine models, evidenced by the decreased motor performance in the rotarod test as early as 8 weeks of age. The motor incoordination worsened over disease course until 36 weeks of age, resulting in a substantial reduction (50%) of the latency to fall at this time point, comparing to WT littermates. Likewise, neuropathological signs were more pronounced, with the presence of mutant Atx2 inclusions inside Purkinje cells only at 4 weeks of age, increasing over disease progression. Moreover, analysis of cerebellum cellular layers demonstrated that expression of Atx2-Q127 led to decreased molecular layer thickness (over 60%) at 12 weeks of age compared to control WT group, while the number of Purkinje cells was significantly lower at 40 weeks of age. The electrophysiological profile of Purkinje cells revealed slower firing frequency in the cells expressing mutant Atx2. Overall, the SCA2-Q127 transgenic mouse model exhibited very robust motor and neuropathological impairments with an early onset, being an advantageous model to study electrophysiological and genetic deregulations in Purkinje cells, as well as assess novel targets for SCA2 treatment. On the downside, the transgene is inserted randomly in the murine genome, as occurs for the Q58 and Q75 transgenic models, which could result in undesirable off-target effects, reducing faithfulness to human disease.

1.4.5.5 SCA2-BAC-Q72 transgenic mouse model

In 2015, Dansithong and co-workers generated a transgenic murine model of SCA2 using a bacterial artificial chromosome (BAC), a DNA clone that allows the insertion of large sequences that might include non-coding regions (Dansithong et al., 2015). The BAC clone used included the complete *ATXN2* gene sequence with edition of exon 1 to harbor the CAG expansion with 72 repeats. A control transgenic line expressing 22 CAGs was also generated using the same methodology (BAC-Q22). Both BAC-Q72 and BAC-Q22 integrated 4 and 10 copies of the transgene, respectively, under the control of the endogenous human promoter, resulting in ubiquitous expression across mice entire organism at the transcript and protein level. Either BAC-72, and BAC-Q22 showed reduced weight loss (30%) in comparison with the WT littermates, parallel to weight changes observed in the Q42 KI model. Regarding analysis of the motor function,

mutant Q72 transgenic mice presented a reduced latency to fall in the accelerated rotarod test at 16 weeks of age, suggesting motor incoordination, a phenotype that progressively aggravated until 36 weeks of age. Similarly, neuropathological abnormalities observed included shrinkage of Purkinje cells dendritic tree, and loss of calbindin-28k and Pcp2 markers in the cerebellum tissue, comparing to both BAC-Q22 and WT littermates. Thus, the BAC-Q72 proved suitable to study RNA-related mechanism as entire *ATXN2* gene is inserted into the murine genome, while ubiquitous expression of Atx2 was also obtained. On the other hand, this model only displayed mild motor and neuropathological deficits, resembling few traits observed in SCA2 disease.

1.4.5.6 SCA2-Q100 knock-in mouse model

The most recent SCA2 mouse model was a knock in murine model with 100 length CAG expansion developed by Sen and colleagues in 2019 (Sen et al., 2019). The authors of this work used the same homologous recombination technology as Q42 KI model, to insert an expansion of 100 trinucleotide repeat units into exon 1 of *ATXN2* murine gene, preserving intact its exon-intro structure and native expression regulation. Genotypical characterization revealed that the Q100 KI model presents polyQ length instability over successive generations and somatic mosaicism, like observed in human SCA2 disease, representing the first model reported to mimic this feature. The monitorization of phenotypic traits until the end of lifespan demonstrated weight loss in all SCA2-Q100 KI mice and a reduced lifespan in homozygous animals, around 14 months when compared to a normal lifespan of 24 months in WT mice. Moreover, mutant mice showed progressive motor deficits compared to WT littermates including hind limb clasping; irregular paw pattern at 48 weeks; decreased forelimb grip strength at 44 weeks of age; progressive decreased latency to fall off the rotarod apparatus from 20 weeks until 14 months of age; and increased hyperactivity activity in the open field test at 10 weeks of age. Accordingly, the expression of expanded Atx2 resulted in a severe and widespread degeneration of brain regions typically affected in SCA2 patients. Particularly, SCA2-Q100 KI mice showed 1C2-positive Atx2 cytosolic aggregates inside cerebellar Purkinje, inferior olivary, pontine nuclei, cerebral cortical, hippocampal, and spinal cord motor neurons.

Furthermore, MRI analysis detected reduced NAA and glutamate levels in the cerebellum of mutant mice. Overall, the SCA2-Q100 KI murine model proved to faithfully reflect several motor and neuropathological features observed in SCA2 patients, as well as metabolic alterations, without the potential off-target effects inherent to a transgenic model. Therefore, this model represents the most suitable tool to study disease mechanisms and novel targets for SCA2 therapy, in comparison to the other available animal models developed so far.

Table 1.5: **Summary of the main phenotypic, motor, and neuropathological features described for the transgenic and knock-in mouse models of SCA2.**

Model	Phenotypic impairments	Onset age (weeks)	Neuropathological alterations	Onset age (weeks)
SCA2-Q58 Tg	Rotarod reduced latency to fall	16	Loss of calbindin-28K immunoreactivity	4
	Irregular footprint	16	Decreased Purkinje cells number	24
	Clasping	32	Cytoplasmic microaggregates	-
	Beamwalk imbalance	32	Decrease in the number and frequency of firing Purkinje cells	24
SCA2-Q75 Tg	Rotarod reduced latency to fall	6	Loss of calbindin-28K immunoreactivity	52
			Loss of dendrites and shrinkage of cell bodies of Purkinje cells	52
SCA2-Q42 KI	Reduced body weight	1	Cytoplasmic insoluble aggregates	56
	Rotarod reduced latency to fall	72		
SCA2-Q127 Tg	Rotarod reduced latency to fall	8	Decreased Purkinje cells number	40
			Perinuclear aggregates	4
			Loss of molecular layer thickness	12
			Slower firing frequency of Purkinje cells	6
SCA2-BAC-Q72 Tg	Reduced body weight	8	Loss of calbindin-28K immunoreactivity	24
	Rotarod reduced latency to fall	16	Shrinkage of dendritic trees in Purkinje cells	-
SCA2-Q100 KI	Reduced body weight	10	Reduced brain weight	56
	Rotarod reduced latency to fall	20		
	Irregular footprint	48	Cytosolic aggregates inside diverse neuronal populations	12
	Clasping	40	Metabolic alterations (reduced N-acetylaspartate and glutamate levels)	12
	Reduced grip strength	44		
	Hyperactivity activity	10		

(Adapted from Alves-Cruzeiro et al., 2016).

1.4.6 Pathogenic mechanisms

As reported for other PolyQ diseases, the genetic mutation responsible for SCA2 disease is well known, however the pathogenic events that lead to the widespread neurodegeneration observed are not fully established. Several molecular pathways and systems, also common to SCA3 disease, were demonstrated to play a role in SCA2 pathogenesis (Fig. 1.8).

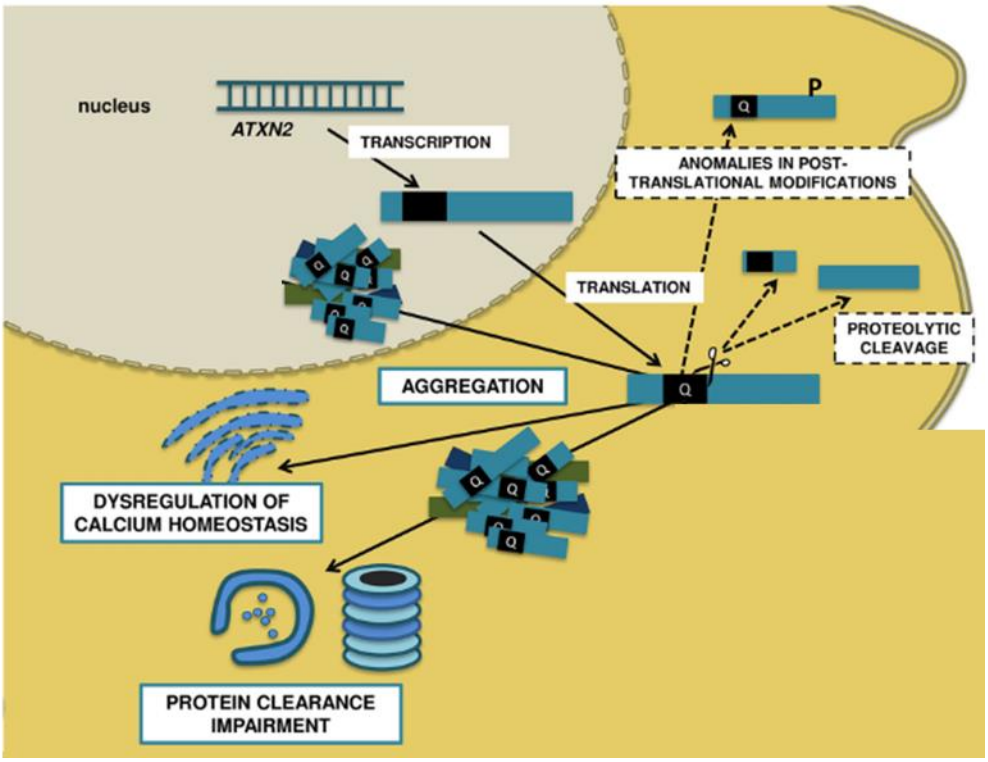

Fig. 1.8. **Cellular mechanisms and pathways involved in SCA2 pathogenesis**. Several molecular events have been put forth as potential toxic mechanisms underlying SCA2 pathogenesis, including mutant protein aggregation and proteolytic cleavage, transcriptional and translational dysregulation, mitochondrial dysfunction and increased oxidative stress, protein clearance mechanisms impairments, and calcium homeostasis deregulation. (Adapted from Alves-Cruzeiro et al., 2016).

1.4.6.1 Mutant Protein Aggregation

The aggregation of polyQ-expanded proteins into nuclear or cytoplasmic insoluble inclusions is a prominent pathological feature of SCA3 and other polyQ disease (Bauer and Nukina, 2009). Likewise, as a polyQ-expanded protein, mutant Atx2 is proposed to undergo conformational alterations, shifting to a β-sheet-rich structure, followed by assembly into oligomers and consequent

formation of insoluble amyloid-like fibrillar structures (Takeuchi and Nagai, 2017; Wen et al., 2017). In fact, histological analysis of SCA2 *post mortem* brain tissues revealed the presence of cytoplasmic and nuclear mutant inclusion bodies inside neurons (Seidel et al., 2017). However, the role of ataxin-2 aggregation in SCA2 pathophysiology is still controversial. A study aiming to assess the aggregation pathology in the brainstem of SCA2 patients, established that disease severity correlated to the existence of different types of mutant inclusion species. The authors noticed that the presence of granular cytoplasmic staining significantly associated with a more severe neurodegeneration pattern, whereas neuronal nuclear inclusions appeared to have a protective role (Seidel et al., 2017). Moreover, a study using 1C2 (polyQ) antibody for analysis of subcellular immunoreactivity patterns, demonstrated that occurrence of granular cytoplasmic staining related to early disease stages, cytoplasmic and nuclear pattern corresponded to active disease stages, and nuclear inclusions correlated with final disease stages (Koyano et al., 2014). On the other hand, the existence of mutant ataxin-2 inclusions in cerebellar Purkinje cells, a neuronal population profoundly degenerated in SCA2 disease, is still unclear, as only few studies reported non-ubiquitinated cytoplasmic aggregates in mouse models (Huynh et al., 1999; Damrath et al., 2012; Sen et al., 2019). Overall, SCA2 seems to be characterized by the presence of Atx2 aggregates, although its role in the disease pathogenesis is yet unclear.

1.4.6.2 Proteolytic cleavage and ubiquitin-proteasome system impairment

The generation of toxic polyQ-products, as a result of proteolytic cleavage, has been proposed as a pathogenic event in SCA3 and other polyQ diseases (Ikeda et al., 1996; Matos et al., 2017). In SCA2, a 42 kDa fragment, reactive to the polyQ-specific 1C2 antibody, was detected in brain samples from SCA2 patients and mouse models (Huynh et al., 1999, 2000; Koyano et al., 1999). The origin of this fragment is explained by the identification of a consensus site for caspase-3 cleavage (Huynh et al., 2000). Strikingly, this fragment was not detected in control samples, suggesting a possible role of proteolytic cleavage and SCA2 pathogenesis. The impairment of the UPS system has also been associated with increased proteolysis of mutant misfolded proteins, generating more toxic

fragments (Li et al., 2010). In SCA2, UPS impairment is suggested by sequestration of proteasome players (FBXW8 and PARK2) into mutant ataxin-2 aggregates in cellular and SCA2-Q42 KI mouse models (Damrath et al., 2012; Halbach et al., 2015). These results could reinforce a role of proteolytic cleavage in SCA2 disease, possibly exacerbated by the dysfunction of the ubiquitin proteasome system.

1.4.6.3 Mitochondrial Dysfunction and Oxidative Stress

Mitochondria play several important roles in cells, such as cellular energy production, calcium signaling, and regulation of cell death through apoptosis or necrosis (McBride et al., 2006). Mitochondrial dysfunction and increased oxidative stress has been reported for SCA3 and other polyQ diseases (Matsuishi et al., 1996; Orr et al., 2008). In SCA2 disease, a study on fibroblasts derived from patients revealed alterations in SOD and catalase levels, key mediators of oxidative stress, both at the transcript and protein levels (Cornelius et al., 2017). These alterations resulted in increased mitochondrial oxidative stress along with dysfunctions in mitochondrial morphology and respiratory chain enzymatic activity. Accordingly, other authors also reported that SCA2 patients' fibroblasts present increased oxidative stress levels and apoptotic activation, upon autophagic inhibition (Wardman et al., 2020). Moreover, a study on SCA2 patients' blood proposed that higher levels of oxidative stress leads to dyshomeostasis of metals levels, including copper, manganese, zinc and vanadium (Squadrone et al., 2018). Therefore, altered mitochondrial function and increased levels of oxidative stress could play an important role in SCA2 pathogenesis and thus be a potential target for therapeutic intervention.

1.4.6.4 Calcium dysregulation

Multiple lines of evidence imply that calcium dysregulation contributes to polyQ disease pathogenesis (Pchitskaya et al., 2018). In SCA2 disease, Pulst et. al. observed that long normal polyQ repeats in the calcium voltage-gated channel subunit alpha 1A (CACNA1A), explained 5.8% of variation on SCA2 age of onset and correlated with early onset of symptoms (Pulst et al., 2005). The CACNA1A channel subunit is highly expressed in Purkinje cells and is responsible for

mediating CA^{2+} ions entry in these cells (Jun et al., 1999). In SCA2 patients brain, CACNA1A protein was found to co-localize in mutant Atx2 aggregates (Pulst et al., 2005). Moreover, abnormal polyQ expansions in CACNA1A gene results in development of SCA6 disease (Ishikawa et al., 1999). These results suggest a potential role of CACNA1A calcium channel subunit in SCA2 pathogenesis. Later studies on calcium signaling demonstrated that mutant expanded form of Atx2 interacts with the C-terminal of the InsP3R1 receptor (Liu et al., 2009). This interaction results in increased release of intracellular CA^{2+} ions in primary Purkinje cells cultures derived from SCA2-Q58 transgenic mouse model. Furthermore, Kasumu and Bezprozvanny suggested that increased levels of CA^{2+} ions in Purkinje cells, mediated by mutant Atx2 activity, exacerbates cerebellar long-term depression (LTD) resulting in excitotoxicity, and triggering the first symptoms of ataxia in SCA2 patients (Kasumu and Bezprozvanny, 2012). Overall, there is compelling evidence that calcium dysregulation mechanisms contribute to SCA2 pathogenesis, proposed to be responsible for the first physical symptoms of the disorder.

1.4.6.5 Autophagy Impairment

As mutant polyQ proteins tend to aggregate and form large multi-protein inclusions, protein degradation systems are essential to maintain cellular homeostasis. Autophagy, an important protein lysosomal-mediated clearance pathway, has been shown to be impaired in different polyQ diseases (Cortes and La Spada, 2015). Regarding SCA2, few studies have reported evidence of autophagic failure in disease pathogenesis. Analysis of peripheral markers in SCA2 patients' blood cells revealed increased mRNA levels of the autophagy-linked FYVE domain (Puorro et al., 2018). Moreover, Paul and co-workers reported that polyQ-expanded Atx2 leads to abnormal autophagy, along with increased expression of the SGs protein staufen1, in SCA2 patient-derived fibroblasts, and in SCA2-Q127 and SCA2-BAC-Q72 transgenic mice (Paul et al., 2018). More recently, our group reported autophagic dysfunction in a novel lentiviral mouse model of SCA2 disease, as well as *in vitro* models and samples from brain patients (Marcelo et al., 2021a). We observed increased levels of the autophagic marker SQSTM1 at the transcript and protein levels, suggesting

ineffective lysosomal degradation. Moreover, we also found that LC3B-II levels, a player required for autophagosome formation, were decreased upon expression of mutant Atx2. Also, detection of abnormal accumulation of autophagic markers in cerebellum and striatum tissues of SCA2 patients further reinforced autophagic impairment in this pathology. Additionally, Wardman et. al. reported that mutant ataxin-2 is eliminated by autophagy rather than by the proteasome system, indicating that autophagic impairment could aggravate the accumulation of misfolded Atx2 protein, promoting its aggregation (Wardman et al., 2020). Overall, studies on autophagic pathway establish that dysfunction of this essential biological mechanism could contribute to SCA2 disease and be a potential target to develop therapeutic approaches.

1.4.7 Therapeutic perspectives for SCA2

SCA2 is a highly debilitating and fatal rare disease that brings devastating consequences for affected individuals and their families. The current treatment options rely only on pharmacological drugs that relief motor symptoms. However, these compounds cannot stop or delay disease progression. So far, several research studies have attempted to develop potential therapeutic strategies that could mitigate SCA2 manifestations and neuropathology in a preclinical setting. Some of these studies will be briefly described in the following section.

1.4.7.1 Antisense oligonucleotide therapy

One of the most promising approaches studied in the context of SCA2 disease is the ASO therapy. This type of therapy has also been investigated in other polyQ disorders, including SCA3 and HD (Moore et al., 2017; Lane et al., 2018; McLoughlin et al., 2018). In this therapy, the oligonucleotide sequence selected is complementary to a target mRNA, suppressing its translation, thus, reducing the protein levels encoded by the target transcript. In 2017, Scoles and collaborators performed an *in vitro* screening of 152 ASOs designed *in silico* for targeting human *ATXN2* gene (Scoles et al., 2017). They found that ASO7 had the most promising results in downregulating ataxin-2 mRNA and protein levels. The authors further tested whether intracerebroventricular injection of ASO7

could mitigate the phenotype observed in two disease mouse models, the SCA2-Q127 and the SCA2-BAC-72Q animals. In fact, administration of ASO7 led to decreased levels of Atx2 expression (more than 75%) in the cerebellum. Importantly, treated mice from both models exhibited significant improved performance in the rotarod test compared to saline-treated animals. Additionally, ASO7 therapy resulted in normalization of several SCA2-related proteins' levels in Purkinje cells, such as Rgs8, Pcp2, Pcp4, Homer3, Cep76 and Fam107b, as well as, led to stabilization of firing frequency in Purkinje neuronal population. Therefore, these findings support ASOs as a potential gene therapy for SCA2 disease. However, the method of ASO delivery to cerebellar cells of SCA2 patients brings about some concerns. Anionic oligonucleotides cross the blood-brain barrier very poorly or not at all, leaving intravenous administration as an unsuitable choice, while the direct injection into the cerebellum through surgery is a highly invasive method carrying safety issues. To overcome these limitations, Ashizawa and co-workers developed a novel liposome formulation that efficiently incorporated oligonucleotides, designated DCL64, for delivery into cerebellar Purkinje cells (Ashizawa et al., 2018). Indeed, intravenous administration of the particles proved to be effective in distributing oligonucleotides in the cerebellum. Overall, the use of ASO therapy holds promising results in pre-clinical studies of SCA2 disease, however further studies on delivery and efficiency are required before moving towards a clinical context.

1.4.7.2 Promoting neuronal protection

Stem cells therapy is a research field that has been shown to bear great potential to treat neurodegenerative disorders, including diverse polyQ diseases (Barros et al., 2020). From the group of therapies using adult stem cells, mesenchymal stromal cells (MSCs) have been in particular focus as they possess several properties, including low immunogenicity, easy accessibility and harvesting, and releasing of neurotrophic factors that promote neuronal protection (Paul and Anisimov, 2013). In SCA2 disease, a study on SCA2-Q58 transgenic mice to assess the potential of MSCs, using two different delivery methods was performed (Chang et al., 2011). Mice that received several intravenous infusions of human mesenchymal stromal cells (hMSCs) showed improved motor function,

as well as Purkinje cells survival. On the other hand, these effects were not so noticeable when animals were treated with a single intracranial injection of hMSCs. These results showed that continuous treatment with MSCs could lead to promising benefits in SCA2 disease. Clinical trials that have also investigated the therapeutic potential of MSCs in patients suffering from different SCAs also corroborated this hypothesis. In these trials, affected individuals presented alleviation of motor deficits upon transplantation of MSCs, however, few months after the treatment most patients returned to previous disease state or showed an aggravation of symptoms (Dongmei et al., 2011; Jin et al., 2013; Miao et al., 2015). Overall, cell therapies using MSCs could be promising approaches for the treatment of SCA2 disease, nevertheless further studies to improve therapeutic outcomes as well as safety issues are required.

1.4.7.3 Targeting calcium dysregulation

As referred above, disturbed calcium signaling was proposed to contribute to SCA2 pathogenesis. Several studies investigated the potential of approaches to block calcium-mediated excitotoxity in Purkinje cells, by modulating binding to calcium channels and suppressing intracellular entry of CA^{2+} ions. The use of ryanodine or dantrolene on SCA2-Q58 transgenic mice resulted in inactivation of the ER calcium channels RyRs, leading to amelioration of motor deficits and decreased Purkinje cells degeneration (Liu et al., 2009). Moreover, the use of specific positive modulators of small-conductance calcium-activated potassium channels (SK) 2 and 3 led to stabilization of Purkinje cells firing rates and had a benefic effect in SCA2-Q58 transgenic mice (Kasumu et al., 2012a). Upon elevated levels of intracellular calcium, the SK channels slow down cerebellar Purkinje cells activity (Meera et al., 2016). Thus, therapeutic modulation of the channels could be a potential target for SCA2 disease. In line with this, the treatment with riluzole, a molecule that binds and allosterically modulates the SK2 channels, ameliorated the pathological phenotype of SCA2-iPSC-derived neurons (Chuang et al., 2019). Therefore, pre-clinical studies showed that modulation of intracellular calcium signaling could reduce Purkinje cells dysfunction, being a potential therapeutic strategy for SCA2 pathology.

1.4.7.4 Enhancing autophagic pathway and protein clearance

The autophagic pathway has been shown to be impaired in several polyQ diseases, including SCA2 disorder as described earlier (Marcelo et al., 2021a). However, few studies targeting the autophagy mechanism as a therapeutic target for SCA2 have been published. Wardman and co-workers demonstrated that trealose, a non-reducing disaccharide shown to induce autophagy, reduced mutant Atx2 levels in SCA2 patients-derived fibroblasts (Wardman et al., 2020). Moreover, recent work from our group showed a potential therapeutic effect of the pharmacological compound cordycepin in SCA2 disease models, similar to results obtained in our previous study on SCA3 models (Marcelo et al., 2018, 2021a). The treatment with cordycepin resulted in decreased number of cells with polyQ-expanded Atx2 aggregates. Importantly, intraperitoneal injections of Cordycepin significantly reduced the number of Atx2-positive inclusions in the striatum of a lentiviral mouse model, as well as reduced loss of neuronal markers and levels of cell death. Overall, these results suggest that enhancement of autophagy could be a promising approach in treating SCA2 disease and further studies on toxicity and efficacy of these targets should be conducted.

1.5 Closing remarks on SCA3 and SCA2

As discussed above, the PolyQ diseases are a group of rare and fatal dominantly transmitted neurodegenerative disorders. The diseases are caused by an abnormal CAG expansion in the disease-causing genes, leading to an abnormal polyQ tract into the respective translated proteins. The clinically heterogenous PolyQ group includes SCA3 and SCA2 diseases, which are the first and the second most frequent SCAs worldwide, respectively. These disorders share common features, such as: i) the existence of a positive correlation between the variable CAG repeat number and both the severity and precocity of symptoms; ii) propensity for the protein products to aggregate and to constitute large intracellular multiprotein inclusions that are detected in patients' neuronal tissue; and (iii) the involvement of common pathways and mechanisms in disease pathogenesis, including toxicity induced by polyQ-expanded protein aggregation, proteolytic cleavage, impairment of protein clearance systems, transcriptional and translational deregulation, calcium dysregulation, mitochondrial dysfunction and oxidative stress. The dysfunction of these and other pathways might promote a stress environment for which cells (and particularly neurons) need to overcome, ensuring survival. An important player in the cellular stress response is the formation of specialized membraneless compartments, designated stress SGs. Several studies have been linking SGs to different human conditions such as cancer (Anderson et al., 2015), aging (Masuda et al., 2009) and neurodegenerative diseases (Asadi et al., 2021). In this line, several findings also provided some hints of a possible implication of SGs in PolyQ diseases. Recently, we published a review discussing the evidence supporting the existence of a link between SGs functionality and PolyQ diseases (Marcelo et al., 2021b). In the following section and based in this review, SGs biology and its implication in this group of pathologies will be outlined.

1.6 Stress granules

1.6.1 What are stress granules?

Stress granules are cytoplasmic non-membranous organelles that consist of messenger ribonucleoprotein (mRNPs) complexes, which are stalled upon inhibition of translation initiation (Buchan and Parker, 2009). SGs formation might be triggered by decreased translation initiation rates during a cellular response to different stressors, including endoplasmic reticulum stress, heat or cold shock, oxidative stress, starvation, or viral infection (Vanderweyde et al., 2013). Moreover, the addition of translation blocking drugs (Dang et al., 2006; Mazroui et al., 2006; Mokas et al., 2009), knockdown of specific translation factors (Mokas et al., 2009) or overexpression of specific RBPs that repress translation (Mazroui et al., 2002; Gilks et al., 2004; Kedersha et al., 2005; Wilczynska et al., 2005; De Leeuw et al., 2007) induces the assembly of SGs.

SGs were first described in tomato cell lines upon cellular stress induction mediated by heat shock, and were denominated heat-stress granules (HSG) (Nover et al., 1983). Through electron microscopy, it was observed that the granular aggregates were highly enriched with HSP17. Later, the assembly of SGs was described in fibroblasts derived from chicken embryos, where the authors detected the presence of HSP24 protein concentrated in distinct aggregates in the cytoplasm after a heat shock stimulus (Collier and Schlesinger, 1986; Collier et al., 1988). Since then, several studies demonstrated SGs formation in different *in vitro* models including plants, protozoa, yeast, *C. elegans* and mammalian cells, as well as, in animal tissues, and in human samples, including in a pathological condition.

1.6.2 Stress granules formation and dynamics

A defining and important feature of SGs is their dynamics, as they quickly assemble upon stress and rapidly diffuse after stress removal. However, the assembly and composition of SGs depends on the type of stress, the type of cell, and the particular stressing factors involved and the signalling pathways that are activated (Kedersha et al., 2005).

In the canonical SGs formation pathway (Fig. 1.9), the first step is the phosphorylation of Eukaryotic translation initiation factor 2A (eIF2α) (Anderson and Kedersha, 2002), by one of the four eIF2α kinases that have in its structure specific regulatory regions that recognize different stress stimulus (Wek et al., 2006; Vanderweyde et al., 2013). The general control non-derepressible-2 (GCN2) (or eIF2α kinase 4 (EIF2AK4)) surveils amino acid levels in cells and responds to starvation stimulus. The pancreatic eIF2α kinase (PEK) (or PKR-like ER kinase (PERK) or eIF2α kinase 3 (EIF2AK3)) belongs to the ER system and is activated upon accumulation of unfolded proteins in ER lumen. The protein kinase R (PKR) is activated upon cells exposition to heat, UV radiation and viral infections. The fourth kinase is the haem-regulated inhibitor (HRI) (or eIF2α kinase 1 (EIF2AK1), which perceives oxidative stress levels (Wek et al., 2006). Phosphorylation of eIF2α by one of the four kinases leads to translation arrestment and dissociation of translation initiation complexes from polysomes (Wolozin, 2012). This results in the accumulation of mRNAs, transcription factors, RBPs and other proteins that have intrinsically disordered domains (IDDs) or prion-like domains (PLDs) (Gilks et al., 2004). These regions of the proteins are low complexity glycine-rich sequences with the ability to reversibly aggregate. They promote numerous electrostatic interactions between different regions of the protein and between different proteins, giving rise to two distinct states within the SGs: a stable core, surrounded by a dynamic shell (Molliex et al., 2015). Firstly, core components of SGs located in the cytoplasm bind to each other, as well as to polyadenylated mRNAs and 40S ribosomal subunits, promoting the recruitment of other proteins and initiating the process of granule assembly (Khong et al., 2017). This event is denominated primary aggregation and results in the formation of a stable core. In the secondary aggregation event, SGs nucleators induce several interactions between different SGs components, resulting in the maturation of SGs and forming the shell, where numerous dynamic weaker protein interactions occur. This state resembles a liquid-liquid phase separation that allow the transition of several proteins and RNA remodelling complexes between the core and the shell of these foci and even within the surrounding cytosol (Jain et al., 2016).

It has also been reported the assembly of SGs independent of eIF2α phosphorylation, defined as a non-canonical pathway. The inhibition of the

Eukaryotic initiation factor 4F (eIF4F) complex, prevents the formation of the 48S initiation complex, inhibiting ribossome activity and arresting translation initiation, resulting in SGs formation (Mazroui et al., 2006).

SGs are rapidly dispersed upon stress removal, allowing the recycling of its components to immediate cellular use, a process that is regulated by molecular chaperons (Alberti et al., 2017). In neurons, autophagy seems also to be implicated in SGs disassembly (Buchan et al., 2013; Matus et al., 2014), although it might not be the preferred pathway for their clearance (Ganassi et al., 2016; Mateju et al., 2017). SGs disassembly correlates positively with a recovery in overall protein synthesis and in the translation of several mRNAs (Mazroui et al., 2007; Tsai et al., 2008; Lian and Gallouzi, 2009).

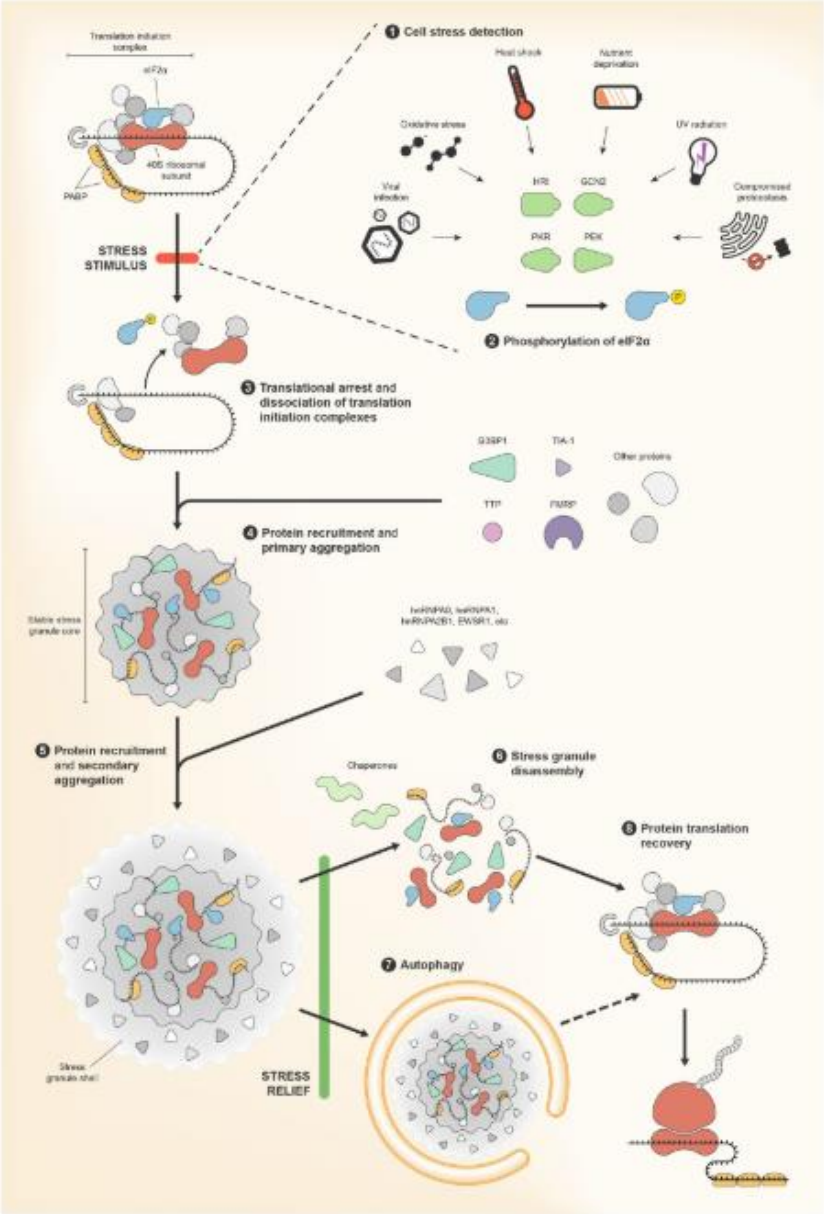

Fig. 1.9. **The canonical stress granule assembly pathway.** (1) Formation of SGs can be triggered by diverse cell damaging conditions, including viral infection, oxidative stress, heat shock, nutrient deprivation, ultraviolet radiation or proteotoxic stress. Stress conditions are detected by specific kinases, protein kinase R (PKR), haem-regulated inhibitor (HRI), general control non-derepressible-2 (GCN2) and pancreatic eIF2α kinase (PEF), that then become activated and (2) phosphorylate eukaryotic translation initiation factor 2 subunit alpha (eIF2α). (3) eIF2α is involved in the formation of translation initiation complexes and, when phosphorylated, leads to dissociation of these complexes and to translational arrest. (4) mRNAs, 40S ribosomal subunits, and proteins involved in translation start to accumulate and to assemble, along with other proteins that are recruited to the forming SGs. This primary aggregation process produces a stable SG core. (5) A secondary aggregation step resulting from additional, albeit weaker, intermolecular interactions originate the shell of the SGs. (6) When stress conditions abate, SGs are either disassembled by molecular chaperons or (7) are cleared by autophagy. (8) Disassembly allows for a rapid recovery of protein synthesis (Marcelo et al., 2021b).

1.6.3 Stress granules components

Although SGs constitution depends on the cell type and the type of stimulus that induces the stress response (Vanderweyde et al., 2013), these cytoplasmic *foci* are mainly composed of stalled pre-initiation complexes: 40S ribosomal subunits, translation initiation factors, poly(A)$^+$ mRNAs and RBPs (Fig. 1.10). The SGs components also include protein kinases, RNA helicases, calcium binding proteins, hydrolases, and even cytoskeletal proteins. Core components involved in the primary aggregation step include G3BP1 (ras GTPase-activating protein-binding protein 1), TIA-1 (T-cell intracellular antigen-1), TIAR (TIA-1 related), TTP (tristetraprolin), and FMRP (fragile X mental retardation protein) (Khong et al., 2017). However, several other proteins have been described as participating in SGs formation. In fact, our group has identified all mammalian SGs components, gathering the information of studies published so far, and listed them in an open access database (Nunes et al., 2019). Our database comprises to date, 464 proteins identified as components of SGs, categorizing them according to their molecular function or subcellular localization, also providing information about the type of cell or stress stimulus used to identify the components. From the 464 proteins identified, 252 (54%) are classified as RBPs (Castello *et al*., 2012). This high prevalence of RBPs in SGs assemblies might be explained by their low complexity domains, which make RBPs prone to aggregation and facilitates protein-protein interactions (Hennig et al., 2015). Overall, this complex composition of SGs seems to underlie the variety of pathways and mechanisms in which they could be involved, and the crucial role of their assembly/disassembly in the context of normal cellular function, which will be discussed in the following section.

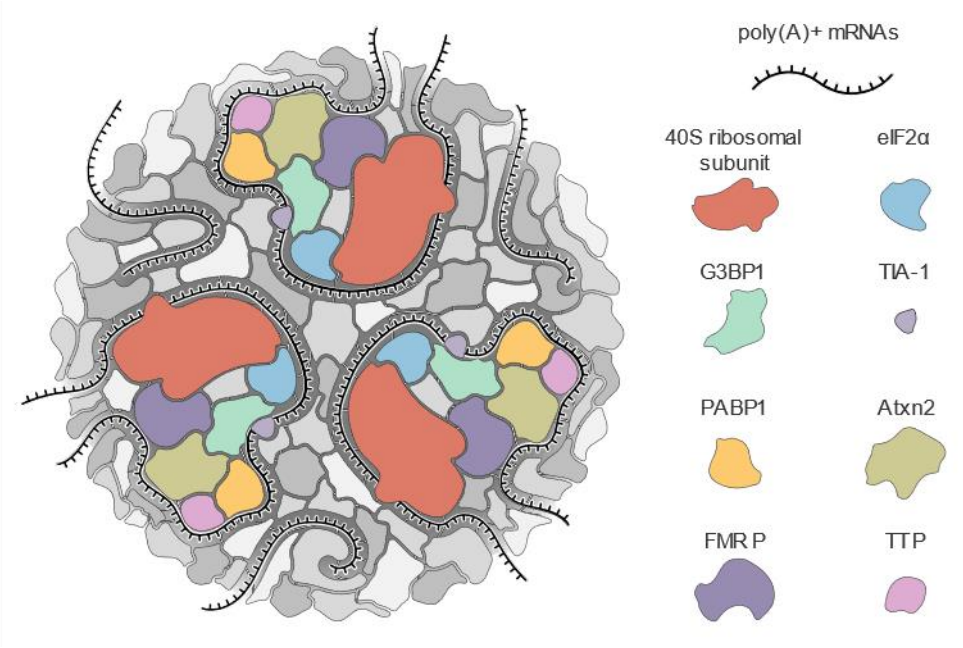

Fig. 1.10. **Stress granule components.** Stress granules are multimolecular cytoplasmic foci that assemble as part of the cellular response to stress. They largely derive from stalled pre-initiation translation complexes and are mainly comprised of poly(A)$^+$ mRNA molecules, 40S ribosomal subunits and a vast array of proteins (more than 450 described so far). The majority of these are RBPs (54%) that bind to each other and to the other SGs components. They include eukaryotic translation initiation factor 2 subunit alpha (eIF2α), ras GTPase-activating protein-binding protein 1 (G3BP1), T-cell intracellular antigen-1 (TIA-1), polyadenylate-binding protein 1 (PABP1), ataxin-2, fragile X mental retardation protein (FMRP) and tristetraprolin (TTP). The unspecified shapes coloured in grayscale represent the remaining proteins counted among the numerous SGs protein components (Marcelo et al., 2021b).

1.6.4 Stress granules functions

As mentioned before, SGs play an important role in cellular response, through a set of different functions that are interconnected (Fig. 1.11) (see Marcelo et al., 2021b for a detailed review of these functions). Kedersha and co-workers firstly proposed that SGs participate in translational arrest during a stress response (Kedersha et al., 1999). They observed that upon phosphorylation of the translation initiation factor eIF2α, SGs were assembled leading to translation arrest, therefore suggesting that these *foci* have functions connected with mRNA translation and localization. Later, it was hypothesized that transiently-formed SGs act as sites where RNA translation is repressed and reprogramed under stress conditions (Anderson and Kedersha, 2008). The hypothesis that SGs might be active effectors of translational repression is further reinforced by the

fact that small ribosomal subunits, translation initiation factors, and other components involved in translation are also recruited into SGs (Anderson and Kedersha, 2009). Moreover, SGs formation is positively correlated with a decrease in global translation levels (Anderson and Kedersha, 2009) and several SGs components are known to function as translational repressors. On the other hand, opposing studies have suggested that SGs formation is not essential for global translation repression during stress (Loschi et al., 2009; Mokas et al., 2009) and that the impairment of SGs assembly does not influence global protein synthesis (Ohn et al., 2008; Mokas et al., 2009). Therefore, it is not completely clear if SGs assembly are essential for translational repression and further studies are needed to clearly establish SGs role in these mechanisms.

SGs are also proposed to function as transient storage sites for mRNAs released from disassembled polysomes during stress. In fact, upon SGs formation, mRNAs of housekeeping genes are stored inside these foci (Anderson & Kedersha, 2009; N Kedersha & Anderson, 2002; Matsuki *et al*., 2013). When the stressful period ceases, SGs are disassembled and the stored mRNAs can either move back to polysomes to restart translation, or be degraded in the PBs (Kedersha & Anderson, 2002; Kedersha & Anderson, 2007). This confers an energetic advantage to the cells to overcome homeostasis after stress removal, since *de novo* protein synthesis is an energetically expensive process for the cell. Consequently, SGs have been implicated in the mRNA triage process (Kedersha & Anderson, 2002; Kedersha & Anderson, 2007), through which mRNA molecules from disassembling polysomes are sorted and the fate of individual transcripts is determined. It was observed that in the presence of cellular stress, both SGs and PBs, which constitute a type of cytoplasmic granules involved in mRNA degradation, assemble (Kedersha et al., 2005). SGs an PBs can dock for the exchange of different components among them, prioritizing the translation or degradation of some mRNA transcripts over others, thereby altering the cell proteome, until stress conditions subside. Whereas specific transcripts are selected for decay by destabilizing proteins, other transcripts are bound by stabilizing proteins for transport or storage, within the SGs or elsewhere (Anderson and Kedersha, 2008). Additionally, it was hypothesized that SGs assembly may help cells prevent the accumulation of misfolded proteins by reducing the synthesis of certain transcripts, while optimizing the translation of

mRNAs involved in the stress response. For example, several mRNAs encoding proteins involved in stress response, like heat shock proteins, are not found inside SGs (Kedersha et al., 2005).

Additionally, multiple lines of evidence support that SGs regulate diverse signalling pathways, by sequestering diverse signalling molecules, thus interfering with cell survival, metabolism and growth processes (Kedersha et al, 2013). For example, SGs were shown to play a role in cellular growth by regulation of the mTOR pathway, which monitors nutrient levels and energy availability to promote cell growth (Hofmann et al., 2012; Fournier et al., 2013; Thedieck et al., 2013; Wippich et al., 2013; Fan et al., 2017). Importantly, SGs assembly and dynamics may be important in the cellular decision of undergoing apoptosis or not, upon a stress stimulus. These *foci* sequester numerous apoptosis regulatory factors, possibly inhibiting or delaying stress-induced cell death signalling (Kedersha et al., 2013). For example, during severe, apoptosis-inducing, stress, the receptor of activated protein C kinase 1 (RACK1) protein binds to the stress-responsive MAP 3 kinase (MTK1) and facilitates its activation; during modest stress RACK1 is recruited to SGs, limiting MTK1 kinase activation and avoiding apoptosis (Arimoto et al., 2008). Furthermore, in stressed cells, SGs formation reduces the production of reactive oxygen species, thereby also preventing apoptosis (Takahashi et al., 2013).

Several studies also suggested a role of SGs in the inhibition of viral replication, by sequestering and binding cell components, as part of their role in translational arrest and RNA decay (Onomoto et al., 2012; Ruggieri et al., 2012; White and Lloyd, 2012; Yoo et al., 2014; Reineke et al., 2015; Mccormick and Khaperskyy, 2017; Reineke and Neilson, 2019).

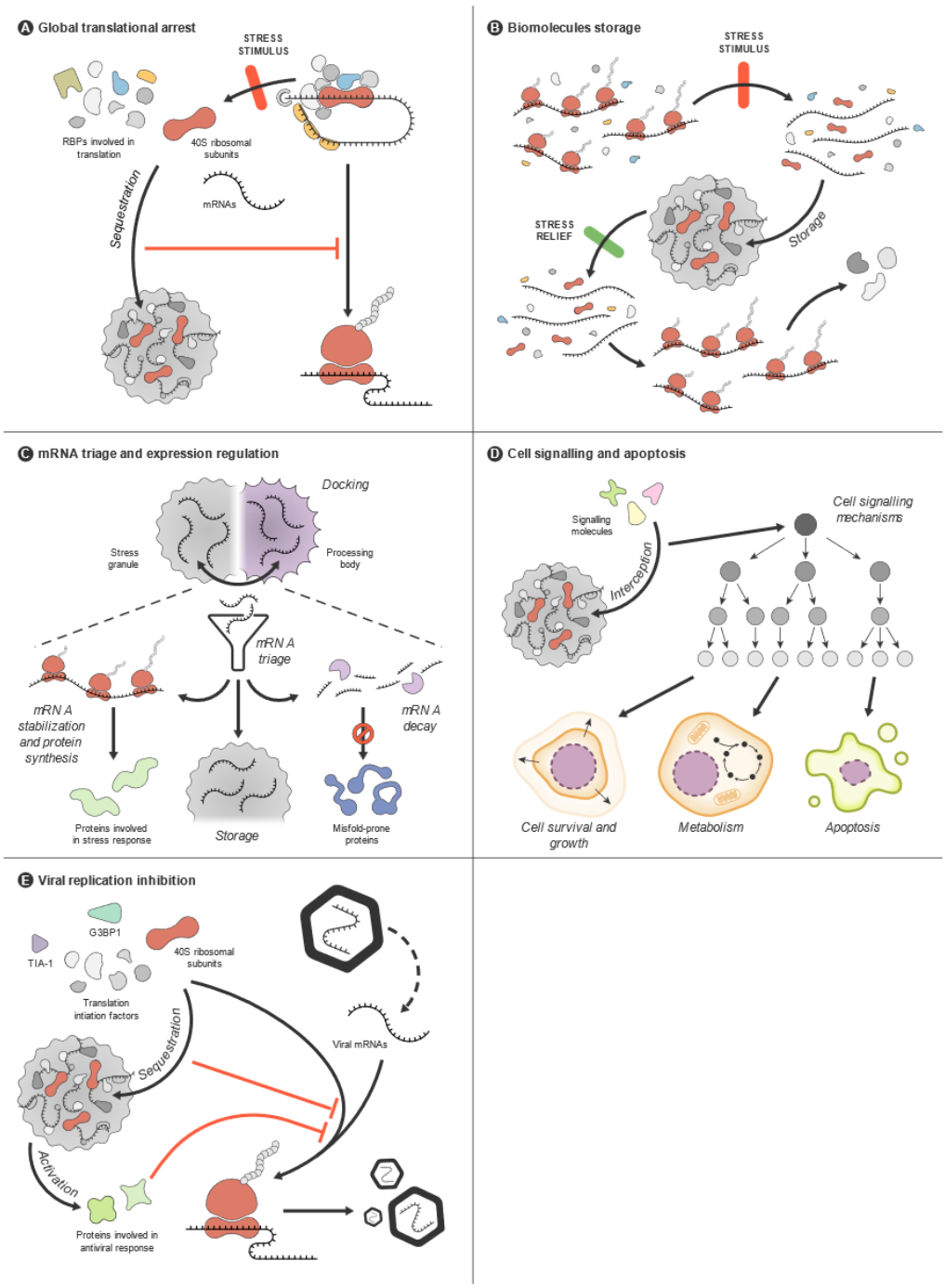

Fig. 1.11. **Stress granules functions.** SGs participate in the cellular response to stress through a set of different actions that are interconnected and derive from the individual activities of SG components and from the assembly/disassembly of these foci. **A)** SG formation involves the disassembly of translation initiation complexes and the coalescence of mRNAs molecules, ribosomal subunits and many proteins involved in translation, resulting in translational arrest and protein synthesis suppression. Additionally, several SG components are known to act as translational repressors. **B)** SGs function as stores of RNAs in cells under stress, allowing a rapid mobilization of these molecules when the damaging conditions subside. **C)** SGs may modulate the

expression of specific proteins during stress, by directing specific mRNA species to different possible fates. This action appears to involve an exchange of mRNAs between SGs and PBs, upon docking of these two types of RNA granules. Translation of some proteins involved in stress responses may be prioritized, some mRNAs may be kept stored in SGs or elsewhere, while others, such as those codifying proteins prone to misfolding, may be targeted for degradation by the processing bodies. **D)** By sequestering signaling molecules, SGs may trigger signaling cascades that regulate or modify cell growth, survival or metabolism, or which promote apoptosis. **E)** SGs play a role in the cellular response against viral infection, by sequestering the endogenous translational machinery necessary for viral protein expression (Marcelo et al., 2021b).

1.6.5 Stress granules and Polyglutamine diseases

More recently, several studies have focused on investigating SGs involvement in the context of human disease. In fact, they have been implicated in different human conditions such as cancer (Anderson et al., 2015), aging (Masuda et al., 2009) and neurodegenerative diseases (Wolozin, 2012). However, the role that SGs assembly/disassembly and its components might play in polyQ diseases pathogenesis has not been so far elucidated. Considering that SGs are structures which result from a multi-protein assembly process during a stress response, and that polyQ-expanded proteins expression induces a multifactorial and permanent state of cell stress, it seems relevant to look for the relation that SGs formation may have with the aberrant protein aggregation observed in the PolyQ disorders. In this section, it will be discussed the hypothesis whereby SGs dysfunctionality, might play a pivotal role in the pathogenesis of PolyQ diseases.

1.6.5.1 Cell stress in polyQ diseases

While the molecular and cellular physiopathology of polyQ diseases remains unclear, it is increasingly clear that it involves the dysfunctionality of several biological systems. As discussed in SCA3 and SCA2 diseases sections, current evidence suggests that cells affected by polyQ toxicity are subjected to cell stress from more than one source. Particularly, it has been reported that polyQ-expanded protein expression triggers proteotoxic and oxidative stress. PolyQ-expanded proteins pose challenges to the mechanisms responsible for

proteostasis, as they are prone to aggregate and to engage in abnormal intermolecular interactions. Proteotoxic stress is associated with a collapse of the protein quality control mechanisms, including autophagy and UPS degradation systems (Labbadia and Morimoto, 2013; Koyuncu et al., 2017). These mechanisms have been described to be affected by PolyQ protein expression, in different PolyQ diseases (Nóbrega and Pereira de Almeida, 2018). Endoplasmic reticulum stress, translated as an accumulation of proteins of the secretory pathway in this cell compartment, may also constitute a source of proteotoxic stress in polyQ diseases. Moreover, one of the targets of polyQ protein toxicity is mitochondrial function (Johri and Beal, 2012; Egorova and Bezprozvanny, 2019; Matos et al., 2019; Paul and Snyder, 2019). As previously discussed, in experimental models of several polyQ diseases, including SCA3 and SCA2, changes in these organelles have been associated with the disruption of the redox equilibrium and the production of reactive oxygen species, the effectors of oxidative damage to biomolecules (Araujo et al., 2011; Laço et al., 2012; Cornelius et al., 2017; Hsu et al., 2017; Wardman et al., 2020). These and other sources of cell stress may contribute to a state of chronic stress in cells affected by polyQ protein toxicity.

1.6.5.2 Sequestration of SGs components into polyQ aggregates

It has been demonstrated that several SGs components are found in the neuropathological protein aggregates that are characteristic of polyQ diseases (Elden et al., 2010; Furukawa et al., 2009; Uchihara et al., 2001; Waelter et al., 2001). For example, it was reported that TIA-1 co-localizes with perinuclear mutant Htt aggregates, in cell cultures (Waelter et al., 2001), and with the Htt mutant aggregates of a HD mouse model (Furukawa et al., 2009). In SCA2 brain patients, TDP-43 co-localizes with pathological inclusions of mutant ataxin-2, which is a SG component (Elden et al., 2010). Moreover, the SGs component ataxin-2 localizes to pathological inclusions in SCA3 patients brain (Uchihara et al., 2001b). This sequestration of SGs components into polyQ-expanded mutant aggregates might disturb SGs formation, having a negative impact on the cell, possibly affecting stress responses and RNA metabolism, ultimately contributing to cytotoxicity.

1.6.5.3 Altered stress granules assembly and disassembly

As mentioned before, the biological features of SGs composition can be altered depending on stress effector or duration of the stress stimulus. In an acute, transient, stress state, induced by conditions such as oxidative, metabolic, hypoxic, or thermal stress, SGs form in the cytoplasm of the cells. Chronic SGs are different from the ones assembled during acute stress conditions. Although only a limited number of reports regarding the composition of chronic SGs is available, this type of granules appears to act as a nidus for the aggregation of some disease-linked proteins. During persistent periods of stress, the phase-separated proteins of the shell can mature to become a gel-like layer, promoting aggregation, and turning into more stable complexes (Wolozin and Ivanov, 2019). A chronic state of cell stress may also interfere with the normal functionality of stress response mechanisms, which may, in turn, have a deleterious effect on cell survival. The pathological aggregation of polyQ proteins and the abnormal interactions in which they engage can result in significant changes in the protein clearance mechanisms and in the cellular stress response pathways (Cowan et al., 2003; Takahashi and Ohnishi, 2009), which could prevent formed SGs from disassembling and/or hindering SG assembly in response to stress. One possible cause for imbalance of SG formation in polyQ diseases concerns the autophagy pathway. It has been shown that enhanced autophagy activity reduces the number of SGs (Ryu et al., 2014). It was also shown that SGs are cleared by autophagy in mammalian cells, as their clearance is reduced by the inhibition of autophagy or by the depletion of VCP/p97, which is implicated in the pathway (Buchan, 2014). Later, it was shown that SGs are cleared by autophagy, through the promotion of the formation of autophagosomes due to the recruitment of Syk kinase, another protein involved in autophagy, to SGs (Krisenko et al., 2015). Autophagy has been demonstrated to be impaired in PolyQ diseases, including SCA3 and SCA2 pathologies (Nixon, 2005; Zheng et al., 2010; Nascimento-Ferreira et al., 2011, 2013; Marcelo et al., 2021a). Thus, autophagy dysregulation may lead to the persistence of SGs, and the consequent sequestering of components involved in cellular response to stress. In turn, this process may contribute to the consolidation of the pathological protein aggregates. This

hypothesis is supported by the fact that normal SGs are free of misfolded proteins and autophagy players, whereas aberrant SGs contain misfolded proteins, which attract autophagy machinery components to SGs (Ganassi et al., 2016; Mateju et al., 2017).

1.6.5.4 Stress granules proposed involvement in polyQ diseases pathogenesis

Multiple evidence supports an involvement of SGs in the pathogenesis of polyQ diseases (Fig. 1.12). On one side, SGs components are found in polyQ-expanded mutant aggregates, which might impact SGs formation and affect normal cell responses to stress, thus contributing to cytotoxicity. Additionally, the expression of polyQ-expanded proteins leads to the dysfunctionality of several biological systems, including protein clearance, ER, and mitochondrial systems. The dysregulation of these biological processes triggers cellular stress inside affected cells, further contributing to a state of chronic stress in cells affected by polyQ protein toxicity. Moreover, SGs removal in neurons seems to be linked to the autophagic pathway, which is dysregulated in several polyQ disorders. Thus, autophagy impairment may contribute to the persistence of SGs, conditioning the availability of translational factors, mRNAs and other agents that are important to cellular function and that constitute SGs.

Overall, the idea that SGs play a relevant role in polyQ diseases pathogenesis opens a new avenue of research and interest in the field of polyQ disorders, further linking it with the cellular mechanisms implicated in stress response.

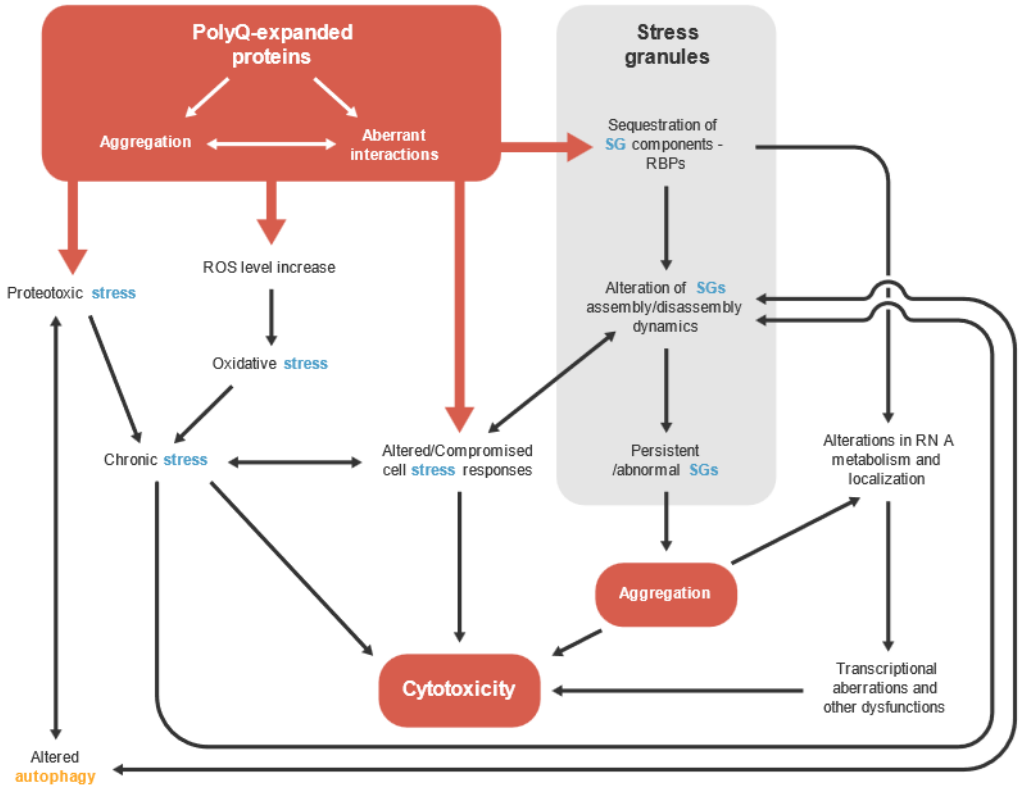

Fig. 1.12. **The putative involvement of stress granules in the molecular pathophysiology of polyglutamine diseases.** Proteins bearing an expanded polyglutamine (PolyQ) tract display a tendency to aggregate and to engage in aberrant intermolecular interactions. Association of PolyQ- expanded proteins with stress granules (SGs) components, in particular RNA-binding proteins (RBPs) that are often prone to aggregate, may alter the dynamics of SGs assembly and disassembly. This can compromise SGs functionality, contributing to the globally deficient cell stress response that has been described to be a component of the molecular pathophysiology of PolyQ diseases. Oxidative stress (associated with an increase in reactive oxidative species - ROS - levels) and proteotoxic stress, which are known to result from expanded PolyQ protein expression, may culminate in a state of chronic cell stress, which may add to the abnormal SG assembly/disassembly dynamics and lead to the persistence of SGs. SGs formed under chronic stress are known to acquire abnormal properties and to seed toxic aggregation. Defects in autophagy caused by PolyQ protein expression may also contribute to the persistence of SGs and to their altered dynamics. Additionally, both the sequestration of RBPs to PolyQ aggregates and the toxic aggregation triggered by SGs may alter RNA metabolism and its subcellular localization, which in turn may lead to transcriptional aberrations. Chronic stress, a reduced ability to cope with cell stress, transcriptional alterations and a pernicious cascade of protein aggregation involving both the PolyQ-expanded proteins and the SGs may combine to produce the cytotoxic profile with is at the basis of cell dysfunction and loss, in PolyQ diseases (Marcelo et al., 2021b).

1.7 Objectives

Despite important data suggestive of SGs involvement in PolyQ diseases, their exact role in these disorders remains unclear. Therefore, the general goal of this project is to contribute to the clarification of SGs and its components' role in the context of PolyQ diseases pathogenesis, trying to identify new pathways and targets for therapeutic intervention, using spinocerebellar ataxia type 3 and type 2 (SCA3 and SCA2) as PolyQ disease models. From this general goal, two broad specific objectives were outlined:

I) To evaluate which SGs components have their expression altered in SCA3 mouse models and modulate selected components as possible therapeutic targets.

Previous evidence showed that SGs components are sequestered into polyQ-expanded aggregates in patients' brain. Moreover, SGs components gene expression levels were found to be significantly altered in individuals affected with neurodegenerative diseases, including the PolyQ disease HD. Therefore, we aimed to investigate which SGs components had their levels up- or downregulated in a SCA3 transgenic mice. The two most significant and relevant components were selected to assess its modulation impact in *in vitro* and *in vivo* models. For these studies, we used cellular and animal models which featured several SCA3 characteristics, including mutant protein aggregation as well as neuropathological and motor function impairments. Finally, it was investigated whether selected components mechanism of action was associated with SGs formation.

II) To develop and characterize a novel and suitable mouse model for assessment of novel potential therapeutic targets for SCA2 disease.

The generation of animal models highly improved the understanding of PolyQ diseases, including SCA3 and SCA2 disorders. Nevertheless, mouse models that exhibit early and substantial phenotypic alterations resembling SCA2 disease are not available. Moreover, the existing models only focus on cerebellar pathology, while degeneration of other brain regions have been described. Thus, we aimed to develop a mouse model using lentiviral vectors to express the mutant Atx2 in

the striatum tissue. We fully characterized the neuropathological alterations induced by expression of mutant protein. Additionally, we assessed whether our novel lentiviral mouse model could be a suitable tool to investigate potential therapeutic targets, by investigating the impact of one of the selected SGs components.

Chapter 2. Modulation of stress granules components as a therapeutic approach for spinocerebellar ataxia type 3

2.1 Introduction

Polyglutamine diseases are a group of rare highly debilitating neurodegenerative disorders that, so far, remain uncurable. These pathologies are caused by abnormal repetitions of the triplet CAG in the disease causing genes, resulting in a toxic polyQ stretch in the respective translated proteins, which have a tendency to aggregate in large multiprotein inclusions (Nóbrega and Pereira de Almeida, 2018). Within the PolyQ group, spinocerebellar ataxia type 3 is the second most common PolyQ disease, as well as, it is the most frequent SCA, affecting 1.5 in 100.000 individuals (Gardiner et al., 2019). The gene implicated in SCA3 disease is *ATXN3* and the respective translated protein is ataxin-3 (Kawaguchi et al., 1994). Besides carrying the CAG/polyQ repeat expansion, the genes and proteins associated with PolyQ diseases do not share significant homology, having distinct biological functions (Paulson, 2018). Nevertheless, these disorders share among them several features, including common pathogenic mechanisms. The most notorious neuropathological hallmark is the presence of insoluble mutant polyQ-expanded protein aggregates, which are found in patients' neuronal tissues (Ross et al., 1999). The polyQ-expanded proteins engage in aberrant interactions and recruit several other functional proteins to aggregates assembly, including RBPs, chaperones, proteasome components and transcription factors (McCampbell et al., 2000; Muchowski et al., 2000; Chai et al., 2001). The formation of insoluble large aggregates and sequestration of important cellular players may compromise the functioning of diverse biological pathways, such as transcription, protein quality control systems and mitochondrial function (Bauer and Nukina, 2009). The dysfunction of important cellular pathways, eventually, leads to the progressive cell death of numerous neuronal populations, which results in an extensive degeneration in various brain regions and severe clinical manifestations in affected individuals (Seidel et al., 2017).

On the other hand, the dysregulation of biological mechanisms increases the levels of cellular stress, which triggers cells to activate several responses to overcome the stress. An important player in the cellular stress response is the formation of stress granules, which are specialized membraneless compartments composed of messenger ribonucleoprotein complexes stalled upon inhibition of

translation initiation (Buchan and Parker, 2009). Several studies have been linking SGs to different human conditions, including different neurodegenerative disorders (Asadi et al., 2021). Moreover, a recent manuscript from our group outlined the studies reporting the involvement of SGs in PolyQ diseases (Marcelo et al., 2021b). In this line, multiple evidence supports an important role of SGs in PolyQ diseases pathogenesis, including: (i) SGs components are recruited and found in polyQ-expanded mutant aggregates, which might impact SGs formation and affect normal cell responses to stress, thus contributing to cytotoxicity; (ii) the expression of polyQ-expanded proteins leads to the dysfunctionality of several biological systems, triggering cellular stress, further contributing to a state of chronic stress in cells; (iii) impairment of protein clearance systems, particularly autophagy, may compromise SGs disassembly and contribute to the persistence of SGs, conditioning the availability of translational factors, mRNAs and other agents that are important to cellular function. Overall, the hypothesis that SGs play a relevant role in PolyQ diseases pathogenesis opens a new avenue of research and interest in the field of these group of neurodegenerative diseases, particularly for the discovery of novel targets for a therapeutic intervention.

Therefore, the aim of this part was to study the role of selected components of SGs in the context of SCA3 disease. Specifically, we analysed the gene expression of SGs components, retrieved from a transcriptomic data set of a SCA3 transgenic mouse model to search which components have their levels altered in the disease context. Importantly, the SGs components whose levels were most altered were selected for modulation in cellular and mouse models of SCA3, to evaluate whether SGs and/or these components could be potential therapeutic targets for SCA3 disease.

2.2 Material and Methods

2.2.1 Gene expression data and ontology analysis

Expression profile for all the 464 identified mammalian SGs components, listed in the Mammalian Stress Granules Proteome (MSGP) database (https://msgp.pt/), were extracted from a transcriptome data set of *Mus musculus* pons samples available in Gene Expression Omnibus (GEO accession: GSE117605). In total, 6 wild-type mice, 4 SCA3-Q15 transgenic mice and 4 SCA3-Q84 transgenic mice were used for RNA-sequencing. Gene expression levels were statistically analyzed using one-way ANOVA followed by *post hoc* Tukey's multiple comparison test in GraphPad software (La Jolla, USA), comparing the different groups: WT versus Q15, WT versus Q84, and Q15 versus Q84. An adjusted P value < 0.05 evaluated the SGs components that were statistically different among the three groups. Additionally, differential gene expression levels for some mammalian SGs components from a SCA2-Q100 KI mouse model compared to wild-type littermates were kindly provided by the authors of the study (Sen et al., 2019).
The PANTHER (Protein ANalysis THrough Evolutionary Relationships, http://www.pantherdb.org/) classification system was used to perform gene ontology analysis for molecular function of the genes statistically up- or downregulated in SCA3 and SCA2 mouse models.

2.2.2 Neuroblastoma cell culture and transfection

Mouse neuroblastoma line-derived cells (N2A), obtained from the American Type Culture Collection cell biology bank (CCL-131), were cultured in Dulbecco's modified Eagle's medium (DMEM) supplemented with 10% fetal bovine serum (FBS), 100 U/ml penicillin and 100 mg/ml streptomycin (Gibco) at 37◦C in 5% CO2/air atmosphere. For transfection assays, complexes of 3µl PEI solution (polyethylenimine 1mg/ml, Tebu-bio) with 500ng of DNA plasmids were formed in 10µl DMEM without supplementation and added to cells previously cultured in 12-well plates for 24h. Transfection reagents were left in cells for a 48h-period incubation, following cells harvest for immunocytochemistry or Western blot

assays. For SGs induction, cells were treated with 0.05 M sodium arsenite (SA, Sigma Aldrich 10 µg/mL), during 1h before harvest. The following DNA constructs were used: human full-length ataxin-3 with an EGFP (enhanced green fluorescent protein) tag carrying a mutant polyQ segment (84Q – Atx3MUT) (Addgene #22123, kindly provided by Dr. Henry Paulson); a CRISPR (Clustered Regularly Interspaced Short Palindromic Repeats) -Cas9 system with a guide RNA for *CARHSP1 Mus musculus* gene under the expression of the U6 promoter and inserted in a lentiviral vector LV05 (Cr-Carhsp1) (Sigma-Aldrich); a CRISPR-Cas9 system with a guide RNA for *PUM1 mus musculus* gene under the expression of the U6 promoter and inserted in a lentiviral vector LV05 (Cr-Pum1) (Sigma-Aldrich); a CRISPR-Cas9 system with a guide RNA for *Escherichia coli* lac Z gene under the expression of the U6 promoter and inserted in a lentiviral vector LV02 (Cr-CT) (Addgene #52961), which has been validated as having no targets in *mus musculus* cells (Platt et al., 2014).

2.2.3 Animals

For this work, C57/BL6 mice and SCA3-Q69 transgenic mice were breed in the animal house facility of the Algarve Biomedical Center Research Institute (ABC-RI) of University of Algarve. All animals were housed in a temperature-controlled room on a 12h light/dark cycle, with food and water were supplied ad libitum. All proceedings were carried out in accordance with the European Community directive (86/609/EEC) for the care and use of laboratory animals. The researchers received certified training (FELASA course) and approval to perform the experiments from the Portuguese authorities (Direcção Geral de Alimentação e Veterinária) in the project Neuropath (421/2019). The SCA3-Q69 transgenic mouse model was developed and characterized by Torashima and collaborators in 2008 (Torashima et al., 2008). In this model, C57BL/6 background mice express the N-terminal truncated human ataxin-3 protein, carrying 69 glutamine repeats, and a N-terminal haemagglutinin (HA) epitope, under the regulation of the L7 promoter, which drives transgene expression into cerebellar Purkinje cells. The truncated Atx3 fragment lacks the Josephin domain and two UIMs domains, consisting only in 69 glutamine repeats with 4 and 42 amino acids at its N-terminus and C-terminus, respectively. The breeding of these animals occurred

by backcrossing heterozygous males with C57BL/6 females. At 3 weeks of age, an ear punch of all animals was collected for genomic DNA extraction, using the GeneJET Genomic DNA Purification Kit (ThermoFisher Cientific), followed by DNA concentration and purity assessment using the NanoDropTM 2000 (ThermoFisher Scientific). Posteriorly, samples genotyping was performed by PCR using DreamTaq DNA Polymerase (ThermoFisher Cientific), according to manufacturer instructions, in a C1000 Touch Thermal Cycler (BioRad). The sequence of primers used for DNA amplification were the following: ATXN3 transgene – Forward 5'ATGTACCCATACGATGTTCC 3', Reverse 5' CTAGCGAGGGAATGAAGAAT 3'; B-actin control gene – Forward 5' GGAGACGGGGTCACCCACAC 3'; Reverse 5' AGCCTCAGGGCATCGGAACC 3'.

2.2.4 Lentiviral vectors

LVs encoding for human full-length mutant ataxin-3 with 84 glutamines (Atx3MUT) under the control of the mouse phosphoglycerate kinase 1 (PGK) promoter were produced in HEK (human embryonic kidney) 293T cells using a four-plasmid system, described elsewhere (Pereira de Almeida et al., 2001), by our research group in ABC-RI facility, University of Algarve. LVs encoding for CRISPR-Cas 9 system guided for *Escherichia coli* lac Z gene under the control of the eukaryotic EF-1 alpha promoter were produced in HEK 293T by our research group in ABC-RI facility, University of Algarve. The LVs titer was quantified using the Lentivirus qPCR Titer Kit (Applied Biological Materials Inc, Vancouver, Canada), allowing the determination of the virus titer in infectious units per ml (IU/ml).

Additionally, LVs encoding for CRISPR-Cas 9 system guided for Carhsp1 (Cr-Carhsp1) and Pum1 (Cr-Pum1) under the control of the eukaryotic EF-1 alpha promoter were produced in HEK (human embryonic kidney) 293T and quantified by p24 antigen ELISA (RETROtek, Gentaur, France) by ViraVector facility, University of Coimbra.

2.2.5 Modulation of Carhsp1 and Pum1 levels in mouse striatum

For modulation of Carhsp1 and Pum1 levels in mouse striatum tissue, concentrated LVs viral stocks encoding for Cr-Carhsp1, Cr-Pum1 and Cr-CT were thawed on ice and homogenized. Adult (8/10-week-old) C57/BL6 mice were anesthetized through intraperitoneal injection (IP) of a mixture of ketamine (75mg/kg, Nimatek, Dechra) with medetomidine (0.75mg/kg, DOMTOR®, Esteve). LVs were administered through a stereotaxic surgery into the left and the right hemisphere of the striatum according to the following brain coordinates relative to bregma: antero-posterior (+0.6mm); lateral (±1.8mm); ventral (-3.3mm). A total concentration of 400ng (Cr-Carhsp1 and Cr-Pum1) of p24 antigen of LVs, while 2E9 IU (Cr-CT) of LVs, were injected at a rate of 0.25µl/min, by means of an automatic injector (Stoelting Co., Wood Dale, IL, USA), into mice striatum using a 34-gauge blunt-tip needle linked to a Hamilton syringe (Hamilton, Reno, NV, USA). Four weeks after surgery, mice were sacrificed through cervical dislocation and striatal punches were collected for posterior Western blot analysis.

2.2.6 SCA3 striatal lentiviral mouse model

To generate the SCA3 lentiviral mice, concentrated LVs viral stocks encoding for Atx3MUT, Cr-Carhsp1, Cr-Pum1 and Cr-CT were thawed on ice and homogenized. Adult (8/10-week-old) C57/BL6 mice were anesthetized through IP of a mixture of ketamine (75mg/kg, Nimatek, Dechra) with medetomidine (0.75mg/kg, DOMTOR®, Esteve). LVs were administered through a stereotaxic surgery into the left and the right hemisphere of the striatum according to the following brain coordinates relative to bregma: antero-posterior (+0.6mm); lateral (±1.8mm); ventral (-3.3mm). A total concentration of 400ng (Cr-Carhsp1 and Cr-Pum1) of p24 antigen of LVs, while 1E8 IU (Atx3MUT) and 1E9 IU (Cr-CT) of LVs, were injected at a rate of 0.25µl/min, by means of an automatic injector (Stoelting Co., Wood Dale, IL, USA), into mice striatum using a 34-gauge blunt-tip needle linked to a Hamilton syringe (Hamilton, Reno, NV, USA). Four weeks after surgery, mice were sacrificed for posterior analysis.

2.2.7 SCA3-Q69 transgenic mice cerebellar injections

To downregulate the levels of Carhsp1 and Pum1, concentrated LVs viral stocks encoding for Cr-Carhsp1, Cr-Pum1 and Cr-CT were thawed on ice and homogenized. Juvenile (4/5-week-old) SCA3-Q69 transgenic mice were anesthetized through intraperitoneal injection (IP) of a mixture of ketamine (75mg/kg, Nimatek, Dechra) with medetomidine (0.75mg/kg, DOMTOR®, Esteve). LVs were administered through a stereotaxic surgery into the cerebellar vermis according to the following brain coordinates: − 1.6 mm rostral to lambda, 0.0 mm midline, and − 1.0 mm ventral to the skull surface, with the mouth bar set at − 3.3 mm. A total concentration of 1000ng (Cr-Carhsp1) and 800ng (Cr-Pum1) of p24 antigen of LVs were injected at a rate of 0.25µl/min, by means of an automatic injector (Stoelting Co., Wood Dale, IL, USA), into mice striatum using a 34-gauge blunt-tip needle linked to a Hamilton syringe (Hamilton, Reno, NV, USA). Also, 2E9 IU of Cr-CT LVs were injected at the same 0.25µl/min rate. Mice were subjected to behavioral analysis and were sacrificed ten weeks after surgery.

2.2.8 Behavioral assessment

One day before and 3-, 6- and 9-weeks after surgery, SCA3-Q69 transgenic mice were subjected to different motor tests to assess motor function performance, following the same protocol described before (Nóbrega et al., 2013b). Motor coordination and balance were evaluated in a rotarod apparatus (47650 Rota-Rod NG, Ugo Basile). Mice were placed on the rotarod at a constant speed (5 rpm) for a maximum of 5 min and at an accelerating speed (4–40 rpm, in 5 min) and the latency to fall was registered. Motor coordination and equilibrium were also evaluated in the beam walking test. Animals were placed in an elevated beam, with different narrow diameters (1,9 and 1,1 cm) and 54 cm of length, and the time taken to cross the beam until reaching a safe platform was recorded. Moreover, the swimming performance was also used to analyze motor coordination by placing mice inside a tank full of water (100x10.5x20 cm) and registering the time taken to transverse the tank and reach an escape platform at the end. All animals performed three trials for each motor test with a 15min rest

between trials and the mean latency to fall off the rotarod, and the mean time to cross the beams and the swimming pool were used for statistical analysis. Additionally, the footprint test was used to evaluate mice gait. For that purpose, hind and front paws were coated with different color, nontoxic ink, and the animals were allowed to walk along a 100-cm-long, 11-cm-wide runaway (with 35-cm high walls) over a fresh sheet of white paper, leaving a trail of footprints. The footprint patterns were analyzed for fore and hind paw overlap, stride length, and hind-base and front-base width. Measures from the center of six consecutive right and left footprints were taken, excluding steps made at the beginning and end of the run.

2.2.9 Tissue preparation

For all immunohistochemical assays, animals received an anesthesia (mixture described above) overdose, followed by a transcardial perfusion with 4% paraformaldehyde (PFA) solution SigmaAldrich). Upon removal, brains were left 24h in 4% PFA solution, dehydrated in a 30% sucrose/0.1M phosphate buffer solution (PBS) for 48h and cryoprotected at -80°C degrees. Posteriorly, coronal brain slices of 20µm thickness and sagittal brain slices of 30µm thickness were obtained using a cryostat (Cryostar NX50, ThermoFisher Scientific) and stored in freefloating PBS with 0.05µm sodium azide solution at 4°C. For western blotting procedures, animals received an anesthesia overdose, followed by cervical dislocation. Brains were removed and striatal punches, using a Harris Core pen with 2.5 mm diameter (Ted Pella Inc., Redding, California, USA), were collected and stored at -80°C until subsequent processing.

2.2.10 Immunochemical procedures

2.2.10.1 Immunocytochemistry

Immunocytochemistry procedure was performed based on protocols described elsewhere (Mendonça et al., 2015; Nóbrega et al., 2015a). Briefly, for cells harvest, we washed cultures with PBS and fixed it with 4% PFA for 20min. Cells were permeabilized with 1% Triton™ X-100 (Sigma) and blocked using 3%

Bovine Serum Albumin (Nzytech) in PBS. Incubation with primary antibodies was done overnight at 4°C. After PBS washes for antibodies removal, cells were incubated in secondary antibodies for 2h at room temperature (RT). Finally, cells were washed with PBS and coverslips were mounted on microscope slides using Fluoromount-G™ medium with DAPI (4′,6′-Diamidino-2′-phenylindole) (ThermoFisher Scientific). Images were acquired with 40x objective in a Zeiss Axio Imager Z2 for the quantification of number of cells with aggregates, and with 63x objective in a Zeiss LSM710 confocal microscope for figure representation.

2.2.10.2 Immunohistochemistry – free floating incubation

Immunohistochemistry assays were performed based on protocols described elsewhere (Nascimento-Ferreira et al., 2011; Nóbrega et al., 2013a, 2014). For visible microscopy analysis, mouse brain slices were incubated in PBS/0.1% diphenylhydrazine for 30min at 37°C. Then, all sections were left in PBS/10% normal goat serum (Gibco)/0.1% Triton X blocking solution for 1h at RT, followed by overnight incubation with primary antibodies at 4°C. Posteriorly, slices were incubated in biotinylated secondary antibodies (1:200, Vector Laboratories) for 2h at RT and then in a reaction with the Vectastain elite avidin-biotin-peroxidase kit and by 3,3′-diaminobenzidine substrate (both from Vector Laboratories). After, sections were assembled over microscope slides, dehydrated in increasing degree ethanol solutions (75, 96 and 100%) and xylene, and finally coverslipped using mounting medium Eukitt (O. Kindler GmbH & CO, Freiburg, Germany). For fluorescence-labeling procedures, sections were incubated in the same blocking solution, followed primary and secondary fluorescent antibodies incubation as described above. After antibodies probing, slices were mounted in microscope slides and coverslipped using the Fluoromount-G™ medium with DAPI. Images were acquired with 20x objective in a Zeiss Axio Imager Z2 and Axio Scan.Z1 Slide Scanner microscopes.

2.2.10.3 Immunochemical antibodies

For immunochemical procedures, the following primary antibodies were used: mouse anti-ataxin-3 (1:1000, ref. 650402, BioLegend); rabbit anti-DARP-32 (1:1000, ref. AB10518, Merck Millipore); mouse anti-FLAG (1:1000, ref. F1804,

Sigma-Aldrich); rabbit anti-G3BP1 (1:1000, ref. 07-1801, Merck Millipore); mouse anti-calbindin-D-28K (1:1000, ref. C9848, Sigma Aldrich); rabbit anti-HA (1:1000, ref. ab9110, Abcam). The following secondary antibodies were used: goat biotinylated anti-mouse (1:200, ref. BA-9200, Vector Laboratories); goat biotinylated anti-rabbit (1:200, ref. BA-1000, Vector Laboratories); goat Alexa Fluor® 594 anti-mouse (1:500, ref. A11005, Invitrogen); goat Alexa Fluor® 594 anti-rabbit (1:500, ref. A11012, Invitrogen); goat Alexa Fluor® 488 anti-rabbit (1:500, ref. A11008, Invitrogen); goat Alexa Fluor® 488 anti-mouse (1:500, ref. A11001, Invitrogen).

2.2.11 Immunochemistry quantitative analysis

For quantification of mutant Atx3 aggregates and DARPP-32 staining loss in the SCA3 lentiviral mouse model, 18 coronal sections per animal were analyzed in ZEN lite software (Zeiss), so that a complete rostrocaudal picture of the striatum was obtained (14-16 transduced sections). Atx3 inclusions were manually counted in all animals. DARPP-32 neuronal lesion area was manually measured for all animals, allowing quantification of depleted volume according to the formula: volume = d*(a1 + a2 + a3), where d is the distance between serial sections (160 µm) and a1 + a2 + a3 are depleted areas for each individual section.

For quantification of Atx3 aggregates and Purkinje cells number in SCA3-Q69 transgenic mouse model, 8 sagittal sections per animal were analyzed using the Image J software (USA). For each section, the number of mutant Atx3 aggregates and Purkinje cells, as well as the area of cerebellar lobes II&III, IX and X were counted blindly using the Analyze Particle tool and Measurement tool.

2.2.12 Western blot

Cell extracts were lysed in 10x RIPA solution (Merck Millipore) and mouse striatal punches were homogenized in a urea/DTT solution, both containing a cocktail of protease inhibitors (Roche pharmaceuticals), followed ultrasound sonication. Protein concentration levels were determined using Pierce™ BCA Protein Assay

Kit (Thermo Scientific) for cell lysates and using NZYBradford reagent (Nzytech) for mouse samples. Sixty to eighty protein µg were resolved in SDS-polyacrylamide gels (7.5%, 10% and 12.5%). Followed by protein transfer to PVDF membrane (Merck Millipore) and antibody probing using the following antibodies: rabbit anti-Carhsp1 (1:1000, ref. PA5-21471, Invitrogen, ThermoFisher Scientific); rabbit anti-Pum1 (1:1000, ref. PA5-30327, Invitrogen, ThermoFisher Scientific); mouse anti-ataxin-3 (1:1000, ref. 650402, BioLegend); mouse anti-β-actin (1:5000, ref. A5316, Sigma Aldrich). Optical densiometric analysis was carried out using Image J software (USA).

2.2.13 Statistical analysis

All statistical analysis was performed using Student's *t*-test for two groups or one-way ANOVA followed by *post hoc* Tukey's multiple comparison test for three groups, using GraphPad software (La Jolla, USA).

2.3 Results

2.3.1 CARHSP1 and PUM1 genes are upregulated in SCA3 and SCA2 mouse models

SGs sequester for its assembly several proteins, depending on the cell type and the type of stress stimulus induced (Vanderweyde et al., 2013). Recently, our group has identified 464 mammalian SGs components, gathering the information of studies published so far, and listing them in an open access database (Nunes et al., 2019). In this study, it was also analysed published transcriptomic data, in which we found that several SGs components have their expression altered in several neurodegenerative disorders, including the PolyQ disease HD. Taking all these information into consideration, we aimed at identifying the SGs components whose expression is significantly altered in the context of SCA3 disease, through gene profile analysis of transcriptional data from a transgenic mouse model, available in Gene Expression Omnibus (GEO accession: GSE117605). The transcriptome data set was retrieved from RNA-sequencing of pons tissue from 6 WT mice, 4 SCA3-Q15 transgenic mice and 4 SCA3-Q84 transgenic mice. We compared gene expression levels from mutant mice (Q84) with non-pathogenic polyQ-expansion mice (Q15) and WT animals for the 464 SGs components and found that 15 components were significantly upregulated while 3 components had their levels downregulated (Fig. 2.1A). Additionally, as SGs formation is a conservative process of the cellular response to a stress and polyQ diseases have common pathogenic mechanisms, we complemented this analysis with data from a SCA2 mouse model. We obtained the gene expression levels for some SGs components from SCA2-Q100 KI mice, kindly provided by the authors of the study (Sen et al., 2019). We observed that 10 components were significantly upregulated, whereas 6 components were downregulated in SCA2 mice compared to WT littermates (Fig. 2.1A). Next, we performed a gene ontology analysis of the 32 SGs components that were significantly altered in SCA3 and SCA2 mice, using the PANTHER classification system. Regarding the molecular function, most genes have binding activity (54,2%), while the rest of the genes are divided into catalytic activity function (18,2%), molecular regulator function (9,1%), and translation regulation activity (6,1%) (Fig. 2.1B). Overall,

upon analysis of all transcriptomic data gathered and taking also in consideration their molecular function, we selected two genes to test in *in vitro* and in vivo models of SCA3 (Fig. 2.1C). The first protein selected was the calcium-regulated heat stable protein 1 (CARHSP1) which showed to be upregulated in both SCA3 and SCA2 mouse models. The second SGs component selected was the Pumilio homolog 1 (PUM1), which had its levels upregulated in SCA3 disease, while no data in SCA2 condition could be obtained. Both proteins have RNA binding activity and, therefore, constitute interesting targets in the context of neurodegenerative diseases (Conlon and Manley, 2017).

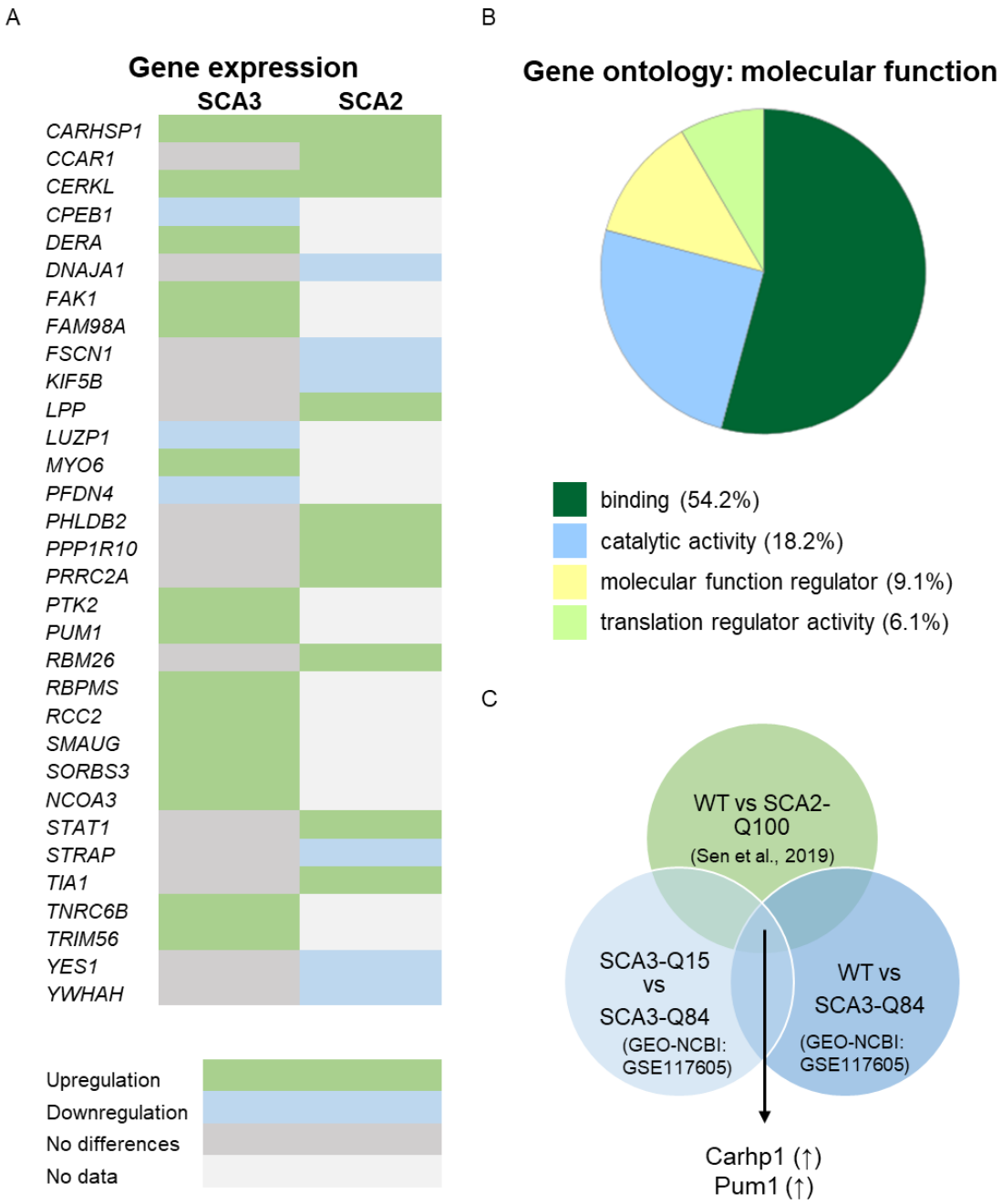

Fig. 2.1. **Gene expression profile analysis for selected SGs components in SCA3 and SCA2 mouse models.** Gene expression levels for the 464 SGs components identified in the MSGP database were obtained from a transcriptome data set of *Mus musculus* for WT, SCA3-Q15 and SCA3-Q84 transgenic mouse models. Additionally, gene expression levels for some SGs components were obtained from SCA2-Q100 KI mouse model. (A) Heat map of SGs proteins that are significantly upregulated (in green), downregulated (in blue), not altered (in dark grey) or no data could be obtained (in light grey), for SCA3 and SCA2 mouse models compared to non-disease controls. (B) Gene ontology analysis of the molecular function for the 32 SGs components that were significantly altered in SCA3 and SCA2 disease revealed that more than half of the proteins have binding activity. (C) From gene expression comparisons between the different groups (WT vs SCA3-Q84), (SCA3-Q15 vs SCA3-Q84) and (WT vs SCA2-Q100), it was selected the proteins Carhsp1 and Pum1 as the most significantly altered and relevant targets for modulation in different models of SCA3 disease.

2.3.2 CRISPR–Cas genome-editing system efficiently downregulates Carhsp1 and Pum1 levels in mouse cells

The SGs components *CARHSP1* and *PUM1* gene levels were found to be upregulated in SCA3 and SCA2 disease mouse models. Thus, we hypothesized whether modulation of these molecules' levels could be a target for these diseases. Recently, gene editing tools like the CRISPR-Cas system have been validated as tools for gene silencing at the DNA level (Nóbrega et al., 2020). Therefore, we acquired a predesigned CRISPR-Cas system with a guide RNA for *Mus musculus CARHSP1* and *PUM1* genes*,* that we named Cr-Carhsp1 and Cr-Pum1 respectively. In this system, the Cas9 protein with endonuclease activity binds to the target DNA locus in a protospacer adjacent motif (PAM), mediated by a single guide RNA (sgRNA) sequence with 20 bases complementary to the DNA (Fig. 2.2A). Upon binding, the Cas9 creates a double-strand break at the targeted genome that can be repaired by the different cellular DNA repair mechanisms, resulting in either reading frame shifts or stop codons insertions, leading to functional knockout of the gene (Nóbrega et al., 2020). We first assessed whether the use of CRISPR-Cas system could silence Carhsp1 and Pum1 expression and reduce its protein levels *in vivo*. For that, lentiviral vectors (LVs) encoding for Cr-Carhsp1 or Cr-Pum1 were stereotaxically injected in WT mice left and right hemisphere (Fig. 2.2B). Additionally, we used a control CRISPR-Cas9 system, Cr-CT, which has a guide RNA for *Escherichia coli* lac Z gene that has been validated as having no targets in *Mus musculus* (Platt et al., 2014) (Fig. 2.2B). By immunohistochemistry staining against the polypeptide protein FLAG tag inserted in the CRISPRs sequence, we confirmed that LVs efficiently transduced striatal cells (Fig. 2.2C). Western blot analysis of brain striatal punches revealed that Cr-Carhsp1 led to a significant decrease of Carhsp1 protein levels compared to Cr-CT and WT conditions (Fig. 2.2D). Likewise, Cr-Pum1 significantly decreased the levels of Pum1 protein in mouse striatal cells, compared to WT animals (Fig. 2.2E). Therefore, the use of CRISPR-Cas system efficiently downregulates the levels of Carhsp1 and Pum1 SGs components to more than 50%, proving to be a successful approach to modulate thee expression of these targets.

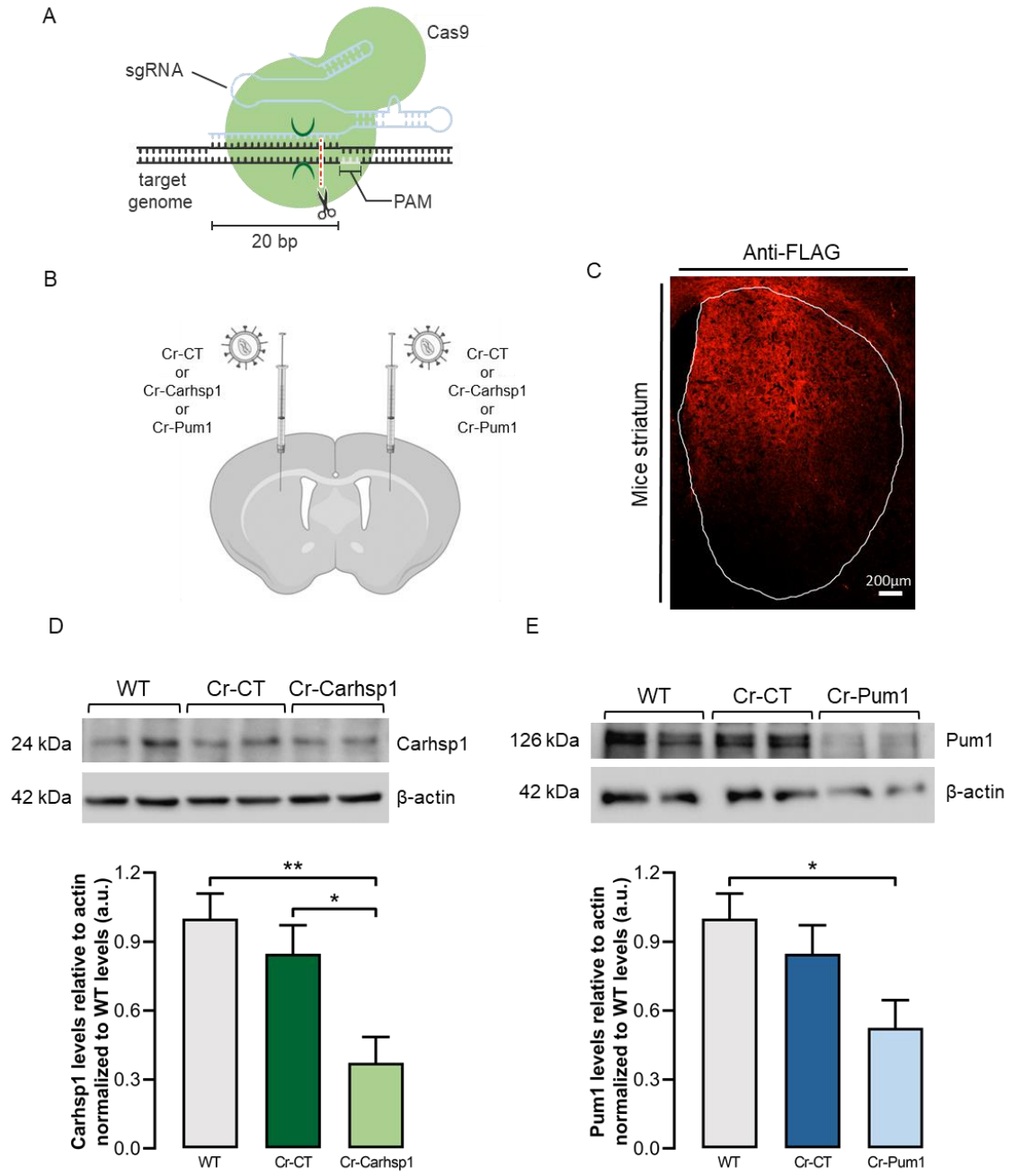

Fig. 2.2. **Assessment of CRISPR-Cas gene editing system in silencing Carhsp1 and Pum1 expression.** (A) CRISPR-Cas tool used in this study is composed by a Cas9 protein with endonuclease activity that binds to double-strand DNA in a protospacer adjacent motif (PAM), mediated by a single guide RNA (sgRNA) sequence with 20 bases complementary to the targeted DNA locus, and creates a double-strand break at the targeted genome, leading to knockout of the gene (adapted from (Nóbrega et al., 2020). (B) LVs encoding for Cr-Carhsp1, Cr-Pum1 or Cr-CT (control CRISPR sequence) were stereotaxically injected in WT mice left and right hemisphere. (C) Fluorescence microscopy images of CRISPRs FLAG tag staining revealed LVs-transduced mice striatum region. (D) Western blot analysis of mice striatal punches showed that Cr-Carhsp1 significantly reduced Carhsp1 protein levels compared to Cr-CT and WT animals. (E) Western blot analysis of mice striatal punches showed that Cr-Pum1 significantly decreased Pum1 protein levels in injected mice compared to WT group. Values are expressed as mean ± SEM *n*=4 per group; *P < 0.05, **P < 0.01; one-way ANOVA followed by post hoc Tukey's multiple comparison test.

2.3.3 Cr–Carhsp1 reduces the number of cells with Atx3MUT aggregates in N2A cells

As *CARHSP1* gene expression is altered in the context of SCA3 mouse models, we started evaluating whether reducing its protein levels could mitigate the phenotype in a SCA3 cellular model. For that, we transfected N2A cells with mutant ataxin-3 carrying 84 glutamines and an EGFP tag (Atx3MUT) as well as with Cr-Carhsp1 construct. Through fluorescence microscopy, we observed that Cr-Carhsp1 expression resulted in a significant decrease in the number of N2A with Atx3MUT aggregates, compared to control (Fig. 2.3A-E). On the other hand, western blot analysis showed that Cr-Carhsp1 did not alter the soluble levels of Atx3MUT, compared to control conditions (Atx3MUT and Cr-CT) (Fig. 2.3F-G).

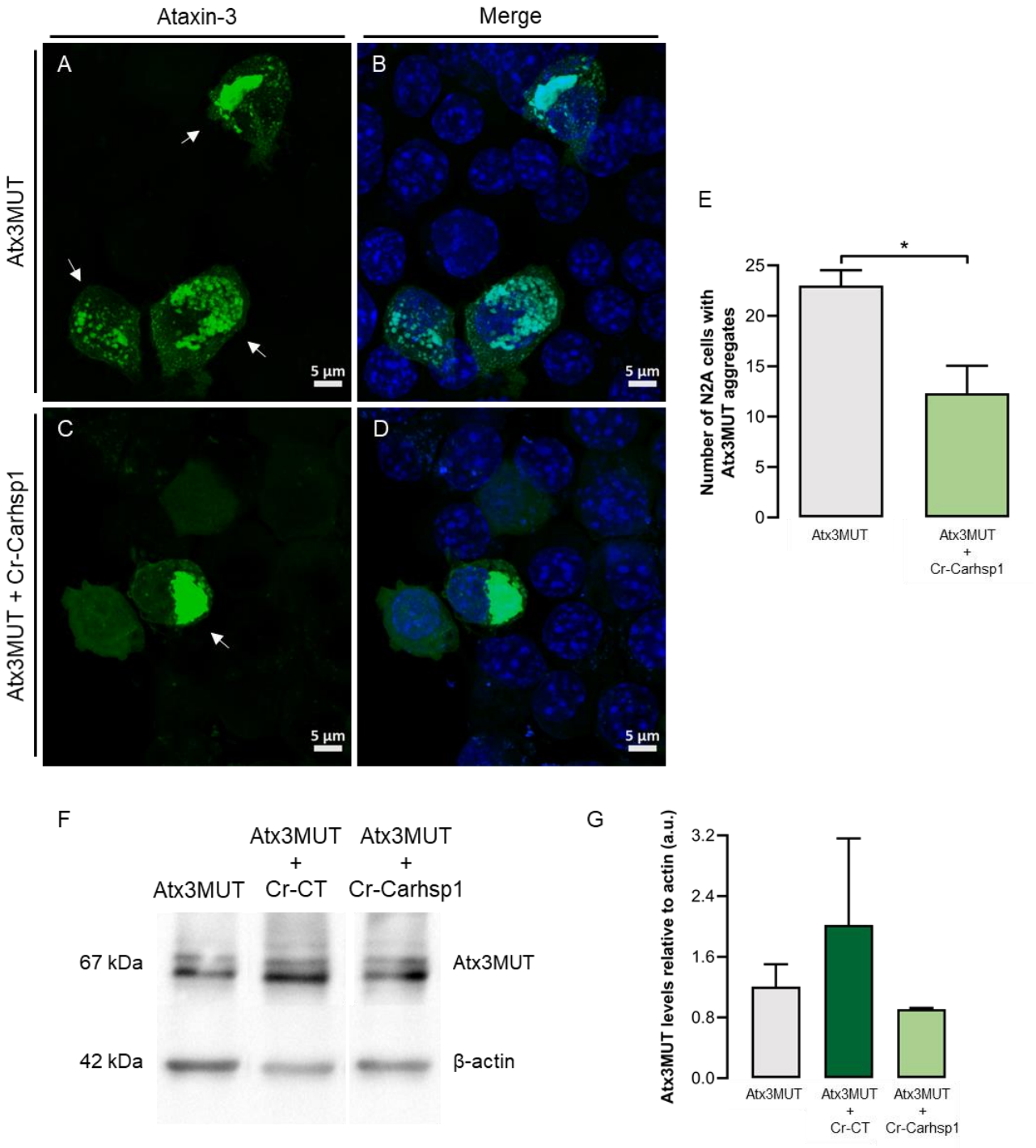

Fig. 2.3. **Assessment of Cr-Carhsp1 expression in Atx3MUT aggregation and soluble levels in N2A cells.** Cultured N2A cells were transfected with human full-length mutant ataxin-3 containing 84Q and an EGFP tag (Atx3MUT) and either with Cr-CT and Cr-Carhsp1. (A-D) Confocal microscopy imagens showing N2A cells with Atx3MUT aggregates, indicated by white arrows. (E) Upon quantification of 100 transfected cells, it was observed that Cr-Carhsp1 reduced the number of cells with Atx3MUT aggregates compared to non-treated condition. (F-G) Western blot analysis of cell extracts showed that Cr-Carhsp1 does not alter soluble Atx3MUT protein levels compared to Atx3MUT and Cr-CT conditions. Values are expressed as mean ± SEM *n*=3 independent experiments; *P < 0.05; unpaired Student's *t*-test; one-way ANOVA followed by post hoc Tukey's multiple comparison test.

2.3.4 Cr–Carhsp1 reduces Atx3MUT aggregates in a SCA3 striatal lentiviral mouse model

After *in vitro* results showing that downregulation of CARHSP1 decreased the mutant Atx3 aggregation levels, we next aimed at investigating the impact of Cr-Carhsp1 in a SCA3 lentiviral mouse model with striatal pathology. In this model, expression of polyQ-expanded Atx3 results in the formation of insoluble protein inclusions inside neurons, as well as loss of neuronal markers (Alves et al., 2008b), which are neuropathological traits observed in post-mortem human tissue (Paulson et al., 1997b; Seidel et al., 2017). Thus, LVs encoding for human full-length mutant Atx3 with 84 glutamines (Atx3MUT) were injected in the right and left striatum hemisphere of adult C57/BL6 mice (Fig. 2.4A). Additionally, other animals received LVs encoding for Cr-CT or Cr-Carhsp1, together with Atx3MUT (Fig. 2.4A). We found that Cr-Carhsp1 led to a significant reduction in the number of Atx3MUT aggregates, compared to the control groups (Atx3MUT and Cr-CT) (Fig. 2.4B-D, H). On the other hand, administration of CRISPRs constructs seem to increase the loss of DARPP-32 neuronal marker staining volume compared to Atx3MUT alone (Fig. 2.4E-G, I). Overall, our results suggest that downregulation of CARHSP1 SGs component levels reduces the mutant Atx3 aggregation, which could have an impact in SCA3 disease.

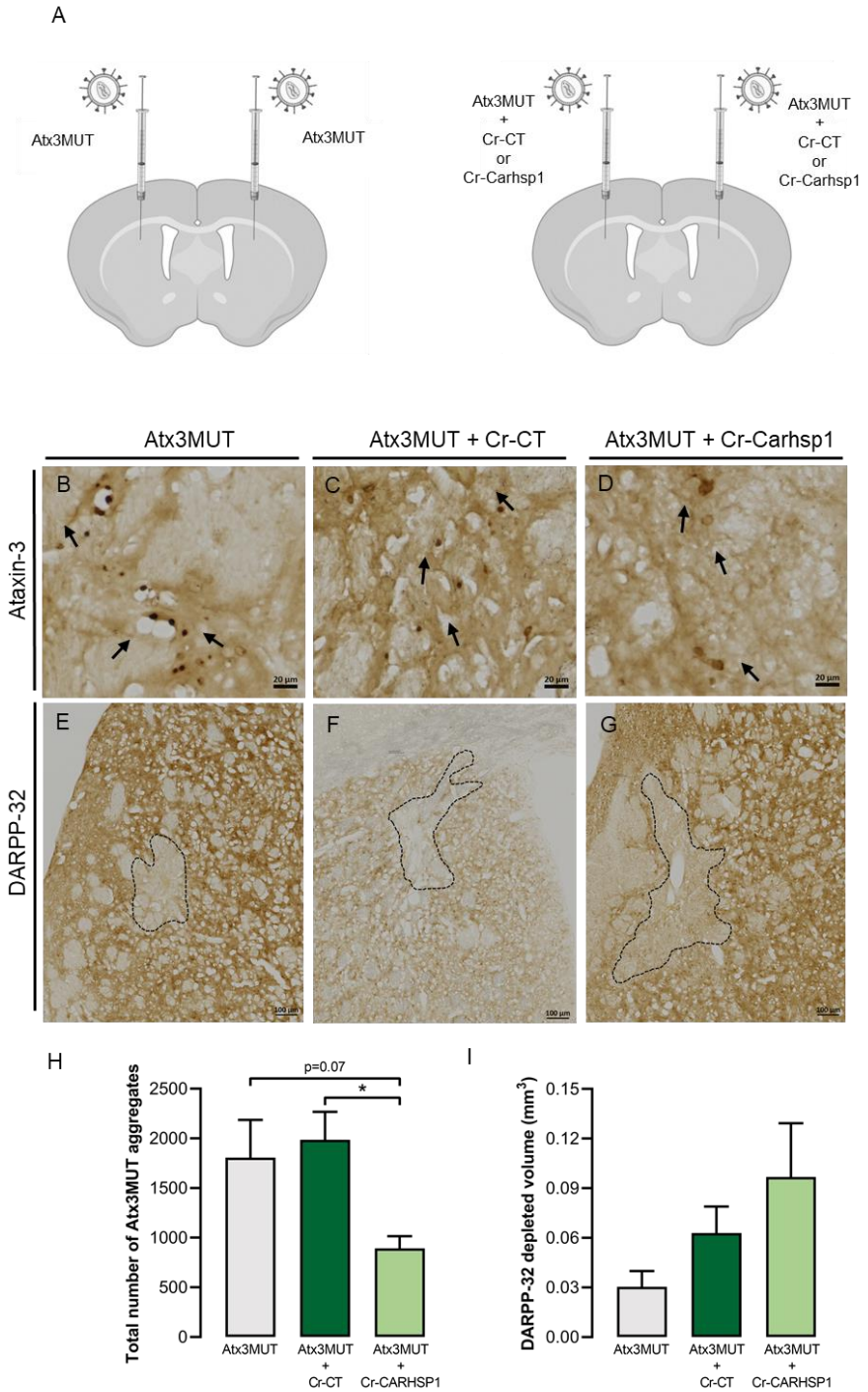

Fig. 2.4. **Assessment of Cr-Carhsp1 impact on aggregation and neuronal markers preservation in a SCA3 striatal lentiviral mouse model.** (A) LVs encoding for human full-length mutant Atx3 (Atx3MUT) were injected in mice striatum, as well as LVs encoding for Cr-CT and Cr-Carhsp1. (B-D) Brain slices were immunoassayed for Atx3 protein and (E-G) the neuronal marker DARPP-32. (H) Upon quantification of the total number of Atx3MUT aggregates, it was observed that Cr-Carhsp1 significantly reduced the number of mutant inclusions compared to control conditions. (I) Quantification of DARPP-32 staining loss volume suggested that Cr-CT and Cr-Carhsp1 showed a tendency to induce higher depletion of staining for the neuronal marker. Values are expressed as mean ± SEM *n*=6 per condition; *P < 0.05; one-way ANOVA followed by post hoc Tukey's multiple comparison test.

2.3.5 Cr–Carhsp1 ameliorates motor coordination in SCA3-Q69 transgenic mouse model

SCA3 disease is characterized by progressive and extensive degeneration of several brain regions, which leads to severe motor deficits in patients (Rüb et al., 2008). Therefore, we next aimed to investigate whether downregulation of Carhsp1 levels could impact motor deficits in a SCA3 transgenic mouse model (Torashima et al., 2008). As early as 3 weeks of age, the SCA3-Q69 mice already displayed cerebellar atrophy, accompanied by motor coordination and gait disturbances, being suitable for testing molecular therapies after disease onset. At 4-5 weeks of age, transgenic mice were injected with either Cr-Carhsp1 or the control construct (Cr-CT) into the cerebellum through stereotaxic surgery (Fig. 2.5A). Mice were subjected to a battery of motor tests one day before the surgery (0 weeks) and every 3 weeks after LVs injection, until 9 weeks of experiment (Fig. 2.5B). We observed that Cr-Carhsp1 group showed a lower latency to fall off rotarod apparatus at constant rotation (5rpm) at 6 weeks of experiment, however this was a temporary effect, as latency to fall showed a tendency to increase at 9 weeks compared to control group (Fig. 2.5C). Regarding the accelerating rotarod and the different beams walking tests, no significant differences were observed between Cr-CT and Cr-Carhsp1 animals at the different timepoints analysed (Fig. 2.5D, F-G). Importantly, the injection of Cr-Carhsp1 resulted in a significant decrease in the time taken to cross the swimming tank, at 9 weeks of LVs expression compared to non-treated mice, suggesting an improved motor performance (Fig. 2.5E). We further assessed animals' gait by measuring different footprint parameters. At 9 weeks post-injection, no significant differences were found in the overlap distance between fore and hind paws between the two experimental groups (Fig. 2.5H). Moreover, front, and hind stride length (Fig. 2.5I-J), as well as front and hind base width measures (Fig. 2.5K-L), were not significantly altered upon injection of LVs encoding Cr-Carhsp1 at the end of the treatment (9 weeks). Overall, the expression of Cr-Carhsp1 improves motor coordination as suggested by different behaviour measures, suggesting downregulation of CARHSP1 SGs component could be a potential target for SCA3 disease.

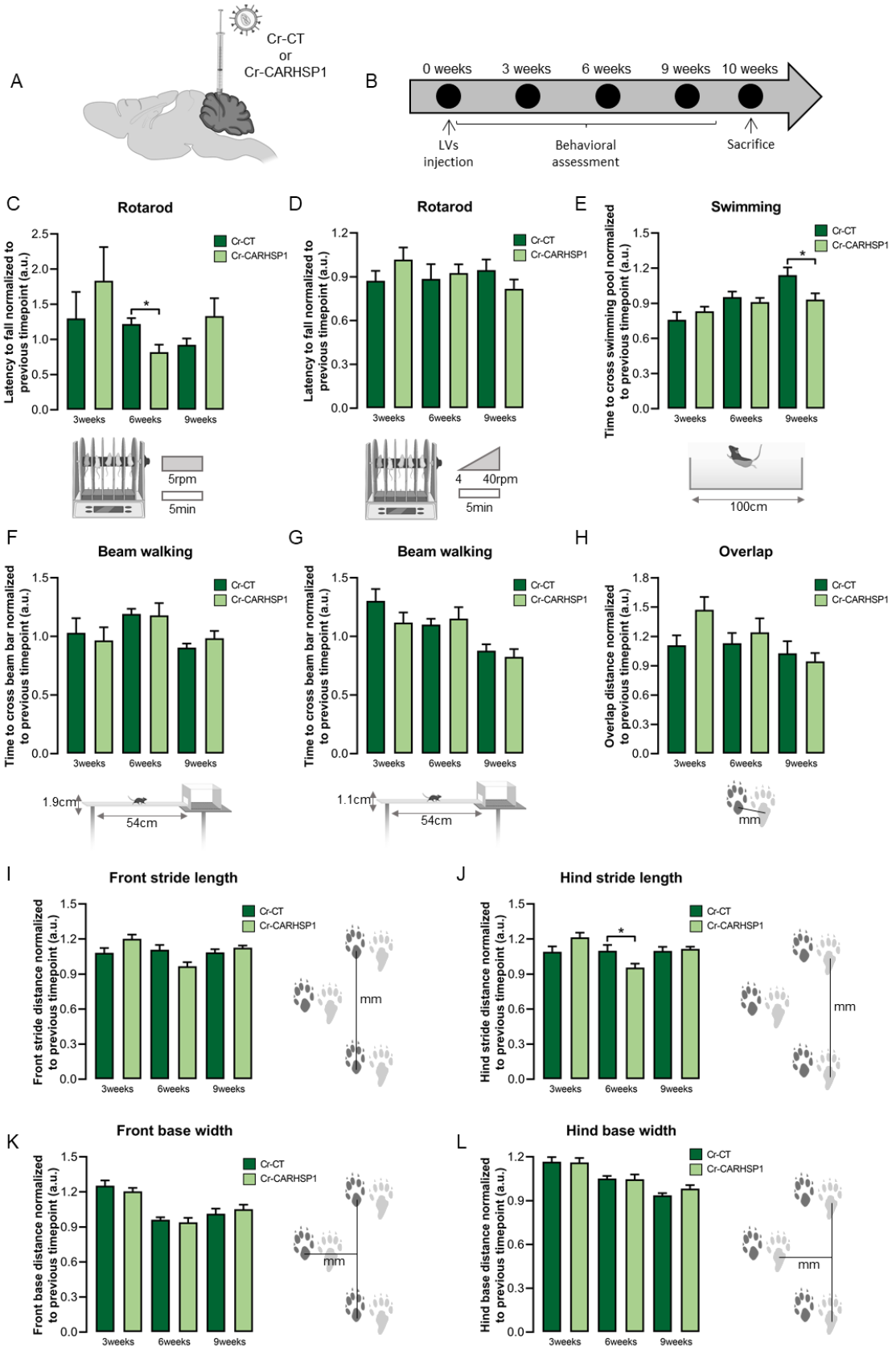

Fig. 2.5. **Assessment of Cr-Carhsp1 expression impact on motor deficits in SCA3-Q69 transgenic mouse model.** (A) LVs encoding for Cr-Carhsp1 or Cr-CT were injected in the cerebellum of 4-5-weeks old SCA3-Q69 transgenic mice. (B) One day before injection (0 weeks) and 3-, 6- and 9-weeks after, mice were subjected to behavioral

analysis. (C) Cr-Carhsp1 mice showed a significant decreased latency to fall off in constant rotarod test at 6 weeks post-injection. Cr-Carhsp1 treatment did not alter motor performance in accelerating rotarod test (D), as well as in thicker (F) and thinner (G) beam walking tests. (E) Injection of Cr-Carhsp1 significantly reduced the time taken by mice to cross the swimming pool at 9 weeks of treatment, compared to control group. (H) Overlap distance between fore and hind paws measure is not significantly altered in Cr-Carhsp1 animals compared to Cr-CT. (I-L) Treatment with Cr-Carhsp1 did not alter front and hind stride length, nor front and hind base width. Values are expressed as mean ± SEM normalized to the previous timepoint; *n*=8 (Cr-Carshp1) and *n*=6 (Cr-CT); *P < 0.05; unpaired Student's *t*-test between Cr-Carshp1 and Cr-CT groups for each timepoint.

2.3.6 Cr–Carhsp1 mitigates neuropathological traits in a SCA3-Q69 transgenic mouse model

The severe clinical manifestations observed in SCA3 patients are a result of an extensive degeneration in several regions of the central nervous system, being the cerebellum the most affected area (Rüb et al., 2008). Therefore, we next aimed to investigate whether downregulation of Carhsp1 levels could impact the neuropathological features associated with the SCA3-Q69 transgenic mouse model. In this model, the expression of mutant Atx3 (tagged with an HA epitope) under the control of the L7 promoter results in marked cerebellar atrophy, with reduced lobules' volume, loss of Purkinje cells and the presence of mutant inclusions (Torashima et al., 2008). Injection of LVs encoding for the CRISPRs constructs led to the transduction of neuronal cells, mainly in lobules 2&3, and in lobules 9 and 10 of the cerebellum. Therefore, we decided to quantify the number of Atx3MUT aggregates, as well as the number of Purkinje cells in these cerebellar lobules. We observed a significantly decreased number of mutant inclusions in animals injected with Cr-Carhsp1 (Fig. 2.6A-C), while no alterations in Purkinje cells were observed (data not shown). Importantly, the area of lobules 2&3 and 10 are significantly increased in Cr-Carhsp1 group, compared to control animals (Fig. 2.6D-I). Additionally, we observed that the volume of transduced lobules (2&3, 9 and 10) is significantly higher upon injection of Cr-Carhsp1, compared to control construct (Fig. 2.6J). Overall, the expression of Cr-Carhsp1 reduces the number of mutant Atx3 aggregates and area and volume of cerebellar lobules, suggesting that the downregulation of CARHSP1 SGs component mitigates neuropathological aggregation and cerebellar atrophy in this SCA3 disease model.

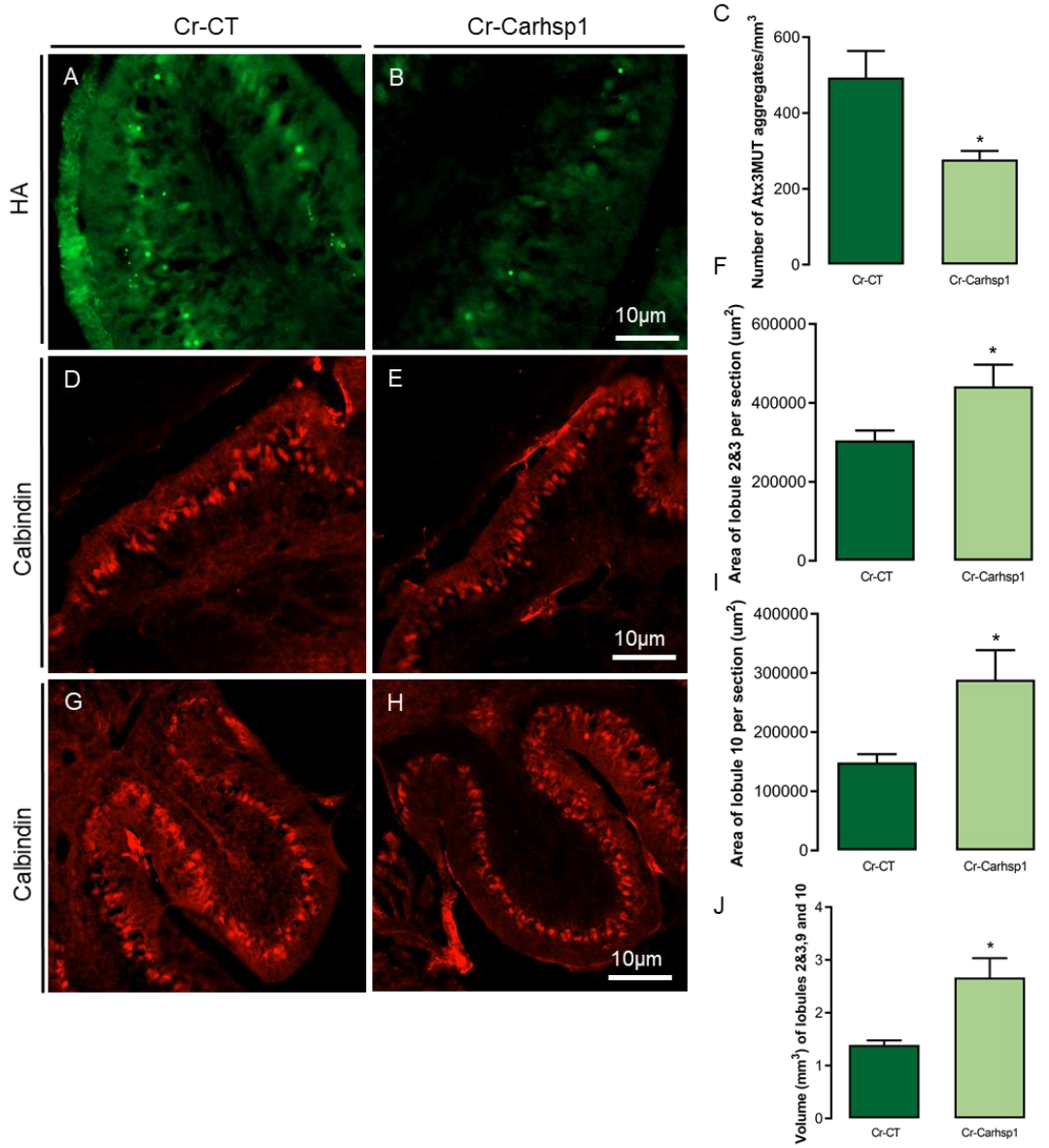

Fig. 2.6. **Assessment of Cr-Carhsp1 expression on neuropathological features in the SCA3-Q69 transgenic mouse model.** (A-B) Brain slices of SCA3-Q69 mice injected with Cr-CT or Cr-Carhsp1 were immunoassayed for HA epitope present in Atx3MUT construct. (C) Upon quantification of HA-positive inclusions, we observed a reduced number of aggregates in lobules 2&3, 9 and 10 in Cr-Carhsp1 animals compared to control group. Brain slices immunoassayed for calbindin showing cerebellar lobules 2&3 (D-E) and lobule 10 (G-H). Quantification of lobules area per slice revealed significantly increased lobules 2&3 (F) and 10 (I) area upon administration of Cr-Carhsp1. (J) Quantification of lobules 2&3, 9 and 10 volumes showed that Cr-Carhsp1 results in preservation of cerebellar lobules volume compared to control condition, suggesting reduced cerebellar atrophy. Values are expressed as mean ± SEM; *n*=4 (Cr-Carshp1) and *n*=3 (Cr-CT); *P < 0.05; unpaired Student's *t*-test.

2.3.7 Cr–Carhsp1 reduces the number of cells with SGs in N2A cell line

As downregulation of Carhsp1 protein levels resulted in decreased mutant Atx3 aggregation and motor improvements in SCA3 mouse models, we next aimed at investigating by which mechanism CARHSP1 could be leading to this reduced aggregation. We hypothesized whether CARHSP1 could impact SGs formation, which we proposed to be involved in PolyQ diseases pathogenesis (Marcelo et al., 2021b). For that, we transfected N2A cells with Cr-CT and Cr-Carhsp1 and induced oxidative stress by treating cells with sodium arsenite. We performed an immunocytochemistry for the SGs component and marker G3BP1 (Fig. 2.7A, D, G) and for the FLAG tag present in Cr-Carshp1 plasmid (Fig. 2.7B, E, H). We observed that Cr-Carhsp1 expression resulted in a significant reduction in the number of N2A cells with SGs, compared to control conditions (Fig. 2.7J). These results indicate that downregulation of CARHSP1 levels impact the assembly of SGs foci, resulting in the reduction of its levels.

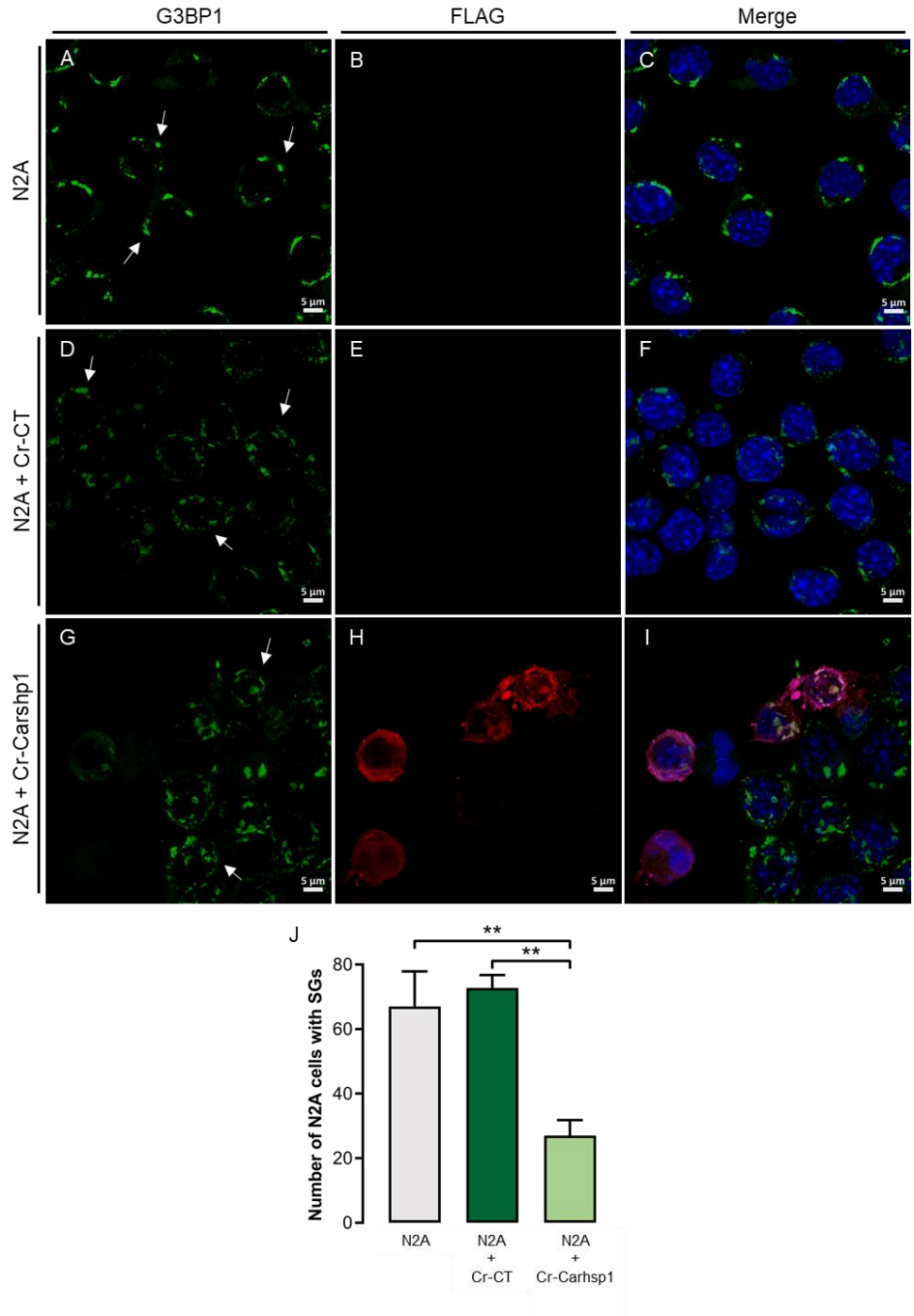

Fig. 2.7. **Assessment of Cr-Carhsp1 impact in SGs assembly in N2A cells.** Cultured N2A cells were transfected with Cr-CT and Cr-Carshp1, following treatment with 0.05M sodium arsenite during 1h for induction of SGs formation. (A, D, G) Confocal microscopy images showing N2A cells with SGs, stained for G3BP1 marker. (B, E, H) Fluorescence microscopy images showing N2A cells transfected with Cr-Carhsp1, stained for FLAG marker. (J) Upon quantification of 100 transfected cells, it was observed that Cr-Carhsp1 reduced the number of cells with SGs compared to non-treated conditions (Cr-CT and N2A). Values are expressed as mean ± SEM n=4 independent experiments; **P < 0.01; one-way ANOVA followed by post hoc Tukey's multiple comparison test.

2.3.8 Cr–Pum1 reduces the number of cells with Atx3MUT aggregates in N2A cells

As *PUM1* gene expression was also altered in the context of SCA3 mouse models, we next evaluated whether reducing Pum1 protein levels could mitigate the phenotype in a SCA3 cellular model. For that, we transfected N2A cells with mutant ataxin-3 carrying 84 glutamines and an EGFP tag (Atx3MUT) as well as with Cr-Pum1 construct. Through fluorescence microscopy, we observed that Cr-Pum1 did not decrease the number of N2A with Atx3MUT aggregates, compared to control (Fig. 2.8A-E). Moreover, Western blot analysis showed that Cr-Pum1 did not alter the soluble levels of Atx3MUT, compared to control conditions (Atx3MUT and Cr-CT) (Fig. 2.8F-G).

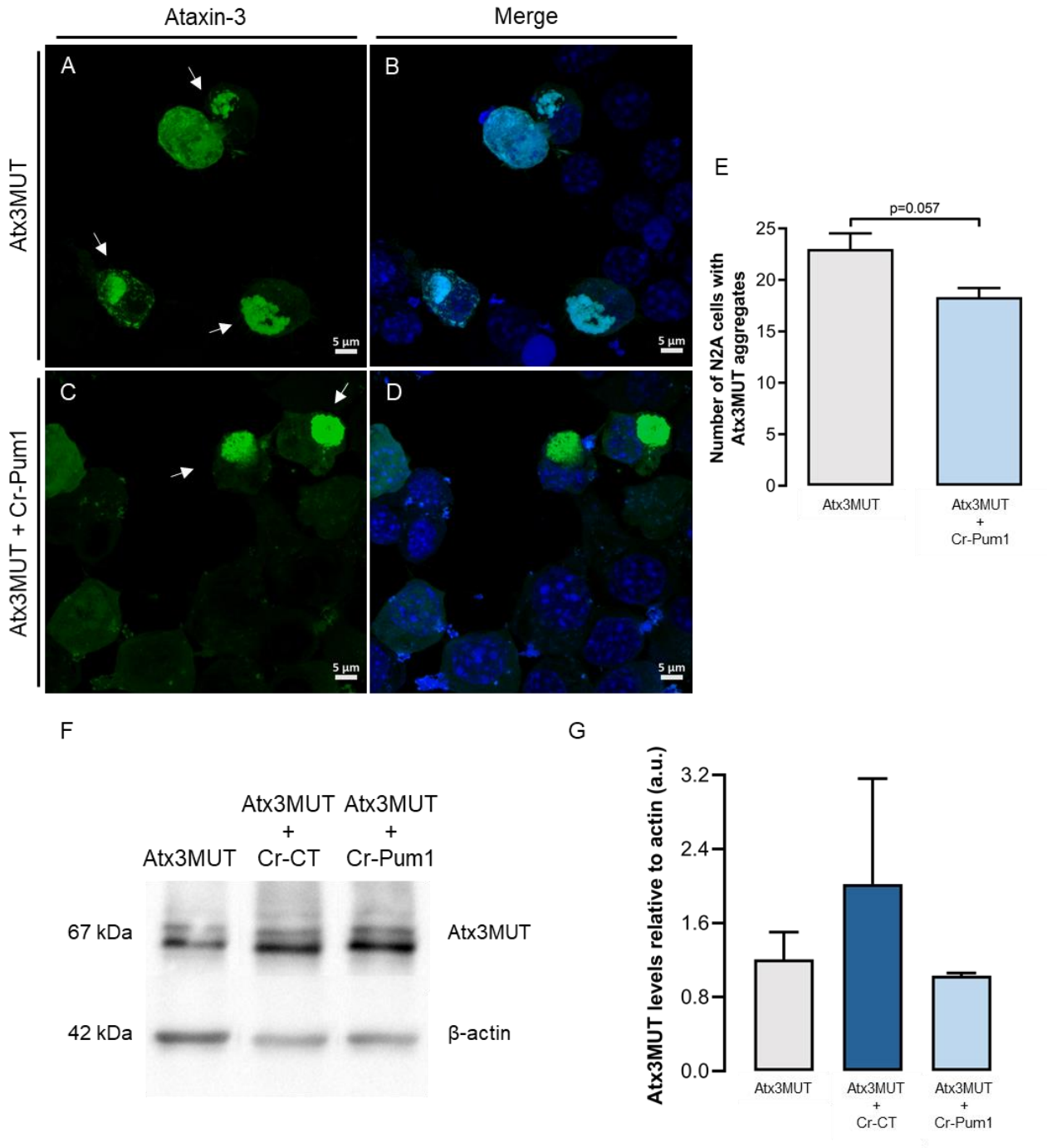

Fig. 2.8. **Assessment of Cr-Pum1 expression impact in Atx3MUT aggregation and protein soluble levels in N2A cells.** Cultured N2A cells were transfected with human full-length mutant ataxin-3 containing 84Q and an EGFP tag (Atx3MUT) and either with Cr-CT and Cr-Pum1. (A-D) Confocal microscopy imagens showing N2A cells with Atx3MUT aggregates. (E) Upon quantification of 100 transfected cells, it was observed that Cr-Pum1 reduced the number of cells with Atx3MUT aggregates compared to non-treated condition. (F-G) Western blot analysis of cell extracts showed that Cr-Pum1 does not alter soluble Atx3MUT protein levels compared to Atx3MUT and Cr-CT conditions. Values are expressed as mean ± SEM of *n*=3 independent experiments; *P < 0.05; unpaired Student's *t*-test; one-way ANOVA followed by post hoc Tukey's multiple comparison test.

2.3.9 Cr–Pum1 increases Atx3MUT aggregates in a SCA3 striatal lentiviral mouse model

Although downregulation of Pum1 did not decrease the mutant Atx3 aggregation levels in the SCA3 *in vitro* model, we decided to also investigate the impact of Cr-Pum1 in the SCA3 striatal lentiviral mouse model. As previously, LVs encoding for human full-length mutant Atx3 with 84 glutamines (Atx3MUT) were injected in the right and left striatum hemisphere of adult C57/BL6 mice (Fig. 2.9A). In this case, other animals received LVs encoding for Cr-CT or Cr-Pum1, together with Atx3MUT (Fig. 2.9A). We found that Cr-Pum1 led to a significant increase in the number of Atx3MUT aggregates, compared to the control groups (Atx3MUT and Cr-CT) (Fig. 2.9B-D, H). Like the results obtained for Cr-Carhsp1, the administration of CRISPRs constructs increases the loss of DARPP-32 neuronal marker staining volume, compared to Atx3MUT (Fig. 2.9E-G, I). Overall, our results suggest that downregulation of PUM1 SGs component levels increases mutant Atx3 aggregation, which could worsen SCA3 pathology.

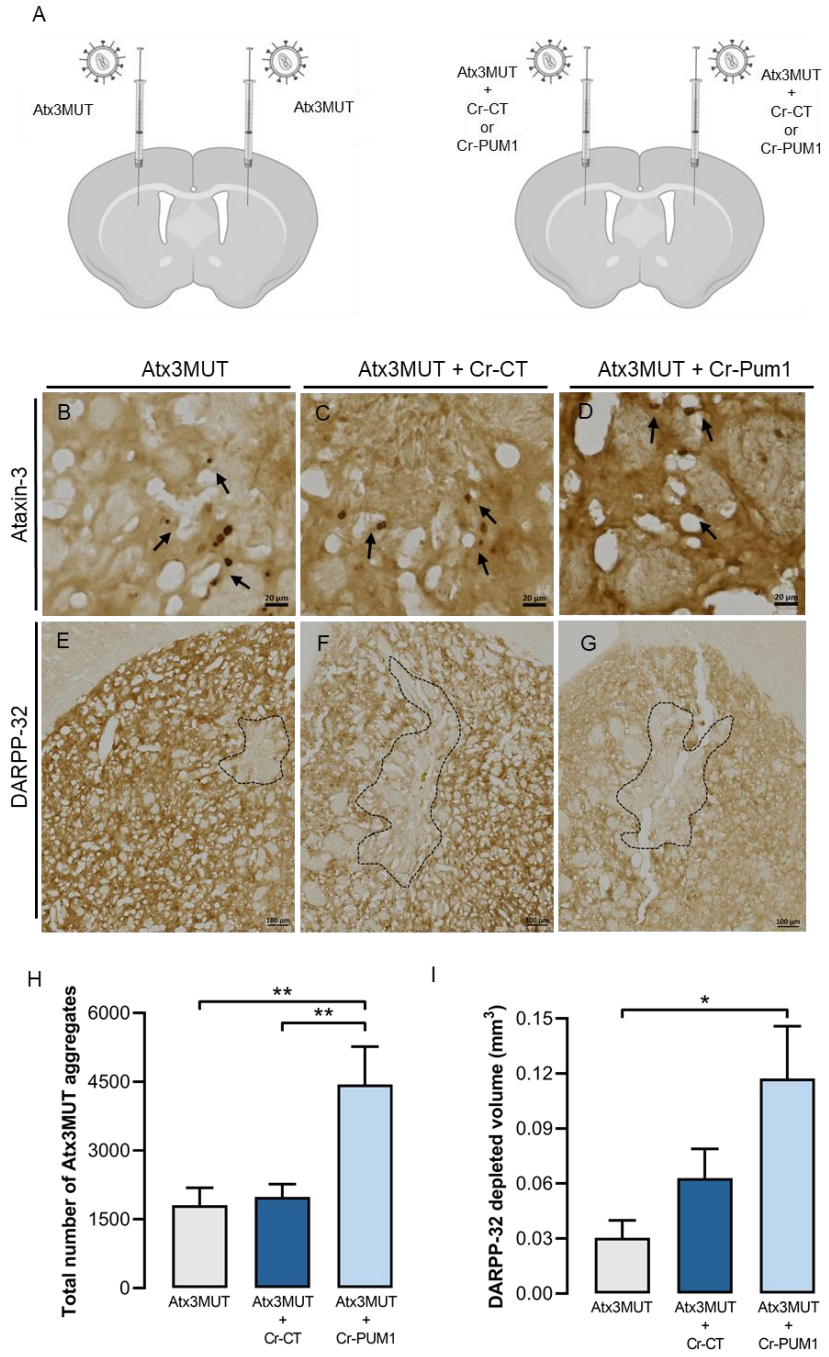

Fig. 2.9. **Assessment of Cr-Pum1 impact on aggregation and neuronal markers preservation in SCA3 striatal lentiviral mouse model.** (A) LVs encoding for human full-length mutant Atx3 (Atx3MUT) were injected in mice striatum, as well as LVs encoding for Cr-CT and Cr-Pum1. (B-D) Brain slices were immunoassayed for Atx3 protein and (E-G) the neuronal marker DARPP-32. (H) Upon quantification of the total number of Atx3MUT aggregates, it was observed that Cr-Pum1 significantly increased the number of mutant inclusions compared to control conditions. (I) Quantification of DARPP-32 staining loss volume suggested that Cr-Pum1 induce higher depletion of staining for the neuronal marker. Values are expressed as mean ± SEM *n*=6 per condition; *P < 0.05; **P < 0.01; one-way ANOVA followed by post hoc Tukey's multiple comparison test.

2.3.10 Cr–Pum1 aggravates gait dysfunction in SCA3-Q69 transgenic mouse model

Even if the downregulation of PUM1 protein levels exacerbates mutant Atx3 aggregation, we went to investigate the impact of Cr-Pum1 in the motor deficits of the SCA3-Q69 mice. Like for the Cr-Carhsp1 experiments, 4-5 weeks old transgenic mice were injected with either Cr-Pum1 or the control construct (Cr-CT) into the cerebellum of the animals, through stereotaxic surgery (Fig. 2.10A). Mice were subjected to a battery of motor tests, one day before the surgery (0 weeks) and every 3 weeks after LVs injection, until 9 weeks post-injection (Fig. 2.10B). The rotarod test, beam walking and swimming tests did not show significant alterations in animals' performance between the Cr-CT and Cr-Pum1 at any timepoints assessed, suggesting Cr-Pum1 did not worse or ameliorate motor coordination function (Fig. 2.10C-G). Moreover, administration of Cr-Pum1 did not alter paws overlap, nor front stride length or hind base width footprint patterns (Fig. 2.10H, I, L). However, Cr-Pum1 injected animals presented decreases hind stride length at 9 weeks of experiment, as well as enlarged front base width at 6 weeks, compared to non-injected mice (Fig. 2.10J-K). Thus, the treatment with Cr-Pum1 seems to aggravate mice gait as suggested by the footprint test, suggesting that downregulation of PUM1 SGs component could have a negative impact in SCA3 disease.

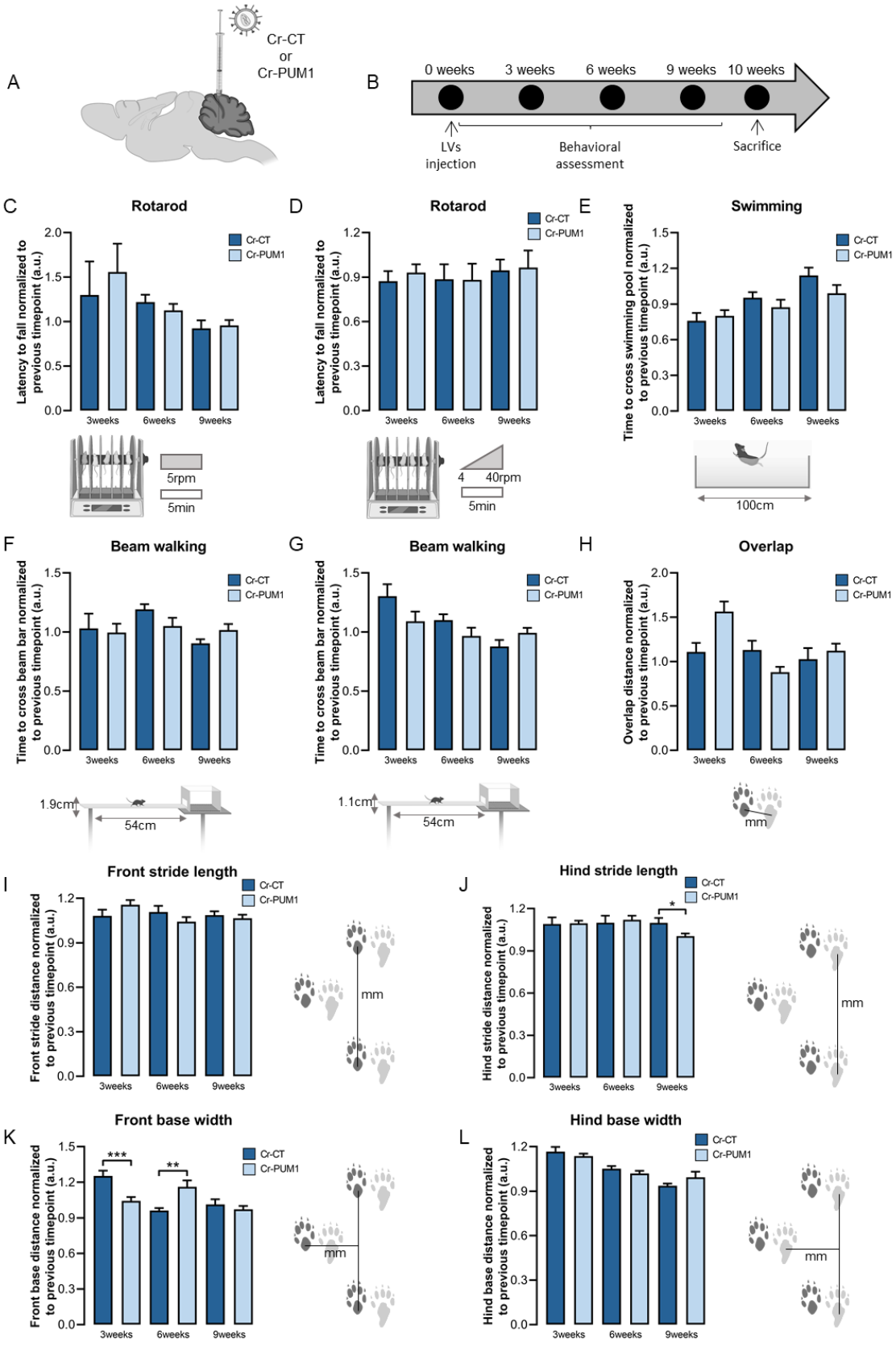

Fig. 2.10. **Assessment of Cr-Pum1 impact on motor deficits in SCA3-Q69 transgenic mouse model.** (A) LVs encoding for Cr-Pum1 or Cr-CT were injected in the cerebellum of 4-5-weeks old SCA3-Q69 transgenic mice. (B) One day before injection (0 weeks) and 3-, 6- and 9-weeks after, mice were subjected to behavioral analysis. Cr-

Pum1 injected mice present no alterations in latency to fall off in constant rotarod test (C), in accelerating rotarod test (D), as well as no differences were observed in the time taken to transverse the swimming tank (E), the thicker (F) or the thinner (G) beam walking test. (H) Overlap distance between fore and hind paws, (I) front stride length or (L) hind base width, compared to Cr-CT. (J-K) The expression of Cr-Pum1 worsens hind stride length and front base width. Values are expressed as mean ± SEM normalized to the previous timepoint; *n*=8 (Cr-Pum1) and *n*=6 (Cr-CT); *P < 0.05; **P < 0.01; ***P < 0.001; unpaired Student's *t*-test between Cr-Pum1 and Cr-CT groups for each timepoint.

2.3.11 Cr–Pum1 does not impact neuropathological features in the SCA3-Q69 transgenic mouse model

As Cr-Pum1 seems to aggravate mice motor function performance, we went to investigate whether motor alterations correlated with neuropathological alterations. Like for the Cr-Carhsp1 experiments, we quantified the number of Atx3MUT aggregates, as well as the number of Purkinje cells in these cerebellar lobules. We observed no alterations in the number of mutant inclusions in animals injected with Cr-Pum1 (Fig. 2.11A-C), as well as no differences in Purkinje cells number were detected, compared to control animals (Fig. 2.11D-F). Likewise, injection of Cr-Pum1 did not influence the volume of transduced cerebellar lobules (2&3, 9 and 10) (Fig. 2.11G-I). Overall, the expression of Cr-Pum1 does not induce neuropathological alterations, suggesting downregulation of PUM1 SGs does not significantly impact cerebellar pathology in SCA3 disease model.

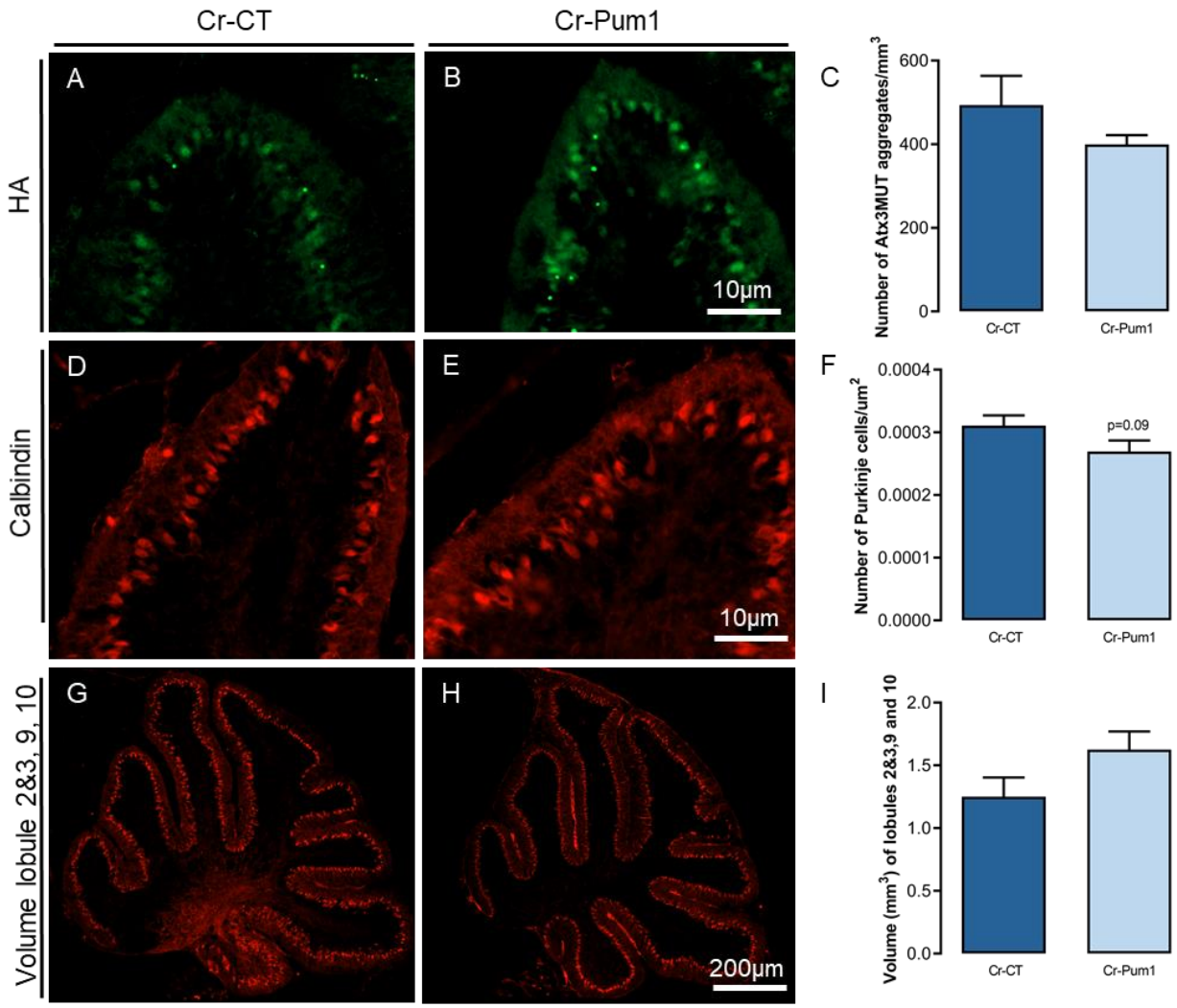

Fig. 2.11. **Assessment of Cr-Pum1 expression on neuropathological features in the SCA3-Q69 transgenic mouse model.** (A-B) Brain slices of SCA3-Q69 mice injected with Cr-CT or Cr-Pum1 were immunoassayed for HA epitope present in Atx3MUT construct. (C) Upon quantification of HA-positive inclusions, no alterations in the number of aggregates in lobules 2&3, 9 and 10 were observed between both experimental groups. (D-E) Brain slices were immunoassayed for the Purkinje cells marker calbindin. (C) Upon quantification of Purkinje cells, no alterations in the number of these cells were observed in Cr-CT or Cr-Pum1 animals. (G-I) Brain slices immunoassayed for calbindin showing cerebellar lobules 2&3, 9 and 10. (L) Quantification of lobules 2&3, 9 and 10 volumes showed that Cr-Pum1 does not impact cerebellar lobules volume compared to control condition. Values are expressed as mean ± SEM; *n*=4 (Cr-Carshp1) and *n*=3 (Cr-CT); *P < 0.05; unpaired Student's *t*-test.

2.3.12 Cr–Pum1 does not influence the number of cells with SGs in N2A cell line

As downregulation of Pum1 protein levels resulted in increased mutant Atx3 aggregation and aggravation of motor impairments in SCA3 mouse models, we aimed at elucidating whether PUM1 could exacerbate SGs formation. For that, we transfected N2A cells with Cr-CT and Cr-Pum1 and induced oxidative stress by treating cells with sodium arsenite compound. We also performed an immunocytochemistry for the SGs component and marker G3BP1 (Fig. 2.12A, D, G) and for the FLAG tag present in Cr-Pum1 plasmid (Fig. 2.12B, E, H). We observed that Cr-Pum1 did not alter the number of N2A cells with SGs, compared to control conditions (Fig. 2.12J). These results indicate that downregulation of PUM1 levels does not impact the assembly of SGs foci.

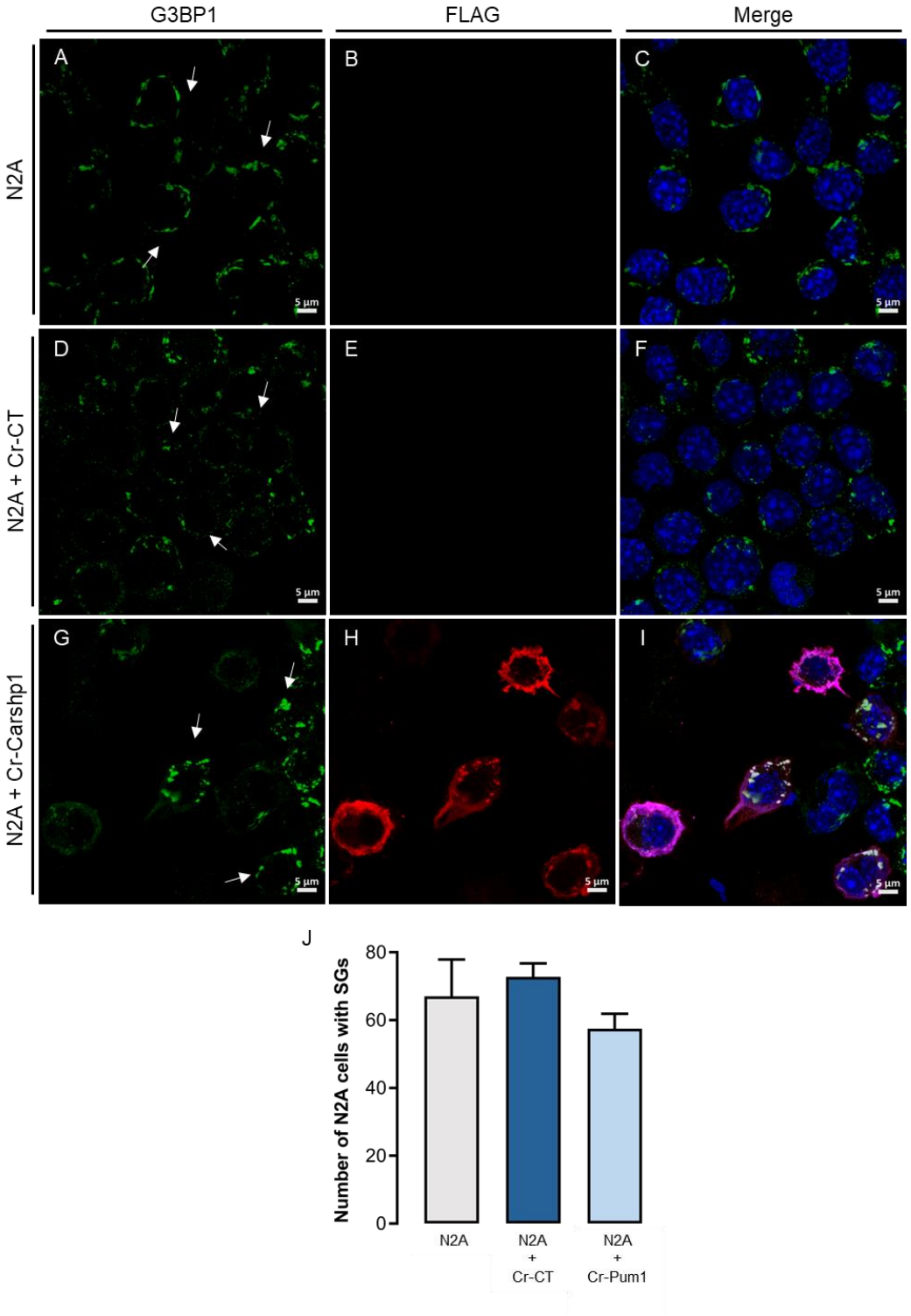

Fig. 2.12. **Assessment of Cr-Pum1 impact in SGs assembly in N2A cells.** Cultured N2A cells were transfected with Cr-CT and Cr-Pum1, following treatment with 0.05M sodium arsenite during 1h for induction of SGs formation. (A, D, G) Fluorescence microscopy images showing N2A cells with SGs, stained for G3BP1 marker. (B, E, H) Fluorescence microscopy images showing N2A cells transfected with Cr-Pum1, stained for FLAG marker. (J) Upon quantification of 100 transfected cells, it was observed that Cr-Pum1 did not alter the number of cells with SGs compared to non-treated conditions (Cr-CT and N2A). Values are expressed as mean ± SEM *n*=4 independent experiments; one-way ANOVA followed by post hoc Tukey's multiple comparison test.

2.4 Discussion

During their lifetime, cells are subjected to different stressing factors that they need to overcome, to maintain homeostasis and assure survival. Among the different pathways activated to manage stress, the formation of stress granules is a key mechanism in the cellular response to stress (Alberti et al., 2017). SGs are membraneless organelles transiently formed after a stress stimuli, which are rapidly disassembled when the stress factor is removed (Buchan, 2014). SGs contain in their structure diverse components, including ribosomal subunits, mRNA molecules, and several proteins while, so far, 464 mammalian proteins have been described to be present in SGs (Nunes et al., 2019). The complex composition of SGs underlies the variety of pathways and mechanisms in which they are suggested to be involved, such as global translation arrest, mRNA triage and expression regulation, cell signaling and apoptosis (Marcelo et al., 2021b). Though the assembly of SGs is essential for cell functioning and survival upon stress conditions, multiple lines of evidence have proposed that a chronic state of cellular state, in which SGs assembly becomes persistent, could contribute to aging or neurodegenerative diseases (Masuda et al., 2009; Asadi et al., 2021). Among neurodegenerative diseases, PolyQ diseases constitute a group of dominantly inherited pathologies characterized by an extensive degeneration of brain tissues and severe motor and neurological symptoms (Nóbrega and Pereira de Almeida, 2018). In these diseases, an abnormal expansion of CAG trinucleotide repeats causes a mutation in the causative genes, resulting in a toxic polyQ stretch into the translated proteins, leading to the formation of insoluble multiprotein aggregates inside diverse neuronal populations (Wen et al., 2017). Although several research groups have already provided some hints into the mechanisms implicated in the neurodegeneration process underlying these disorders, the exact cascade of events that triggers the progressive cell death observed in selective neuronal populations is yet unclear. Emerging evidence supports that SGs play a relevant role in PolyQ diseases pathogenesis, opening a new avenue of research in this field (Marcelo et al., 2021b). Thus, in this study, we aimed at investigating the role of SGs and its components in the context of the PolyQ disease SCA3.

SGs components have been demonstrated to be sequestered to the neuropathological protein aggregates found in PolyQ diseases, which could affect the biological functions of these molecules and its normal cellular levels (Uchihara et al., 2001b; Furukawa et al., 2009; Elden et al., 2010; Nunes et al., 2019). In fact, a previous study from our group reported that 395 SGs components have their gene expression altered in HD patients, with 195 having their expression increased and 200 repressed (Nunes et al., 2019). Accordingly, we observed that 32 SGs components had their gene expression levels significantly different in SCA3 and SCA2 disease mouse models, compared to WT samples, being 23 genes upregulated and 9 downregulated. This evidence suggests that modulation of SGs components levels could impact PolyQ diseases. Therefore, in the present study we selected the SGs components, CARHSP1 and PUM1, whose levels were significantly upregulated in SCA3 mice, to investigate the effect of their downregulation in *in vitro* and *in vivo* models. Moreover, CARHSP1 and PUM1 gene levels were also found augmented in HD patients' samples (Nunes et al., 2019), strengthening the hypothesis that these proteins could be relevant targets for PolyQ diseases.

SCA3 disease is caused when the number of CAGs in the *ATXN3* gene is above 61 repeats, leading to polyQ-expanded Atx3 protein to aggregate (Maciel et al., 2001; Ellisdon et al., 2006). So, in order to modulate CARHSP1 levels we used mouse cellular and *in vivo* models that present the neuropathological Atx3 aggregates observed in SCA3 patients (Alves et al., 2008b; Torashima et al., 2008). We further observed that the downregulation of CARHSP1 levels, using the CRISPR-Cas gene editing system, resulted in reduced aggregation of ataxin-3 *in vitro*, as well as in the lentiviral and the transgenic mouse models. Additionally, reduced levels of CARHSP1 led to a preservation of cerebellar lobules areas and volume, resulting in reduced cerebellar atrophy. Moreover, decreased levels of CARHSP1 also led to improved motor coordination in treated mice, compared to control group. We investigated whether CARHSP1 mechanism in Atx3 aggregation could be related to SGs formation. In fact, the downregulation of CARHSP1 resulted in reduced assembly of SGs, suggesting this protein has an important role in the formation of these cellular *foci*. The function of CARHSP1 mRNA binding activity inside SGs has been previously described (Hou et al., 2011). However, our results demonstrate that CARHSP1

is important for SGs formation induced by oxidative stress. Overall, our study supports that downregulation of CARHSP1 could be a potential therapeutic target for SCA3 disease, although further studies are needed. The impact of CARHSP1 in mutant Atx3 aggregation might be explained by its role in SGs assembly, as a persistent state of cellular stress has been proposed to contribute to PolyQ diseases pathogenesis (Marcelo et al., 2021b). Future studies addressing the role of CARHSP1 as an enhancer of the inflammation mediator TNF-α (tumor necrosis factor alpha) should be performed, as reduced levels of CARHSP1 inhibits TNF-α levels and could result in reduced neuroinflammation levels, a hallmark of diverse neurodegenerative diseases (Pfeiffer et al., 2011).

In this work, we also investigated whether downregulation of PUM1 levels could impact SCA3 disease. PUM1 is an RNA-binding protein (RBP) that is involved in repression of mRNAs (Goldstrohm et al., 2018). Interestingly, *PUM1* knockout mice revealed that PUM1 represses *ATNX1* mRNA, the gene responsible for the PolyQ disease SCA1 (Gennarino et al., 2015). Moreover, the depletion of PUM1 resulted in increased ataxin-1 expression, motor incoordination and loss of Purkinje cells. On the other hand, we observed *PUM1* gene expression levels are upregulated in SCA3 disease, as well as in HD patients (Nunes et al., 2019). Therefore, we aimed at assessing the impact of decreasing PUM1 levels in the SCA3 cellular and mouse models. We observed that knockdown of PUM1 did not influence mutant Atx3 aggregation in a mouse cell line and a transgenic mouse model. However, downregulation of PUM1 levels led to increased levels of mutant aggregates in SCA3 lentiviral mice, along with gait dysfunctions in a SCA3 transgenic mouse model. These results agree with the observations in SCA1 disease, suggesting that depletion of PUM1 levels possibly aggravates the neurodegeneration process in PolyQ diseases. Contrary to CARHSP1 protein, we observed that PUM1 absence does not impair SGs formation. Accordingly, other authors also demonstrated that PUM1 mRNA repression activity occurs under conditions where RNP granules are not present (Goldstrohm et al., 2018). Overall, our results showed that several SGs components levels are altered in the context of PolyQ diseases, while modulation of its levels could differently impact disease models. On one hand, the depletion of CARHSP1 protein resulted in mitigation of neuropathological and motor deficits in SCA3 models, which suggests it could be a potential therapeutic target for SCA3 disease. On the

opposite side, the modulation of PUM1 protein levels aggravated SCA3 traits. Thus, future studies addressing these SGs components are required to further elucidate the role of these molecules in PolyQ diseases.

Chapter 3. Development and characterization of a novel SCA2 lentiviral mouse model with striatal pathology

3.1 Introduction

Spinocerebellar ataxia type 2 (SCA2) is a rare and fatal dominantly-inherited neurodegenerative disorder (Wadia and Swami, 1971; Orozco et al., 1989). SCA2 pathology comprises the clinically and genetically heterogenous group of Polyglutamine (PolyQ) diseases, as it is caused by abnormal repeats of the triplet CAG in the *ATXN2* gene, resulting in an expanded polyQ chain in the ataxin-2 (Atx2) protein (Pulst et al., 1996; Sanpei et al., 1996). In healthy individuals, the protein carries between 13-31 glutamines (Q), while repeats above that threshold lead to disease development (Lastres-Becker et al., 2008b). The mutation results in progressive and widespread degeneration of different neuronal populations, including the cerebellum, pons, basal ganglia, thalamus and midbrain (Seidel et al., 2012). Because of this extensive neurodegeneration, patients affected by the pathology present highly incapacitating cerebellar and extracerebellar symptoms. The clinical manifestations include motor dysfunctions such as progressive gait ataxia, dysarthria, postural tremors and bradykinesia, as well as visual impairments as slow eye saccades and cognitive/psychiatric symptoms like frontal-executive dysfunction and anxiety signs (Magaña et al., 2013; Stezin et al., 2018). Several pre-clinical studies have attempted to develop effective therapeutic approaches to delay or stop SCA2 disease. However, currently, patients rely only on pharmacological compounds to relief symptomatology.

Understanding the molecular mechanisms underlying SCA2 pathogenesis is essential to find new targets and an efficient therapy for this incurable disorder. The development and characterization of several SCA2 cellular and animal models, already provided some hints in the events that lead to neuronal death. The disease-causing polyQ expansion induces conformational alterations in the native Atx2 structure, resulting in formation of insoluble fibrillar bodies that accumulate as aggregates inside neuronal cells (Takeuchi and Nagai, 2017; Wen et al., 2017). Although the role of aggregation in SCA2 pathogenesis remains unresolved, analysis of patients' *post-mortem* brain samples revealed a positive correlation between the presence of mutant Atx2 inclusions and the severity/extension of neuronal degeneration (Seidel et al., 2017). Despite several advances, the exact mechanisms through each mutant Atx2 leads to death of neurons are still controversial and need to be further elucidated. Moreover, most

mouse models developed so far focused mainly on studying neuropathological features in cerebellum tissue, while neuronal degeneration is found in numerous different brain regions (Alves-Cruzeiro et al., 2016; Seidel et al., 2017).

Thus, in this work we aimed at developing a novel lentiviral mouse model of SCA2, with striatal pathology (Marcelo et al., 2021a). We observed that transduction of striatal neurons with lentiviral vectors (LVs) carrying mutant Atx2, resulted in substantial levels of mutant protein inclusions, as well as loss of neuronal markers staining. We further detected increased levels of cell death and neuroinflammation signs upon expression of mutant Atx2 in mice striatum. Importantly, we validated the use of this new lentiviral mouse model to assess the effect of potential therapeutic strategies. Overall, the new mouse model developed in this work resembled diverse neuropathological traits observed in SCA2 patients, constituting a valuable tool to investigate disease mechanisms and to study new targets for a therapeutic intervention for this incurable pathology.

3.2 Material and Methods

3.2.1 Animals

Adult C57/BL6 mice, breed in the animal house facility of the Center for Biomedical Research of University of Algarve, were used in this work. All animals were housed in a temperature-controlled room on a 12h light-12 h dark cycle. Food and water were provided ad libitum. The experiments were carried out in accordance with the European Community directive (86/609/EEC) for the care and use of laboratory animals. The researchers received certified training (FELASA course) and approval to perform the experiments from the Portuguese authorities (Direcção Geral de Alimentação e Veterinária) in the project Neuropath (421/2019).

3.2.2 Lentiviral vectors

Lentiviral particles (LVs) encoding for human full-length ataxin-2 with either normal polyQ segment (23Q – Atx2WT) or mutant polyQ segment (80Q – Atx2MUT) under the control of the mouse phosphoglycerate kinase 1 (PGK) promoter were produced in HEK (human embryonic kidney) 293T cells using a four-plasmid system, described elsewhere (Pereira de Almeida et al., 2001), and quantified by p24 antigen ELISA (RETROtek, Gentaur, France), by ViraVector facility, University of Coimbra. Additionally, LVs encoding for CRISPR-Cas 9 system guided for Carhsp1 (Cr-Carhsp1) under the control of the eukaryotic EF-1 alpha promoter were produced in HEK (human embryonic kidney) 293T and quantified by p24 antigen ELISA (RETROtek, Gentaur, France) by ViraVector facility, University of Coimbra.

LVs encoding for CRISPR-Cas 9 system guided for *Escherichia coli* lac Z gene (Cr-CT) under the control of the eukaryotic EF-1 alpha promoter were produced in HEK 293T by our research group in ABC-RI facility, University of Algarve. The LVs titer was quantified using the Lentivirus qPCR Titer Kit (Applied Biological Materials Inc, Vancouver, Canada), allowing the determination of the virus titer in infectious units per ml (IU/ml).

3.2.3 SCA2 striatal lentiviral mouse model

To develop the SCA2 lentiviral mice, concentrated LVs viral stocks encoding for Atx2WT or Atx2MUT, Cr-Carhsp1 and Cr-CT were thawed on ice and homogenized. Adult (8/10-week-old) C57/BL6 mice were anesthetized through intraperitoneal injection (IP) of a mixture of ketamine (75mg/kg, Nimatek, Dechra) with medetomidine (0.75mg/kg, DOMTOR®, Esteve). LVs were administered through a stereotaxic surgery into the left (Atx2WT) or the right (Atx2MUT) hemisphere of the striatum according to the following brain coordinates relative to bregma: antero-posterior (+0.6mm); lateral (±1.8mm); ventral (-3.3mm). A concentration of 400ng of p24 antigen (2E10 IU/µl) in 2µl of Atx2MUT LVs were injected at a rate of 0.25µl/min, by means of an automatic injector (Stoelting Co., Wood Dale, IL, USA), into mice striatum using a 34-gauge blunt-tip needle linked to a Hamilton syringe (Hamilton, Reno, NV, USA). Four, eight and twelve weeks after surgery, mice were sacrificed for posterior analysis. Additionally, for CRISPRs constructs assessment, a total concentration of 400ng (Atx2MUT and Cr-Carhsp1) of p24 antigen of LVs, while 1E9 IU (Cr-CT) of LVs were injected and mice were sacrificed twelve weeks after surgery.

3.2.4 Tissue preparation

For all immunohistochemical assays, animals received an anesthesia (mixture described above) overdose, followed by a transcardial perfusion with 4% paraformaldehyde (PFA) solution SigmaAldrich). Upon removal, brains were left 24h in 4% PFA solution, dehydrated in a 30% sucrose/0.1M phosphate buffer solution (PBS) for 48h and cryoprotected at -80°C degrees. Posteriorly, coronal brain slices of 20µm thickness were obtained using a cryostat (Cryostar NX50, ThermoFisher Scientific) and stored in freefloating PBS with 0.05µm sodium azide solution at 4°C. For western blotting procedures, animals received an anesthesia overdose, followed by cervical dislocation. Brains were removed and striatal punches, using a Harris Core pen with 2.5 mm diameter (Ted Pella Inc., Redding, California, USA), were collected and stored at -80°C until subsequent processing.

3.2.5 Neuroblastoma cell culture and transfection

Mouse neuroblastoma line-derived cells (Neuro-2A), obtained from the American Type Culture Collection cell biology bank (CCL-131), were cultured in Dulbecco's modified Eagle's medium (DMEM) supplemented with 10% fetal bovine serum (FBS), 100 U/ml penicillin and 100 mg/ml streptomycin (Gibco) at 37◦C in 5% CO2/air atmosphere. For transfection assays, complexes of 3µl PEI solution (polyethylenimine 1mg/ml, Tebu-bio) with 500ng of DNA plasmids were formed in 10µl DMEM without supplementation and added to cells previously cultured in 12-well plates for 24h. Transfection reagents were left in cells for a 48h-period incubation, following cells harvest for immunocytochemistry or western blot assays. The following DNA constructs were used: human full-length ataxin-2 with normal polyQ segment (23Q – Atx2WT) and mutant polyQ segment (80Q – Atx2MUT).

3.2.6 Human post-mortem brain tissue

Post-mortem striatum and cerebellum brain tissue from two clinically and genetically SCA2 confirmed patients were obtained from the NIH NeuroBioBank (USA). Control striatum and cerebellum tissues from healthy individuals, without neurological conditions diagnosed, were obtained from NIH NeuroBioBank (USA). Tissues preserved in 4% PFA solution, were dehydrated in a 30% sucrose/PBS for 48h, cryoprotected at -80°C degrees, dissected in 40µm slices using a cryostat (Cryostar NX50, ThermoFisher Scientific) and stored in free floating PBS/sodium azide solution at 4°C.

3.2.7 Immunochemical procedures

3.2.7.1 Immunocytochemistry

Immunocytochemistry procedure was performed based on protocols described elsewhere (Mendonça et al., 2015; Nóbrega et al., 2015a). Briefly, for cells harvest, we washed cultures with PBS and fixed it with 4% PFA for 20min. Cells were permeabilized with 1% Triton™ X-100 (Sigma) and blocked using 3%

Bovine Serum Albumin (Nzytech) in PBS. Incubation with primary antibodies was done overnight at 4°C. After PBS washes for antibodies removal, cells were incubated in secondary antibodies for 2h at room temperature (RT). Finally, cells were washed with PBS and coverslips were mounted on microscope slides using Fluoromount-G™ medium with DAPI (4′,6′-Diamidino-2′-phenylindole) (ThermoFisher Scientific). Images were acquired with a 100x objective in a Zeiss LSM710 confocal microscope.

3.2.7.2 Immunohistochemistry – free floating incubation

Immunohistochemistry assays were performed based on protocols described elsewhere(Nascimento-Ferreira et al., 2011; Nóbrega et al., 2013a, 2014). For visible microscopy analysis, mouse and human brain slices were incubated in PBS/0.1% diphenylhydrazine for 30min at 37°C. A subsequent step of incubation in Tris-buffered pH=9 antigen retrieval solution for 30min at 95°C was performed for human sections. Then, all sections were left in PBS/10% normal goat serum (Gibco)/0.1% Triton X blocking solution for 1h at RT, followed by overnight incubation with primary antibodies at 4°C. Posteriorly, slices were incubated in biotinylated secondary antibodies (1:200, Vector Laboratories) for 2h at RT and then in a reaction with the Vectastain elite avidin-biotin-peroxidase kit and by 3,3′-diaminobenzidine substrate (both from Vector Laboratories). After, sections were assembled over microscope slides, dehydrated in increasing degree ethanol solutions (75, 96 and 100%) and xylene, and finally coverslipped using mounting medium Eukitt (O. Kindler GmbH & CO, Freiburg, Germany). For fluorescence-labeling procedures, sections were incubated in the same blocking solution, followed primary and secondary antibodies incubation as described above. After antibodies probing, slices were mounted in microscope slides and coverslipped using the Fluoromount-G™ medium with DAPI. Images were acquired with a 20x objective in a Zeiss Axio Imager Z2 and Axio Scan.Z1 Slide Scanner microscopes, and with a 100x objective in a Zeiss LSM710 confocal microscope.

3.2.7.3 Immunochemical antibodies

For immunochemical procedures, the following primary antibodies were used: mouse anti-ataxin-2 (1:1000, ref. 611378, BD Biosciences); rabbit anti-DARP-32 (1:1000, ref. AB10518, Merck Millipore); mouse anti-Iba1/AIF1 (1:1000, ref. MABN92, Merck Millipore); mouse anti-GFAP (1:1000, ref. 644702, BioLegend); rabbit anti-Cleaved Caspase-3 (Asp175) (1:1000, ref. 9661, Cell Signaling); rabbit anti-GFAP (1:500, ref. Z0334, Dako, Agilent); rabbit anti-Iba1 (1:1000, ref. 019-19741, FUJIFILM Wako Pure Chemical Corporation) and rabbit anti-NeuN (1:1000, ref. ABN78, Millipore). The following secondary antibodies were used: goat biotinylated anti-mouse (1:200, ref. BA-9200, Vector Laboratories); goat biotinylated anti-rabbit (1:200, ref. BA-1000, Vector Laboratories); goat Alexa Fluor® 594 anti-mouse (1:500, ref. A11005, Invitrogen); goat Alexa Fluor® 594 anti-rabbit (1:500, ref. A11012, Invitrogen); goat Alexa Fluor® 488 anti-rabbit (1:500, ref. A11008, Invitrogen); goat Alexa Fluor® 488 anti-mouse (1:500, ref. A11001, Invitrogen).

3.2.8 Cresyl violet staining

Coronal mouse brain slices were displayed onto microscope slides, followed by cresyl violet solution staining and ethanol (75, 96 and 100% solutions) and xylene dehydration. Eukitt mounting medium was then used to mount coverslips. Images were acquired with 20x objective in a Zeiss Axio Imager Z2.

3.2.9 Immunochemistry quantitative analysis

For quantification of Atx2 aggregates and DARPP-32 staining loss, 18 coronal sections per animal were analyzed in ZEN lite software (Zeiss), so that a complete rostrocaudal picture of the striatum was obtained (14-16 transduced sections). Atx2 inclusions were manually counted in all animals. DARPP-32 neuronal lesion area was manually measured for all animals, allowing quantification of depleted volume according to the formula: volume = d*(a1 + a2 + a3), where d is the distance between serial sections (160 µm) and a1 + a2 + a3 are depleted areas for each individual section.

3.2.10 Cleaved caspase-3 quantitative analysis

The cleaved caspase-3 puncta were assessed by scanning 14-16 sections of each animal covering the entire transduced striatum using a 20x objective in an Axio Scan.Z1 Slide Scanner microscope. The total number of cleaved caspase-3 puncta was calculated automatically in a blind manner using ImageJ (NIH, USA), as well as the number of Atx2 transduced cells in those sections (Nóbrega et al., 2015a). Data were expressed as the ratio of the total number of cleaved caspase-3 puncta to the total number of Atx2 transduced cells normalized for the control Atx2WT hemisphere.

3.2.11 Neuronal density quantitative analysis

The total number of Atx2 transduced cells was assessed by scanning 14-16 sections of each animal covering the entire transduced striatum using a 20x objective in an Axio Scan.Z1 Slide Scanner microscope. This number was calculated automatically in a blind manner using ImageJ (NIH, USA). Considering the striatal hemisphere volume of 10.75 mm^3 (ref. (Hjorth et al., 2020)) and an average of 20% transduction area per hemisphere, the total number of Atx2 transduced cells in the striatum was used to calculate the number of neurons transduced with Atx2 per mm^3.

3.2.12 Western blot

Cell extracts were lysed in 10x RIPA solution (Merck Millipore) and mouse striatal punches were homogenized in a urea/DTT solution, both containing a cocktail of protease inhibitors (Roche pharmaceuticals), followed ultrasound sonication. Protein concentration levels were determined using Pierce™ BCA Protein Assay Kit (Thermo Scientific) for cell lysates and using NZYBradford reagent (Nzytech) for mouse samples. Sixty to eighty protein µg were resolved in SDS-polyacrylamide gels (7.5% and 12%). Followed by protein transfer to PVDF membrane (Merck Millipore) and antibody probing using the following antibodies: mouse anti-ataxin-2 (1:1000, ref. 611378, BD Biosciences); mouse anti-IC2

(polyQ chain) (1:1000, ref. MAB1574, Merck Millipore); mouse anti-β-actin (1:5000, ref. A5316, Sigma Aldrich). Optical densiometric analysis was carried out using Image J software (USA).

3.2.13 Statistical analysis

All statistical analysis was performed using Student's *t*-test for two groups or one-way ANOVA followed by *post hoc* Tukey's multiple comparison test for three groups, using GraphPad software (La Jolla, USA).

3.3 Results

3.3.1 Atx2 aggregate-like inclusions are detected in SCA2 patients' striatum and cerebellum tissue

Several histological and neuroimaging studies in neuronal tissues from SCA2 patients have already demonstrated that several other brain regions, besides the cerebellum, are affected in this neurodegenerative disorder (Seidel et al., 2012). Thus, we first decided to confirm whether striatum tissue is affected in SCA2 post-mortem brain samples. Upon microscopy analysis, we confirmed the presence of the hallmark mutant Atx2 aggregates in the cerebellum of SCA2 patients (Fig.22C), while these aggregates were not observed in healthy individual brain samples (Fig. 22A). Importantly, mutant Atx2 inclusions were also detected in striatum SCA2-derived tissue (Fig. 22D), whereas these structures were not present in control non-disease brain (Fig.22 B). These findings support that developing a mouse model mimicking striatal pathology could be a useful tool for pre-clinical research studies in SCA2 disease.

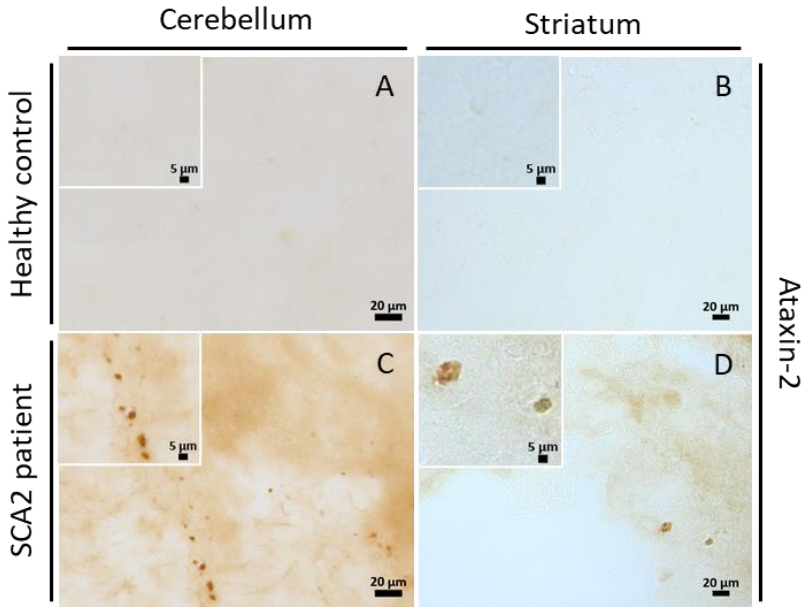

Fig. 3.1: **Atx2 protein inclusions abnormally accumulate in SCA2 patients' brain.** Immunohistochemical analysis of cerebellum post-mortem brain sections of SCA2 patients and healthy controls. (A-B) Staining for ataxin-2 showed no immunoreactivity in cerebellum and striatum tissue of healthy control. (C-D) On the other hand, staining for ataxin-2 revealed the presence of aggregated structures in cerebellum and striatum of SCA2 brain, indicating a disease state.

3.3.2 Overexpression of mutant Atx2 leads to neuropathological abnormalities SCA2-related.

The development and characterization of adequate non-human models of disease is crucial to elucidate disease mechanisms and to investigate new therapies. For SCA2, different cellular and animal models have been developed (Alves-Cruzeiro et al., 2016; Sen et al., 2019). While the use of these models has several advantages, often they only display disease features in advanced ages, which sometimes conditionate the development of research projects in a reasonable timeline. The classical view is that SCA2 selectively impacts the cerebellum, leading to poor movement coordination as the disease progresses. However, clinical evidence from the past 10 years shows that other regions are affected and are the underlying causes for non-ataxia symptoms (Seidel et al., 2012). Therefore, we aimed to develop a new model based in the expression of mutant Atx2 through LVs in the striatum region. A similar approach has been used for Huntington's disease and SCA3 (De Almeida et al., 2002; Alves et al., 2008b). Previously, it was shown that LVs have a high tropism to transduce neurons (Pereira de Almeida et al., 2001). Accordingly, we showed that LVs promote the expression of Atx2 in striatal neurons, stained for the neuronal nuclear marker NeuN, regardless of the length of the polyQ expansion (Fig. 23A-D). Moreover, LVs did not transduce glial cells, such as astrocytes or microglia, as co-localization between Atx2 and the glial markers GFAP and Iba1 was not observed (Fig. 23E-L). Additionally, Atx2 expression was under the control of the mouse phosphoglycerate kinase 1 (PGK) promoter, which allows long-term and sustained transduction of striatum neurons(Alves et al., 2008b; Nóbrega et al., 2013a).

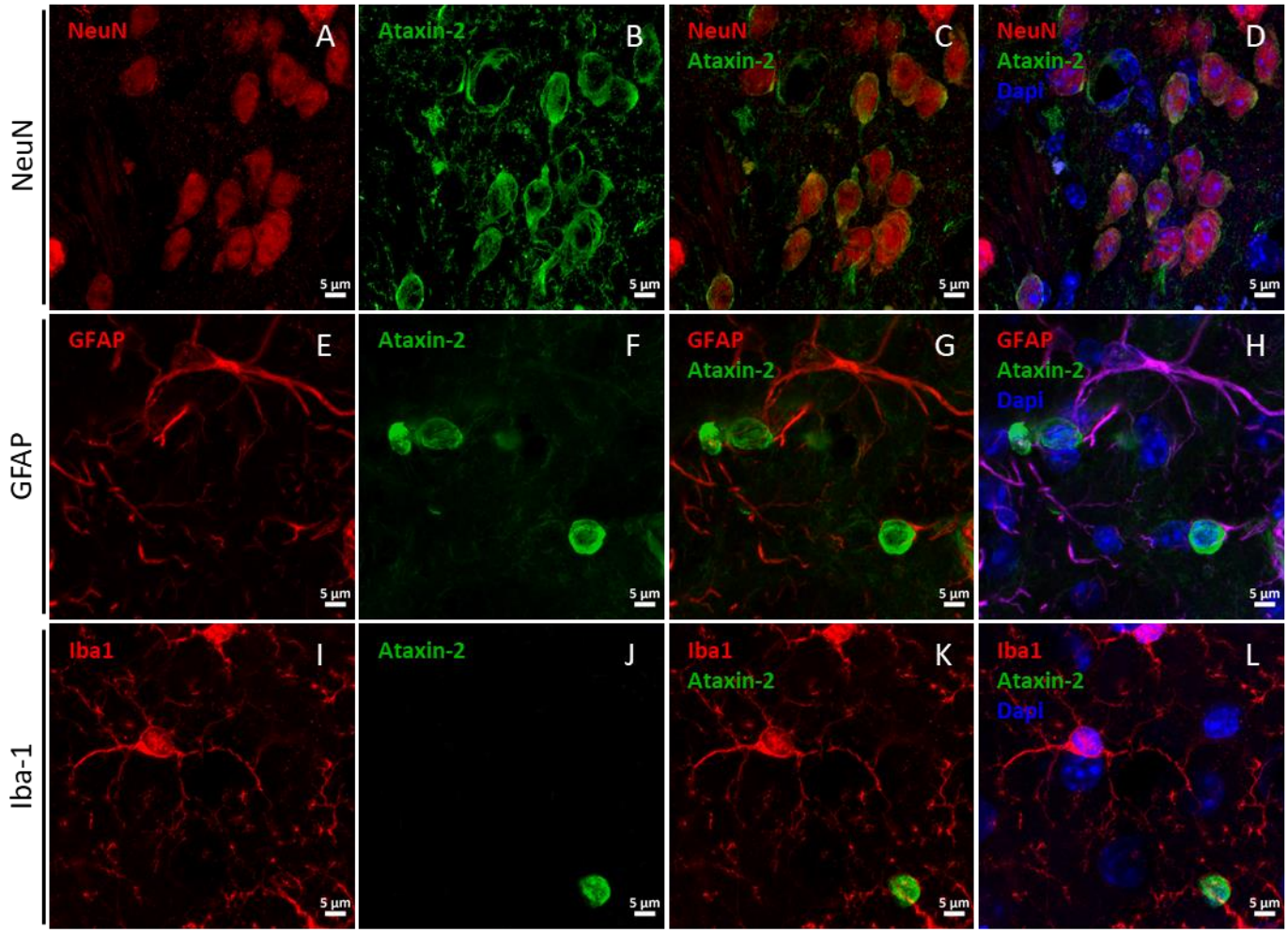

Fig. 3.2: **Lentiviral vectors (LVs) encoding for Atx2 specifically transduces striatal neurons.** LVs encoding for human wild-type Atx2 (Atx2WT) and mutant Atx2 (Atx2MUT) were injected in mice striatum under the control of neuron-specific PGK promoter. Brain sections were immunoassayed for Atx2 protein, the nuclear neuronal marker NeuN, and the glial markers GFAP and Iba1. (A-D) Confocal microscopy revealed that Atx2 is expressed in NeuN positive neurons, surrounding the nucleus of these cells. On the other hand, GFAP marker and Iba1 co-staining showed that LVs do not transduce glial cells, as Atx2 expression does not co-localized with astrocytes (E-H) or microglia (I-L).

For the development of the SCA2 striatal lentiviral mouse model, we used two different ataxin-2 constructs. The wild-type human full-length ataxin-2 had a non-pathogenic polyQ segment with 23 glutamines (23Q – Atx2WT), whereas the human full-length mutant construct used carried an abnormal polyQ-expanded tract with 80 glutamines (80Q – Atx2MUT). Before *in vivo* experiments, we previously validated these constructs in N2A cells, in which we observed the presence of ataxin-2 aggregates upon transfection with Atx2MUT (Fig. 24D-F), while Atx2WT form does not form intracellular aggregated inclusions (Fig. 24A-

C). Moreover, Western blot analysis demonstrated higher levels of polyglutamine chain in Atx2MUT condition compared to Atx2WT (Fig. 24G-H).

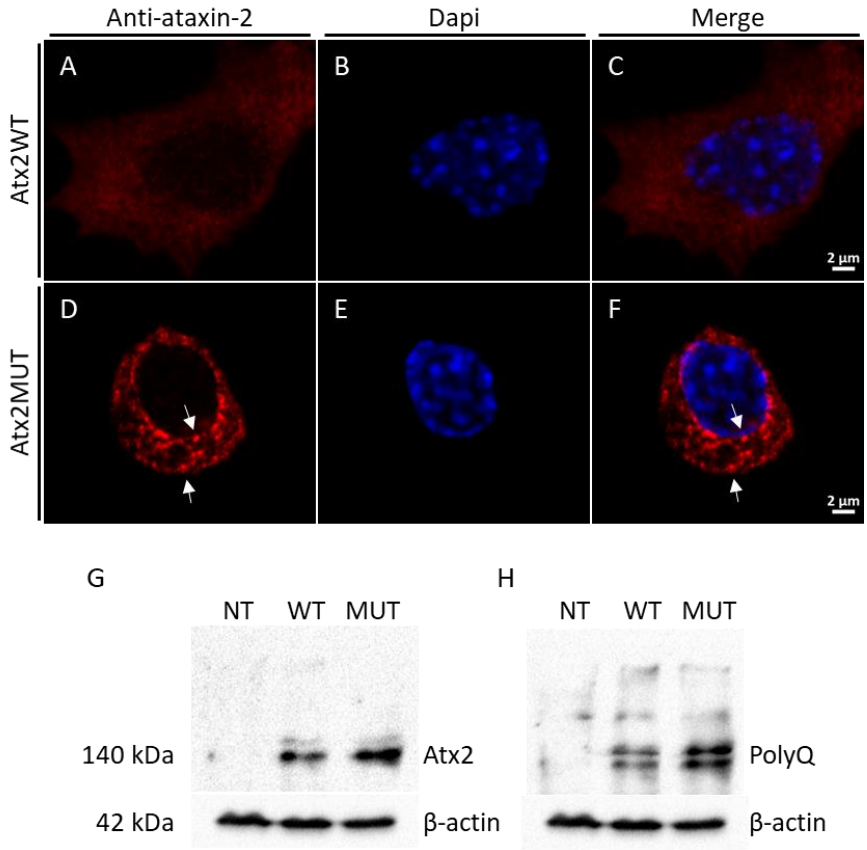

Fig. 3.3: **Atx2MUT construct induces aggregation in N2A cells.** Cultured N2A cells were transfected either with human wild-type ataxin-2 (Atx2WT) or mutant ataxin-2 (Atx2MUT). After 48h of transfection, cells were collected and labelled using anti-ataxin-2 and/or anti-1C2 (polyQ repeats) antibodies through immunocytochemistry and Western Blot assays, respectively. Confocal microscopy revealed the presence of ataxin-2 positive inclusions in the cytoplasm of cells expressing Atx2MUT (D, E, F) while cells transfected with Atx2WT did not present aggregated structures (A, B, C). Western blot results showed higher levels of polyglutamine chain in Atx2MUT condition compared to Atx2WT or non-transfected cells (NT) (G, H).

To develop the striatal lentiviral model for SCA2, LVs encoding for Atx2WT were injected in mice left striatum, while Atx2MUT were injected in the contralateral hemisphere of the same animal, through stereotaxic surgery (Fig. 25A). For immunohistochemical analysis, the injected animals were divided into three different groups and sacrificed at 4-, 8- and 12-weeks post-injection (Fig. 25B). Mutant Atx2 protein is prone to aggregate and form cytoplasmic insoluble inclusions that are found in patients' brain tissue (Koyano et al., 2014). Immunohistochemistry analysis for Atx2 revealed a diffuse staining across Atx2WT injected region (Fig. 25C), while we detected the presence of ataxin-2 aggregates in the Atx2MUT injected hemisphere (Fig. 25D-F). The number of aggregates increased significantly over time, reaching the maximum at 12 weeks post-injection (Fig. 25K). In the SCA3 lentiviral model, the expression of mutant Atx3 resulted in the loss of neuronal markers (Alves et al., 2008b). In line with this, we found that the expression of Atx2MUT led to a depletion of DARPP-32 marker, being the volume of neuronal loss significantly higher at 12 weeks post injection compared to the 4- and 8- weeks timepoints (Fig. 25H-J, L). In the Atx2WT hemisphere there is a residual DARPP-32 staining depletion (Fig. 25G), although it was lower than the marker loss reported upon an injection with PBS (Nóbrega et al., 2019). Importantly, the levels of DARPP-32 loss were similar across all time points (Fig. 25M). These results show that the expression of mutant Atx2, induces neuropathological alterations similar to those observed in SCA2 patients (Koyano et al., 1999; Pang et al., 2002).

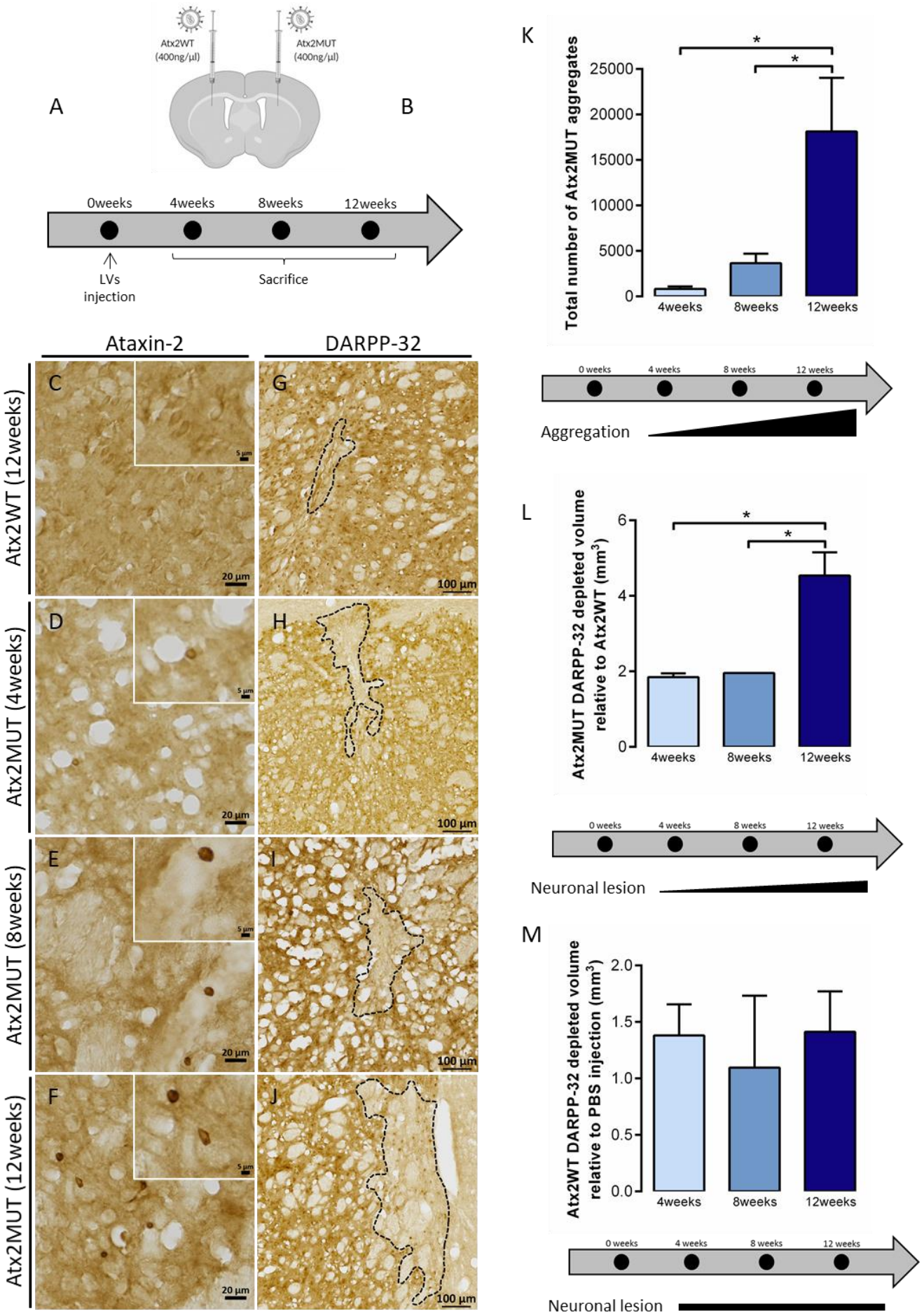
A
B
Atx2WT
(400ng/µl)
Atx2MUT
(400ng/µl)
0weeks
4weeks
8weeks
12weeks
LVs
injection
Sacrifice
Ataxin-2
DARPP-32
Atx2WT (12weeks)
Atx2MUT (4weeks)
Atx2MUT (8weeks)
Atx2MUT (12weeks)
C
D
E
F
G
H
I
J
20 µm
100 µm
5 µm
K
Total number of Atx2MUT aggregates
25000
20000
15000
10000
5000
0
4weeks
8weeks
12weeks
0 weeks
4 weeks
8 weeks
12 weeks
Aggregation
L
Atx2MUT DARPP-32 depleted volume relative to Atx2WT (mm³)
6
4
2
0
Neuronal lesion
M
Atx2WT DARPP-32 depleted volume relative to PBS injection (mm³)
2.0
1.5
1.0
0.5
0.0
Neuronal lesion

Fig. 3.4: **The expression of mutant ataxin-2 in the striatum induces aggregation and loss of neuronal marker.** A) Animals received a stereotaxic injection with lentiviral vectors (LVs) encoding for human wild-type ataxin-2 (Atx2WT) and mutant ataxin-2 (Atx2MUT) in left and right striatum hemisphere, respectively. B) Animals were divided in three groups according to the time of Atx2 expression, for 4-, 8- and 12- weeks after injection. C) Immunohistochemistry of brain sections revealed a general diffuse signal for Atx2 protein expression in Atx2WT hemisphere. In contrast, the overexpression of Atx2MUT resulted in Atx2 aggregates at 4 (D), 8 (E), and 12 (F) weeks of experiment. K) The quantification of the total number of mutant aggregates showed a significant increase over time of Atx2 expression, reaching high levels at 12 weeks (values are expressed as mean ± SEM *n*=3 per timepoint). (G) Immunohistochemistry for DARPP-32 neuronal marker showed that Atx2WT results in reduced marker loss, whereas Atx2MUT induces a higher depletion of staining for DARPP-32 either at 4- and 8-weeks post injection (H, I). These alterations are particularly high at 12 weeks (J, L) (values are expressed as mean ± SEM *n*=3 (4-, 8-weeks) and *n*=8 (12-weeks). Quantification of the neuronal marker depleted volume in mice Atx2WT hemisphere revealed similar levels of DARPP-32 depleted staining at 4-, 8- and 12-weeks after injection, indicating that expression of Atx2WT does not aggravate neuronal marker loss over time (G, M) (values are expressed as mean ± SEM relative to PBS injection n=3). *P < 0.05; one-way ANOVA followed by post hoc Tukey's multiple comparison test).

Moreover, we analyzed a group of injected animals with Atx2WT to confirm the expression of ataxin-2 in both hemispheres through Western blot analysis of striatal punches (Fig. 26A-B). No differences were found in the expression of Atx2WT and Atx2MUT. We further complemented the immunohistochemical studies in the previous group of animals, where we quantified the number of transduced neurons in the striatum per mm^3, by analyzing the transduced sections and automatically counting the Atx2 positive cells. In the same line as what was observed in the western blot analysis, no differences in the expression between Atx2WT and Atx2MUT was observed, thus suggesting similar levels of LVs transduction (Fig. 26C-G).

Altogether, our results show that the expression of mutant Atx2 in the striatum leads to the development of neuropathological abnormalities SCA2-related.

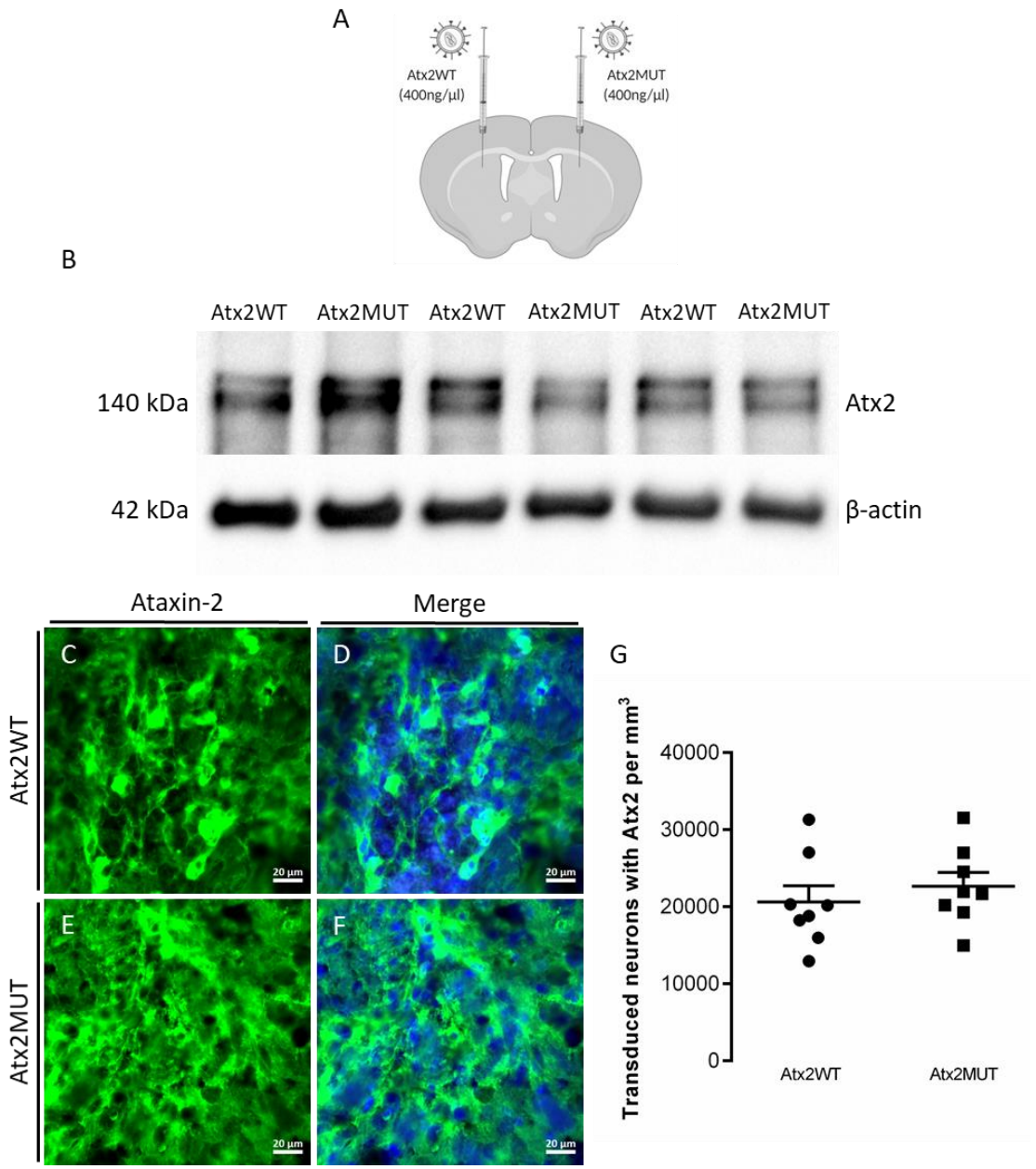

Fig. 3.5: **Lentiviral vectors (LVs) encoding for Atx2WT and Atx2MUT leads to similar expression levels of Atx2 in the striatum.** (A) Mice were stereotaxically injected with LVs encoding for human wild-type ataxin-2 (Atx2WT) and mutant ataxin-2 (Atx2MUT) under the control of PGK promoter in left and right striatum hemisphere, respectively. Striatal punches were collected 12 weeks after LVs expression and analyzed through Western blot for Atx2 protein. (B) We confirmed the expression of Atx2 upon LVs administration in both Atx2WT and Atx2MUT hemispheres. (C-F) Histological staining against Atx2 of striatum sections (14-16) were scanned in a fluorescence microscope. (G) Upon quantification of the number of striatal neurons transduced with Atx2 per mm3, no differences were found in the different constructs suggesting equal levels of transduction. Values are expressed as mean ± SEM *n*=8; unpaired Student's *t*-test.

3.3.3 The expression of mutant Atx2 leads to neuroinflammation and cell death

Neuronal death is the ultimate outcome of the molecular events underlying the SCA2 neuropathological process, which might be related to apoptosis. Therefore, in the injected animals we analyzed cleaved caspase-3 labeling (Fig. 27A-D), the active form of caspase-3 protein, which plays a critical role in apoptosis (McIlwain et al., 2013). We observed that the expression of Atx2MUT led to a significant increase in cleaved caspase-3 puncta over the different timepoints of the experiment, suggesting an increase in cell death through apoptosis (Fig. 27Q). Moreover, the formation of pycnotic nuclei structures occurs during the apoptotic process, as chromatin becomes condensed (Soriano et al., 1993). To assess the presence of these structures upon Atx2MUT expression, we performed a cresyl violet staining of striatal sections. In line with the results depicted above, we observed an increased presence of pycnotic nuclei over time of Atx2MUT expression, suggesting possible cell injury and striatal degeneration (Fig. 27E-H).

Neuroinflammation has been reported in polyQ diseases, as well as in other neurodegenerative disorders (Olejniczak et al., 2015; Hong et al., 2016). In SCA2, reactive astrocytes and microglia, characterized by the expression of GFAP and Iba1 markers, respectively, were observed in different brain tissues of affected individuals (Orozco et al., 1989; Huynh et al., 1999; Hoche et al., 2008). In line with this, we found that Atx2MUT resulted in marked astrogliosis (Fig. 27J-L) and microgliosis (Fig. 27N-P) across mice striata, compared to a minimal presence of reactive astrocytes and microglia in the needle insertion site in the Atx2WT injected hemisphere (Fig. 27I, M). The triggering of neuroinflammation by Atx2MUT is highlighted by the fact that surgically associated gliosis around the injection site is typically reduced over time, while we found that inflammatory response markers reactivity in Atx2MUT injected hemisphere increased over time (Fig. 27M). Overall, these results indicate that expression of mutant Atx2 leads to cell injury and degeneration in mice striatum, while also inducing neuroinflammation.

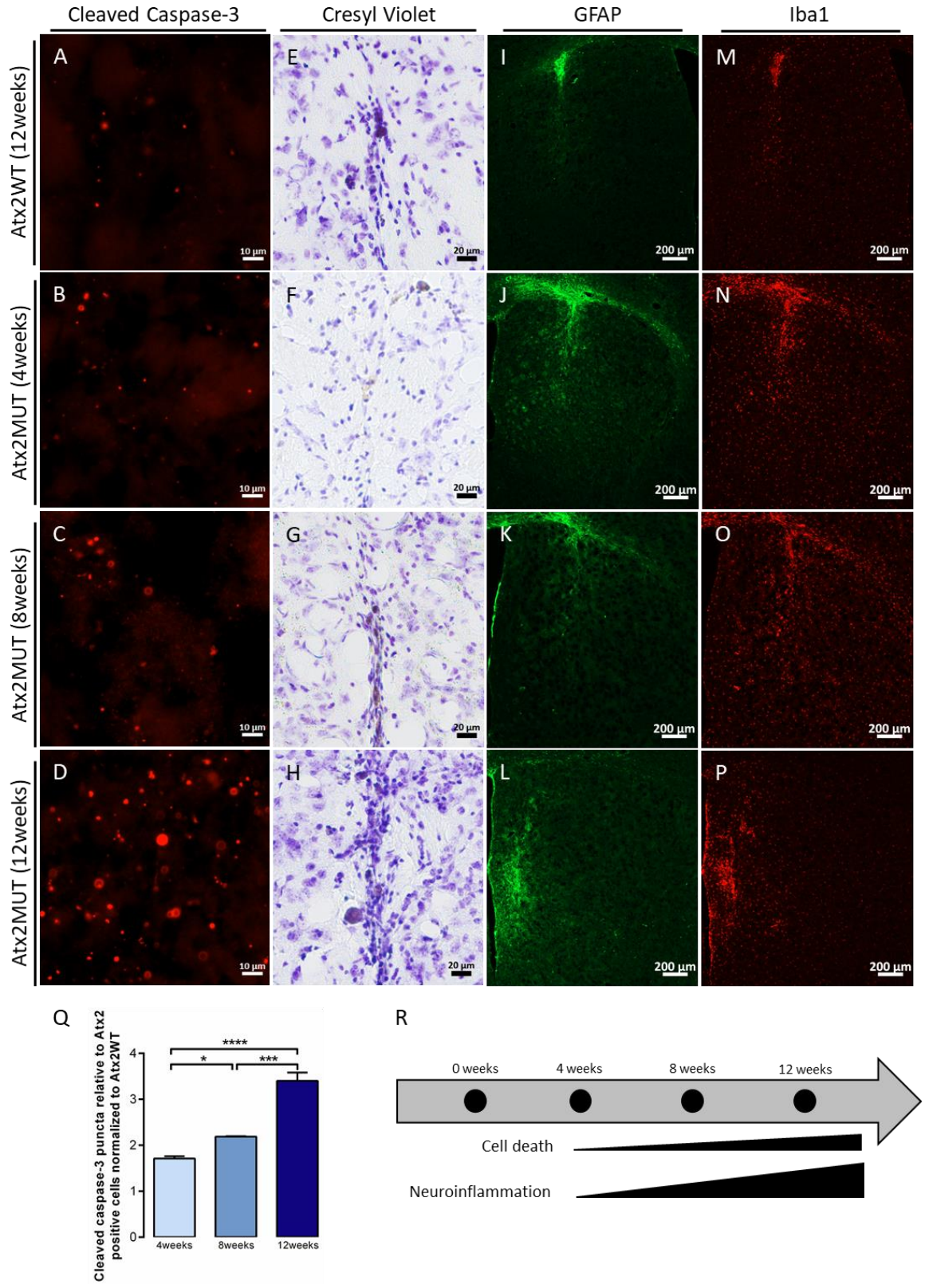

Fig. 3.6: **The expression of mutant Atx2 leads to cell death and neuroinflammation.** Cleaved caspase-3 immunostaining of mouse striatum sections injected with Atx2WT at 12 weeks (A) and Atx2MUT at 4-, 8- and 12- weeks post-injection (B-D). Quantification of cleaved caspase-3 puncta relative to Atx2 positive cells showed that expression of Atx2MUT in the mouse striatum leads to a significant increase of cleaved caspase-3 over the different timepoints, suggesting an increase in apoptosis (Q) (values are expressed

as mean ± SEM *n*=3 per timepoint and normalized to Atx2WT; *P < 0.05, ***P < 0.001, ****P < 0.0001; one-way ANOVA followed by post hoc Tukey's multiple comparison test). (E-H) Cresyl violet staining revealed that expression of Atx2MUT resulted in increased presence of pycnotic nuclei structures over time, suggesting cell lesion and striatal degeneration (R). Immunohistochemistry for GFAP (astrocytes marker) and Iba-1 (microglia marker) revealed low levels of astrogliosis (I) and microgliosis (M) upon expression of Atx2WT. In contrast, the overexpression of Atx2MUT induced an inflammatory response, highlighted by increased staining of GFAP (J-L) and Iba-1 (N-P) at 4-, 8- and 12-weeks after disease beginning. These neuropathological alterations are higher at 12-weeks of experiment (R).

3.3.4 Validation of the SCA2 striatal lentiviral mouse to assess novel targets for therapeutic intervention

As the development of the lentiviral mouse model resulted in striatal pathology resembling neuropathological findings observed in SCA2 patients, we further aimed to validate our model as a tool to assess potential therapeutic targets. Previous results from our work demonstrated that downregulation of the SGs component CARHSP1 resulted in mitigation of the phenotypic alterations in *in vitro* and *in vivo* models of SCA3 disease. Moreover, *CARHSP1* gene levels were found to be upregulated in SCA2-KI100 mouse model. Therefore, we decided to investigate the impact of downregulating Carhsp1 protein levels using the same CRISPR-Cas system (Cr-Carhsp1) used in the SCA3 striatal lentiviral mouse model. Thus, LVs encoding for human full-length mutant Atx2 with 80 glutamines (Atx2MUT) were injected in the right and left striatum hemisphere of adult C57/BL6 mice (Fig. 3.7A). Additionally, other animals received LVs encoding for Cr-CT or Cr-Carhsp1, together with Atx2MUT (Fig. 3.7A). Contrary to results observed in SCA3 models, we found that Cr-Carhsp1 did not alter the number of Atx2MUT aggregates, compared to the control groups (Atx2MUT and Cr-CT) (Fig. 3.7B-D, H). Moreover, the administration of CRISPRs constructs does not impact the loss of DARPP-32 neuronal marker staining volume, compared to Atx2MUT expression alone (Fig. 3.7E-G, I). Overall, our results suggest that downregulation of CARHSP1 SGs component does not impact Atx2 aggregation.

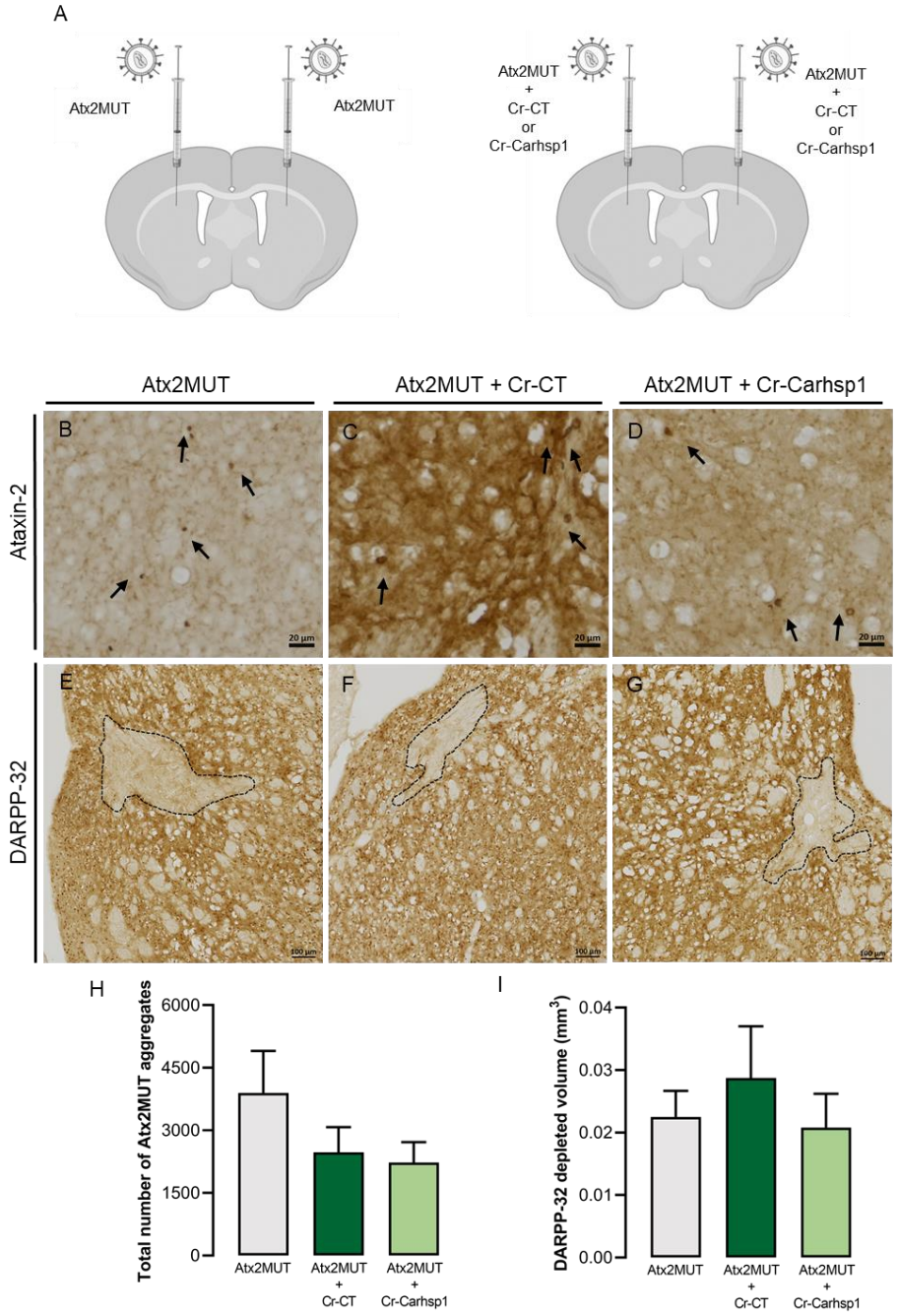

Fig. 3.7. **Assessment of Cr-Carhsp1 expression on aggregation and neuronal markers preservation in a SCA2 striatal lentiviral mouse model.** (A) LVs encoding for human full-length mutant Atx2 (Atx2MUT) were injected in mice striatum, as well as LVs encoding for Cr-CT and Cr-Carhsp1. (B-D) Brain slices were immunoassayed for Atx2 protein and (E-G) the neuronal marker DARPP-32. (H) Upon quantification of the total number of Atx2MUT aggregates, no differences between Cr-Carhsp1 and Cr-CT groups were observed. (I) Quantification of DARPP-32 staining loss volume showed no alterations in Cr-Carhsp1 compared to Cr-CT group. Values are expressed as mean ± SEM *n*=4 per condition; one-way ANOVA followed by post hoc Tukey's multiple comparison test.

3.4 Discussion

SCA2 is an incurable and fatal disease prompting devastating physical and psychological consequences for affected individuals and their families. The causative polyQ-expanded ataxin-2 protein is responsible for the cascade of events that precede neuronal death and degeneration of different brain regions (Huynh et al., 1999). However, the exact mechanisms underlying SCA2 pathogenesis are still controversial and need further elucidation so that a disease-modifying therapy can be developed. Disease models are fundamental tools to study physiological pathways behind human pathologies. Basic models as yeast, *Caenorhabditis elegans* and *Drosophila melanogaster* allowed the study of ataxin-2 biological roles (Kiehl et al., 2000; Satterfield and Pallanck, 2006). On the other hand, more complex models, like murine animals, allow a greater and profound functional knowledge, as well as the investigation of new therapeutic solutions. The existing SCA2 mouse models have several advantages, and have provided valuable insights in disease research (Huynh et al., 2000; Aguiar et al., 2006; Damrath et al., 2012; Hansen et al., 2013; Dansithong et al., 2015; Alves-Cruzeiro et al., 2016; Sen et al., 2019).

While the most affected brain region in SCA2 patients is the cerebellum, and specifically the Purkinje cells (Estrada et al., 1999), it is now clear that several other regions are also profoundly affected in these patients and responsible for the non-ataxia symptoms that SCA2 patients also display (Seidel et al., 2012). However, there is a lack of studies focusing on the striatum or other regions affected in SCA2, despite the fact that mutant ataxin-2 inclusions and neurodegeneration were observed in the striatum in patients' brain (Estrada et al., 1999; Koyano et al., 1999; Pang et al., 2002; Varrone et al., 2004). In fact, the involvement of this region in the disease could explain the parkinsonism symptoms observed in several SCA2 patients (Pirker et al., 2003). Therefore, in this study we aimed at developing a new mouse model featuring striatal pathology through the expression of mutant ataxin-2 under the control of neuron-specific PGK promoter mediated by lentiviral vectors, which are characterized by neuronal tropism and long-term stable expression (Zala et al., 2004).

Using this strategy, we detected mutant ataxin-2 aggregates and loss of a neuronal marker, as early as 4 weeks after the injection of LVs encoding mutant

ataxin-2. These neuropathological alterations increased significantly over time and reached maximum at 12 weeks post injection. Such early SCA2 signs were only detected in the Q127 transgenic mice, in which perinuclear aggregates were detected at 4 weeks of disease, although no sights of neuronal loss was found (Hansen et al., 2013). Moreover, the expression of mutant ataxin-2 resulted in increased levels of cleaved caspase-3 puncta and appearance of condensed chromatin pycnotic nuclei, suggesting cellular injury and death. Further characterization of our model strengthened the role of glial cells in SCA2 pathogenesis. Neuroinflammation actively contributes to increased toxicity and neuronal death in many neurodegenerative disorders (Hong et al., 2016). This process is mediated by astrocytes and microglia cells, that secrete neurotrophic factors and cytokines (Fakhoury, 2017). In fact, reactive astrocytes and microglia are present in affected brain regions of SCA2 patients (Gierga et al., 2005; Hoche et al., 2008). Accordingly, in our study, we observed astrogliosis and microgliosis in the mutant ataxin-2 expressing hemisphere, which worsened during disease progression. Therefore, our observations also support the inflammatory response as a potential target to treat this condition. Overall, our data suggests that the striatal lentiviral mouse model is a robust and fast disease progression model, reproducing several pathological hallmarks present in SCA2 patients.

The use of the SCA2 lentiviral mouse model as a suitable tool to assess novel targets for a therapeutic intervention was also validated in this work. We have previously reported that CARHSP1, an RNA-binding protein important in the formation of SGs, could impact disease phenotype in SCA3 PolyQ disease cellular and animal models. Moreover, we observed that *CARHSP1* gene expression levels are upregulated in brain of SCA2-KI100 transgenic mice. Thus, in this work we aimed to investigate whether knockdown of Carhsp1 levels, using CRISPR-Cas gene editing system, could also impact SCA2 neuropathological signs characterized in SCA2 lentiviral mouse model. Contrary to results obtained in SCA3 lentiviral model, downregulation of CARHSP1 levels did not impact mutant Atx2 protein aggregation. Although PolyQ diseases share common features and mechanisms of pathogenesis, this result reinforces that potential therapeutical targets should be tested for each PolyQ disease, as different outcomes might happen.

In conclusion, in this study we developed a new mouse model that bear resemblance to some of the neuropathological hallmarks observed in SCA2 patients, thus constituting a useful model to study disease mechanisms and therapeutic strategies. Moreover, the suitability of the striatal lentiviral mouse model to study the effect of pharmacological compounds in SCA2 disease was further demonstrated in our recent study (Marcelo et al., 2021a). In this work, the molecular activation of autophagy, using the compound cordycepin, mitigated the neuropathological alterations observed in SCA2 mice.

Chapter 4. Conclusions and future perspectives

Polyglutamine diseases are a group of rare and fatal neurodegenerative pathologies, which are caused by an abnormal expansion of CAG triple repeats within the coding region of disease-causing genes (Nóbrega and Pereira de Almeida, 2018). In all of these human conditions, the trinucleotide expansion is translated into a toxic polyQ stretch in the respective proteins, which tend to aggregate and form large multiprotein inclusions inside specific neuronal populations, ultimately leading to cell death (Gatchel and Zoghbi, 2005). While different, PolyQ diseases share common pathogenic mechanisms, including formation of toxic polyQ-expanded products and alterations of diverse biological processes, including protein clearance systems, transcription and translation, and mitochondrial function (Gatchel and Zoghbi, 2005; Bauer and Nukina, 2009; La Spada and Taylor, 2010). The related-PolyQ diseases features encourages the search of novel targets that have the potential to be therapeutic solutions for all disorders, which remain for now incurable.

Within the PolyQ group, spinocerebellar ataxia type 3 and type 2 represent the first and second most common SCAs in the world (Bird, 1998). SCA3 and SCA2 are caused by an expanded CAG stretch in *ATXN3* and *ATXN2* genes, respectively, resulting in a toxic polyQ tract in the translated proteins, Atx3 and Atx2 (Kawaguchi et al., 1994; Imbert et al., 1996; Pulst et al., 1996; Sanpei et al., 1996). Although Atx3 and Atx2 do not share significant homology or biological functions, when mutated both proteins undergo conformational alterations assembling into large insoluble inclusions that are found in patients brain (Paulson et al., 1997b; Schmidt et al., 1998; Seidel et al., 2017). Despite the exact events underlying selective neuronal death are not fully understood, several mechanisms have been proposed in SCA3 and SCA2 pathogenesis (Takahashi et al., 2010), including toxicity induced by polyQ-expanded protein aggregation, proteolytic cleavage, impairment of protein clearance systems, transcriptional and translational deregulation, calcium dysregulation, mitochondrial dysfunction and oxidative stress. Importantly, the dysfunction of these essential cellular pathways induces a stressful environment which needs to overcome, to cells survival.

The formation of stress granules plays an important role in the cellular response to stress stimulus (Buchan, 2014). In the presence of different stressors, translation initiation process is inhibited leading to the assembly of SGs, which

are composed by stalled pre-initiation complexes such as ribosomal subunits, translation initiation factors, mRNAs and RBPs (Vanderweyde et al., 2013). While essential players in cellular mechanisms, SGs have been associated with human conditions, like cancer (Anderson et al., 2015), aging (Masuda et al., 2009) and neurodegeneration (Asadi et al., 2021). In line with this, multiple evidence support a role of SGs and its components dysfunctionality in PolyQ diseases (Marcelo et al., 2021b). First, SGs components are sequestered and found in polyQ-expanded aggregates (Uchihara et al., 2001a; Waelter et al., 2001; Furukawa et al., 2009; Elden et al., 2010). Moreover, expression of polyQ-expanded proteins induce a persistent state of cellular stress, which could have a deleterious effect on cell survival (Wolozin and Ivanov, 2019). Thus, the main goal of this work was to clarify the role of SGs and its components in the context of PolyQ diseases, trying to identify new pathways and targets for therapeutic intervention using SCA3 and SCA2 as PolyQ diseases models.

We began our study by analyzing SGs components gene expression levels in SCA3 and SCA2 disease mouse models. Mammalian proteins described to be constituents of SGs assemblies have been previously curated and listed in an open access database by our group (Nunes et al., 2019). In this study, from the 464 proteins identified as SGs components, 395 genes have their levels altered in patients with the PolyQ disease HD. Accordingly, through transcriptomic data analysis, in this study we reported that 23 SGs components had their gene levels upregulated, while 9 were downregulated in SCA3 and SCA2 disease. This prompted us to investigate whether modulation of SGs components levels could be a promising therapeutic strategy in these pathologies. From the 32 differentially expressed components, we selected two RNA-binding proteins, CARHSP1 and PUM1, whose levels were found to be upregulated. As well, these proteins gene expression levels were also reported to be significantly increased in HD patients (Nunes et al., 2019). These findings led us to hypothesized whether decreasing CARHSP1 and PUM1 levels could be a potential strategy to treat PolyQ diseases. In order to test our hypothesis, we decided to use CRISPR-Cas gene editing tool to modulate the levels of SGs components selected, which proved to be efficient in downregulating CARHSP1 and PUM1 protein levels to more than 50% in mouse neuronal cells.

Firstly, we assessed the impact of Carhsp1 and Pum1 knockdown in mouse cellular and animal models of SCA3 disease. *In vitro* studies showed that while CARHSP1 resulted in decreased aggregation of mutant Atx3 protein, PUM1 did not alter the number of cells with mutant aggregates. On the other hand, silencing of both targets did not reduce neither increase mutant Atx3 soluble levels. Results in the SCA3 lentiviral mouse model were similar with those found in the cellular model. Whereas downregulation of CARHSP1 significantly reduced the number of mutant protein inclusions, PUM1 downregulation led to increased levels of aggregation. Further analysis also demonstrated that while knockdown of Carhsp1 resulted in reduced aggregation, the use of CRISPRs constructs did not preserve the loss of neuronal markers staining. Future studies on cell survival and death markers are required to evaluate possible toxic effects associated with CRISPR-Cas system. Next, we aimed to investigate the impact of decreasing Carhsp1 and Pum1 levels in a SCA3 transgenic mouse model, which exhibits early disease onset characterized by motor deficits and cerebellar pathology. Knockdown of CARHSP1 levels resulted in mitigation of mice motor incoordination, as well as reduced number of mutant Atx3 aggregates and reduced cerebellar atrophy, compared to non-treated animals. On the other side, PUM1 downregulation failed to rescue mice motor deficits, worsening the ataxic gait, while no evident neuropathological alterations were detected. Finally, we assessed whether the impact of CARHP1 and PUM1 in SCA3 disease could be associated with SGs formation. Our results showed that CARHSP1 is essential for the formation of SGs during oxidative stress and that decreasing its levels led to substantial decreased assembly of these cytoplasmic *foci*. As CARHSP1 was reported to function as a TNF-α mRNA stability enhancer necessary for effective production of this inflammation mediator, and neuroinflammation is a hallmark of SCA3 and other neurodegenerative diseases, posterior studies evaluating the effect of CARHSP1 downregulation in neuroinflammation markers should be performed (Pfeiffer et al., 2011; Hong et al., 2016). Regarding PUM1 component, we observed that downregulating its level did not affect SGs formation, suggesting it as non-essential player in SGs response to oxidative stress. The composition of SGs is variable depending on the cell type or stressing factor induced (Vanderweyde et al., 2013), thus studies using different stress stimulus

and other cell lines should be performed to confirm the role of PUM1 in SGs assembly.

Because downregulation of CARHSP1 levels revealed a promising benefic effect in rescuing several neuropathological and motor deficits in SCA3 disease models, we hypothesized whether this could be a potential therapeutic strategy for other PolyQ diseases. Therefore, we decided to evaluate this strategy in SCA2 disease.

Understanding disease mechanisms is essential to search for potential targets for therapy. Moreover, the screening and assessment of experimental therapies is only possible using disease models. In the case of SCA2, development and characterization of disease models using simple and more complex organisms highly improved the understanding of this incurable pathology. However, we found a lack of suitable models that allowed the study of different SCA2 disease aspects. The mouse models developed so far only focus on cerebellar pathology, while several other brain regions, including the striatum, have also neuronal degeneration (Estrada et al., 1999; Varrone et al., 2004). Moreover, most models manifest late disease, which delays experimental studies and increase their cost (Alves-Cruzeiro et al., 2016). Taking advantage of using viral constructs to expression mutant transgenes, in this work we developed and characterized a novel striatal lentiviral mouse model for SCA2 disease, which could serve the purpose of studying disease mechanisms, as well as, finding targets for a therapeutic intervention (Marcelo et al., 2021a). As LVs show a high tropism to transduce neurons (Pereira de Almeida et al., 2001), we used these viral vectors to promote the expression of mutant Atx2 in mice striatum. We then searched for neuropathological features typically observed in SCA2 patients, including neuronal mutant protein aggregation, neuronal degeneration, and inflammation signs. Twelve weeks after disease onset, we observed substantial levels of mutant inclusions, as well as decreased staining for neuronal markers upon mutant ataxin-2 expression. Moreover, the presence of pycnotic nuclei were observed, while levels of an apoptotic marker were found to be highly increased, upon expression of polyQ-expanded Atx2, suggesting cell death. Additionally, astrogliosis and microgliosis inflammation processes were also reported. Overall, our results supports that the striatal lentiviral mouse model is a robust and fast disease progression model, which resembles several features of SCA2 disease.

As the main goal of this work was to search for promising targets for therapeutic intervention in PolyQ diseases, we further validated the suitability of this model to assess the impact of CARHSP1 downregulation as a potential target in SCA2 disease. Contrary to results observed in SCA3 lentiviral mouse model, downregulation of CARHSP1 levels did not impact mutant ataxin-2 aggregation. Future studies evaluating cell death and neuroinflammation signs described for this mouse model are required to obtain further insight into the impact of CARHSP1 downregulation in SCA2 disease. Importantly, these data strengthen the idea that, although PolyQ diseases share common pathogenic mechanisms, validating novel therapeutic strategies is needed for each one of them, using relevant disease models.

In conclusion, our study identified a SGs component, CARHSP1, that showed promising results in ameliorating neuropathological and motor features in SCA3 disease models, whose potential as therapeutical solution for SCA3 should be further investigated.

References

Afonso-Reis, R., Afonso, I. T., and Nóbrega, C. (2021). Current Status of Gene Therapy Research in Polyglutamine Spinocerebellar Ataxias. *Int. J. Mol. Sci.* 22, 4249. doi:10.3390/IJMS22084249.

Aguiar, J., Fernández, J., Aguilar, A., Mendoza, Y., Vázquez, M., Suárez, J., et al. (2006). Ubiquitous expression of human SCA2 gene under the regulation of the SCA2 self promoter cause specific Purkinje cell degeneration in transgenic mice. *Neurosci. Lett.* 392, 202–206. doi:10.1016/J.NEULET.2005.09.020.

Alberti, S., Mateju, D., Mediani, L., and Carra, S. (2017). Granulostasis: Protein Quality Control of RNP Granules. *Front. Mol. Neurosci.* 10, 84. doi:10.3389/fnmol.2017.00084.

Albrecht, M., Golatta, M., Wüllner, U., and Lengauer, T. (2004). Structural and functional analysis of ataxin-2 and ataxin-3. *Eur. J. Biochem.* 271, 3155–3170. doi:10.1111/J.1432-1033.2004.04245.X.

Almaguer-Mederos, L., Rodríguez, R. A., Zaldivar, Y. G., Gotay, D. A., Almarales, D. C., Mesa, J. L., et al. (2013). Estimation of survival in Spinocerebellar Ataxia type 2 Cuban patients. *Clin. Genet.* 83, 293–294. doi:10.1111/J.1399-0004.2012.01902.X.

Almeida, B., Abreu, I. A., Matos, C. A., Fraga, J. S., Fernandes, S., Macedo, M. G., et al. (2015). SUMOylation of the brain-predominant Ataxin-3 isoform modulates its interaction with p97. *Biochim. Biophys. Acta* 1852, 1950–1959. doi:10.1016/J.BBADIS.2015.06.010.

Alves-Cruzeiro, J. M. D. C., Mendonça, L., Pereira de Almeida, L., and Nóbrega, C. (2016). Motor Dysfunctions and Neuropathology in Mouse Models of Spinocerebellar Ataxia Type 2: A Comprehensive Review. *Front. Neurosci.* 10. doi:10.3389/fnins.2016.00572.

Alves, S., Nascimento-Ferreira, I., Auregan, G., Hassig, R., Dufour, N., Brouillet, E., et al. (2008a). Allele-specific RNA silencing of mutant ataxin-3 mediates neuroprotection in a rat model of Machado-Joseph disease. *PLoS One* 3, e3341. doi:10.1371/journal.pone.0003341.

Alves, S., Régulier, E., Nascimento-Ferreira, I., Hassig, R., Dufour, N., Koeppen, A., et al. (2008b). Striatal and nigral pathology in a lentiviral rat model of Machado-Joseph disease. *Hum. Mol. Genet.* 17, 2071–2083. doi:10.1093/hmg/ddn106.

Anderson, P., and Kedersha, N. (2002). Visibly stressed: the role of eIF2, TIA-1, and stress granules in protein translation. *Cell Stress Chaperones* 7, 213. doi:10.1379/1466-1268(2002)007<0213:VSTROE>2.0.CO;2.

Anderson, P., and Kedersha, N. (2008). Stress granules: the Tao of RNA triage. *Trends Biochem. Sci.* 33, 141–50. doi:10.1016/j.tibs.2007.12.003.

Anderson, P., and Kedersha, N. (2009). RNA granules: post-transcriptional and epigenetic modulators of gene expression. *Mol. Cell Biol.* 10, 430–436. doi:10.1038/nrm2694.

Anderson, P., Kedersha, N., and Ivanov, P. (2015). Stress granules, P-bodies and cancer. *Biochim. Biophys. Acta* 1849, 861–870. doi:10.1016/J.BBAGRM.2014.11.009.

Antenora, A., Bruzzese, D., Lieto, M., Roca, A., Florio, M. T., Peluso, S., et al. (2018). Predictors of survival in spinocerebellar ataxia type 2 population from Southern Italy. *Neurol. Sci.* 39, 1857–1860. doi:10.1007/S10072-018-3504-1.

Araujo, J., Breuer, P., Dieringer, S., Krauss, S., Dorn, S., Zimmermann, K., et al. (2011).

FOXO4-dependent upregulation of superoxide dismutase-2 in response to oxidative stress is impaired in spinocerebellar ataxia type 3. *Hum. Mol. Genet.* 20, 2928–2941. doi:10.1093/HMG/DDR197.

Arimoto, K., Fukuda, H., Imajoh-ohmi, S., Saito, H., and Takekawa, M. (2008). Formation of stress granules inhibits apoptosis by suppressing stress-responsive MAPK pathways. *Nat. Cell Biol.* 10. doi:10.1038/ncb1791.

Asadi, M. R., Sadat Moslehian, M., Sabaie, H., Jalaiei, A., Ghafouri-Fard, S., Taheri, M., et al. (2021). Stress Granules and Neurodegenerative Disorders: A Scoping Review. *Front. Aging Neurosci.* 0, 310. doi:10.3389/FNAGI.2021.650740.

Ashizawa, A. T., Holt, J., Faust, K., Liu, W., Tiwari, A., Zhang, N., et al. (2018). Intravenously Administered Novel Liposomes, DCL64, Deliver Oligonucleotides to Cerebellar Purkinje Cells. *The Cerebellum* 18, 99–108. doi:10.1007/S12311-018-0961-2.

Auburger, G., Diaz, G. O., Capote, R. F., Sanchez, S. G., Perez, M. P., Cueto, M. E. del, et al. (1990). Autosomal dominant ataxia: Genetic evidence for locus heterogeneity from a cuban founder-effect population. *Am. J. Hum. Genet.* 46, 1163. Available at: /pmc/articles/PMC1683834/?report=abstract [Accessed October 26, 2021].

Barros, I., Marcelo, A., Silva, T. P., Barata, J., Rufino-Ramos, D., Pereira de Almeida, L., et al. (2020). Mesenchymal Stromal Cells' Therapy for Polyglutamine Disorders: Where Do We Stand and Where Should We Go? *Front. Cell. Neurosci.* 14. doi:10.3389/FNCEL.2020.584277.

Bauer, P. O., and Nukina, N. (2009). The pathogenic mechanisms of polyglutamine diseases and current therapeutic strategies. *J. Neurochem.* 110, 1737–1765. doi:10.1111/J.1471-4159.2009.06302.X.

Beauchemin, A. M. J., Gottlieb, B., Beitel, L. K., Elhaji, Y. A., Pinsky, L., and Trifiro, M. A. (2001). Cytochrome c oxidase subunit Vb interacts with human androgen receptor: A potential mechanism for neurotoxicity in spinobulbar muscular atrophy. *Brain Res. Bull.* 56, 285–297. doi:10.1016/S0361-9230(01)00583-4.

Bence, N. F., Sampat, R. M., and Kopito, R. R. (2001). Impairment of the Ubiquitin-Proteasome System by Protein Aggregation. *Science (80-.).* 292, 1552–1555. doi:10.1126/SCIENCE.292.5521.1552.

Berger, Z., Ravikumar, B., Menzies, F. M., Oroz, L. G., Underwood, B. R., Pangalos, M. N., et al. (2006). Rapamycin alleviates toxicity of different aggregate-prone proteins. *Hum. Mol. Genet.* 15, 433–442. doi:10.1093/HMG/DDI458.

Berke, S. J. S., Schmied, F. A. F., Brunt, E. R., Ellerby, L. M., and Paulson, H. L. (2004). Caspase-mediated proteolysis of the polyglutamine disease protein ataxin-3. *J. Neurochem.* 89, 908–918. doi:10.1111/J.1471-4159.2004.02369.X.

Bettencourt, C., and Lima, M. (2011). Machado-Joseph Disease : from first descriptions to new perspectives. *Orphanet J. Rare Dis.* 6, 1–12.

Bichelmeier, U., Schmidt, T., Hübener, J., Boy, J., Rüttiger, L., Häbig, K., et al. (2007). Nuclear Localization of Ataxin-3 Is Required for the Manifestation of Symptoms in SCA3: In Vivo Evidence. *J. Neurosci.* 27, 7418–7428. doi:10.1523/JNEUROSCI.4540-06.2007.

Bilen, J., and Bonini, N. M. (2007). Genome-Wide Screen for Modifiers of Ataxin-3 Neurodegeneration in Drosophila. *PLOS Genet.* 3. doi:10.1371/JOURNAL.PGEN.0030177.

Bird, T. D. (1998). Hereditary Ataxia Overview. *GeneReviews®*. Available at: https://www.ncbi.nlm.nih.gov/books/NBK1138/ [Accessed October 26, 2021].

Bonanomi, M., Natalello, A., Visentin, C., Pastori, V., Penco, A., Cornelli, G., et al. (2014). Epigallocatechin-3-gallate and tetracycline differently affect ataxin-3 fibrillogenesis and reduce toxicity in spinocerebellar ataxia type 3 model. *Hum. Mol. Genet.* 23, 6542–6552. doi:10.1093/HMG/DDU373.

Boy, J., Schmidt, T., Schumann, U., Grasshoff, U., Unser, S., Holzmann, C., et al. (2010). A transgenic mouse model of spinocerebellar ataxia type 3 resembling late disease onset and gender-specific instability of CAG repeats. *Neurobiol. Dis.* 37, 284–293. doi:10.1016/J.NBD.2009.08.002.

Braga-Neto, P., Felicio, A. C., Hoexter, M. Q., Pedroso, J. L., Dutra, L. A., Alessi, H., et al. (2012a). Cognitive and olfactory deficits in Machado–Joseph disease: A dopamine transporter study. *Parkinsonism Relat. Disord.* 18, 854–858. doi:10.1016/J.PARKRELDIS.2012.04.015.

Braga-Neto, P., Pedroso, J. L., Alessi, H., Dutra, L. A., Felício, A. C., Minett, T., et al. (2012b). Cerebellar Cognitive Affective Syndrome in Machado Joseph Disease: Core Clinical Features. *Cerebellum* 11, 549–556. doi:10.1007/S12311-011-0318-6.

Brenneis, C., Bösch, S. M., Schocke, M., Wenning, G. K., and Poewe, W. (2003). Atrophy pattern in SCA2 determined by voxel-based morphometry. *Neuroreport* 14, 1799–1802. doi:10.1097/00001756-200310060-00008.

Buchan, J. R. (2014). mRNP granules. Assembly, function, and connections with disease. *RNA Biol.* 11, 1019–1030. doi:10.4161/15476286.2014.972208.

Buchan, J. R., Kolaitis, R., Taylor, J. P., and Parker, R. (2013). Eukaryotic Stress Granules Are Cleared by Autophagy and Cdc48 / VCP Function. *Cell* 153, 1461–1474. doi:10.1016/j.cell.2013.05.037.

Buchan, J. R., and Parker, R. (2009). Eukaryotic Stress Granules: The Ins and Outs of Translation. *Mol. Cell* 36, 932–941. doi:10.1016/J.MOLCEL.2009.11.020.

Budworth, H., and McMurray, C. T. (2013). A brief history of triplet repeat diseases. *Methods Mol. Biol.* 1010, 3–17. doi:10.1007/978-1-62703-411-1_1.

Bunting, E. L., Hamilton, J., and Tabrizi, S. J. (2021). Polyglutamine diseases. *Curr. Opin. Neurobiol.* 72, 39–47. doi:10.1016/j.conb.2021.07.001.

Bürk, K., Fetter, M., Abele, M., Laccone, F., Brice, A., Dichgans, J., et al. (1999a). Autosomal dominant cerebellar ataxia type I: oculomotor abnormalities in families with SCA1, SCA2, and SCA3. *J. Neurol.* 246, 789–797. doi:10.1007/S004150050456.

Bürk, K., Globas, C., Bösch, S., Gräber, S., Abele, M., Brice, A., et al. (1999b). Cognitive deficits in spinocerebellar ataxia 2. *Brain* 122, 769–777. doi:10.1093/BRAIN/122.4.769.

Burnett, B. G., and Pittman, R. N. (2005). The polyglutamine neurodegenerative protein ataxin 3 regulates aggresome formation. *Proc. Natl. Acad. Sci.* 102, 4330–4335. doi:10.1073/PNAS.0407252102.

Burnett, B., Li, F., and Pittman, R. N. (2003). The polyglutamine neurodegenerative protein ataxin-3 binds polyubiquitylated proteins and has ubiquitin protease activity. *Hum. Mol. Genet.* 12, 3195–3205. doi:10.1093/HMG/DDG344.

Cancel, G., Dürr, A., Didierjean, O., Imbert, G., Bürk, K., Lezin, A., et al. (1997).

Molecular and Clinical Correlations in Spinocerebellar Ataxia 2: A Study of 32 Families. *Hum. Mol. Genet.* 6, 709–715. doi:10.1093/HMG/6.5.709.

Carmo-Silva, S., Nobrega, C., Pereira de Almeida, L., and Cavadas, C. (2017). Unraveling the Role of Ataxin-2 in Metabolism. *Trends Endocrinol. Metab.* 28, 309–318. doi:10.1016/J.TEM.2016.12.006.

Carmona, V., Cunha-Santos, J., Onofre, I., Simões, A. T., Vijayakumar, U., Davidson, B. L., et al. (2017). Unravelling Endogenous MicroRNA System Dysfunction as a New Pathophysiological Mechanism in Machado-Joseph Disease. *Mol. Ther.* 25, 1038–1055. doi:10.1016/J.YMTHE.2017.01.021.

Carvalho, D. R., La Rocque-Ferreira, A., Rizzo, I. M., Imamura, E. U., and Speck-Martins, C. E. (2008). Homozygosity Enhances Severity in Spinocerebellar Ataxia Type 3. *Pediatr. Neurol.* 38, 296–299. doi:10.1016/J.PEDIATRNEUROL.2007.12.006.

Castello, A., Fischer, B., Eichelbaum, K., Horos, R., Beckmann, B. M., Strein, C., et al. (2012). Resource Insights into RNA Biology from an Atlas of Mammalian mRNA-Binding Proteins. *Cell* 149, 1393–1406. doi:10.1016/j.cell.2012.04.031.

Cecchin, C. R., Pires, A. P., Rieder, C. R., Monte, T. L., Silveira, I., Carvalho, T., et al. (2007). Depressive Symptoms in Machado-Joseph Disease (SCA3) Patients and Their Relatives. *Community Genet.* 10, 19–26. doi:10.1159/000096276.

Cemal, C. K., Carroll, C. J., Lawrence, L., Lowrie, M. B., Ruddle, P., Al-Mahdawi, S., et al. (2002). YAC transgenic mice carrying pathological alleles of the MJD1 locus exhibit a mild and slowly progressive cerebellar deficit. *Hum. Mol. Genet.* 11, 1075–1094. doi:10.1093/HMG/11.9.1075.

Cendelin, J., Cvetanovic, M., Gandelman, M., Hirai, H., Orr, H. T., Pulst, S. M., et al. (2021). Consensus Paper: Strengths and Weaknesses of Animal Models of Spinocerebellar Ataxias and Their Clinical Implications. *The Cerebellum*, 1–30. doi:10.1007/S12311-021-01311-1.

Chai, Y., Berke, S. S., Cohen, R. E., and Paulson, H. L. (2004). Poly-ubiquitin Binding by the Polyglutamine Disease Protein Ataxin-3 Links Its Normal Function to Protein Surveillance Pathways. *J. Biol. Chem.* 279, 3605–3611. doi:10.1074/JBC.M310939200.

Chai, Y., Koppenhafer, S. L., Bonini, N. M., and Paulson, H. L. (1999a). Analysis of the Role of Heat Shock Protein (Hsp) Molecular Chaperones in Polyglutamine Disease. *J. Neurosci.* 19, 10338–10347. doi:10.1523/JNEUROSCI.19-23-10338.1999.

Chai, Y., Koppenhafer, S. L., Shoesmith, S. J., Perez, M. K., and Paulson, H. L. (1999b). Evidence for proteasome involvement in polyglutamine disease: localization to nuclear inclusions in SCA3/MJD and suppression of polyglutamine aggregation in vitro. *Hum. Mol. Genet.* 8, 673–82. Available at: http://www.ncbi.nlm.nih.gov/pubmed/10072437 [Accessed May 16, 2016].

Chai, Y., Wu, L., Griffin, J. D., and Paulson, H. L. (2001). The Role of Protein Composition in Specifying Nuclear Inclusion Formation in Polyglutamine Disease. *J. Biol. Chem.* 276, 44889–44897. doi:10.1074/JBC.M106575200.

Chang, K. H., Chen, W. L., Lee, L. C., Lin, C. H., Kung, P. J., Lin, T. H., et al. (2013). Aqueous extract of paeonia lactiflora and paeoniflorin as aggregation reducers targeting chaperones in cell models of spinocerebellar ataxia 3. *Evidence-based Complement. Altern. Med.* 2013. doi:10.1155/2013/471659.

Chang, W. H., Tien, C. L., Chen, T. J., Nukina, N., and Hsieh, M. (2009). Decreased

protein synthesis of Hsp27 associated with cellular toxicity in a cell model of Machado–Joseph disease. *Neurosci. Lett.* 454, 152–156. doi:10.1016/J.NEULET.2009.03.004.

Chang, Y., Chen, M., Chiang, Y., Chen, Y., Ma, W., and Tseng, C. (2011). Mesenchymal stem cell transplantation ameliorates motor function deterioration of spinocerebellar ataxia by rescuing cerebellar Purkinje cells. *J. Biomed. Sci.* 18, 54. doi:10.1186/1423-0127-18-54.

Chatterjee, N., Lin, Y., Santillan, B. A., Yotnda, P., and Wilson, J. H. (2015). Environmental stress induces trinucleotide repeat mutagenesis in human cells. *Proc. Natl. Acad. Sci. U. S. A.* 112, 3764. doi:10.1073/PNAS.1421917112.

Chen, C. M., Weng, Y. T., Chen, W. L., Lin, T. H., Chao, C. Y., Lin, C. H., et al. (2014a). Aqueous extract of Glycyrrhiza inflata inhibits aggregation by upregulating PPARGC1A and NFE2L2–ARE pathways in cell models of spinocerebellar ataxia 3. *Free Radic. Biol. Med.* 71, 339–350. doi:10.1016/J.FREERADBIOMED.2014.03.023.

Chen, H.-C., Lirng, J.-F., Soong, B.-W., Guo, W. Y., Wu, H.-M., Chen, C. C.-C., et al. (2014b). The merit of proton magnetic resonance spectroscopy in the longitudinal assessment of spinocerebellar ataxias and multiple system atrophy-cerebellar type. *Cerebellum & Ataxias* 1, 1–10. doi:10.1186/S40673-014-0017-4.

Chen, X., Tang, T.-S., Tu, H., Nelson, O., Pook, M., Hammer, R., et al. (2008). Deranged calcium signaling and neurodegeneration in spinocerebellar ataxia type 3. *J. Neurosci.* 28, 12713–24. doi:10.1523/JNEUROSCI.3909-08.2008.

Chou, A. H., Yeh, T. H., Kuo, Y. L., Kao, Y. C., Jou, M. J., Hsu, C. Y., et al. (2006). Polyglutamine-expanded ataxin-3 activates mitochondrial apoptotic pathway by upregulating Bax and downregulating Bcl-xL. *Neurobiol. Dis.* 21, 333–345. doi:10.1016/J.NBD.2005.07.011.

Chou, A. H., Yeh, T. H., Ouyang, P., Chen, Y. L., Chen, S. Y., and Wang, H. L. (2008). Polyglutamine-expanded ataxin-3 causes cerebellar dysfunction of SCA3 transgenic mice by inducing transcriptional dysregulation. *Neurobiol. Dis.* 31, 89–101. doi:10.1016/J.NBD.2008.03.011.

Choudhry, S., Mukerji, M., Srivastava, A. K., Jain, S., and Brahmachari, S. K. (2001). CAG repeat instability at SCA2 locus: anchoring CAA interruptions and linked single nucleotide polymorphisms. *Hum. Mol. Genet.* 10, 2437–2446. doi:10.1093/HMG/10.21.2437.

Chuang, C. Y., Yang, C. C., Soong, B. W., Yu, C. Y., Chen, S. H., Huang, H. P., et al. (2019). Modeling spinocerebellar ataxias 2 and 3 with iPSCs reveals a role for glutamate in disease pathology. *Sci. Rep.* 9, 1–13. doi:10.1038/s41598-018-37774-2.

Collier, N. C., Heuser, J., Levy, M. A., and Schlesinger, M. J. (1988). Ultrastructural and biochemical analysis of the stress granule in chicken embryo fibroblasts. *J. Cell Biol.* 106, 1131–9. doi:10.1083/jcb.106.4.1131.

Collier, N. C., and Schlesinger, M. J. (1986). The dynamic state of heat shock proteins in chicken embryo fibroblasts. *J. Cell Biol.* 103, 1495–1507. doi:10.1083/jcb.103.4.1495.

Conlon, E. G., and Manley, J. L. (2017). RNA-binding proteins in neurodegeneration: mechanisms in aggregate. *Genes Dev.* 31, 1509–1528. doi:10.1101/GAD.304055.117.

Cornelius, N., Wardman, J. H., Hargreaves, I. P., Neergheen, V., Bie, A. S., Tümer, Z., et al. (2017). Evidence of oxidative stress and mitochondrial dysfunction in spinocerebellar ataxia type 2 (SCA2) patient fibroblasts: Effect of coenzyme Q10 supplementation on these parameters. *Mitochondrion* 34, 103–114. doi:10.1016/J.MITO.2017.03.001.

Cortes, C. J., and La Spada, A. R. (2015). Autophagy in polyglutamine disease: Imposing order on disorder or contributing to the chaos? *Mol. Cell. Neurosci.* 66, 53–61. doi:10.1016/j.mcn.2015.03.010.

Cossée, M., Schmitt, M., Campuzano, V., Reutenauer, L., Moutou, C., Mandel, J.-L., et al. (1997). Evolution of the Friedreich's ataxia trinucleotide repeat expansion: Founder effect and premutations. *Proc. Natl. Acad. Sci.* 94, 7452–7457. doi:10.1073/PNAS.94.14.7452.

Costa, M. do C., and Paulson, H. L. (2012). Toward understanding Machado-Joseph disease. *Prog. Neurobiol.* 97, 239–257. doi:10.1016/J.PNEUROBIO.2011.11.006.

Costa, R. G. (2021). Insights into the spreading of ataxin-2 through extracellular vesicles.

Coutinho, P., and Andrade, C. (1978). Autosomal dominant system degeneration in Portuguese families of the Azores Islands: A new genetic disorder involving cerebellar, pyramidal, extrapyramidal and spinal cord motor functions. *Neurology* 28, 703–709. doi:10.1212/WNL.28.7.703.

Coutinho, P., Ruano, L., Loureiro, J. L., Cruz, V. T., Barros, J., Tuna, A., et al. (2013). Hereditary Ataxia and Spastic Paraplegia in Portugal: A Population-Based Prevalence Study. *JAMA Neurol.* 70, 746–755. doi:10.1001/JAMANEUROL.2013.1707.

Cowan, K. J., Diamond, M. I., and Welch, W. J. (2003). Polyglutamine protein aggregation and toxicity are linked to the cellular stress response. *Hum. Mol. Genet.* 12, 1377–1391. doi:10.1093/hmg/ddg151.

Cunha-Santos, J., Duarte-Neves, J., Carmona, V., Guarente, L., Pereira de Almeida, L., and Cavadas, C. (2016). Caloric restriction blocks neuropathology and motor deficits in Machado–Joseph disease mouse models through SIRT1 pathway. *Nat. Commun.* 7, 1–14. doi:10.1038/ncomms11445.

Cushman-Nick, M., Bonini, N. M., and Shorter, J. (2013). Hsp104 Suppresses Polyglutamine-Induced Degeneration Post Onset in a Drosophila MJD/SCA3 Model. *PLOS Genet.* 9, e1003781. doi:10.1371/JOURNAL.PGEN.1003781.

D'Abreu, A., Jr., M. C. F., Yasuda, C. L., Campos, B. A. G., Lopes-Cendes, I., and Cendes, F. (2012). Neocortical Atrophy in Machado-Joseph Disease: A Longitudinal Neuroimaging Study. *J. Neuroimaging* 22, 285–291. doi:10.1111/J.1552-6569.2011.00614.X.

D'Abreu, A., Jr, M. F., Appenzeller, S., Lopes-Cendes, I., and Cendes, F. (2009a). Axonal Dysfunction in the Deep White Matter in Machado-Joseph Disease. *J. Neuroimaging* 19, 9–12. doi:10.1111/J.1552-6569.2008.00260.X.

D'Abreu, A., Jr, M. F., Conz, L., Friedman, J. H., Nucci, A. M., Cendes, F., et al. (2009b). Sleep symptoms and their clinical correlates in Machado–Joseph disease. *Acta Neurol. Scand.* 119, 277–280. doi:10.1111/J.1600-0404.2008.01092.X.

Damrath, E., Heck, M. V., Gispert, S., Azizov, M., Nowock, J., Seifried, C., et al. (2012). ATXN2-CAG42 Sequesters PABPC1 into Insolubility and Induces FBXW8 in Cerebellum of Old Ataxic Knock-In Mice. *PLOS Genet.* 8, e1002920. doi:10.1371/JOURNAL.PGEN.1002920.

Dang, Y., Kedersha, N., Low, W. K., Romo, D., Gorospe, M., Kaufman, R., et al. (2006). Eukaryotic Initiation Factor 2α-independent Pathway of Stress Granule Induction by the Natural Product Pateamine A. *J. Biol. Chem.* 281, 32870–32878. doi:10.1074/JBC.M606149200.

Dansithong, W., Paul, S., Figueroa, K. P., Rinehart, M. D., Wiest, S., Pflieger, L. T., et al. (2015). Ataxin-2 Regulates RGS8 Translation in a New BAC-SCA2 Transgenic Mouse Model. *PLOS Genet.* 11, e1005182. doi:10.1371/JOURNAL.PGEN.1005182.

De Almeida, L. P., Ross, C. A., Zala, D., Aebischer, P., and Déglon, N. (2002). Lentiviral-Mediated Delivery of Mutant Huntingtin in the Striatum of Rats Induces a Selective Neuropathology Modulated by Polyglutamine Repeat Size, Huntingtin Expression Levels, and Protein Length. *J. Neurosci.* 22, 3473–3483. doi:10.1523/jneurosci.22-09-03473.2002.

de Araújo, M. A., Raposo, M., Kazachkova, N., Vasconcelos, J., Kay, T., and Lima, M. (2016). Trends in the Epidemiology of Spinocerebellar Ataxia Type 3/Machado-Joseph Disease in the Azores Islands, Portugal. *JSM Brain Sci.* 1, 1001. Available at: http://www.orpha.net/orphacom/cahiers/docs/GB/ [Accessed October 13, 2021].

De Leeuw, F., Zhang, T., Wauquier, C., Huez, G., Kruys, V., and Gueydan, C. (2007). The cold-inducible RNA-binding protein migrates from the nucleus to cytoplasmic stress granules by a methylation-dependent mechanism and acts as a translational repressor. *Exp. Cell Res.* 313, 4130–4144. doi:10.1016/J.YEXCR.2007.09.017.

Diallo, A., Jacobi, H., Cook, A., Labrum, R., Durr, A., Brice, A., et al. (2018). Survival in patients with spinocerebellar ataxia types 1, 2, 3, and 6 (EUROSCA): a longitudinal cohort study. *Lancet Neurol.* 17, 327–334. doi:10.1016/S1474-4422(18)30042-5.

do Carmo Costa, M., Bajanca, F., Rodrigues, A.-J., Tomé, R. J., Corthals, G., Macedo-Ribeiro, S., et al. (2010). Ataxin-3 Plays a Role in Mouse Myogenic Differentiation through Regulation of Integrin Subunit Levels. *PLoS One* 5, e11728. doi:10.1371/JOURNAL.PONE.0011728.

Do Carmo Costa, M., Luna-Cancalon, K., Fischer, S., Ashraf, N. S., Ouyang, M., Dharia, R. M., et al. (2013). Toward RNAi Therapy for the Polyglutamine Disease Machado–Joseph Disease. *Mol. Ther.* 21, 1898–1908. doi:10.1038/MT.2013.144.

Dongmei, H., Jing, L., Mei, X., Ling, Z., Hongmin, Y., Zhidong, W., et al. (2011). Clinical analysis of the treatment of spinocerebellar ataxia and multiple system atrophy-cerebellar type with umbilical cord mesenchymal stromal cells. *Cytotherapy* 13, 913–917. doi:10.3109/14653249.2011.579958.

Doss-Pepe, E. W., Stenroos, E. S., Johnson, W. G., and Madura, K. (2003). Ataxin-3 Interactions with Rad23 and Valosin-Containing Protein and Its Associations with Ubiquitin Chains and the Proteasome Are Consistent with a Role in Ubiquitin-Mediated Proteolysis. *Mol. Cell. Biol.* 23, 6469–6483. doi:10.1128/MCB.23.18.6469-6483.2003.

Duarte-Neves, J., Gonçalves, N., Cunha-Santos, J., Simões, A. T., den Dunnen, W. F. A., Hirai, H., et al. (2015). Neuropeptide Y mitigates neuropathology and motor deficits in mouse models of Machado–Joseph disease. *Hum. Mol. Genet.* 24, 5451–5463. doi:10.1093/HMG/DDV271.

Egorova, P. A., and Bezprozvanny, I. B. (2019). Molecular Mechanisms and Therapeutics for Spinocerebellar Ataxia Type 2. *Neurotherapeutics* 16, 1050–1073. doi:10.1007/s13311-019-00777-6.

Elden, A. C., Kim, H.-J., Hart, M. P., Chen-Plotkin, A. S., Johnson, B. S., Fang, X., et al. (2010). Ataxin-2 intermediate-length polyglutamine expansions are associated with increased risk for ALS. *Nature* 466, 1069–1075. doi:10.1038/nature09320.

Ellisdon, A. M., Pearce, M. C., and Bottomley, S. P. (2007). Mechanisms of Ataxin-3 Misfolding and Fibril Formation: Kinetic Analysis of a Disease-associated Polyglutamine Protein. *J. Mol. Biol.* 368, 595–605. doi:10.1016/J.JMB.2007.02.058.

Ellisdon, A. M., Thomas, B., and Bottomley, S. P. (2006). The Two-stage Pathway of Ataxin-3 Fibrillogenesis Involves a Polyglutamine-independent Step. *J. Biol. Chem.* 281, 16888–16896. doi:10.1074/JBC.M601470200.

Esteves, S., Duarte-Silva, S., Naia, L., Neves-Carvalho, A., Teixeira-Castro, A., Rego, A. C., et al. (2015). Limited Effect of Chronic Valproic Acid Treatment in a Mouse Model of Machado-Joseph Disease. *PLoS One* 10, e0141610. doi:10.1371/JOURNAL.PONE.0141610.

Estrada, R., Galarraga, J., Orozco, G., Nodarse, A., and Auburger, G. (1999). Spinocerebellar ataxia 2 (SCA2): Morphometric analyses in 11 autopsies. *Acta Neuropathol.* 97, 306–310. doi:10.1007/s004010050989.

Evers, M. M., Tran, H. D., Zalachoras, I., Pepers, B. A., Meijer, O. C., den Dunnen, J. T., et al. (2013). Ataxin-3 protein modification as a treatment strategy for spinocerebellar ataxia type 3: Removal of the CAG containing exon. *Neurobiol. Dis.* 58, 49–56. doi:10.1016/J.NBD.2013.04.019.

Evert, B. O., Araujo, J., Vieira-Saecker, A. M., Vos, R. A. I. de, Harendza, S., Klockgether, T., et al. (2006). Ataxin-3 Represses Transcription via Chromatin Binding, Interaction with Histone Deacetylase 3, and Histone Deacetylation. *J. Neurosci.* 26, 11474–11486. doi:10.1523/JNEUROSCI.2053-06.2006.

Evert, B. O., Vogt, I. R., Kindermann, C., Ozimek, L., Vos, R. A. I. de, Brunt, E. R. P., et al. (2001). Inflammatory Genes Are Upregulated in Expanded Ataxin-3-Expressing Cell Lines and Spinocerebellar Ataxia Type 3 Brains. *J. Neurosci.* 21, 5389–5396. doi:10.1523/JNEUROSCI.21-15-05389.2001.

Evert, B. O., Vogt, I. R., Vieira-Saecker, A. M., Ozimek, L., de Vos, R. A. I., Brunt, E. R. P., et al. (2003). Gene Expression Profiling in Ataxin-3 Expressing Cell Lines Reveals Distinct Effects of Normal and Mutant Ataxin-3. *J. Neuropathol. Exp. Neurol.* 62, 1006–1018. doi:10.1093/JNEN/62.10.1006.

Fakhoury, M. (2017). Microglia and astrocytes in Alzheimer's disease: implications for therapy. *Curr. Neuropharmacol.* 15. doi:10.2174/1570159x15666170720095240.

Fan, A. C., Leung, A. K. L., and States, U. (2017). RNA Granules and Diseases - A Case Study of Stress Granules in ALS and FTLD. *Adv Exp Med Biol* 907, 263–296. doi:10.1007/978-3-319-29073-7.

Fei, E., Jia, N., Zhang, T., Ma, X., Wang, H., Liu, C., et al. (2007). Phosphorylation of ataxin-3 by glycogen synthase kinase 3β at serine 256 regulates the aggregation of ataxin-3. *Biochem. Biophys. Res. Commun.* 357, 487–492. doi:10.1016/J.BBRC.2007.03.160.

Fernandez, M., McClain, M. E., Martinez, R. A., Snow, K., Lipe, H., Ravits, J., et al. (2000). Late-onset SCA2: 33 CAG repeats are sufficient to cause disease. *Neurology* 55, 569–572. doi:10.1212/WNL.55.4.569.

Ferrigno, P., and Silver, P. A. (2000). Polyglutamine Expansions: Proteolysis, Chaperones, and the Dangers of Promiscuity. *Neuron* 26, 9–12. doi:10.1016/S0896-6273(00)81132-0.

Figueroa, K. P., Coon, H., Santos, N., Velazquez, L., Mederos, L. A., and Pulst, S. M. (2017). Genetic analysis of age at onset variation in spinocerebellar ataxia type 2. *Neurol. Genet.* 3. doi:10.1212/NXG.0000000000000155.

Filla, A., De Michele, G., Santoro, L., Calabrese, O., Castaldo, I., Giuffrida, S., et al. (1999). Spinocerebellar ataxia type 2 in southern Italy: a clinical and molecular study of 30 families. *J. Neurol.* 246, 467–471. doi:10.1007/S004150050385.

Fittschen, M., Lastres-Becker, I., Halbach, M. V., Damrath, E., Gispert, S., Azizov, M., et al. (2015). Genetic ablation of ataxin-2 increases several global translation factors in their transcript abundance but decreases translation rate. *Neurogenetics* 16, 181–192. doi:10.1007/S10048-015-0441-5/FIGURES/4.

Fonville, N. C., Ward, R. M., and Mittelman, D. (2011). Stress-Induced Modulators of Repeat Instability and Genome Evolution. *J. Mol. Microbiol. Biotechnol.* 21, 36–44. doi:10.1159/000332748.

Fournier, M., Coudert, L., Mellaoui, S., Adjibade, P., Gareau, C., and Côté, M. (2013). Inactivation of the mTORC1-Eukaryotic Translation Initiation Factor 4E Pathway Alters Stress Granule Formation. *Mol. Cell. Biol.* 33, 2285–2301. doi:10.1128/MCB.01517-12.

Friedman, J. E. (2011). Anticipation in hereditary disease: the history of a biomedical concept. *Hum. Genet. 2011 1306* 130, 705–714. doi:10.1007/S00439-011-1022-9.

Friedman, J. H., and Amick, M. M. (2008). Fatigue and daytime somnolence in Machado Joseph Disease (Spinocerebellar ataxia type 3). *Mov. Disord.* 23, 1323–1324. doi:10.1002/MDS.22122.

Fu, Y.-H., Pizzuti, A., Fenwick, R. G., JR., King, J., Rajnarayan, S., et al. (1992). An unstable triplet repeat in a gene related to myotonic muscular dystrophy. *Science (80-.).* 255, 1256–1258. doi:10.1126/SCIENCE.1546326.

Fujikake, N., Nagai, Y., Popiel, H. A., Okamoto, Y., Yamaguchi, M., and Toda, T. (2008). Heat Shock Transcription Factor 1-activating Compounds Suppress Polyglutamine-induced Neurodegeneration through Induction of Multiple Molecular Chaperones. *J. Biol. Chem.* 283, 26188–26197. doi:10.1074/JBC.M710521200.

Furukawa, Y., Kaneko, K., Matsumoto, G., Kurosawa, M., and Nukina, N. (2009). Cross-seeding fibrillation of Q/N-rich proteins offers new pathomechanism of polyglutamine diseases. *J. Neurosci.* 29, 5153–62. doi:10.1523/JNEUROSCI.0783-09.2009.

Furusho, K., Yoshizawa, T., and Shoji, S. (2005). Ectoine alters subcellular localization of inclusions and reduces apoptotic cell death induced by the truncated Machado–Joseph disease gene product with an expanded polyglutamine stretch. *Neurobiol. Dis.* 20, 170–178. doi:10.1016/J.NBD.2005.02.011.

Ganassi, M., Mateju, D., Bigi, I., Mediani, L., Poser, I., Lee, H. O., et al. (2016). A Surveillance Function of the HSPB8-BAG3-HSP70 Chaperone Complex Ensures Stress Granule Integrity and Dynamism. *Mol. Cell* 63, 796–810. doi:10.1016/j.molcel.2016.07.021.

Gardiner, S. L., Boogaard, M. W., Trompet, S., De Mutsert, R., Rosendaal, F. R., Gussekloo, J., et al. (2019). Prevalence of Carriers of Intermediate and Pathological Polyglutamine Disease–Associated Alleles Among Large Population-Based Cohorts. *JAMA Neurol.* 76, 650–656. doi:10.1001/JAMANEUROL.2019.0423.

Gatchel, J. R., and Zoghbi, H. Y. (2005). Diseases of Unstable Repeat Expansion: Mechanisms and Common Principles. *Nat. Rev. Genet.* 6, 743–755.

doi:10.1038/nrg1691.

Gennarino, V. A., Singh, R. K., White, J. J., De Maio, A., Han, K., Kim, J. Y., et al. (2015). Pumilio1 Haploinsufficiency Leads to SCA1-like Neurodegeneration by Increasing Wild-Type Ataxin1 Levels. *Cell* 160, 1087–1098. doi:10.1016/J.CELL.2015.02.012.

Geschwind, D. H., Perlman, S., Figueroa, C. P., Treiman, L. J., and Pulst, S. M. (1997). The prevalence and wide clinical spectrum of the spinocerebellar ataxia type 2 trinucleotide repeat in patients with autosomal dominant cerebellar ataxia. *Am. J. Hum. Genet.* 60, 842. Available at: /pmc/articles/PMC1712476/?report=abstract [Accessed October 27, 2021].

Gierga, K., Bürk, K., Bauer, M., Orozco Diaz, G., Auburger, G., Schultz, C., et al. (2005). Involvement of the cranial nerves and their nuclei in spinocerebellar ataxia type 2 (SCA2). *Acta Neuropathol.* 109, 617–631. doi:10.1007/s00401-005-1014-8.

Gilks, N., Kedersha, N., Ayodele, M., Shen, L., Stoecklin, G., Dember, L. M., et al. (2004). Stress granule assembly is mediated by prion-like aggregation of TIA-1. *Mol. Biol. Cell* 15, 5383–5398. doi:10.1091/MBC.E04-08-0715/ASSET/IMAGES/LARGE/ZMK0120429070009.JPEG.

Gispert, S., Twells, R., Orozco, G., Brice, A., Weber, J., Heredero, L., et al. (1993). Chromosomal assignment of the second locus for autosomal dominant cerebellar ataxia (SCA2) to chromosome 12q23–24.1. *Nat. Genet.* 4, 295–299. doi:10.1038/ng0793-295.

Goldstrohm, A. C., Hall, T. M. T., and McKenney, K. M. (2018). Post-transcriptional Regulatory Functions of Mammalian Pumilio Proteins. *Trends Genet.* 34, 972–990. doi:10.1016/J.TIG.2018.09.006.

Goti, D., Katzen, S. M., Mez, J., Kurtis, N., Kiluk, J., Ben-Haïem, L., et al. (2004). A Mutant Ataxin-3 Putative-Cleavage Fragment in Brains of Machado-Joseph Disease Patients and Transgenic Mice Is Cytotoxic above a Critical Concentration. *J. Neurosci.* 24, 10266–10279. doi:10.1523/JNEUROSCI.2734-04.2004.

Goto, J., Watanabe, M., Ichikawa, Y., Yee, S. B., Ihara, N., Endo, K., et al. (1997). Machado–Joseph disease gene products carrying different carboxyl termini. *Neurosci. Res.* 28, 373–377. doi:10.1016/S0168-0102(97)00056-4.

Guimarães, R. P., D'Abreu, A., Yasuda, C. L., França, M. C., Silva, B. H. B., Cappabianco, F. A. M., et al. (2013). A multimodal evaluation of microstructural white matter damage in spinocerebellar ataxia type 3. *Mov. Disord.* 28, 1125–1132. doi:10.1002/MDS.25451.

Gunawardena, S., and Goldstein, L. S. B. (2005). Polyglutamine Diseases and Transport Problems: Deadly Traffic Jams on Neuronal Highways. *Arch. Neurol.* 62, 46–51. doi:10.1001/ARCHNEUR.62.1.46.

Gwinn–Hardy, K., Chen, J. Y., Liu, H.-C., Liu, T. Y., Boss, M., Seltzer, W., et al. (2000). Spinocerebellar ataxia type 2 with parkinsonism in ethnic Chinese. *Neurology* 55, 800–805. doi:10.1212/WNL.55.6.800.

Haacke, A., Hartl, F. U., and Breuer, P. (2007). Calpain Inhibition Is Sufficient to Suppress Aggregation of Polyglutamine-expanded Ataxin-3. *J. Biol. Chem.* 282, 18851–18856. doi:10.1074/JBC.M611914200.

Hagerman, R. J., Leehey, M., Heinrichs, W., Tassone, F., Wilson, R., Hills, J., et al. (2001). Intention tremor, parkinsonism, and generalized brain atrophy in male carriers of fragile X. *Neurology* 57, 127–130. doi:10.1212/WNL.57.1.127.

Halbach, M. V., Stehning, T., Damrath, E., Jendrach, M., Şen, N. E., Başak, A. N., et al. (2015). Both Ubiquitin Ligases FBXW8 and PARK2 Are Sequestrated into Insolubility by ATXN2 PolyQ Expansions, but Only FBXW8 Expression Is Dysregulated. *PLoS One* 10, e0121089. doi:10.1371/JOURNAL.PONE.0121089.

Hansen, S. T., Meera, P., Otis, T. S., and Pulst, S. M. (2013). Changes in Purkinje cell firing and gene expression precede behavioral pathology in a mouse model of SCA2. *Hum. Mol. Genet.* 22, 271–283. doi:10.1093/HMG/DDS427.

Heir, R., Ablasou, C., Dumontier, E., Elliott, M., Fagotto-Kaufmann, C., and Bedford, F. K. (2006). The UBL domain of PLIC-1 regulates aggresome formation. *EMBO Rep.* 7, 1252–1258. doi:10.1038/SJ.EMBOR.7400823.

Hennig, S., Kong, G., Mannen, T., Sadowska, A., Kobelke, S., Blythe, A., et al. (2015). Prion-like domains in RNA binding proteins are essential for building subnuclear paraspeckles. *J. Cell Biol.* 210, 529–539. doi:10.1083/JCB.201504117.

Hjorth, J. J. J., Kozlov, A., Carannante, I., Frost Nylén, J., Lindroos, R., Johansson, Y., et al. (2020). The microcircuits of striatum in silico. *Proc. Natl. Acad. Sci. U. S. A.* 117, 9554–9565. doi:10.1073/PNAS.2000671117.

Hoche, F., Seidel, K., Brunt, E. R., Auburger, G., Schöls, L., Bürk, K., et al. (2008). Involvement of the auditory brainstem system in spinocerebellar ataxia type 2 (SCA2), type 3 (SCA3) and type 7 (SCA7). *Neuropathol. Appl. Neurobiol.* 34, 479–491. doi:10.1111/J.1365-2990.2007.00933.X.

Hofmann, S., Cherkasova, V., Bankhead, P., Bukau, B., and Stoecklin, G. (2012). Translation suppression promotes stress granule formation and cell survival in response to cold shock. *Mol. Biol. Cell* 23, 3786–3800. doi:10.1091/mbc.E12-04-0296.

Hong, H., Kim, B. S., and Im, H.-I. (2016). Pathophysiological role of neuroinflammation in neurodegenerative diseases and psychiatric disorders. *Int. Neurourol. J.* 20, S2–S7. doi:10.5213/inj.1632604.302.

Hou, H., Wang, F., Zhang, W., Wang, D., Li, X., Bartlam, M., et al. (2011). Structure-Functional Analyses of CRHSP-24 Plasticity and Dynamics in Oxidative Stress Response. *J. Biol. Chem.* 286, 9623–9635. doi:10.1074/JBC.M110.177436.

Hsu, J. Y., Jhang, Y. L., Cheng, P. H., Chang, Y. F., Mao, S. H., Yang, H. I., et al. (2017). The truncated C-terminal fragment of mutant ATXN3 disrupts mitochondria dynamics in spinocerebellar ataxia type 3 models. *Front. Mol. Neurosci.* 10. doi:10.3389/fnmol.2017.00196.

Hu, J., Matsui, M., Gagnon, K. T., Schwartz, J. C., Gabillet, S., Arar, K., et al. (2009). Allele-specific silencing of mutant huntingtin and ataxin-3 genes by targeting expanded CAG repeats in mRNAs. *Nat. Biotechnol.* 27, 478–484. doi:10.1038/nbt.1539.

Huang, F., Zhang, L., Long, Z., Chen, Z., Hou, X., Wang, C., et al. (2014). miR-25 alleviates polyQ-mediated cytotoxicity by silencing ATXN3. *FEBS Lett.* 588, 4791–4798. doi:10.1016/J.FEBSLET.2014.11.013.

Hübener, J., Weber, J. J., Richter, C., Honold, L., Weiss, A., Murad, F., et al. (2013). Calpain-mediated ataxin-3 cleavage in the molecular pathogenesis of spinocerebellar ataxia type 3 (SCA3). *Hum. Mol. Genet.* 22, 508–518. doi:10.1093/HMG/DDS449.

Huen, N. Y. M., and Chan, H. Y. E. (2005). Dynamic regulation of molecular chaperone gene expression in polyglutamine disease. *Biochem. Biophys. Res. Commun.* 334,

1074–1084. doi:10.1016/J.BBRC.2005.07.008.

Huynh, D. P., Del Bigio, M. R., Ho, D. H., and Pulst, S.-M. (1999). Expression of Ataxin-2 in Brains from Normal Individuals and Patients with Alzheimer's Disease and Spinocerebellar Ataxia 2. 45, 232–241. doi:10.1002/1531-8249.

Huynh, D. P., Figueroa, K., Hoang, N., and Pulst, S.-M. (2000). Nuclear localization or inclusion body formation of ataxin-2 are not necessary for SCA2 pathogenesis in mouse or human. *Nat. Genet.* 26, 44–50. doi:10.1038/79162.

Huynh, D. P., Yang, H.-T., Vakharia, H., Nguyen, D., and Pulst, S. M. (2003). Expansion of the polyQ repeat in ataxin-2 alters its Golgi localization, disrupts the Golgi complex and causes cell death. *Hum. Mol. Genet.* 12, 1485–1496. doi:10.1093/HMG/DDG175.

Ichikawa, Y., Goto, J., Hattori, A., Toyoda, M., Ishii, K., Jeong, S.-Y., et al. (2001). The genomic structure and expression of MJD, the Machado-Joseph disease gene. *J. Hum. Genet.* 46, 413–422.

Ikeda, H., Yamaguchi, M., Sugai, S., Aze, Y., Narumiya, S., and Kakizuka, A. (1996). Expanded polyglutamine in the Machado–Joseph disease protein induces cell death in vitro and in vivo. *Nat. Genet.* 13, 196–202. doi:10.1038/ng0696-196.

Imbert, G., Saudou, F., Yvert, G., Devys, D., Trottier, Y., Garnier, J.-M., et al. (1996). Cloning of the gene for spinocerebellar ataxia 2 reveals a locus with high sensitivity to expanded CAG/glutamine repeats. *Nat. Genet.* 14, 285–291. doi:10.1038/ng1196-285.

Infante, J., Combarros, O., Volpini, V., Corral, J., Llorca, J., and Berciano, J. (2005). Autosomal dominant cerebellar ataxias in Spain: molecular and clinical correlations, prevalence estimation and survival analysis. *Acta Neurol. Scand.* 111, 391–399. doi:10.1111/J.1600-0404.2005.00400.X.

Ishikawa, K., Fujigasaki, H., Saegusa, H., Ohwada, K., Fujita, T., Iwamoto, H., et al. (1999). Abundant Expression and Cytoplasmic Aggregations of α1A Voltage-Dependent Calcium Channel Protein Associated with Neurodegeneration in Spinocerebellar Ataxia Type 6. *Hum. Mol. Genet.* 8, 1185–1193. doi:10.1093/HMG/8.7.1185.

Ito, N., Kamiguchi, K., Nakanishi, K., Sokolovskya, A., Hirohashi, Y., Tamura, Y., et al. (2016). A novel nuclear DnaJ protein, DNAJC8, can suppress the formation of spinocerebellar ataxia 3 polyglutamine aggregation in a J-domain independent manner. *Biochem. Biophys. Res. Commun.* 474, 626–633. doi:10.1016/J.BBRC.2016.03.152.

Jain, S., Wheeler, J. R., Walters, R. W., Agrawal, A., Barsic, A., Parker, R., et al. (2016). ATPase-Modulated Stress Granules Contain a Diverse Proteome and Substructure Article ATPase-Modulated Stress Granules Contain a Diverse Proteome and Substructure. *Cell*, 1–12. doi:10.1016/j.cell.2015.12.038.

Jana, N. R., Dikshit, P., Goswami, A., Kotliarova, S., Murata, S., Tanaka, K., et al. (2005). Co-chaperone CHIP Associates with Expanded Polyglutamine Protein and Promotes Their Degradation by Proteasomes. *J. Biol. Chem.* 280, 11635–11640. doi:10.1074/JBC.M412042200.

Jin, J., Liu, Z., Lu, Z., Guan, D., Wang, C., Chen, Z., et al. (2013). Safety and Efficacy of Umbilical Cord Mesenchymal Stem Cell Therapy in Hereditary Spinocerebellar Ataxia. 1, 11–20.

Johri, A., and Beal, M. F. (2012). Antioxidants in Huntington's disease. *Biochim. Biophys.*

Acta - Mol. Basis Dis. 1822, 664–674. doi:10.1016/j.bbadis.2011.11.014.

Jun, K., Piedras-Rentería, E. S., Smith, S. M., Wheeler, D. B., Lee, S. B., Lee, T. G., et al. (1999). Ablation of P/Q-type Ca2+ channel currents, altered synaptic transmission, and progressive ataxia in mice lacking the α1A-subunit. *Proc. Natl. Acad. Sci.* 96, 15245–15250. doi:10.1073/PNAS.96.26.15245.

Kanai, K., Kuwabara, S., Arai, K., Sung, J., Ogawara, K., and Hattori, T. (2003). Muscle cramp in Machado–Joseph diseaseAltered motor axonal excitability properties and mexiletine treatment. *Brain* 126, 965–973. doi:10.1093/BRAIN/AWG073.

Kasumu, A., and Bezprozvanny, I. (2012). Deranged calcium signaling in purkinje cells and pathogenesis in spinocerebellar ataxia 2 (SCA2) and other ataxias. *Cerebellum* 11, 630–639. doi:10.1007/s12311-010-0182-9.

Kasumu, A. W., Hougaard, C., Rode, F., Jacobsen, T. A., Sabatier, J. M., Eriksen, B. L., et al. (2012a). Selective Positive Modulator of Calcium-Activated Potassium Channels Exerts Beneficial Effects in a Mouse Model of Spinocerebellar Ataxia Type 2. *Chem. Biol.* 19, 1340–1353. doi:10.1016/J.CHEMBIOL.2012.07.013.

Kasumu, A. W., Liang, X., Egorova, P., Vorontsova, D., and Bezprozvanny, I. (2012b). Chronic Suppression of Inositol 1,4,5-Triphosphate Receptor-Mediated Calcium Signaling in Cerebellar Purkinje Cells Alleviates Pathological Phenotype in Spinocerebellar Ataxia 2 Mice. *J. Neurosci.* 32, 12786–12796. doi:10.1523/JNEUROSCI.1643-12.2012.

Kawaguchi, Y., Okamoto, T., Taniwaki, M., Aizawa, M., Inoue, M., Katayama, S., et al. (1994). CAG expansions in a novel gene for Machado-Joseph disease at chromosome 14q32.1. *Nat. Genet.* 8, 221–228. doi:10.1038/ng1194-221.

Kedersha, N., and Anderson, P. (2002). Stress granules : sites of mRNA triage that regulate mRNA stability Stress granules (SGs): a historical perspective. *Biochem. Soc. Trans.* 30, 963–969.

Kedersha, N., and Anderson, P. (2007). Mammalian Stress Granules and Processing Bodies. *Methodos Enzymol.* 431. doi:10.1016/S0076-6879(07)31005-7.

Kedersha, N., Ivanov, P., and Anderson, P. (2013). Stress granules and cell signaling: more than just a passing phase? *Trends Biochem. Sci.* 38, 494–506. doi:10.1016/j.tibs.2013.07.004.

Kedersha, N. L., Gupta, M., Li, W., Miller, I., and Anderson, P. (1999). RNA-Binding Proteins Tia-1 and Tiar Link the Phosphorylation of Eif-2α to the Assembly of Mammalian Stress Granules. *J. Cell Biol.* 147, 1431–1442. doi:10.1083/JCB.147.7.1431.

Kedersha, N., Stoecklin, G., Ayodele, M., Yacono, P., Lykke-Andersen, J., Fitzler, M. J., et al. (2005). Stress granules and processing bodies are dynamically linked sites of mRNP remodeling. *J. Cell Biol.* 169, 871–884. doi:10.1083/JCB.200502088.

Khan, L. A., Bauer, P. O., Miyazaki, H., Lindenberg, K. S., Landwehrmeyer, B. G., and Nukina, N. (2006). Expanded polyglutamines impair synaptic transmission and ubiquitin–proteasome system in Caenorhabditis elegans. *J. Neurochem.* 98, 576–587. doi:10.1111/J.1471-4159.2006.03895.X.

Khong, A., Matheny, T., Jain, S., Mitchell, S. F., Wheeler, J. R., Parker, R., et al. (2017). The Stress Granule Transcriptome Reveals Principles of mRNA Accumulation in Stress Granules Resource The Stress Granule Transcriptome Reveals Principles of mRNA Accumulation in Stress Granules. *Mol. Cell* 68, 808-820.e5. doi:10.1016/j.molcel.2017.10.015.

Kiehl, T. R., Nechiporuk, A., Figueroa, K. P., Keating, M. T., Huynh, D. P., and Pulst, S. M. (2006). Generation and characterization of Sca2 (ataxin-2) knockout mice. *Biochem. Biophys. Res. Commun.* 339, 17–24. doi:10.1016/J.BBRC.2005.10.186.

Kiehl, T. R., Shibata, H., and Pulst, S. M. (2000). The ortholog of human ataxin-2 is essential for early embryonic patterning in C. elegans. *J. Mol. Neurosci.* 15, 231–241. doi:10.1385/JMN:15:3:231.

Kieling, C., Prestes, P., Saraiva-Pereira, M., and Jardim, L. (2007). Survival estimates for patients with Machado–Joseph disease (SCA3). *Clin. Genet.* 72, 543–545. doi:10.1111/J.1399-0004.2007.00910.X.

Kinoshita, A., Hayashi, M., Oda, M., and Tanabe, H. (1995). Clinicopathological study of the peripheral nervous system in Machado-Joseph disease. *J. Neurol. Sci.* 130, 48–58. doi:10.1016/0022-510X(94)00285-V.

Kish, S. J., Mastrogiacomo, F., Guttman, M., Furukawa, Y., Taanman, J.-W., Dozic, S., et al. (1999). Decreased Brain Protein Levels of Cytochrome Oxidase Subunits in Alzheimer's Disease and in Hereditary Spinocerebella Ataxia Disorders: A Nonspecific Change? *J. Neurochem.* 72, 700–707. doi:10.1046/J.1471-4159.1999.0720700.X.

Kleiger, G., and Mayor, T. (2014). Perilous journey: a tour of the ubiquitin–proteasome system. *Trends Cell Biol.* 24, 352–359. doi:10.1016/J.TCB.2013.12.003.

Klockgether, T., Lüdtke, R., Kramer, B., Abele, M., Bürk, K., Schöls, L., et al. (1998). The natural history of degenerative ataxia: a retrospective study in 466 patients. *Brain* 121, 589–600. doi:10.1093/BRAIN/121.4.589.

Klockgether, T., Schöls, L., Abele, M., Bürk, K., Topka, H., Andres, F., et al. (1999). Age related axonal neuropathy in spinocerebellar ataxia type 3/Machado-Joseph disease (SCA3/MJD). *J. Neurol. Neurosurg. Psychiatry* 66, 222–224. doi:10.1136/JNNP.66.2.222.

Koch, P., Breuer, P., Peitz, M., Jungverdorben, J., Kesavan, J., Poppe, D., et al. (2011). Excitation-induced ataxin-3 aggregation in neurons from patients with Machado–Joseph disease. *Nature* 480, 543–546. doi:10.1038/nature10671.

Kopito, R. R. (2000). Aggresomes, inclusion bodies and protein aggregation. *Trends Cell Biol.* 10, 524–530. doi:10.1016/S0962-8924(00)01852-3.

Koyano, S., Uchihara, T., Fujigasaki, H., Nakamura, A., Yagishita, S., and Iwabuchi, K. (1999). Neuronal intranuclear inclusions in spinocerebellar ataxia type 2: Triple-labeling immunofluorescent study. *Neurosci. Lett.* 273, 117–120. doi:10.1016/S0304-3940(99)00656-4.

Koyano, S., Yagishita, S., Kuroiwa, Y., Tanaka, F., and Uchihara, T. (2014). Neuropathological Staging of Spinocerebellar Ataxia Type 2 by Semiquantitative 1C2-Positive Neuron Typing. Nuclear Translocation of Cytoplasmic 1C2 Underlies Disease Progression of Spinocerebellar Ataxia Type 2. *Brain Pathol.* 24, 599–606. doi:10.1111/BPA.12146.

Koyuncu, S., Fatima, A., Gutierrez-Garcia, R., and Vilchez, D. (2017). Proteostasis of huntingtin in health and disease. *Int. J. Mol. Sci.* 18. doi:10.3390/ijms18071568.

Krisenko, M. O., Higgins, R. L., Ghosh, S., Zhou, Q., Trybula, J. S., Wang, W. H., et al. (2015). Syk is recruited to stress granules and promotes their clearance through autophagy. *J. Biol. Chem.* 290, 27803–27815. doi:10.1074/jbc.M115.642900.

La Spada, A. R., and Taylor, J. P. (2010). Repeat expansion disease: Progress and

puzzles in disease pathogenesis. *Nat. Rev. Genet.* 11, 247–258. doi:10.1038/nrg2748.

Labbadia, J., and Morimoto, R. I. (2013). Huntington's disease: Underlying molecular mechanisms and emerging concepts. *Trends Biochem. Sci.* 38, 378–385. doi:10.1016/j.tibs.2013.05.003.

Laço, M. N., Oliveira, C. R., Paulson, H. L., and Rego, A. C. (2012). Compromised mitochondrial complex II in models of Machado-Joseph disease. *Biochim. Biophys. Acta - Mol. Basis Dis.* 1822, 139–149. doi:10.1016/j.bbadis.2011.10.010.

Laffita-Mesa, J. M., Almaguer-Mederos, L. E., Kourí, V., Bauer, P. O., Vázquez-Mojena, Y., Mariño, T. C., et al. (2014). Large normal alleles and SCA2 prevalence: lessons from a nationwide study and analysis of the literature. *Clin. Genet.* 86, 96–98. doi:10.1111/CGE.12221.

Laffita-Mesa, J. M., Velázquez-Pérez, L. C., Santos Falcón, N., Cruz-Mariño, T., González Zaldívar, Y., Vázquez Mojena, Y., et al. (2011). Unexpanded and intermediate CAG polymorphisms at the SCA2 locus (ATXN2) in the Cuban population: evidence about the origin of expanded SCA2 alleles. *Eur. J. Hum. Genet.* 20, 41–49. doi:10.1038/ejhg.2011.154.

Landau, W. M., Schmidt, R. E., McGlennen, R. C., and Reich, S. G. (2000). Hereditary Spastic Paraplegia and Hereditary Ataxia. Part 2: A Family Demonstrating Various Phenotypic Manifestations With the SCA3 Genotype. *Arch. Neurol.* 57, 733–739. doi:10.1001/ARCHNEUR.57.5.733.

Lane, R. M., Smith, A., Baumann, T., Gleichmann, M., Norris, D., Bennett, C. F., et al. (2018). Translating Antisense Technology into a Treatment for Huntington's Disease. *Methods Mol. Biol.* 1780, 497–523. doi:10.1007/978-1-4939-7825-0_23.

Lastres-Becker, I., Brodesser, S., Lütjohann, D., Azizov, M., Buchmann, J., Hintermann, E., et al. (2008a). Insulin receptor and lipid metabolism pathology in ataxin-2 knock-out mice. *Hum. Mol. Genet.* 17, 1465–1481. doi:10.1093/HMG/DDN035.

Lastres-Becker, I., Rüb, U., and Auburger, G. (2008b). Spinocerebellar ataxia 2 (SCA2). *Cerebellum* 7, 115–124. doi:10.1007/s12311-008-0019-y.

Li, F., Macfarlan, T., Pittman, R. N., and Chakravarti, D. (2002). Ataxin-3 Is a Histone-binding Protein with Two Independent Transcriptional Corepressor Activities. *J. Biol. Chem.* 277, 45004–45012. doi:10.1074/JBC.M205259200.

Li, X., Wang, C.-E., Huang, S., Xu, X., Li, X.-J., Li, H., et al. (2010). Inhibiting the ubiquitin–proteasome system leads to preferential accumulation of toxic N-terminal mutant huntingtin fragments. *Hum. Mol. Genet.* 19, 2445–2455. doi:10.1093/HMG/DDQ127.

Lian, X. J., and Gallouzi, I.-E. (2009). Oxidative Stress Increases the Number of Stress Granules in Senescent Cells and Triggers a Rapid Decrease in p21waf1/cip1 Translation. *J. Biol. Chem.* 284, 8877–87. doi:10.1074/jbc.M806372200.

Lim, C., and Allada, R. (2013). ATAXIN-2 Activates PERIOD Translation to Sustain Circadian Rhythms in Drosophila. *Science (80-.).* 340, 875–879. doi:10.1126/SCIENCE.1234785.

Liman, J., Deeg, S., Voigt, A., Voßfeldt, H., Dohm, C. P., Karch, A., et al. (2014). CDK5 protects from caspase-induced Ataxin-3 cleavage and neurodegeneration. *J. Neurochem.* 129, 1013–1023. doi:10.1111/JNC.12684.

Linnemann, C., Tezenas du Montcel, S., Rakowicz, M., Schmitz-Hübsch, T., Szymanski,

S., Berciano, J., et al. (2015). Peripheral Neuropathy in Spinocerebellar Ataxia Type 1, 2, 3, and 6. *The Cerebellum* 15, 165–173. doi:10.1007/S12311-015-0684-6.

Liquori, C. L., Ricker, K., Moseley, M. L., Jacobsen, J. F., Kress, W., Naylor, S. L., et al. (2001). Myotonic dystrophy type 2 caused by a CCTG expansion in intron I of ZNF9. *Science (80-.).* 293, 864–867. doi:10.1126/science.1062125.

Lirng, J.-F., Wang, P.-S., Chen, H.-C., Soong, B.-W., Guo, W. Y., Wu, H.-M., et al. (2012). Differences between Spinocerebellar Ataxias and Multiple System Atrophy-Cerebellar Type on Proton Magnetic Resonance Spectroscopy. *PLoS One* 7, e47925. doi:10.1371/JOURNAL.PONE.0047925.

Liu, J., Tang, T.-S., Tu, H., Nelson, O., Herndon, E., Huynh, D. P., et al. (2009). Deranged Calcium Signaling and Neurodegeneration in Spinocerebellar Ataxia Type 2. *J. Neurosci.* 29, 9148–9162. doi:10.1523/JNEUROSCI.0660-09.2009.

Liu, J., Yu, D., Aiba, Y., Pendergraff, H., Swayze, E. E., Lima, W. F., et al. (2013). ss-siRNAs allele selectively inhibit ataxin-3 expression: multiple mechanisms for an alternative gene silencing strategy. *Nucleic Acids Res.* 41, 9570–9583. doi:10.1093/NAR/GKT693.

Lo, R. Y., Figueroa, K. P., Pulst, S. M., Perlman, S., Wilmot, G., Gomez, C., et al. (2016). Depression and Clinical Progression in Spinocerebellar Ataxias. *Park. Relat. Disord.* 22, 87. doi:10.1016/J.PARKRELDIS.2015.11.021.

Lodi, R., Schapira, A. H. V., Manners, D., Styles, P., Wood, N. W., Taylor, D. J., et al. (2000). Abnormal in vivo skeletal muscle energy metabolism in Huntington's disease and dentatorubropallidoluysian atrophy. *Ann. Neurol.* 48, 72–76. Available at: https://pubmed.ncbi.nlm.nih.gov/10894218/ [Accessed October 21, 2021].

Loschi, M., Leishman, C. C., Berardone, N., and Boccacio, G. L. (2009). Dynein and kinesin regulate stress-granule and P-body dynamics. *J. Cell Sci.* 122, 3973–3982. doi:10.1242/jcs.051383.

Maciel, P., Costa, M. do C., Ferro, A., Rousseau, M., Santos, C. S., Gaspar, C., et al. (2001). Improvement in the Molecular Diagnosis of Machado-Joseph Disease. *Arch. Neurol.* 58, 1821–1827. doi:10.1001/ARCHNEUR.58.11.1821.

Magaña, J. J., Velázquez-Pérez, L., and Cisneros, B. (2013). Spinocerebellar ataxia type 2: Clinical presentation, molecular mechanisms, and therapeutic perspectives. *Mol. Neurobiol.* 47, 90–104. doi:10.1007/s12035-012-8348-8.

Marcelo, A., Afonso, I. T., Afonso-Reis, R., Brito, D. V. C., Costa, R. G., Rosa, A., et al. (2021a). Autophagy in Spinocerebellar ataxia type 2, a dysregulated pathway, and a target for therapy. *Cell Death Dis.*

Marcelo, A., Brito, F., Carmo-Silva, S., Matos, C. A., Alves-Cruzeiro, J., Vasconcelos-Ferreira, A., et al. (2018). Cordycepin activates autophagy through AMPK phosphorylation to reduce abnormalities in Machado–Joseph disease models. *Hum. Mol. Genet.* doi:10.1093/hmg/ddy328.

Marcelo, A., Koppenol, R., de Almeida, L. P., Matos, C. A., and Nóbrega, C. (2021b). Stress granules, RNA-binding proteins and polyglutamine diseases: too much aggregation? *Cell Death Dis.* 12, 1–17. doi:10.1038/s41419-021-03873-8.

Markossian, K. A., and Kurganov, B. I. (2004). Protein Folding, Misfolding, and Aggregation. Formation of Inclusion Bodies and Aggresomes. *Biochem.* 69, 971–984. doi:10.1023/b:biry.0000043539.07961.4c.

Masino, L., Musi, V., Menon, R. P., Fusi, P., Kelly, G., Frenkiel, T. A., et al. (2003).

Domain architecture of the polyglutamine protein ataxin-3: a globular domain followed by a flexible tail. *FEBS Lett.* 549, 21–25. doi:10.1016/S0014-5793(03)00748-8.

Masino, L., Nicastro, G., De Simone, A., Calder, L., Molloy, J., and Pastore, A. (2011). The Josephin Domain Determines the Morphological and Mechanical Properties of Ataxin-3 Fibrils. *Biophys. J.* 100, 2033–2042. doi:10.1016/J.BPJ.2011.02.056.

Masuda, K., Marasa, B., Martindale, J. L., Halushka, M. K., and Gorospe, M. (2009). Tissue- and age-dependent expression of RNA-binding proteins that influence mRNA turnover and translation. *Aging (Albany. NY).* 1, 681–698. doi:10.18632/AGING.100073.

Mateju, D., Franzmann, T. M., Patel, A., Kopach, A., Boczek, E. E., Maharana, S., et al. (2017). An aberrant phase transition of stress granules triggered by misfolded protein and prevented by chaperone function. *EMBO J.* 36, 1669–1687. doi:10.15252/embj.201695957.

Matos, C. A., Almeida, L. P. de, and Nóbrega, C. (2019). Machado–Joseph disease/spinocerebellar ataxia type 3: lessons from disease pathogenesis and clues into therapy. *J. Neurochem.* 148, 8–28. doi:10.1111/JNC.14541.

Matos, C. A., Macedo-Ribeiro, S. de, and Carvalho, A. L. (2011). Polyglutamine diseases : The special case of ataxin-3 and Machado – Joseph disease. *Prog. Neurobiol. jo* 95, 26–48. doi:10.1016/j.pneurobio.2011.06.007.

Matos, C. A., Nóbrega, C., Louros, S. R., Almeida, B., Ferreiro, E., Valero, J., et al. (2016). Ataxin-3 phosphorylation decreases neuronal defects in spinocerebellar ataxia type 3 models. *J. Cell Biol.* 212, 465–480. doi:10.1083/JCB.201506025.

Matos, C. A., Pereira de Almeida, L., and Nobrega, C. (2017). Proteolytic Cleavage of Polyglutamine Disease-Causing Proteins: Revisiting the Toxic Fragment Hypothesis. *Curr. Pharm. Des.* 23, 753–775. doi:10.2174/1381612822666161227121912.

Matsuishi, T., Sakai, T., Naito, E., Nagamitsu, S., Kuroda, Y., Iwashita, H., et al. (1996). Elevated cerebrospinal fluid lactate/pyruvate ratio in Machado-Joseph disease. *Acta Neurol. Scand.* 93, 72–75. doi:10.1111/J.1600-0404.1996.TB00174.X.

Matsuki, H., Takahashi, M., Higuchi, M., and Makokha, G. N. (2013). Both G3BP1 and G3BP2 contribute to stress granule formation. *Genes to Cells* 18, 135–146. doi:10.1111/gtc.12023.

Matsumoto, M., Yada, M., Hatakeyama, S., Ishimoto, H., Tanimura, T., Tsuji, S., et al. (2004). Molecular clearance of ataxin-3 is regulated by a mammalian E4. *EMBO J.* 23, 659–669. doi:10.1038/SJ.EMBOJ.7600081.

Matus, S., Bosco, D. A., and Hetz, C. (2014). Autophagy meets fused in sarcoma-positive stress granules. *Neurobiol. Aging* 35, 2832–2835. doi:10.1016/j.neurobiolaging.2014.08.019.

Mazroui, R., Di Marco, S., Kaufman, R. J., and Gallouzi, I.-E. (2007). Inhibition of the Ubiquitin-Proteasome System Induces Stress Granule Formation. *Mol. Biol. Cell* 18, 2603–2618. doi:10.1091/mbc.e06-12-1079.

Mazroui, R., Hout, M. E., Tremblay, S., Fillion, C., Labelle, Y., and Khandjian, E. W. (2002). Trapping of messenger RNA by Fragile X Mental Retardation protein into cytoplasmic granules induces translation repression. *Hum. Mol. Genet.* 11, 3007–3017. doi:10.1093/HMG/11.24.3007.

Mazroui, R., Sukarieh, R., Bordeleau, M. E., Kaufman, R. J., Northcote, P., Tanaka, J., et al. (2006). Inhibition of ribosome recruitment induces stress granule formation independently of eukaryotic initiation factor 2α phosphorylation. *Mol. Biol. Cell* 17, 4212–4219. doi:10.1091/MBC.E06-04-0318/ASSET/IMAGES/LARGE/ZMK0100678020005.JPEG.

Mazzucchelli, S., De Palma, A., Riva, M., D'Urzo, A., Pozzi, C., Pastori, V., et al. (2009). Proteomic and biochemical analyses unveil tight interaction of ataxin-3 with tubulin. *Int. J. Biochem. Cell Biol.* 41, 2485–2492. doi:10.1016/J.BIOCEL.2009.08.003.

McBride, H. M., Neuspiel, M., and Wasiak, S. (2006). Mitochondria: More Than Just a Powerhouse. *Curr. Biol.* 16, R551–R560. doi:10.1016/J.CUB.2006.06.054.

McCampbell, A., Taylor, J. P., Taye, A. A., Robitschek, J., Li, M., Walcott, J., et al. (2000). CREB-binding protein sequestration by expanded polyglutamine. *Hum. Mol. Genet.* 9, 2197–2202. doi:10.1093/HMG/9.14.2197.

Mccormick, C., and Khaperskyy, D. A. (2017). Translation inhibition and stress granules in the antiviral immune response. *Nat. Rev. Immunol.* 17, 647–660. doi:10.1038/nri.2017.63.

McIlwain, D. R., Berger, T., and Mak, T. W. (2013). Caspase functions in cell death and disease. *Cold Spring Harb. Perspect. Biol.* 5, 1–28. doi:10.1101/cshperspect.a008656.

McLoughlin, H. S., Moore, L. R., Chopra, R., Komlo, R., McKenzie, M., Blumenstein, K. G., et al. (2018). Oligonucleotide therapy mitigates disease in spinocerebellar ataxia type 3 mice. *Ann. Neurol.* 84, 64–77. doi:10.1002/ANA.25264.

McMurray, C. T. (2010). Mechanisms of trinucleotide repeat instability during human development. *Nat. Rev. Genet.* 11, 786–799. doi:10.1038/nrg2828.

Mederos, L. A., Proenza, C., Almira, Y. R., Batallán, K. E., Falcón, N. S., Góngora, E. M., et al. (2008). Age-dependent risks in genetic counseling for spinocerebellar ataxia type 2. *Clin. Genet.* 74, 571–573. doi:10.1111/J.1399-0004.2008.01073.X.

Meera, P., Pulst, S. M., and Otis, T. S. (2016). Cellular and circuit mechanisms underlying spinocerebellar ataxias. *J. Physiol.* 594, 4653–4660. doi:10.1113/JP271897.

Mendonça, L. S., Nóbrega, C., Hirai, H., Kaspar, B. K., and Pereira de Almeida, L. (2015). Transplantation of cerebellar neural stem cells improves motor coordination and neuropathology in Machado-Joseph disease mice. *Brain* 138, 320–335. doi:10.1093/brain/awu352.

Menzies, F. M., Huebener, J., Renna, M., Bonin, M., Riess, O., and Rubinsztein, D. C. (2010). Autophagy induction reduces mutant ataxin-3 levels and toxicity in a mouse model of spinocerebellar ataxia type 3. *Brain* 133, 93–104. doi:10.1093/brain/awp292.

Miao, X., Wu, X., and Shi, W. (2015). Umbilical cord mesenchymal stem cells in neurological disorders: A clinical study. *Indian J. Biochem. Biophys.* 52, 140–146.

Michalik, A., and Van Broeckhoven, C. (2003). Pathogenesis of polyglutamine disorders: aggregation revisited. *Hum. Mol. Genet.* 12, R173–R186. doi:10.1093/HMG/DDG295.

Mittelman, D., Sykoudis, K., Hersh, M., Lin, Y., and Wilson, J. H. (2010). Hsp90 modulates CAG repeat instability in human cells. *Cell Stress Chaperones* 15, 753–759. doi:10.1007/S12192-010-0191-0.

Mokas, S., Mills, J. R., Garreau, C., Fournier, M. J., Robert, F., Arya, P., et al. (2009). Uncoupling stress granule assembly and translation initiation inhibition. *Mol. Biol. Cell* 20, 2673–2683. doi:10.1091/MBC.E08-10-1061/ASSET/IMAGES/LARGE/ZMK0110990680007.JPEG.

Molliex, A., Temirov, J., Lee, J., Coughlin, M., Kanagaraj, A. P., Kim, H. J., et al. (2015). Phase separation by low complexity domains promotes stress granule assembly and drives pathological fibrillization. *Cell* 163, 123–33. doi:10.1016/j.cell.2015.09.015.

Moore, L. R., Rajpal, G., Dillingham, I. T., Qutob, M., Blumenstein, K. G., Gattis, D., et al. (2017). Evaluation of Antisense Oligonucleotides Targeting ATXN3 in SCA3 Mouse Models. *Mol. Ther. - Nucleic Acids* 7, 200–210. doi:10.1016/J.OMTN.2017.04.005.

Muchowski, P. J., Schaffar, G., Sittler, A., Wanker, E. E., Hayer-Hartl, M. K., and Hartl, F. U. (2000). Hsp70 and Hsp40 chaperones can inhibit self-assembly of polyglutamine proteins into amyloid-like fibrils. *Proc. Natl. Acad. Sci. U. S. A.* 97, 7841–7846. doi:10.1073/pnas.140202897.

Mulley, J. C., Yu, S., Loesch, D. Z., Hay, D. A., Donnelly, A., Gedeon, A. K., et al. (1995). FRAXE and mental retardation. *J. Med. Genet.* 32, 162. doi:10.1136/JMG.32.3.162.

Nagai, Y., Fujikake, N., Ohno, K., Higashiyama, H., Popiel, H. A., Rahadian, J., et al. (2003). Prevention of polyglutamine oligomerization and neurodegeneration by the peptide inhibitor QBP1 in Drosophila. *Hum. Mol. Genet.* 12, 1253–1259. doi:10.1093/HMG/DDG144.

Nakano, K. K., Dawson, D. M., and Spence, A. (1972). Machado disease. A hereditary ataxia in Portuguese emigrants to Massachusetts. *Neurology* 22, 49–55. doi:10.1212/WNL.22.1.49.

Nascimento-Ferreira, I., Nóbrega, C., Vasconcelos-Ferreira, A., Onofre, I., Albuquerque, D., Aveleira, C., et al. (2013). Beclin 1 mitigates motor and neuropathological deficits in genetic mouse models of Machado–Joseph disease. *Brain* 136, 2173–2188. doi:10.1093/brain/awt144.

Nascimento-Ferreira, I., Santos-Ferreira, T., Sousa-Ferreira, L., Auregan, G., Onofre, I., Alves, S., et al. (2011). Overexpression of the autophagic beclin-1 protein clears mutant ataxin-3 and alleviates Machado–Joseph disease. *Brain* 134, 1400–1415. doi:10.1093/brain/awr047.

Natalello, A., Frana, A. M., Relini, A., Apicella, A., Invernizzi, G., Casari, C., et al. (2011). A Major Role for Side-Chain Polyglutamine Hydrogen Bonding in Irreversible Ataxin-3 Aggregation. *PLoS One* 6, e18789. doi:10.1371/JOURNAL.PONE.0018789.

Nechiporuk, T., Huynh, D. P., Figueroa, K., Sahba, S., Nechiporuk, A., and Pulst, S. M. (1998). The Mouse SCA2 Gene: cDNA Sequence, Alternative Splicing and Protein Expression. *Hum. Mol. Genet.* 7, 1301–1309. doi:10.1093/HMG/7.8.1301.

Nixon, R. A. (2005). Endosome function and dysfunction in Alzheimer's disease and other neurodegenerative diseases. in *Neurobiology of Aging* (Neurobiol Aging), 373–382. doi:10.1016/j.neurobiolaging.2004.09.018.

Nóbrega, C., Carmo-Silva, S., Albuquerque, D., Vasconcelos-Ferreira, A., Vijayakumar, U.-G., Mendonça, L., et al. (2015a). Re-establishing ataxin-2 downregulates translation of mutant ataxin-3 and alleviates Machado–Joseph disease. *Brain* 138, 3537–3554. doi:10.1093/BRAIN/AWV298.

Nóbrega, C., Carmo-silva, S., Albuquerque, D., Vasconcelos-ferreira, A., Vijayakumar, U., Mendonc, L., et al. (2015b). Re-establishing ataxin-2 downregulates translation of mutant ataxin-3 and alleviates Machado – Joseph disease. *Brain* 138, 3537–3554. doi:10.1093/brain/awv298.

Nóbrega, C., Codêsso, J. M., Mendonça, L., and Pereira De Almeida, L. (2019). RNA Interference Therapy for Machado-Joseph Disease: Long-Term Safety Profile of Lentiviral Vectors Encoding Short Hairpin RNAs Targeting Mutant Ataxin-3. *Hum. Gene Ther.* 30, 841–854. doi:10.1089/hum.2018.157.

Nóbrega, C., Mendonça, L., and Matos, C. A. (2020). *A Handbook of Gene and Cell Therapy*. Springer International Publishing doi:10.1007/978-3-030-41333-0_1.

Nóbrega, C., Nascimento-Ferreira, I., Onofre, I., Albuquerque, D., Conceição, M., Déglon, N., et al. (2013a). Overexpression of Mutant Ataxin-3 in Mouse Cerebellum Induces Ataxia and Cerebellar Neuropathology. *The Cerebellum* 12, 441–455. doi:10.1007/s12311-012-0432-0.

Nóbrega, C., Nascimento-Ferreira, I., Onofre, I., Albuquerque, D., Déglon, N., and Pereira de Almeida, L. (2014). RNA Interference Mitigates Motor and Neuropathological Deficits in a Cerebellar Mouse Model of Machado-Joseph Disease. *PLoS One* 9, e100086. doi:10.1371/journal.pone.0100086.

Nóbrega, C., Nascimento-Ferreira, I., Onofre, I., Albuquerque, D., Hirai, H., Déglon, N., et al. (2013b). Silencing Mutant Ataxin-3 Rescues Motor Deficits and Neuropathology in Machado-Joseph Disease Transgenic Mice. *PLoS One* 8, e52396. doi:10.1371/journal.pone.0052396.

Nóbrega, C., and Pereira de Almeida, L. (2018). *Polyglutamine Disorders*. doi:10.1007/978-3-319-71779-1_6.

Nonhoff, U., Ralser, M., Welzel, F., Piccini, I., Balzereit, D., Yaspo, M. L., et al. (2007). Ataxin-2 interacts with the DEAD/H-box RNA helicase DDX6 and interferes with P-bodies and stress granules. *Mol. Biol. Cell* 18, 1385–1396. doi:10.1091/MBC.E06-12-1120/ASSET/IMAGES/LARGE/ZMK0040780170009.JPEG.

Nover, L., Scharf, K. D., and Neumann, D. (1983). Formation of cytoplasmic heat shock granules in tomato cell cultures and leaves. *Mol. Cell. Biol.* 3, 1648–55. doi:10.1128/mcb.3.9.1648.

Nunes, C., Mestre, I., Marcelo, A., Koppenol, R., Matos, C. A., and Nóbrega, C. (2019). MSGP: the first database of the protein components of the mammalian stress granules. *Database* 2019, 31. doi:10.1093/DATABASE/BAZ031.

Ohn, T., Kedersha, N., Hickman, T., Tisdale, S., and Anderson, P. (2008). A functional RNAi screen links O-GlcNAc modification of ribosomal proteins to stress granule and processing body assembly. *Nat. Cell Biol.* 10, 1224–1231. doi:10.1038/ncb1783.

Olejniczak, M., Urbanek, M. O., and Krzyzosiak, W. J. (2015). The role of the immune system in triplet repeat expansion diseases. *Mediators Inflamm.* 2015. doi:10.1155/2015/873860.

Oliveira Miranda, C., Marcelo, A., Silva, T. P., Barata, J., Vasconcelos-Ferreira, A., Pereira, D., et al. (2018). Repeated Mesenchymal Stromal Cell Treatment Sustainably Alleviates Machado-Joseph Disease. *Mol. Ther.* 26, 2131–2151. doi:10.1016/j.ymthe.2018.07.007.

Onomoto, K., Jogi, M., Yoo, J. S., Narita, R., Morimoto, S., Takemura, A., et al. (2012). Critical role of an antiviral stress granule containing RIG-I and PKR in viral detection

and innate immunity. *PLoS One* 7. doi:10.1371/journal.pone.0043031.

Orozco, G., Estrada, R., Perry, T. L., Araña, J., Fernandez, R., Gonzalez-Quevedo, A., et al. (1989). Dominantly inherited olivopontocerebellar atrophy from eastern Cuba: Clinical, neuropathological, and biochemical findings. *J. Neurol. Sci.* 93, 37–50. doi:10.1016/0022-510X(89)90159-7.

Orphanet (2021). Prevalence and incidence of rare diseases: Bibliographic data. Available at: www.orpha.net [Accessed October 13, 2021].

Orr, A. L., Li, S., Wang, C.-E., Li, H., Wang, J., Rong, J., et al. (2008). N-Terminal Mutant Huntingtin Associates with Mitochondria and Impairs Mitochondrial Trafficking. *J. Neurosci.* 28, 2783–2792. doi:10.1523/JNEUROSCI.0106-08.2008.

Orr, H. T., and Zoghbi, H. Y. (2007). Trinucleotide Repeat Disorders. *http://dx.doi.org/10.1146/annurev.neuro.29.051605.113042* 30, 575–621. doi:10.1146/ANNUREV.NEURO.29.051605.113042.

Ostrowski, L. A., Hall, A. C., and Mekhail, K. (2017). Ataxin-2: From RNA Control to Human Health and Disease. *Genes (Basel).* 8, 2–21. doi:10.3390/GENES8060157.

Pang, J. T., Giunti, P., Chamberlain, S., An, S. F., Vitaliani, R., Scaravilli, T., et al. (2002). Neuronal intranuclear inclusions in SCA2: A genetic, morphological and immunohistochemical study of two cases. *Brain* 125, 656–663. doi:10.1093/brain/awf060.

Paul, B. D., and Snyder, S. H. (2019). Impaired redox signaling in Huntington's disease: Therapeutic implications. *Front. Mol. Neurosci.* 12. doi:10.3389/fnmol.2019.00068.

Paul, G., and Anisimov, S. V (2013). The secretome of mesenchymal stem cells : Potential implications for neuroregeneration. *Biochimie* 95, 2246–2256. doi:10.1016/j.biochi.2013.07.013.

Paul, S., Dansithong, W., Figueroa, K. P., Scoles, D. R., and Pulst, S. M. (2018). Staufen1 links RNA stress granules and autophagy in a model of neurodegeneration. *Nat. Commun.* 9. doi:10.1038/s41467-018-06041-3.

Paulson, H. (2018). "Repeat expansion diseases," in *Handbook of Clinical Neurology*, 105–123. doi:10.1016/B978-0-444-63233-3.00009-9.

Paulson, H. L., Das, S. S., Crino, P. B., Perez, M. K., Patel, S. C., Gotsdiner, D., et al. (1997a). Machado-Joseph disease gene product is a cytoplasmic protein widely expressed in brain. *Ann. Neurol.* 41, 453–462. doi:10.1002/ANA.410410408.

Paulson, H. L., Perez, M. K., Trottier, Y., Trojanowski, J. Q., Subramony, S. H., Das, S. S., et al. (1997b). Intranuclear Inclusions of Expanded Polyglutamine Protein in Spinocerebellar Ataxia Type 3. *Neuron* 19, 333–344. doi:10.1016/S0896-6273(00)80943-5.

Pchitskaya, E., Popugaeva, E., and Bezprozvanny, I. (2018). Calcium signaling and molecular mechanisms underlying neurodegenerative diseases. *Cell Calcium* 70, 87–94. doi:10.1016/J.CECA.2017.06.008.

Pedroso, J. L., França, M. C., Braga-Neto, P., D'Abreu, A., Saraiva-Pereira, M. L., Saute, J. A., et al. (2013). Nonmotor and extracerebellar features in Machado-Joseph disease: A review. *Mov. Disord.* 28, 1200–1208. doi:10.1002/MDS.25513.

Pellistri, F., Bucciantini, M., Invernizzi, G., Gatta, E., Penco, A., Frana, A. M., et al. (2013). Different ataxin-3 amyloid aggregates induce intracellular Ca2 + deregulation by different mechanisms in cerebellar granule cells. *Biochim. Biophys.*

Acta 1833, 3155–3165. doi:10.1016/J.BBAMCR.2013.08.019.

Pereira de Almeida, L., Zala, D., Aebischer, P., and Déglon, N. (2001). Neuroprotective Effect of a CNTF-Expressing Lentiviral Vector in the Quinolinic Acid Rat Model of Huntington's Disease. *Neurobiol. Dis.* 8, 433–446. doi:10.1006/nbdi.2001.0388.

Pfeffer, M., Gispert, S., Auburger, G., Wicht, H., and Korf, H.-W. (2017). Impact of Ataxin-2 knock out on circadian locomotor behavior and PER immunoreaction in the SCN of mice. *Chronobiol. Int.* 34, 129–137. doi:10.1080/07420528.2016.1245666.

Pfeiffer, J. R., McAvoy, B. L., Fecteau, R. E., Deleault, K. M., and Brooks, S. A. (2011). CARHSP1 Is Required for Effective Tumor Necrosis Factor Alpha mRNA Stabilization and Localizes to Processing Bodies and Exosomes. *Mol. Cell. Biol.* 31, 277–286. doi:10.1128/MCB.00775-10/SUPPL_FILE/SUPPLEMENTAL_FIGURE_2.ZIP.

Pirker, W., Back, C., Gerschlager, W., Laccone, F., and Alesch, F. (2003). Chronic thalamic stimulation in a patient with spinocerebellar ataxia type 2. *Mov. Disord.* 18, 222–225. doi:10.1002/mds.10192.

Platt, R. J., Chen, S., Zhou, Y., Yim, M. J., Swiech, L., Kempton, H. R., et al. (2014). CRISPR-Cas9 Knockin Mice for Genome Editing and Cancer Modeling. *Cell* 159, 440–455. doi:10.1016/J.CELL.2014.09.014.

Polo, S., Sigismund, S., Faretta, M., Guidi, M., Capua, M. R., Bossi, G., et al. (2002). A single motif responsible for ubiquitin recognition and monoubiquitination in endocytic proteins. *Nature* 416, 451–455. doi:10.1038/416451a.

Pulst, S.-M., Nechiporuk, A., Nechiporuk, T., Gispert, S., Chen, X.-N., Lopes-Cendes, I., et al. (1996). Moderate expansion of a normally biallelic trinucleotide repeat in spinocerebellar ataxia type 2. *Nat. Genet.* 14, 269–276. doi:10.1038/ng1196-269.

Pulst, S.-M., Nechiporuk, A., and Starkman, S. (1993). Anticipation in spinocerebellar ataxia type 2. *Nat. Genet.* 5, 8–10. doi:10.1038/ng0993-8c.

Pulst, S. M., Santos, N., Wang, D., Yang, H., Huynh, D., Velazquez, L., et al. (2005). Spinocerebellar ataxia type 2: polyQ repeat variation in the CACNA1A calcium channel modifies age of onset. *Brain* 128, 2297–2303. doi:10.1093/BRAIN/AWH586.

Puorro, G., Marsili, A., Sapone, F., Pane, C., De Rosa, A., Peluso, S., et al. (2018). Peripheral markers of autophagy in polyglutamine diseases. *Neurol. Sci.* 39, 149–152. doi:10.1007/s10072-017-3156-6.

Ralser, M., Albrecht, M., Nonhoff, U., Lengauer, T., Lehrach, H., and Krobitsch, S. (2005). An Integrative Approach to Gain Insights into the Cellular Function of Human Ataxin-2. *J. Mol. Biol.* 346, 203–214. doi:10.1016/J.JMB.2004.11.024.

Ramos, A., Kazachkova, N., Silva, F., Maciel, P., Silva-Fernandes, A., Duarte-Silva, S., et al. (2015). Differential mtDNA Damage Patterns in a Transgenic Mouse Model of Machado–Joseph Disease (MJD/SCA3). *J. Mol. Neurosci.* 55, 449–453. doi:10.1007/S12031-014-0360-1.

Ravikumar, B., Duden, R., and Rubinsztein, D. C. (2002). Aggregate-prone proteins with polyglutamine and polyalanine expansions are degraded by autophagy. *Hum. Mol. Genet.* 11, 1107–1117. doi:10.1093/HMG/11.9.1107.

Reineke, L. C., Kedersha, N., Langereis, M. A., van Kuppeveld, F. J. M., and Lloyd, R. E. (2015). Stress granules regulate double-stranded RNA-dependent protein kinase activation through a complex containing G3BP1 and Caprin1. *MBio* 6.

doi:10.1128/mBio.02486-14.

Reineke, L. C., and Neilson, J. R. (2019). Differences between acute and chronic stress granules, and how these differences may impact function in human disease. *Biochem. Pharmacol.* 162, 123–131. doi:10.1016/j.bcp.2018.10.009.

Reynaldo-Armiñán, R. D., Reynaldo-Hernández, R., Paneque-Herrera, M., Prieto-Ávila, L., and Pérez-Ruiz, E. (2002). Mental disorders in patients with spinocerebellar ataxia type 2 in Cuba. *Rev. Neurol.* 35, 818–821. doi:10.33588/RN.3509.2002300.

Rezende, T. J. R. de, D'Abreu, A., Guimarães, R. P., Lopes, T. M., Lopes-Cendes, I., Cendes, F., et al. (2015). Cerebral cortex involvement in Machado−Joseph disease. *Eur. J. Neurol.* 22, 277-e24. doi:10.1111/ENE.12559.

Richards, B. W., Sylvester, P. E., and Brooker, C. (1981). Fragile X-linked mental retardation: the Martin-Bell syndrome. *J. Ment. Defic. Res.* 25 Pt 4, 253–265. doi:10.1111/J.1365-2788.1981.TB00115.X.

Riess, O., Rüb, U., Pastore, A., Bauer, P., and Schöls, L. (2008). SCA3: Neurological features, pathogenesis and animal models. *The Cerebellum* 7, 125–137. doi:10.1007/S12311-008-0013-4.

Rodrigues, A.-J., Coppola, G., Santos, C., Costa, M. do C., Ailion, M., Sequeiros, J., et al. (2007). Functional genomics and biochemical characterization of the C. elegans orthologue of the Machado-Joseph disease protein ataxin-3. *FASEB J.* 21, 1126–1136. doi:10.1096/FJ.06-7002COM.

Rodrigues, A. J., do Carmo Costa, M., Silva, T. L., Ferreira, D., Bajanca, F., Logarinho, E., et al. (2010). Absence of ataxin-3 leads to cytoskeletal disorganization and increased cell death. *Biochim. Biophys. Acta* 1803, 1154–1163. doi:10.1016/J.BBAMCR.2010.07.004.

Rodriguez-Graña, T., Rodríguez-Labrada, R., Santana-Porbén, S., Reynaldo-Cejas, L., Medrano-Montero, J., Canales-Ochoa, N., et al. (2021). Weight loss is correlated with disease severity in Spinocerebellar ataxia type 2: a cross-sectional cohort study. *Nutr. Neurosci.*, 1–9. doi:10.1080/1028415X.2021.1895479.

Rodríguez-Labrada, R., Velázquez-Pérez, L., Auburger, G., Ziemann, U., Canales-Ochoa, N., Medrano-Montero, J., et al. (2016). Spinocerebellar ataxia type 2: Measures of saccade changes improve power for clinical trials. *Mov. Disord.* 31, 570–578. doi:10.1002/MDS.26532.

Rodríguez-Labrada, R., Velázquez-Pérez, L., Seigfried, C., Canales-Ochoa, N., Auburger, G., Medrano-Montero, J., et al. (2011). Saccadic latency is prolonged in Spinocerebellar Ataxia type 2 and correlates with the frontal-executive dysfunctions. *J. Neurol. Sci.* 306, 103–107. doi:10.1016/J.JNS.2011.03.033.

Rodríguez-Lebrón, E., Costa, M. D., Luna-Cancalon, K., Peron, T. M., Fischer, S., Boudreau, R. L., et al. (2013). Silencing Mutant ATXN3 Expression Resolves Molecular Phenotypes in SCA3 Transgenic Mice. *Mol. Ther.* 21, 1909–1918. doi:10.1038/MT.2013.152.

Romanul, F. C. A., Fowler, H. L., Radvany, J., Feldman, R. G., and Feingold, M. (1977). Azorean disease of the nervous system. *N. Engl. J. Med.* 296, 1505–1508.

Rosenberg, R. N. (1992). Machado-Joseph disease: an autosomal dominant motor system degeneration. *Mov. Disord.* 7, 193–203. doi:10.1002/MDS.870070302.

Rosenberg, R. N., Nyhan, W. L., Bay, C., and Shore, P. (1976). Autosomal dominant striatonigral degeneration: A clinical, pathologic, and biochemical study of a new

genetic disorder. *Neurology* 26, 703–714. doi:10.1212/WNL.26.8.703.

Ross, C. A., Wood, J. D., Schilling, G., Peters, M. F., Nucifora, F. C., Cooper, J. K., et al. (1999). Polyglutamine pathogenesis. *Philos. Trans. R. Soc. B Biol. Sci.* 354, 1005–1011. doi:10.1098/rstb.1999.0452.

Rüb, U., Brunt, E. R., and Deller, T. (2008). New insights into the pathoanatomy of spinocerebellar ataxia type 3 (Machado-Joseph disease). *Curr. Opin. Neurol.* 21, 111–116. doi:10.1097/WCO.0B013E3282F7673D.

Rüb, U., Schöls, L., Paulson, H., Auburger, G., Kermer, P., Jen, J. C., et al. (2013). Clinical features, neurogenetics and neuropathology of the polyglutamine spinocerebellar ataxias type 1, 2, 3, 6 and 7. *Prog. Neurobiol.* 104, 38–66. doi:10.1016/J.PNEUROBIO.2013.01.001.

Rüb, U., Seidel, K., Özerden, I., Gierga, K., Brunt, E. R., Schöls, L., et al. (2007). Consistent affection of the central somatosensory system in spinocerebellar ataxia type 2 and type 3 and its significance for clinical symptoms and rehabilitative therapy. *Brain Res. Rev.* 53, 235–249. doi:10.1016/J.BRAINRESREV.2006.08.003.

Ruggieri, A., Dazert, E., Metz, P., Hofmann, S., Bergeest, J. P., Mazur, J., et al. (2012). Dynamic Oscillation of Translation and Stress Granule Formation Mark the Cellular Response to Virus Infection. *Cell Host Microbe* 12, 71–85. doi:10.1016/j.chom.2012.05.013.

Ryu, H. H., Jun, M. H., Min, K. J., Jang, D. J., Lee, Y. S., Kim, H. K., et al. (2014). Autophagy regulates amyotrophic lateral sclerosis-linked fused in sarcoma-positive stress granules in neurons. *Neurobiol. Aging* 35, 2822–2831. doi:10.1016/j.neurobiolaging.2014.07.026.

Sahba, S., Nechiporuk, A., Figueroa, K. P., Nechiporuk, T., and Pulst, S. M. (1998). Genomic Structure of the Human Gene for Spinocerebellar Ataxia Type 2 (SCA2) on Chromosome 12q24.1. *Genomics* 47, 359–364. doi:10.1006/GENO.1997.5131.

Sánchez-Cruz, G., Velázquez-Pérez, L., Gómez-Peña, L., Martínez-Góngora, E., Castellano-Sánchez, G., and Santos-Falcón, N. (2001). Dysautonomic features in patients with cuban type 2 spinocerebellar ataxia. *Rev. Neurol.* 33, 428–433. doi:10.33588/RN.3305.2001244.

Sanpei, K., Takano, H., Igarashi, S., Sato, T., Oyake, M., Sasaki, H., et al. (1996). Identification of the spinocerebellar ataxia type 2 gene using a direct identification of repeat expansion and cloning technique, DIRECT. *Nat. Genet.* 14, 277–284. doi:10.1038/ng1196-277.

Santarriaga, S., Haver, H. N., Kanack, A. J., Fikejs, A. S., Sison, S. L., Egner, J. M., et al. (2018). SRCP1 Conveys Resistance to Polyglutamine Aggregation. *Mol. Cell* 71, 216-228.e7. doi:10.1016/J.MOLCEL.2018.07.008.

Satterfield, T. F., and Pallanck, L. J. (2006). Ataxin-2 and its Drosophila homolog, ATX2, physically assemble with polyribosomes. *Hum. Mol. Genet.* 15, 2523–2532. doi:10.1093/HMG/DDL173.

Scherzed, W., Brunt, E. R., Heinsen, H., de Vos, R. A., Seidel, K., Bürk, K., et al. (2012). Pathoanatomy of Cerebellar Degeneration in Spinocerebellar Ataxia Type 2 (SCA2) and Type 3 (SCA3). *The Cerebellum* 11, 749–760. doi:10.1007/S12311-011-0340-8.

Schmidt, J., and Schmidt, T. (2018). Animal Models of Machado-Joseph Disease. *Adv. Exp. Med. Biol.* 1049, 289–308. doi:10.1007/978-3-319-71779-1_15.

Schmidt, T., Landwehrmeyer, G. B., Schmitt, I., Trottier, Y., Auburger, G., Laccone, F., et al. (1998). An Isoform of Ataxin-3 Accumulates in the Nucleus of Neuronal Cells in Affected Brain Regions of SCA3 Patients. *Brain Pathol.* 8, 669–679. doi:10.1111/J.1750-3639.1998.TB00193.X.

Schmitt, I., Linden, M., Khazneh, H., Evert, B. O., Breuer, P., Klockgether, T., et al. (2007). Inactivation of the mouse Atxn3 (ataxin-3) gene increases protein ubiquitination. *Biochem. Biophys. Res. Commun.* 362, 734–739. doi:10.1016/J.BBRC.2007.08.062.

Schmitz-Hübsch, T., Coudert, M., Bauer, P., Giunti, P., Globas, C., Baliko, L., et al. (2008). Spinocerebellar ataxia types 1, 2, 3, and 6: Disease severity and nonataxia symptoms. *Neurology* 71, 982–989. doi:10.1212/01.WNL.0000325057.33666.72.

Schulz, J. B., Borkert, J., Wolf, S., Schmitz-Hübsch, T., Rakowicz, M., Mariotti, C., et al. (2010). Visualization, quantification and correlation of brain atrophy with clinical symptoms in spinocerebellar ataxia types 1, 3 and 6. *Neuroimage* 49, 158–168. doi:10.1016/J.NEUROIMAGE.2009.07.027.

Scoles, D. R., Meera, P., Schneider, M. D., Paul, S., Dansithong, W., Figueroa, K. P., et al. (2017). Antisense oligonucleotide therapy for spinocerebellar ataxia type 2. *Nature* 544, 362–366. doi:10.1038/nature22044.

Scoles, D. R., Pflieger, L. T., Thai, K. K., Hansen, S. T., Dansithong, W., and Pulst, S.-M. (2012). ETS1 regulates the expression of ATXN2. *Hum. Mol. Genet.* 21, 5048–5065. doi:10.1093/HMG/DDS349.

Seidel, K., den Dunnen, W. F. A., Schultz, C., Paulson, H., Frank, S., de Vos, R. A., et al. (2010). Axonal inclusions in spinocerebellar ataxia type 3. *Acta Neuropathol.* 120, 449–60. doi:10.1007/s00401-010-0717-7.

Seidel, K., Siswanto, S., Brunt, E. R. P., Den Dunnen, W., Korf, H. W., and Rüb, U. (2012). Brain pathology of spinocerebellar ataxias. *Acta Neuropathol.* 124, 1–21. doi:10.1007/s00401-012-1000-x.

Seidel, K., Siswanto, S., Fredrich, M., Bouzrou, M., Dunnen, W. F. A. den, Özerden, I., et al. (2017). On the distribution of intranuclear and cytoplasmic aggregates in the brainstem of patients with spinocerebellar ataxia type 2 and 3. *Brain Pathol.* 27, 345–355. doi:10.1111/BPA.12412.

Sen, N.-E., Canet-Pons, J., Halbach, M. V., Arsovic, A., Pilatus, U., Chae, W. H., et al. (2019). Generation of an Atxn2-CAG100 knock-in mouse reveals N-acetylaspartate production deficit due to early Nat8l dysregulation. *Neurobiol. Dis.* 132, 104559. doi:10.1016/J.NBD.2019.104559.

Shih, S. C., Katzmann, D. J., Schnell, J. D., Sutanto, M., Emr, S. D., and Hicke, L. (2002). Epsins and Vps27p/Hrs contain ubiquitin-binding domains that function in receptor endocytosis. *Nat. Cell Biol.* 4, 389–393. doi:10.1038/ncb790.

Silva-Fernandes, A., Duarte-Silva, S., Neves-Carvalho, A., Amorim, M., Soares-Cunha, C., Oliveira, P., et al. (2014). Chronic Treatment with 17-DMAG Improves Balance and Coordination in A New Mouse Model of Machado-Joseph Disease. *Neurotherapeutics* 11, 433–449. doi:10.1007/S13311-013-0255-9.

Simões, A. T., Gonçalves, N., Koeppen, A., Déglon, N., Kügler, S., Duarte, C. B., et al. (2012). Calpastatin-mediated inhibition of calpains in the mouse brain prevents mutant ataxin 3 proteolysis, nuclear localization and aggregation, relieving Machado–Joseph disease. *Brain* 135, 2428–2439. doi:10.1093/BRAIN/AWS177.

Simões, A. T., Gonçalves, N., Nobre, R. J., Duarte, C. B., and Pereira de Almeida, L.

(2014). Calpain inhibition reduces ataxin-3 cleavage alleviating neuropathology and motor impairments in mouse models of Machado–Joseph disease. *Hum. Mol. Genet.* 23, 4932–4944. doi:10.1093/HMG/DDU209.

Sisodia, S. S. (1998). Nuclear Inclusions in Glutamine Repeat Disorders: Are They Pernicious, Coincidental, or Beneficial? *Cell* 95, 1–4. doi:10.1016/S0092-8674(00)81743-2.

Soriano, E., Del Rio, J. A., and Auladell, C. (1993). Characterization of the phenotype and birthdates of pyknotic dead cells in the nervous system by a combination of DNA staining and immunohistochemistry for 5'-bromodeoxyuridine and neural antigens. *J. Histochem. Cytochem.* 41, 819–827. doi:10.1177/41.6.8315274.

Sowa, A. S., Martin, E., Martins, I. M., Schmidt, J., Depping, R., Weber, J. J., et al. (2018). Karyopherin α-3 is a key protein in the pathogenesis of spinocerebellar ataxia type 3 controlling the nuclear localization of ataxin-3. *Proc. Natl. Acad. Sci.* 115, E2624–E2633. doi:10.1073/PNAS.1716071115.

Spada, A. R. La, Paulson, H. L., and Fischbeck, K. H. (1994). Trinucleotide repeat expansion in neurological disease. *Ann. Neurol.* 36, 814–822. doi:10.1002/ANA.410360604.

Squadrone, S., Brizio, P., Mancini, C., Abete, M. C., and Brusco, A. (2018). Altered homeostasis of trace elements in the blood of SCA2 patients. *J. Trace Elem. Med. Biol.* 47, 111–114. doi:10.1016/J.JTEMB.2018.02.011.

Sreenu, V. B., Kumar, P., Nagaraju, J., and Nagarajaram, H. A. (2006). Microsatellite polymorphism across the M. tuberculosis and M. bovis genomes: implications on genome evolution and plasticity. *BMC Genomics* 7. doi:10.1186/1471-2164-7-78.

Srivastava, D., Ahmad, M. M., Shamim, M., Maurya, R., Srivastava, N., Pandey, P., et al. (2019). Modulation of Gene Expression by Microsatellites in Microbes. *New Futur. Dev. Microb. Biotechnol. Bioeng. Microb. Genes Biochem. Appl.*, 209–218. doi:10.1016/B978-0-444-63503-7.00012-7.

Stephen, C. D., and Schmahmann, J. D. (2019). Eye Movement Abnormalities Are Ubiquitous in the Spinocerebellar Ataxias. *The Cerebellum* 18, 1130–1136. doi:10.1007/S12311-019-01044-2.

Stezin, A., Venkatesh, S. D., Thennarasu, K., Purushottam, M., Jain, S., Yadav, R., et al. (2018). Non-ataxic manifestations of Spinocerebellar ataxia-2, their determinants and predictors. *J. Neurol. Sci.* 394, 14–18. doi:10.1016/j.jns.2018.08.024.

Sudarsky, L., and Coutinho, P. (1995). Machado-Joseph disease. *Clin. Neurosci.* 3, 17–22. Available at: http://www.ncbi.nlm.nih.gov/pubmed/7614089 [Accessed September 6, 2017].

Suite, N. D. A., Sequeiros, J., and McKhann, G. M. (1986). Machado-Joseph Disease in a Sicilian-American Family. *J. Neurogenet.* 3, 177–182. doi:10.3109/01677068609106847.

Takahashi, A., and Ohnishi, T. (2009). Molecular mechanisms involved in adaptive responses to radiation, UV light, and Heat. *J. Radiat. Res.* 50, 385–393. doi:10.1269/jrr.09048S.

Takahashi, M., Higuchi, M., Matsuki, H., Yoshita, M., Ohsawa, T., Oie, M., et al. (2013). Stress Granules Inhibit Apoptosis by Reducing Reactive Oxygen Species Production. *Mol. Cell. Biol.* 33, 815–829. doi:10.1128/MCB.00763-12.

Takahashi, T., Katada, S., and Onodera, O. (2010). Polyglutamine Diseases: Where

does Toxicity Come from? What is Toxicity? Where are We Going? *J. Mol. Cell Biol.* 2, 180–191. doi:10.1093/JMCB/MJQ005.

Takao, M., Aoyama, M., Ishikawa, K., Sakiyama, Y., Yomono, H., Saito, Y., et al. (2011). Spinocerebellar ataxia type 2 is associated with Parkinsonism and Lewy body pathology. *Case Reports* 2011, bcr0120113685. doi:10.1136/BCR.01.2011.3685.

Takeuchi, T., and Nagai, Y. (2017). Protein misfolding and aggregation as a therapeutic target for polyglutamine diseases. *Brain Sci.* 7. doi:10.3390/brainsci7100128.

Takiyama, Y., Nishizawa, M., Tanaka, H., Kawashima, S., Sakamoto, H., Karube, Y., et al. (1993). The gene for Machado–Joseph disease maps to human chromosome 14q. *Nat. Genet.* 4, 300–304. doi:10.1038/ng0793-300.

Thedieck, K., Holzwarth, B., Prentzell, M. T., Boehlke, C., Ruf, S., Sonntag, A. G., et al. (2013). Inhibition of mTORC1 by Astrin and Stress Granules Prevents Apoptosis in Cancer Cells. *Cell* 154, 859–874. doi:10.1016/j.cell.2013.07.031.

Todi, S. V., and Paulson, H. L. (2011). Balancing act: deubiquitinating enzymes in the nervous system. *Trends Neurosci.* 34, 370–382. doi:10.1016/J.TINS.2011.05.004.

Todi, S. V, Winborn, B. J., Scaglione, K. M., Blount, J. R., Travis, S. M., and Paulson, H. L. (2009). Ubiquitination directly enhances activity of the deubiquitinating enzyme ataxin-3. *EMBO J.* 28, 372–382. doi:10.1038/EMBOJ.2008.289.

Toonen, L. J. A., Rigo, F., van Attikum, H., and van Roon-Mom, W. M. C. (2017). Antisense Oligonucleotide-Mediated Removal of the Polyglutamine Repeat in Spinocerebellar Ataxia Type 3 Mice. *Mol. Ther. - Nucleic Acids* 8, 232–242. doi:10.1016/J.OMTN.2017.06.019.

Toonen, L. J. A., Schmidt, I., Luijsterburg, M. S., van Attikum, H., and van Roon-Mom, W. M. C. (2016). Antisense oligonucleotide-mediated exon skipping as a strategy to reduce proteolytic cleavage of ataxin-3. *Sci. Reports 2016 61* 6, 1–11. doi:10.1038/srep35200.

Torashima, T., Koyama, C., Iizuka, A., Mitsumura, K., Takayama, K., Yanagi, S., et al. (2008). Lentivector-mediated rescue from cerebellar ataxia in a mouse model of spinocerebellar ataxia. *EMBO Rep.* 9, 393–399. doi:10.1038/embor.2008.31.

Tower, C., Fu, L., Gill, R., Prichard, M., Lesort, M., and Sztul, E. (2011). Human cytomegalovirus UL97 kinase prevents the deposition of mutant protein aggregates in cellular models of Huntington's disease and Ataxia. *Neurobiol. Dis.* 41, 11–22. doi:10.1016/J.NBD.2010.08.013.

Trottier, Y., Cancel, G., An-Gourfinkel, I., Lutz, Y., Weber, C., Brice, A., et al. (1998). Heterogeneous Intracellular Localization and Expression of Ataxin-3. *Neurobiol. Dis.* 5, 335–347. doi:10.1006/NBDI.1998.0208.

Tsai, H. F., Tsai, H. J., and Hsieh, M. (2004). Full-length expanded ataxin-3 enhances mitochondrial-mediated cell death and decreases Bcl-2 expression in human neuroblastoma cells. *Biochem. Biophys. Res. Commun.* 324, 1274–1282. doi:10.1016/J.BBRC.2004.09.192.

Tsai, N.-P., Ho, P.-C., and Wei, L.-N. (2008). Regulation of stress granule dynamics by Grb7 and FAK signalling pathway. *EMBO J.* 27, 715–26. doi:10.1038/emboj.2008.19.

Tuin, I., Voss, U., Kang, J.-S., Kessler, K., Rüb, U., Nolte, D., et al. (2006). Stages of sleep pathology in spinocerebellar ataxia type 2 (SCA2). *Neurology* 67, 1966–1972. doi:10.1212/01.WNL.0000247054.90322.14.

Uchihara, T., Fujigasaki, H., Koyano, S., Nakamura, A., Yagishita, S., and Iwabuchi, K. (2001a). Non-expanded polyglutamine proteins in intranuclear inclusions of hereditary ataxias--triple-labeling immunofluorescence study. *Acta Neuropathol.* 102, 149–52. Available at: http://www.ncbi.nlm.nih.gov/pubmed/11563629 [Accessed March 27, 2017].

Uchihara, T., Fujigasaki, H., Koyano, S., Nakamura, A., Yagishita, S., and Iwabuchi, K. (2001b). Non-expanded polyglutamine proteins in intranuclear inclusions of hereditary ataxias – triple-labeling immunofluorescence study. *Acta Neuropathol.* 102, 149–152. doi:10.1007/S004010100364.

van de Loo, S., Eich, F., Nonis, D., Auburger, G., and Nowock, J. (2009). Ataxin-2 associates with rough endoplasmic reticulum. *Exp. Neurol.* 215, 110–118. doi:10.1016/J.EXPNEUROL.2008.09.020.

Vanderweyde, T., Youmans, K., Liu-Yesucevitz, L., and Wolozin, B. (2013). Role of Stress Granules and RNA-Binding Proteins in Neurodegeneration: A Mini-Review. *Gerontology* 59, 524–533. doi:10.1159/000354170.

Varrone, A., Salvatore, E., De Michele, G., Barone, P., Sansone, V., Pellecchia, M. T., et al. (2004). Reduced Striatal [123I]FP-CIT Binding in SCA2 Patients without Parkinsonism. *Ann. Neurol.* 55, 426–430. doi:10.1002/ana.20054.

Velázquez-Pérez, L. C., Rodríguez-Labrada, R., and Fernandez-Ruiz, J. (2017). Spinocerebellar Ataxia Type 2: Clinicogenetic Aspects, Mechanistic Insights, and Management Approaches. *Front. Neurol.* 8, 472. doi:10.3389/FNEUR.2017.00472.

Velázquez-Pérez, L., Fernandez-Ruiz, J., Díaz, R., González, R. P.-, Ochoa, N. C., Cruz, G. S., et al. (2006). Spinocerebellar ataxia type 2 olfactory impairment shows a pattern similar to other major neurodegenerative diseases. *J. Neurol.* 253, 1165–1169. doi:10.1007/S00415-006-0183-2.

Velázquez-Pérez, L., Rodríguez-Labrada, R., García-Rodríguez, J. C., Almaguer-Mederos, L. E., Cruz-Mariño, T., and Laffita-Mesa, J. M. (2011a). A Comprehensive Review of Spinocerebellar Ataxia Type 2 in Cuba. *The Cerebellum* 10, 184–198. doi:10.1007/S12311-011-0265-2.

Velázquez-Pérez, L., Seifried, C., Santos-Falcón, N., Abele, M., Ziemann, U., Almaguer, L. E., et al. (2004). Saccade velocity is controlled by polyglutamine size in spinocerebellar ataxia 2. *Ann. Neurol.* 56, 444–447. doi:10.1002/ANA.20220.

Velázquez-Pérez, L., Voss, U., Rodríguez-Labrada, R., Auburger, G., Ochoa, N. C., Cruz, G. S., et al. (2011b). Sleep Disorders in Spinocerebellar Ataxia Type 2 Patients. *Neurodegener. Dis.* 8, 447–454. doi:10.1159/000324374.

Velázquez Pérez, L., Cruz, G. S., Santos Falcón, N., Enrique Almaguer Mederos, L., Escalona Batallan, K., Rodríguez Labrada, R., et al. (2009). Molecular epidemiology of spinocerebellar ataxias in Cuba: Insights into SCA2 founder effect in Holguin. *Neurosci. Lett.* 454, 157–160. doi:10.1016/J.NEULET.2009.03.015.

Wadia, N. H., and Swami, R. K. (1971). A new form of heredo-familial spinocerebellar degeneration with slow eye movements (nine families). *Brain* 94, 359–374. doi:10.1093/brain/94.2.359.

Waelter, S., Boeddrich, A., Lurz, R., Scherzinger, E., Lueder, G., Lehrach, H., et al. (2001). Accumulation of mutant huntingtin fragments in aggresome-like inclusion bodies as a result of insufficient protein degradation. *Mol. Biol. Cell* 12, 1393–407. Available at: http://www.ncbi.nlm.nih.gov/pubmed/11359930 [Accessed March 28, 2017].

Wang, H., Jia, N., Fei, E., Wang, Z., Liu, C., Zhang, T., et al. (2007). p45, an ATPase subunit of the 19S proteasome, targets the polyglutamine disease protein ataxin-3 to the proteasome. *J. Neurochem.* 101, 1651–1661. doi:10.1111/J.1471-4159.2007.04460.X.

Wang, H., Ying, Z., and Wang, G. (2012). Ataxin-3 Regulates Aggresome Formation of Copper-Zinc Superoxide Dismutase (SOD1) by Editing K63-linked Polyubiquitin Chains. *J. Biol. Chem.* 287, 28576–28585. doi:10.1074/JBC.M111.299990.

Wang, Q., Li, L., and Ye, Y. (2006). Regulation of retrotranslocation by p97-associated deubiquitinating enzyme ataxin-3. *J. Cell Biol.* 174, 963–971. doi:10.1083/JCB.200605100.

Wardman, J. H., Henriksen, E. E., Marthaler, A. G., Nielsen, J. E., and Nielsen, T. T. (2020). Enhancement of Autophagy and Solubilization of Ataxin-2 Alleviate Apoptosis in Spinocerebellar Ataxia Type 2 Patient Cells. *Cerebellum* 19, 165–181. doi:10.1007/s12311-019-01092-8.

Warrick, J. M., Chan, H. Y. E., Gray-Board, G. L., Chai, Y., Paulson, H. L., and Bonini, N. M. (1999). Suppression of polyglutamine-mediated neurodegeneration in Drosophila by the molecular chaperone HSP70. *Nat. Genet.* 23, 425–428. doi:10.1038/70532.

Watchon, M., Yuan, K. C., Mackovski, N., Svahn, A. J., Cole, N. J., Goldsbury, C., et al. (2017). Calpain Inhibition Is Protective in Machado–Joseph Disease Zebrafish Due to Induction of Autophagy. *J. Neurosci.* 37, 7782–7794. doi:10.1523/JNEUROSCI.1142-17.2017.

Wek, R. C., Jiang, H., and Anthony, T. G. (2006). Coping with stress : eIF2 kinases and translational control. *Biochem. Soc.* 34, 7–11.

Wellington, C. L., Ellerby, L. M., Hackam, A. S., Margolis, R. L., Trifiro, M. A., Singaraja, R., et al. (1998). Caspase Cleavage of Gene Products Associated with Triplet Expansion Disorders Generates Truncated Fragments Containing the Polyglutamine Tract. *J. Biol. Chem.* 273, 9158–9167. doi:10.1074/JBC.273.15.9158.

Wen, J., Scoles, D. R., and Facelli, J. C. (2017). Effects of the enlargement of polyglutamine segments on the structure and folding of ataxin-2 and ataxin-3 proteins. *J. Biomol. Struct. Dyn.* 35, 504–519. doi:10.1080/07391102.2016.1152199.

White, J. P., and Lloyd, R. E. (2012). Regulation of stress granules in virus systems. *Trends Microbiol.* 20, 175–183. doi:10.1016/j.tim.2012.02.001.

Wilczynska, A., Aigueperse, C., Kress, M., Dautry, F., and Weil, D. (2005). The translational regulator CPEB1 provides a link between dcp1 bodies and stress granules. *J. Cell Sci.* 118, 981–992. doi:10.1242/JCS.01692.

Williams, A. J., Knutson, T. M., Colomer Gould, V. F., and Paulson, H. L. (2009). In vivo suppression of polyglutamine neurotoxicity by C-terminus of Hsp70-interacting protein (CHIP) supports an aggregation model of pathogenesis. *Neurobiol. Dis.* 33, 342–353. doi:10.1016/J.NBD.2008.10.016.

Williams, A., Jahreiss, L., Sarkar, S., Saiki, S., Menzies, F. M., Ravikumar, B., et al. (2006). Aggregate-Prone Proteins Are Cleared from the Cytosol by Autophagy: Therapeutic Implications. *Curr. Top. Dev. Biol.* 76, 89–101. doi:10.1016/S0070-2153(06)76003-3.

Wilusz, C. J., and Wilusz, J. (2005). Eukaryotic Lsm proteins: lessons from bacteria. *Nat.*

Struct. Mol. Biol. 12, 1031–1036. doi:10.1038/nsmb1037.

Winborn, B. J., Travis, S. M., Todi, S. V., Scaglione, K. M., Xu, P., Williams, A. J., et al. (2008). The Deubiquitinating Enzyme Ataxin-3, a Polyglutamine Disease Protein, Edits Lys63 Linkages in Mixed Linkage Ubiquitin Chains. *J. Biol. Chem.* 283, 26436–26443. doi:10.1074/JBC.M803692200.

Wippich, F., Bodenmiller, B., Trajkovska, M. G., Wanka, S., Aebersold, R., and Pelkmans, L. (2013). Dual Specificity Kinase DYRK3 Couples Stress Granule Condensation / Dissolution to mTORC1 Signaling. *Cell* 152, 791–805. doi:10.1016/j.cell.2013.01.033.

Wolozin, B. (2012). Regulated protein aggregation: Stress granules and neurodegeneration. *Mol. Neurodegener.* 7, 1–12. doi:10.1186/1750-1326-7-56/FIGURES/4.

Wolozin, B., and Ivanov, P. (2019). Stress granules and neurodegeneration. *Nat. Rev. Neurosci.* 20, 649–666. doi:10.1038/s41583-019-0222-5.

Woods, B. T., and Schaumburg, H. H. (1972). Nigro-spino-dentatal Degeneration with Nuclear Ophthalmoplegia: A Unique and Partially Treatable Clinico-pathological Entity. *J. Neurol. Sci.* 17, 149–166. doi:10.1016/0022-510X(72)90137-2.

Wu, D., Vonk, J. J., Salles, F., Vonk, D., Haslbeck, M., Melki, R., et al. (2019). The N terminus of the small heat shock protein HSPB7 drives its polyQ aggregation–suppressing activity. *J. Biol. Chem.* 294, 9985–9994. doi:10.1074/JBC.RA118.007117.

Yamada, M., Tsuji, S., and Takahashi, H. (2000). Pathology of CAG repeat diseases. *Neuropathology* 20, 319–325.

Yeh, T.-H., Lu, C.-S., Chou, Y.-H. W., Chong, C.-C., Wu, T., Han, N.-H., et al. (2005). Autonomic Dysfunction in Machado-Joseph Disease. *Arch. Neurol.* 62, 630–636. doi:10.1001/ARCHNEUR.62.4.630.

Yokoshi, M., Li, Q., Yamamoto, M., Okada, H., Suzuki, Y., and Kawahara, Y. (2014). Direct Binding of Ataxin-2 to Distinct Elements in 3′ UTRs Promotes mRNA Stability and Protein Expression. *Mol. Cell* 55, 186–198. doi:10.1016/J.MOLCEL.2014.05.022.

Yoo, J. S., Takahasi, K., Ng, C. S., Ouda, R., Onomoto, K., Yoneyama, M., et al. (2014). DHX36 Enhances RIG-I Signaling by Facilitating PKR-Mediated Antiviral Stress Granule Formation. *PLoS Pathog.* 10. doi:10.1371/journal.ppat.1004012.

Yoshida, H., Yoshizawa, T., Shibasaki, F., Shoji, S., and Kanazawa, I. (2002). Chemical Chaperones Reduce Aggregate Formation and Cell Death Caused by the Truncated Machado–Joseph Disease Gene Product with an Expanded Polyglutamine Stretch. *Neurobiol. Dis.* 10, 88–99. doi:10.1006/NBDI.2002.0502.

Yu, Y.-C., Kuo, C.-L., Cheng, W.-L., Liu, C.-S., and Hsieh, M. (2009). Decreased antioxidant enzyme activity and increased mitochondrial DNA damage in cellular models of Machado-Joseph disease. *J. Neurosci. Res.* 87, 1884–1891. doi:10.1002/JNR.22011.

Zala, D., Bensadoun, J. C., De Almeida, L. P., Leavitt, B. R., Gutekunst, C. A., Aebischer, P., et al. (2004). Long-term lentiviral-mediated expression of ciliary neurotrophic factor in the striatum of Huntington's disease transgenic mice. *Exp. Neurol.* 185, 26–35. doi:10.1016/j.expneurol.2003.09.002.

Zheng, S., Clabough, E. B. D., Sarkar, S., Futter, M., Rubinsztein, D. C., and Zeitlin, S.

O. (2010). Deletion of the huntingtin polyglutamine stretch enhances neuronal autophagy and longevity in mice. *PLoS Genet.* 6. doi:10.1371/journal.pgen.1000838.

Zhivotovsky, B., and Orrenius, S. (2011). Calcium and cell death mechanisms: A perspective from the cell death community. *Cell Calcium* 50, 211–221. doi:10.1016/J.CECA.2011.03.003.

Zhong, X., and Pittman, R. N. (2006). Ataxin-3 binds VCP/p97 and regulates retrotranslocation of ERAD substrates. *Hum. Mol. Genet.* 15, 2409–2420. doi:10.1093/HMG/DDL164.

Zoghbi, H. Y., and Orr, H. T. (2000). Glutamine Repeats and Neurodegeneration. *Annu. Rev. Neurosci.* 23, 217–247. doi:10.1146/ANNUREV.NEURO.23.1.217.